Novel Methodology for the Synthesis of Amino Acids with Applications in Biological Imaging

Leanne M. Riley, MChem

A thesis submitted in part fulfilment of the requirements of the degree of Doctor of Philosophy

School of Chemistry

College of Science and Engineering

University of Glasgow

June 2022

Abstract

The aim of this PhD was the synthesis and development of novel unnatural amino acids for imaging. The first project focused on the preparation of fluorescent pyridine derived *α*-amino acids. The key step in this methodology was ring formation through an inverse demand hetero-Diels Alder reaction of enone derived amino acids. A methoxy substituted analogue, previously shown to have good photophysical properties, was synthesised, and explored as a potential pH probe. Novel analogues with extended conjugation were prepared through regioselective bromination and Suzuki-Miyaura cross-coupling reactions. These amino acids displayed solvatochromic properties and sensitivity to changes in pH and solvent viscosity.

The next project investigated the synthesis of benzotriazole derived *α*-amino acids with extended conjugation though alkynyl and alkenyl substituents. The formation of an iodinated-benzotriazole amino acid was achieved through diazotisation and cyclisation of a 1,2-aryldiamine, utilising a mild polymer supported nitrite reagent. Sonogashira cross-coupling reactions gave the alkynes and subsequent reduction allowed access to the alkenes. Both classes showed improved photophysical properties compared to previously published truncated analogues.
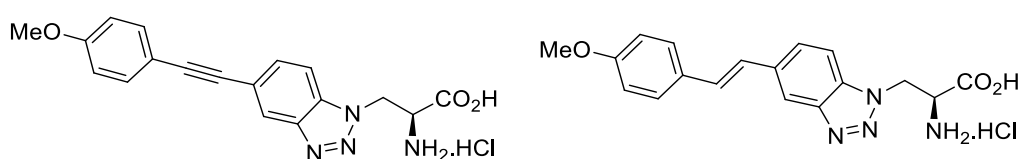
In the final project, novel precursors to *cis*- and *trans*-4-fluoroprolines were synthesised. These analogues utilised a novel protecting group strategy, which allowed deprotection under mild conditions following fluorination. Ultimately, the synthesis of these precursors facilitated the design of an improved, automated, radiosynthesis of *cis*- and *trans*-4-[18F]-fluoroproline.

Table of Contents

Acknowledgements

members – Holly, Amy, Rochelle, Nina, Lachlan and Valeria, as well as Joe and Becca from the Hartley group who have been around for the duration of my PhD. You guys have been incredible both in answering all of my questions inside the lab and providing endless laughs outside of the lab. P.S. Sorry for making every night out a burger night.

Authors Declaration

I declare that, except where explicit reference is made to the contribution of others, this thesis represents the original work of Leanne M. Riley and has not been submitted for any other degree at the University of Glasgow or any other institution. The research was carried out at the University of Glasgow in the Loudon Laboratory under the supervision of Professor Andrew Sutherland between October 2018 to April 2022. Aspects of the work described herein have been published elsewhere as listed below.

T. E. F. Morgan, L. M. Riley, A. A. S. Tavares and A. Sutherland, Automated Radiosynthesis of *cis*- and *trans*-4-[^{18}F]Fluoro-L-proline Using [^{18}F]Fluoride, *J. Org. Chem.*, 2021, **86**, 14054-14060.

Abbreviations

°C	Degrees centigrade
4-AP	4-Aminophthalimide
4-DMAP	4-(*N,N*-dimethylamino)phthalimide
6-DMN	6-N,N-dimethylamino-2,3-naphthalimide
Abs	Absorbance
Ac	Acetyl
ANAP	3-(6-acetylnaphthalen-2-ylamino)-2- aminopropanoic acid
Ar	Aromatic
AzuAla	β-(1-azulenyl)-L-alanine
Boc	*tert*-Butyloxycarbonyl
BODIPY	Boron-dipyrromethene
br	Broad
Cbz	Carboxybenzyl
CI	Chemical ionisation
COSY	Correlated spectroscopy
d	Doublet
Δ	Reflux
DANA	6-(2-dimethylaminonaphthoyl)alanine
DAST	Diethylaminosulfur trifluoride
DDQ	2,3-Dichloro-5,6-dicyano-1,4-benzoquinone
DEPT	Distortionless enhancement polarisation transfer
DIPEA	Diisopropylethylamine
DMABN	4-(Dimethylamino)benzonitrile
DMAP	4-Dimethylaminopyridine
DMF	Dimethylformamide
DMSO	Dimethyl sulfoxide
ee	Enantiomeric excess
EI	Electron impact
Em	Emission
er	Enantiomeric ratio
ESI	Electrospray ionisation
Et	Ethyl
Fmoc	Fluorenylmethyloxycarbonyl

Fmoc-Osu	Fmoc *N*-hydroxysuccinimide ester
g	Grams
GFP	Green fluorescent protein
h	Hour
HBTU	*O*-(Benzotriazol-1-yl)-*N,N,N',N'*-tetramethyluronium hexafluorophosphate
HIV	Human immunodeficiency virus
HMTA	Hexamethylenetetramine
HOBt	Hydroxybenzotriazole
HOMO	Highest occupied molecular orbital
HPLC	High-performance liquid chromatography
HSQC	Heteronuclear single quantum correlation spectroscopy
Hz	Hertz
ICT	Intramolecular charge transfer
IR	Infrared
J	NMR spectra coupling constant
KRT1	Keratin 1
LE	Locally Excited
LiHMDS	Lithium bis(trimethylsilyl)amide
m-	*Meta-*
m	Multiplet
M	Molar
m/z	Mass to charge
Me	Methyl
mg	Milligrams
MHz	Megahertz
mL	Millilitres
mM	Millimolar
μM	Micromolar
mmol	Millimole
mol	Mole
Ms	Mesyl
MW	Microwave
NBD	7-Chloro-4-nitrobenzo-2-oxa-1,3-diazole
NBS	*N*-Bromosuccinimide

nm	nanometers
NMR	Nuclear magnetic resonance
o-	*Ortho-*
p-	*Para-*
PBS	Phosphate-buffered saline
PET	Positron emission tomography
Ph	Phenyl
PRODAN	6-Propionyl-2-(dimethylamino)naphthalene
q	Quartet
rt	Room temperature
s	Singlet
S_0	Ground state
S_1	First excited state
S_2	Second excited state
S_NAr	Nucleophilic aromatic substitution
SPPS	Solid phase peptide synthesis
t	Triplet
TBAF	Tetra-*n*-butylammonium fluoride
Tf	Triflyl
TFA	Trifluoroacetic acid
THF	Tetrahydrofuran
TICT	Twisted intramolecular charge transfer
TLC	Thin layer chromatography
TMS	Trimethylsilyl
TPPTS	Triphenylphosphine-3,3',3''-trisulfonate
Trp	Tryptophan
TrpB	Tryptophan synthase *β*-subunit
Ts	Tosyl
UV	Ultraviolet
Vis	Visible
ε	Molar attenuation coefficient
λ_{abs}	Absorbance maximum
λ_{em}	Emission maximum
φ	Fluorescence quantum yield

1.0 Introduction

Fluorophores have played a critical role in biological research in recent decades, with fluorescence spectroscopy allowing for the visualisation of biological and biochemical processes.[1] Small molecule fluorophores have been used to image cells and study the processes within them, due to their inexpensive nature and ease of use, as well as their ability to be tuned for specific applications.[2] Simple modifications to common small molecule fluorophores can provide probes with specific emission wavelengths and differing behaviours depending on environment.[3] As well as the common naturally occurring fluorophores and derivatives thereof, significant work has been undertaken in the design of novel fluorophores based on an understanding of how the structures of organic molecules impact the resulting fluorescence properties.[1]

Proteins and peptides play a crucial role in many biological processes, however the lack of intrinsic fluorescence of these structures limits the ability of fluorescence spectroscopy to visualise them.[4,5] To overcome these limitations, protein labelling has been successfully employed, allowing both visualisation and studies of crucial processes such as enzyme activity, protein interactions and ligand induced conformational changes.[6,7] Such strategies for protein labelling include the use of naturally fluorescent proteins such as green fluorescent protein (GFP) or the use of self-labelling tags (such as HALO tags). While these approaches allow for the imaging of proteins and peptides, and have provided valuable insight into biological processes, often such modifications involve a large conformational or structural change to the protein structure of interest. These modifications can thus disrupt the natural function and reactivity of the protein or peptide and subsequently alter the biomolecular properties of the target. Some naturally occurring amino acids which contain aromatic groups exhibit fluorescent properties, however imaging of proteins and peptides using these compounds is limited.[8] These limitations are a result of the poor photophysical properties of most of these amino acids, and due to the fact that the presence of multiple residues within a peptide or protein may complicate spectroscopy. As an alternative, small fluorescent probes appended to an amino acid side-chain, which can thus be incorporated into a peptide or protein have been developed.[9] Owing to their relatively small size, these probes may be incorporated with minimal disruption to protein structure. These fluorescent amino acids can be

incorporated efficiently into peptides by methodology such as solid phase peptide synthesis (SPPS) or into larger protein structures by genetic encoding.[4]

1.1 Fluorescence in Organic Compounds

Fluorescence in organic compounds occurs as a result of conjugated π systems. Absorption of a photon of light at a specific wavelength allows for excitation of a π (HOMO) electron into a π* (LUMO) orbital - thus creating an excited state of the molecule.[10] Frequently, this involves excitation to the first or second excited state (S_1 or S_2) energy levels. Each of these levels is made up of various vibrational and rotational states, and any of these states may be occupied, as often represented in a Jablonski diagram (**Figure 1**). However, before the emission of light from a fluorophore, the molecule will usually relax to the lowest available vibrational state of the S_1 energy level. This process occurs by internal conversion, which due to a very short timespan (10^{-12} s), is almost always complete before emission can occur. The initial excited state of the molecule is also known as the excited singlet state (S_1'), which after undergoing conformational changes relaxes into a lower energy singlet state (S_1).

Fluorescence occurs when a molecule reverts to the ground state (S_0) from the lowest energy S_1 state. This return to the ground state releases a photon of lower energy (longer wavelength) than initially absorbed. The difference in energy between the wavelength absorbed and the wavelength emitted can be attributed to the different solvation states of the ground state and excited state molecules,[2] as well as conformational changes or other radiative decay processes leading to the dissipation of energy before the electron can relax to the ground state.[11] The molecule may initially relax to any of the vibrational levels of S_0, followed by rapid thermal conversion to the lowest vibrational level. It is worth noting that during fluorescence, this emission from the S_1 state is an allowed transition, due to spin pairing of the excited electron with that of the ground state electron. As a result, fluorescence lifetimes are often short (10^{-9} s).
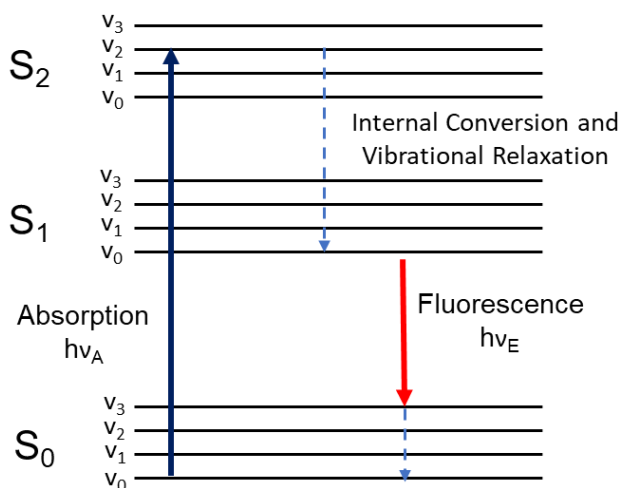
Figure 1: Jablonski Diagram showing absorption of a photon of light and subsequent internal conversion and emission processes.

The emission spectrum of a compound is often the mirror image of its absorption spectrum.[10] This results from the absorption of photons which excite a molecule to any of the available vibrational levels of the S_1/S_2 excited states. Following relaxation to the lowest energy S_1 state, emission of a photon may occur to relax the molecule to any of the S_0 vibrational states. The vibrational energy level spacing of a molecule is not altered significantly by the excitation, and so vibrational energy level gaps are similar in both the ground state and excited state, resulting in analogous spectra. Generally emission spectra will be the mirror image of the absorption shown for the S_0–S_1 absorption, but without a band corresponding to S_0–S_2 absorption, as no emission occurs from this level. This clear structural detail in a UV-Vis spectrum of vibrational transitions is often observed in more rigid compounds, such as anthracene (**Figure 2**). However, in compounds which are more flexible, a large number of rotational energy levels often results in a broadening of absorption and emission peaks.
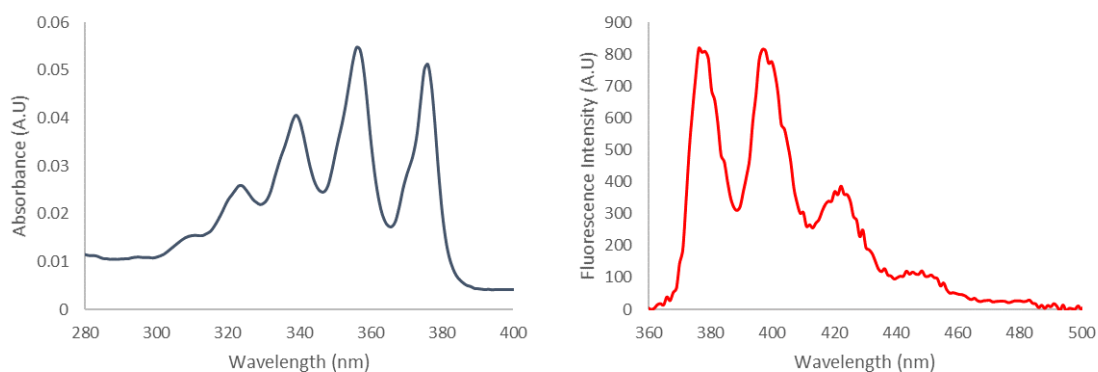
Figure 2: *Absorbance and emission spectra for anthracene. Measured at 10 µM in ethanol.*

Another consequence of the almost immediate relaxation of the molecule to the lowest available energy S_1 state, is a phenomenon known as Kasha's rule.[12] Kasha's rule dictates that emission spectra are usually independent of the excitation wavelength. There are exceptions to the rule, which include molecules which exist in two ionisation states, and those which emit from the S_2 level (although this is rare).

In addition to the wavelength at which a fluorophore absorbs and emits light, there are several parameters which are useful to summarise the properties of a fluorophore.[1] These include Stokes shift, quantum yield, molar attenuation coefficient and brightness. The difference in wavelength between the absorption maximum (λ_{abs}) and emission maximum (λ_{em}) of a compound is known as the Stokes Shift. A large Stokes Shift is a beneficial property in a fluorophore, as it minimises reabsorption of emitted light. The molar attenuation coefficient (ε) is a measure of how strongly a molecule absorbs light at a given wavelength (usually reported at λ_{abs}). The fluorescence quantum yield (ϕ) is a ratio of the number of photons emitted to those absorbed. As such, it is a measure of decay by emission, rather than by other non-radiative decay processes, and the closer to unity this value, the brighter a fluorophore is likely to be. Multiplication of the quantum yield and molar attenuation coefficient ($\phi \times \varepsilon$) gives the brightness value of the fluorophore.

1.1.1 Tuning the Properties of Small Molecule Fluorescent Probes

A range of small molecule fluorescent probes have been designed for use in fluorescence imaging. A large majority of fluorophores used to date are results of modifications to a set of "core" scaffolds.[1] Among the smaller of these examples are structures based upon well-defined fluorophores, such as quinoline, coumarin or styrene scaffolds (**Figure 3**). These small scaffolds generally show absorption maxima below 400 nm, and emission maxima around 450 nm, with precise values depending on the nature of substituents present.
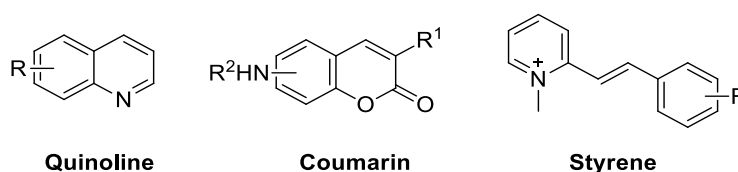
Figure 3: Small 'core' scaffolds frequently found in fluorophores. R groups indicate common sites of functionalisation.

Frequently, when designing fluorophores, substituents are modified in a way which allows for charge transfer across the molecule (**Scheme 1**).[1] For example, where an electron withdrawing group is present in the core scaffold, electron donating groups may be added in order to provide a donor-π-acceptor moiety. This framework results in intramolecular charge transfer (ICT) which is known to produce favourable photophysical properties such as red shifted UV-Vis and emission spectra. For biological imaging, chromophores which can be excited at longer wavelengths are generally favoured to avoid damage to biological samples.[13] In particular, wavelengths above 300 nm are required to avoid certain biological damage, however much longer wavelengths are preferable for many biological applications.
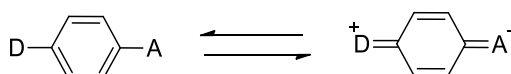
Scheme 1: Intramolecular charge transfer resulting from a donor-π-acceptor framework in organic fluorophores.

Another approach to red-shift the absorption and emission spectra of a compound is to increase π-conjugation.[1] As a result of this, larger "core" scaffolds containing more aromatic rings generally have higher absorption and emission maxima. Such scaffolds include fluorescein, BODIPY, naphthalimide and rhodamine structures

(**Figure 4**). These larger dyes generally display absorption maxima between 450 nm and 500 nm, with slightly higher emission maxima of 510–550 nm, however this again depends on the nature of the substituents present.
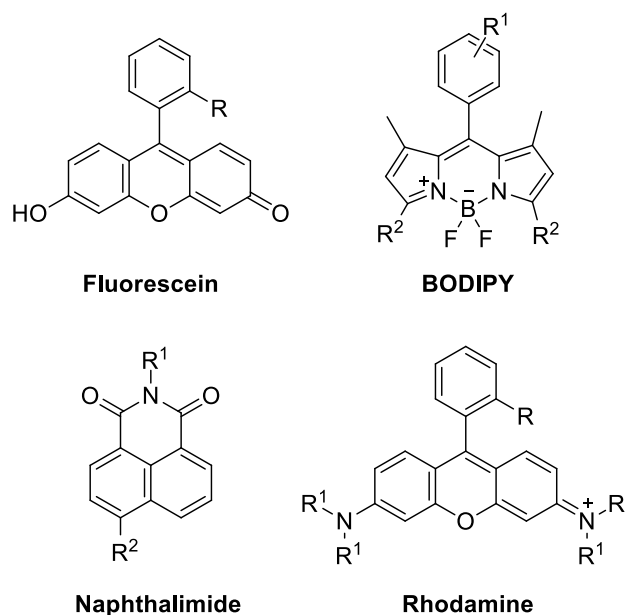
Figure 4: *Core scaffolds of fluorescein, BODIPY, naphthalimide and rhodamine fluorophores. R groups represent common sites of functionalisation.*

This increase in π-conjugation may also be achieved by the addition of alkenyl or alkynyl groups into a fluorophore, and such extended linear conjugation also has the effect of red-shifting the absorption maximum.[14] For example, in work by Michl and co-workers, the inclusion of a styryl unit was shown to shift the absorption maximum of a fluorophore centred around a 4,5-dicyanoimidazole unit from 279 nm to 334 nm (**Figure 5**).[15]
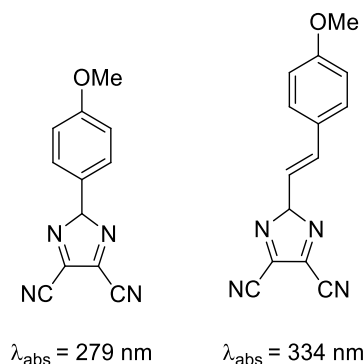
Figure 5: *Inclusion of an alkenyl group into 4,5-dicyanoimidazole based fluorophores.*

The replacement of heteroatoms with group 14 elements such as tin, germanium or silicon has also been shown to improve the photophysical properties of fluorophores.[16] For example, the inclusion of these atoms into a xanthene structure allowed for a bathochromic shift in absorbance spectra when compared to the oxygenated parent compound (**Figure 6**). This was proposed to be a result of LUMO stabilisation through the $\sigma*-\pi*$ conjugation between $\sigma*$ orbitals (Si-C, Ge-C, or Sn-C) and a $\pi*$ orbital of the fluorophore.

λ_{abs} = 547 nm

λ_{abs} = 614 nm

λ_{abs} = 621 nm

λ_{abs} = 634 nm
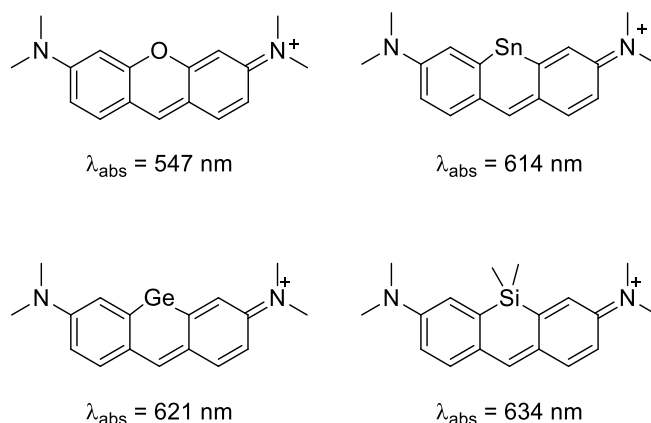
Figure 6: Modification of xanthene structures with group 14 elements.

Another example of the effect of altering a bridging group was shown by Vendrell and co-workers in a series of small fluorophores based on a 7-chloro-4-nitrobenzo-2-oxa-1,3-diazole (NBD) structure.[17] These SCOTfluors (Small, Conjugatable, Orthogonal, Tunable) demonstrated emission across the visible spectrum due to different bridging groups (**Figure 7**). In particular, the Se and C bridged derivatives displayed red and NIR emission respectively, which was proposed to be a result of a reduced HOMO-LUMO gap.

| λ_{abs} = | 420 nm | 476 nm | 510 nm | 546 nm | 564 nm |
| λ_{em} = | 460 nm | 548 nm | 606 nm | 650 nm | 650 nm |
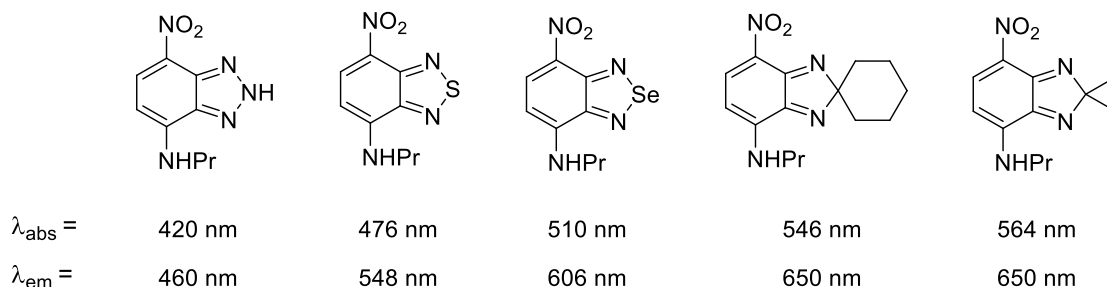
Figure 7: SCOTfluors, with different bridging groups.

Bright fluorophores are frequently desired for biological imaging.[18] A general method for improving the brightness or quantum yield of fluorophores is to restrict bond

rotation.[1,19,20] Usually, fluorophores with a more rigid structure display a larger quantum yield and subsequent brightness. This is a result of the limited number of rotational de-excitation pathways, and greater π overlap due to conformational restrictions. For example, the rigidification of cyanine **1** to give polycyclic analogue **2** resulted in a remarkable increase in quantum yield from 0.15 to 0.69 (**Figure 8**).[21] A consequence of restricting the rotation available to a molecule, however, is a reduction in the Stokes shift, which may result in reabsorption of emitted light.[10]

1
λ_{abs} = 638 nm
λ_{em} = 657 nm
ϕ = 0.15

2
λ_{abs} = 662 nm
λ_{em} = 677 nm
ϕ = 0.69
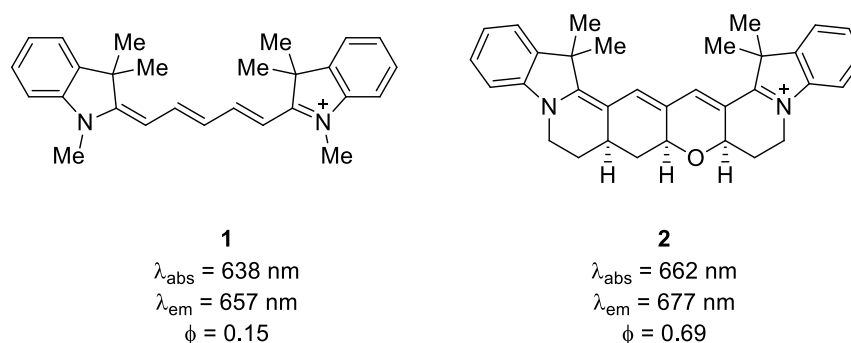
***Figure 8**: The rigidification of cyanine **1** and resulting increase in quantum yield.*

Another example of restricted bond rotation resulting in an increase in quantum yield was observed in the general strategy of replacing dimethylamino groups with azetidine rings.[19] This exchange was reported to increase the rotational barrier around the C-N bond and thus eliminate quenching through twisted intramolecular charge transfer (TICT). In 2017, Lavis and co-workers investigated the replacement of dialkylamino groups in rhodamines with azetidine rings, and showed that replacement allowed for an increase in quantum yield of 0.41 to 0.88 (**Figure 9a**).[22] This strategy was shown to be general, with application to other fluorophores, including coumarins, also allowing for a large increase in quantum yield (**Figure 9b**).

a)

λ_{abs} = 548 nm
λ_{em} = 572 nm
ϕ = 0.41

λ_{abs} = 549 nm
λ_{em} = 571 nm
ϕ = 0.88

b)

λ_{abs} = 372 nm
λ_{em} = 470 nm
ϕ = 0.19

λ_{abs} = 354 nm
λ_{em} = 467 nm
ϕ = 0.96
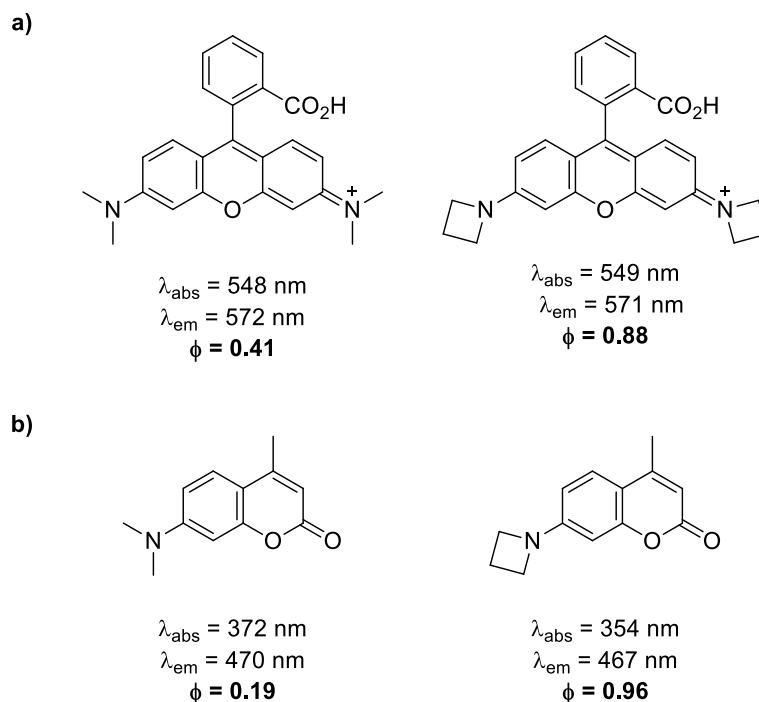
Figure 9: The influence on quantum yield of replacing a dimethylamino group with an azetidine ring. Fluorescence properties measured in aqueous solution.

1.1.2 Environmentally Sensitive Fluorophores

In addition to being used in simple imaging techniques, fluorophores may also report on environmental changes. For example, certain fluorophores exhibit enhanced brightness, quenching, or a change in emission wavelength upon exposure to different environments. Such environmental changes can include a change in polarity (usually indicated by solvatochromism),[23] pH or viscosity.[24,25] Probes which exhibit a change in photophysical properties upon exposure to cations have also been developed, allowing for the detection of cations, such as calcium within cells.[26]

Solvatochromism is a good indicator of the environmental sensitivity of a fluorophore, as it is directly proportional to the response of the fluorophore to a general polarity change.[10,23] Typically, a fluorophore has a larger dipole moment in the excited state than in the ground state. As this excited state is increasingly stabilised by increasingly polar solvents, the excited state energy is lowered and emission wavelength becomes red-shifted.[10] This effect is most pronounced for fluorophores which contain a considerable dipole, and a result of this is that compounds which display charge-transfer properties are often highly solvatochromic. Nonpolar compounds are generally much less sensitive to solvent polarity. This response to environmental polarity may be described in simple terms

by the Lippert-Mataga equation (**Equation 1**).[27] As most of the parameters in this equation are constant, it is possible to plot a graph of Stokes shift (v_A–v_F) versus orientation polarisability (Δf) for a fluorophore.[10] This may be used to gain information about the dipole across the compound (μ_E–μ_G)^2 where μ_E and μ_G are the excited state dipole and ground state dipole respectively.

$$\dot{v}_A - \dot{v}_F = \frac{2\Delta f}{hca^3}(\mu_E - \mu_G)^2 + k$$

Equation 1: Simplified Lippert-Mataga equation. Where h= Planck's constant (6.6256×10^{-34} m^2 kg s^{-1}), c = speed of light in a vacuum (2.997×10^8 m s^{-1}), a is the radius of the cavity in which the fluorophore resides, $\bar{v}_A$ and $\bar{v}_F$ are the wavenumbers (cm^{-1}) of absorption and emission respectively. Δf is the orientation polarisability of the solvent.

In this equation, Δf is the orientation polarisability of the solvent (**Equation 2**). This is dependent upon the dielectric constant of the solvent, as well as the solvent refractive index.

$$\Delta f = \frac{\varepsilon - 1}{2\varepsilon + 1} - \frac{\eta^2 - 1}{2n^2 + 1}$$

Equation 2: The orientation polarisability of a solvent, where ε is the solvent dialectric constant and n is the solvent refractive index.

As the Lippert-Mataga equation is only an approximation, it does not take into account the shape of the fluorophore or any specific solvent interactions. As such, deviations from this equation may be used to indicate specific solvent effects, such as hydrogen bonding, preferential solvation, and charge-transfer interactions. For example, a Lippert-Mataga plot for spiro compound **3**, showed deviations from a straight line in protic solvents, which indicated specific solvent-fluorophore interactions were present (**Figure 10**).[28] More complex equations have since been developed which account for some of these parameters, but the Lippert-Mataga equation continues to allow for a simple visualisation of general and specific solvent effects.[10]
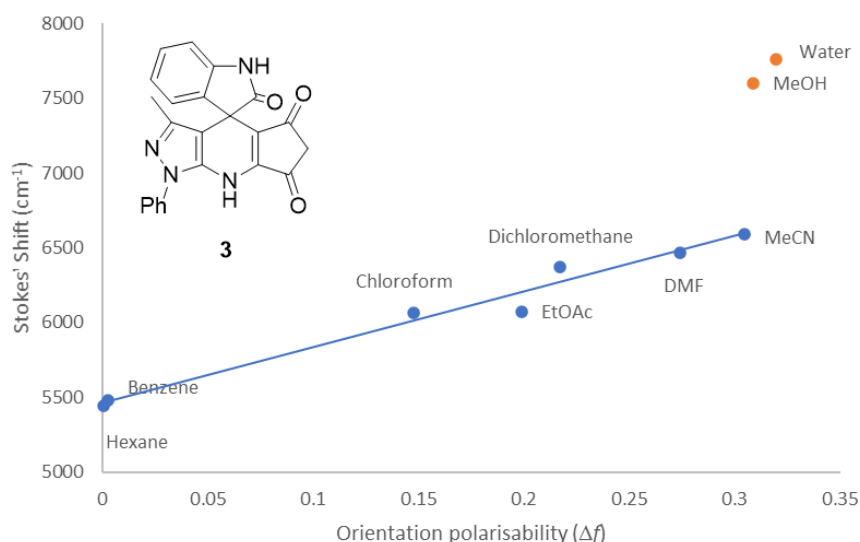
Figure 10*: Lippert-Mataga plot showing the solvent sensitivity of spiro analogue **3**. Graph reproduced from publication by Khurana and co-workers.*[28]

Two solvatochromic fluorophores were recently described by Nagy and co-workers, in their work on isocyanoanthracene dyes.[29] A comparison between diaminoanthracene **4** and 1-amino-5-isocyanoanthracene **5** showed that cyano analogue **5** demonstrated a larger shift of wavelength in solvents of different polarities (**Figure 11**). The difference in emission maxima between the least polar solvent hexane, and most polar solvent, DMSO, for diamino analogue **4** was 36 nm, whereas for cyano analogue **5** a shift of 49 nm was observed. This was proposed to be because this analogue displayed more "push-pull" characteristics typical of ICT fluorophores, with an electron-donating amino group and electron-withdrawing cyano group which create a dipole across the compound.

4
λ_{em}(hexane) = 475 nm
λ_{em}(DMSO) = 511 nm

$\Delta\lambda_{em}$ = 36 nm

5
λ_{em}(hexane) = 527 nm
λ_{em}(DMSO) = 576 nm

$\Delta\lambda_{em}$ = 49 nm
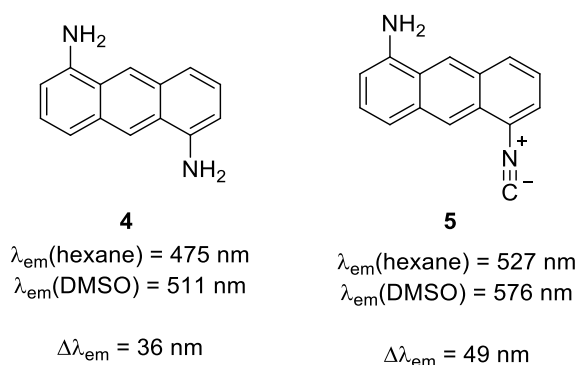
Figure 11*: Solvatochromic properties of diaminoanthracene **4** and 1-amino-5-iosocyanoanthracene **5**.*

Fluorophores which display pH sensitivity often contain a heteroatom which is capable of either being protonated in an acidic environment or deprotonated in a basic environment.[30] These changes can alter the resulting photophysical properties of the fluorophore. As the pH across cellular environments can vary from as low as 4.5 in lysosomes up to 8.0 in the mitochondria, and pH changes are frequently involved in biological processes, fluorophores which can detect such changes are valuable tools.[31]

For many probes, a change in quantum yield or complete fluorescence quenching results from a change in pH.[30] However in rarer cases, such as reported by Ihmels and co-workers in 2004, a change in pH may result in a shift in absorption and emission wavelength.[32] As quenching may also be caused by other external factors, a change in wavelength can be a more reliable indicator of pH change. Among the fluorophores synthesised by the group was pyridine analogue **6** (**Scheme 2**). It was shown that upon the addition of acid, the emission maximum of this analogue shifted from 443 nm to 540 nm because of the increased charge transfer across the chromophore.

6
λ_{em} = 443 nm λ_{em} = 540 nm
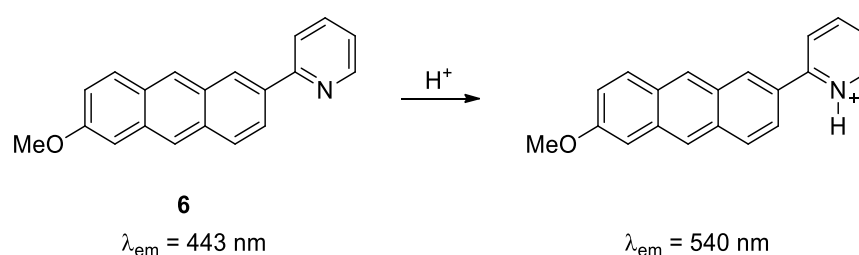
Scheme 2: *Protonation of pyridine **6** and subsequent shift in emission maximum.*

Finally, an emerging area of interest with regards to environmentally sensitive fluorophores are molecular rotors. This term is used to describe fluorophores which can twist in the excited state. Many such fluorophores have found use as viscosity sensors.[33] The formation of a TICT state upon photoexcitation gives a low energy excited state which has the possibility to decay either through a radiative (and usually red-shifted) emission pathway (**Figure 12**) or through non-radiative decay.[24,33,34] When the non-radiative decay pathway is favoured, fluorescence quenching is observed, and so many methods for reducing TICT in fluorophores have been devised.[19] However, when a TICT state shows radiative decay, the resulting red-shifted emission may be considered a beneficial property.
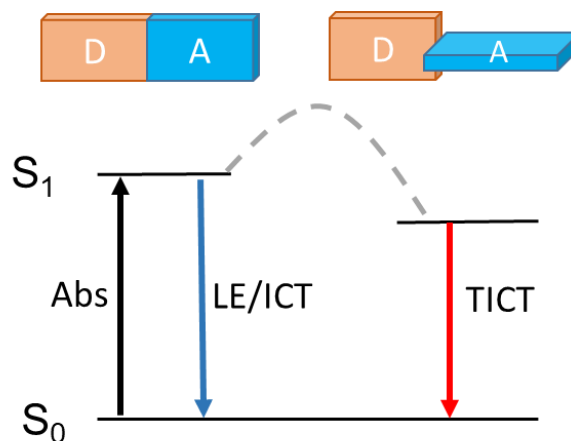
Figure 12: Formation of a TICT state.

For molecular rotors which emit from the TICT state, exposure to a higher-viscosity solvent may result in a blue-shifted emission being observed as the fluorophore is forced to emit from the planar (LE or ICT) state.[24] As such, a blue-shift in emission maxima may be used to indicate an environment of high viscosity when fluorophores which exhibit TICT are used. The first observation of TICT was in the emission spectra of 4-(dimethylamino)benzonitrile (DMABN), whereby an unexpected red-shifted peak appeared in more polar solvents. It was ultimately discovered that this was due to stabilisation of the TICT state (**Scheme 3**).
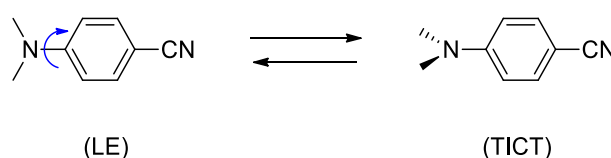
Scheme 3: TICT observed in DMABN.

1.2 Fluorescent Amino Acids

Imaging of proteins and peptides is often difficult due to limited localisation of probes into the site of interest, and as such, the development of fluorescent amino acids is of great interest.[4] The use of small molecule fluorophores as amino acid side-chains has allowed for the imaging of peptides and proteins.[35] Small fluorophores are beneficial to avoid disruptions to natural protein folding and conformations, although some flexibility in fluorophore size may be exerted depending on the application. Fluorophores which are larger than naturally occurring amino acids are frequently required to achieve the desired photophysical properties. Fluorescent amino acids have been designed for numerous applications, allowing for a large range of choice

when selecting an amino acid for imaging purposes.[9,36] However, there is no "one size fits all" fluorophore and new efficient methods for the synthesis of known fluorescent amino acids, as well as the discovery of novel fluorescent amino acids, are consistently of interest to widen the toolbox of available fluorophores.

Tryptophan, tyrosine and phenylalanine are three naturally occurring amino acids which show fluorescent properties (**Figure 13**), and some imaging of proteins and peptides using these amino acids has been possible.[37] However, their optical properties are suboptimal for most biological imaging purposes. Both tyrosine and phenylalanine demonstrate low attenuation coefficients. Tryptophan is the most fluorescent of these amino acids, however, it absorbs and emits light within the UV range and shows a low photostability, which make it a poor fluorescent probe, particularly for *in vivo* applications. Additionally, the presence of multiple residues within a protein can complicate fluorescence spectroscopy. The need for small fluorescent probes similar in size to these amino acids, as well as their intrinsic fluorescent properties, however, makes them a good starting point for further modifications.

L-Tryptophan
λ_{abs} = 279 nm
λ_{em} = 365 nm
ε = 5.58 × 10^3 M^{-1} cm^{-1}
Φ = 0.01–0.4

L-Tyrosine
λ_{abs} = 275 nm
λ_{em} = 310 nm
ε = 1.41 × 10^3 M^{-1} cm^{-1}
Φ = 0.14

L-Phenylalanine
λ_{abs} = 258 nm
λ_{em} = 282 nm
ε = 0.20 × 10^3 M^{-1} cm^{-1}
Φ = 0.024
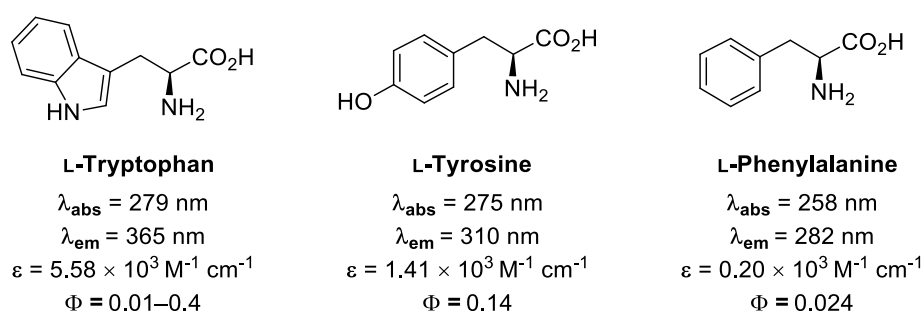
Figure 13*: Naturally occurring fluorescent amino acids, L-tryptophan, L-tyrosine and L-phenylalanine.*

1.2.1 Fluorescent Probes based on Natural Amino Acids

Among the smallest of fluorescent probes produced by the modification of a naturally occurring fluorescent amino acid are a range of cyanotryptophan analogues.[4] In particular, 4-cyanotryophan **9** described by Hilaire and co-workers showed good all-round photophysical properties.[38] The probe showed an absorbance at 325 nm (red-shifted relative to native tryptophan), emission maximum at 405 nm in methanol, and a large quantum yield (0.8). Unfortunately, the route to 4-cyanotryptophan was limited by the high cost starting material **7**. Protection with

toxic TMS-diazomethane was then required, which, after Boc-protection, gave **8** in 48% yield. This was followed by a low yielding Pd-catalysed cyanation step, which gave product **9** (**Scheme 4**).
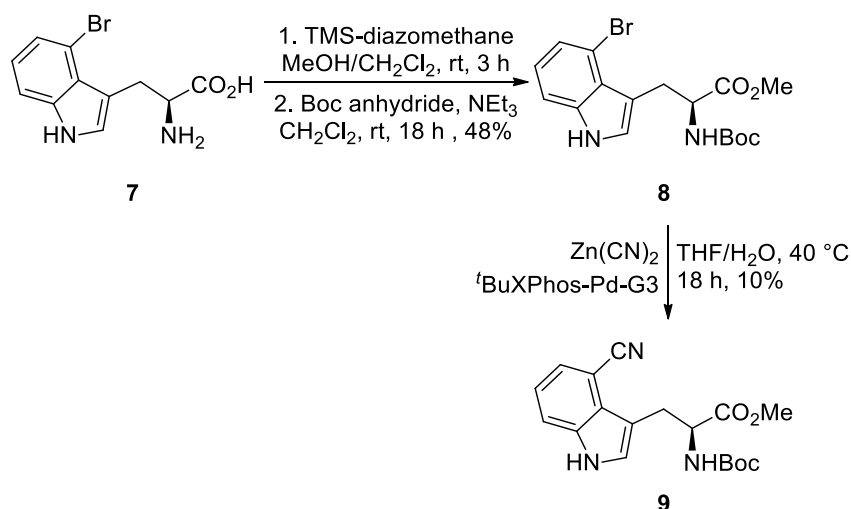
Scheme 4: *Initial synthetic route to protected 4-cyanotryptophan **9**.*

Following the initial report of 4-cyanotryptophan as a useful fluorescent probe, alternative syntheses have been reported. Of these, many have proven low yielding or only provided access to the racemic compound.[39,40] One of the more successful syntheses required the use of a genetically modified enzyme, limiting this approach to labs with expertise in protein expression.[41] In 2019, however, a more accessible approach was reported by Zhang and co-workers (**Scheme 5**).[42] The route started from 4-cyanoindole **10**, which was subjected to a previously well documented three-step procedure (a Mannich reaction, followed by alkylation and reduction)[43] to give racemic amine **11**. This allowed for production on a multi-gram scale. Acetylation of **11**, followed by hydrolysis with lithium hydroxide gave carboxylic acid **13**. Enzymatic hydrolysis of racemic *N*-acyl amino acid **13**,[44] using *Amano acylase* gave L-amino acid **14** in >99% ee. Finally, Fmoc protection of the compound was achieved under standard conditions to produce **15** in 62% of the theoretical yield over 2 steps.
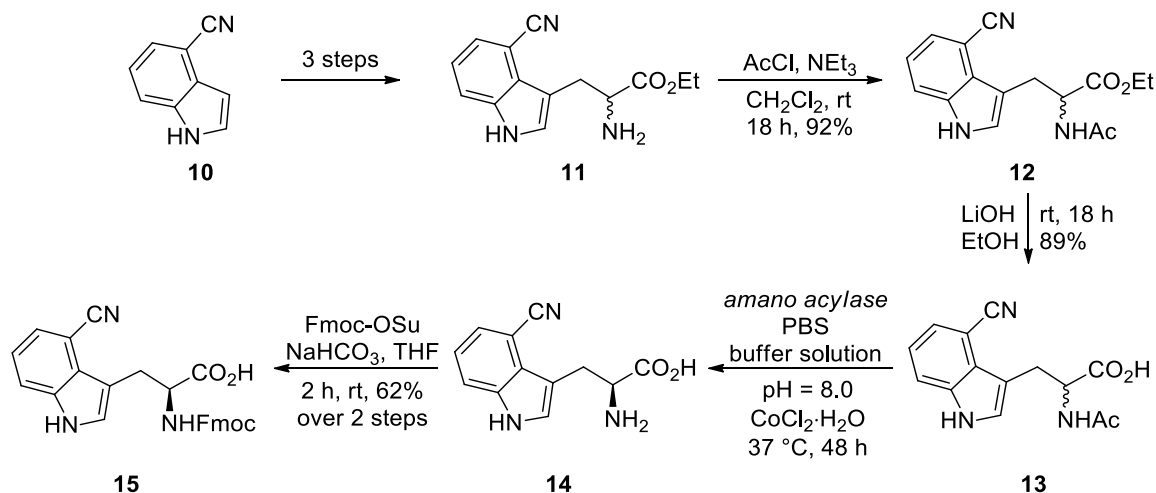
Scheme 5: *Synthesis of 4-cyanotryptophan **15** as reported by Zhang and co-workers, starting with 4-cyanoindole **10**.*

In 2021, a novel route towards 4-cyanotryptophan **14** using a non-enzymatic strategy was described.[45] This route exploited an asymmetric phase-transfer alkylation of **16** (**Scheme 6**). Precursor **16** was initially synthesised in 64% yield over four steps from 4-cyanoindole **10**, via a Vilsmeier-Haack formylation, followed by Boc-protection, reduction of the aldehyde and subsequent bromination. It was noted that these steps were achieved in high purity without the need for column chromatography. Subsequently, the phase-transfer alkylation step was investigated through reaction of **16** with glycine derived imine **17**, in the presence of phase transfer catalyst **18**. Reaction conditions were based on literature precedent for the phase-transfer alkylation of the equivalent 4-iodoindole analogue.[46] The conversion to imine **19** proceeded smoothly, with 77% yield and >98% ee, on a 10 g scale. Hydrolysis of the resulting imine **19** and deprotection gave deprotected 4-cyanotryptophan **14** in 91% yield over two steps.
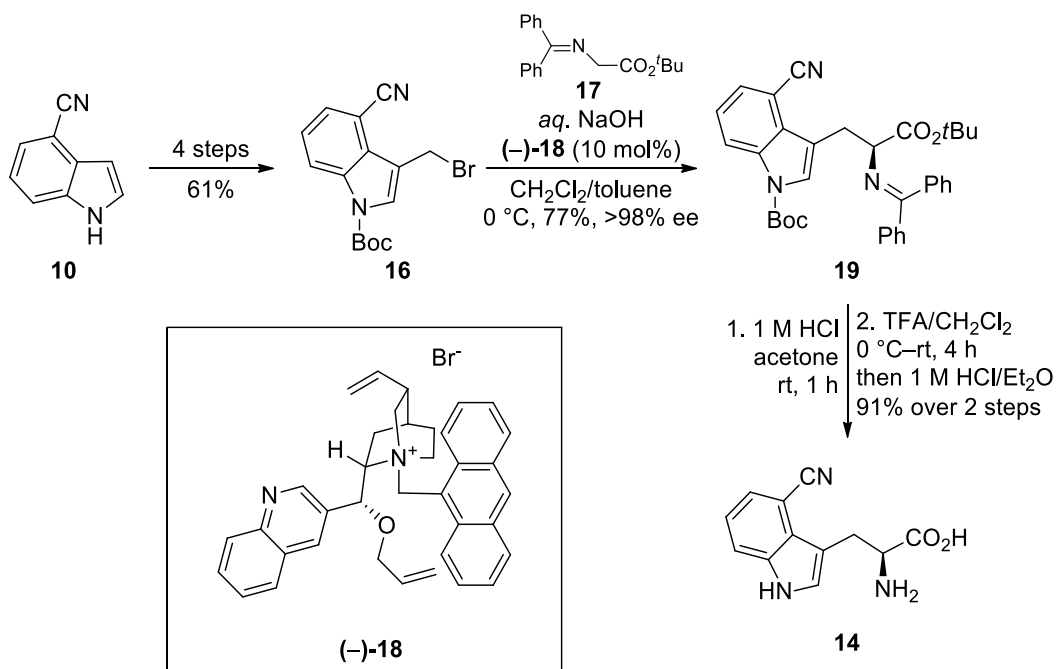
Scheme 6: *Synthesis of 4-cyanotryptophan 14 via phase-transfer alkylation.*

As well as 4-cyanotryptophan, other small molecule analogues of tryptophan have been described. In one example, replacement of the indole ring by an azulene ring was reported.[47] This isostere, β-(1-azulenyl)-L-alanine (AzuAla), was shown to be incorporated into proteins in place of tryptophan without disruption of protein structure and function (**Figure 14**).[48] AzuAla did not demonstrate any environmental sensitivity, which can be advantageous in ensuring the fluorophore's emission profile is simple to analyse.[48] This analogue was reported to demonstrate distinct absorption bands compared to tryptophan, and can be excited at 342 nm, while maintaining a similar brightness.

Tryptophan
λ_{abs} = 279 nm
λ_{em} = 365 nm

AzuAla
λ_{abs} = 340 nm
λ_{em} = 380 nm
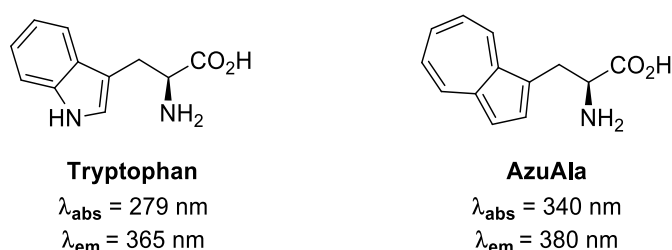
Figure 14: *Structures of tryptophan and AzuAla.*

Previously reported syntheses of AzuAla have proven time sensitive and required precious metal catalysts,[49] whereas the route recently presented by Arnold and co-workers used an engineered enzyme, TrpB.[50] While the native TrpB enzyme performs a conjugate addition reaction between indole and serine to make

tryptophan, in this work, the enzyme was used to perform the same reaction, with an azulene ring as the nucleophile (**Scheme 7**). Directed evolution was used to produce a biocatalyst which was able to produce AzuAla in 57% yield, and in >99% ee. Crude azulene from the reaction was isolated and reused in order to maximise efficiency.
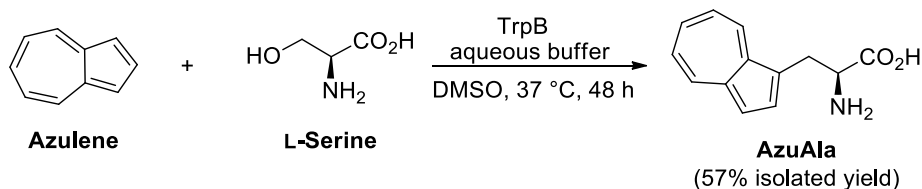
Scheme 7: *Enzymatic synthesis of AzuAla*

The expansion of the tryptophan moiety by additional conjugation was reported by Sewald and co-workers, who prepared a series of compounds by coupling of 7-bromotryptophan **20** with styryl residues via a Heck reaction (**Scheme 8**).[51] This reaction was reported to work in aqueous conditions with unprotected 7-bromotryptophan **20** (initially produced by biocatalytic bromination of L-tryptophan).[52] Palladium acetate was used for the Heck cross-coupling reactions in the presence of water-soluble phosphine ligand triphenylphosphine-3,3',3''-trisulfonate (TPPTS) and potassium carbonate. While the reaction with the water-soluble 4-carboxystyrene occurred in water, a dioxane/water co-solvent mixture was used for the coupling of other, less water-soluble styrenes with bromotryptophan **20**. Amongst the synthesised analogues, the trifluoromethyl analogue was found to have the most red-shifted absorption and emission spectra, with an absorption maximum of 371 nm and emission maximum of 448 nm. This was proposed to be a result of ICT between the electron donating nitrogen of the indole ring and electron withdrawing trifluoromethyl group. All of the coupled products were shown to have bathochromically shifted absorption and emission wavelengths when compared to aryl analogues previously produced by the group *via* Suzuki-Miyaura cross-coupling reactions.[53] These novel stretched, styrene analogues showed the positive impact of the incorporation of additional conjugation.

R = 4-CO$_2$H, **51%***
R = 3-F, **66%**
R = 4-CF$_3$, **70%**
R = 4-OMe, **64%**
R = 3-NO$_2$, **30%**
R = H, **28%**

* Solvent = H$_2$O
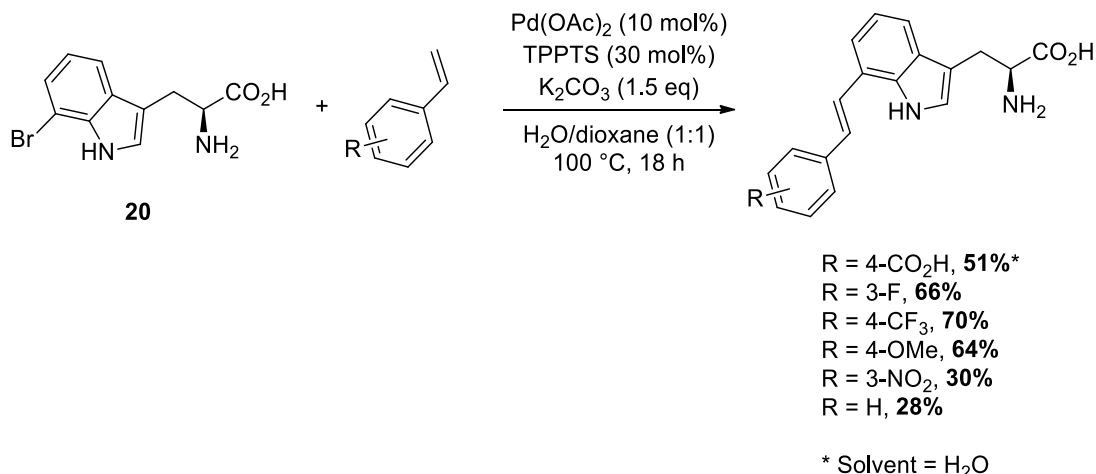
Scheme 8: *Heck reaction of 7-bromotryptophan **20**.*

Other naturally fluorescent amino acids, such as tyrosine have also been used as a starting point for modifications to produce fluorescent probes. One example of this was shown by Wang and co-workers (**Scheme 9**).[54] As above, a Heck cross-coupling reaction was used in order to increase conjugation of the amino acid. Both mono- and di-styryl substituted analogues were synthesised from mono-iodinated tyrosine **21** and di-iodinated tyrosine **22**, respectively. The extended analogues showed a red-shift in absorption and emission maxima relative to native tyrosine as a result of the extra conjugation. The most red-shifted of these analogues in both series was the nitro analogue, likely as a result of the electron donating character of the phenol moiety and the withdrawing character of the nitro group providing a push-pull system. However, the nitro analogue was strongly quenched in polar environments, and so the analogues featuring a pyridyl or pyridinium ring are more notable. These analogues had a strongly red-shifted absorption maximum (570 nm) and were not subject to quenching effects.
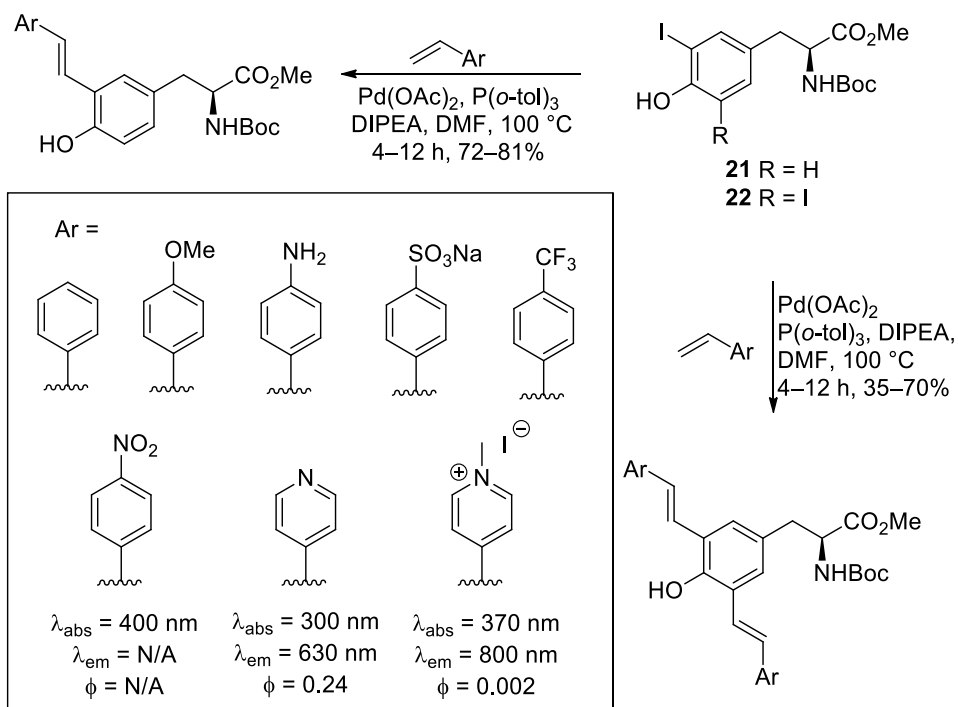
Scheme 9: Synthesis of extended tyrosine analogues. Selected fluorescence properties are shown for bis substituted analogues, measured in DMSO.

Investigative work was undertaken on di-substituted pyridyl analogue **23,** which contained two groups likely to be sensitive to pH changes – the pyridyl group and the phenol moiety (**Figure 15**). It was shown under acidic conditions that protonation of the pyridine led to a red-shift in emission maximum from 435 nm to 623 nm. This was likely a result of the increased electron-accepting nature of the pyridinium which in turn increased the charge-transfer across the fluorophore. A similar effect was observed under basic conditions, in which the phenol group was deprotonated to provide a stronger electron-donating effect, resulting in red-shifted emission maximum (from 435 nm to 535 nm).
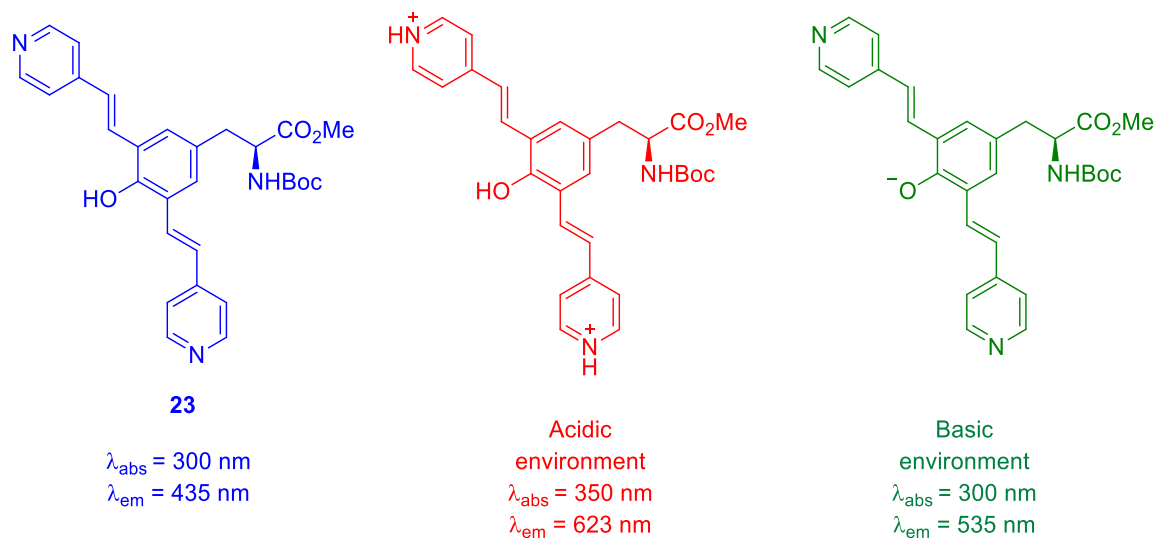
Figure 15: *The pH sensitivity of tyrosine derived amino acid **23**. Measured in acetonitrile with addition of p-toluenesulfonic acid to create an acidic environment and NaOH for a basic environment.*

1.2.2 Amino Acid Probes Incorporating Established Fluorophores

A range of established fluorophore scaffolds including coumarin, fluorescein, BODIPY, rhodamine and cyanine cores have been used for the design of fluorescent amino acids.[4] While these scaffolds each have applications as fluorescent probes, traditionally there are problems with the delivery of probes to sites of interest. Incorporating the fluorophores as side-chains of amino acids as a method of installing them into proteins is one way to overcome this issue.

The incorporation of a coumarin derived amino acid into a protein was demonstrated by the Schultz lab.[55] A 7-hydoxycoumarin moiety was chosen, as this scaffold shows a large Stokes shift, has a small size and demonstrated pH sensitivity. The fluorescent amino acid was synthesised in three steps from glutamic acid derivative **24**. Initially, **24** was reacted with *N,N'*-carbonyldiimidazole to form an acyl-imidazole intermediate (**Scheme 10**). This was used for coupling with ethyl magnesium malonate to give β-keto ester **25**. Subsequent reaction with 1,3-dihydroxybenzene in methanesulfonic acid gave 7-hydroxycoumarin product **26**. This analogue demonstrated an absorption maximum of 360 nm and emission maximum of around 450 nm, with a large brightness.
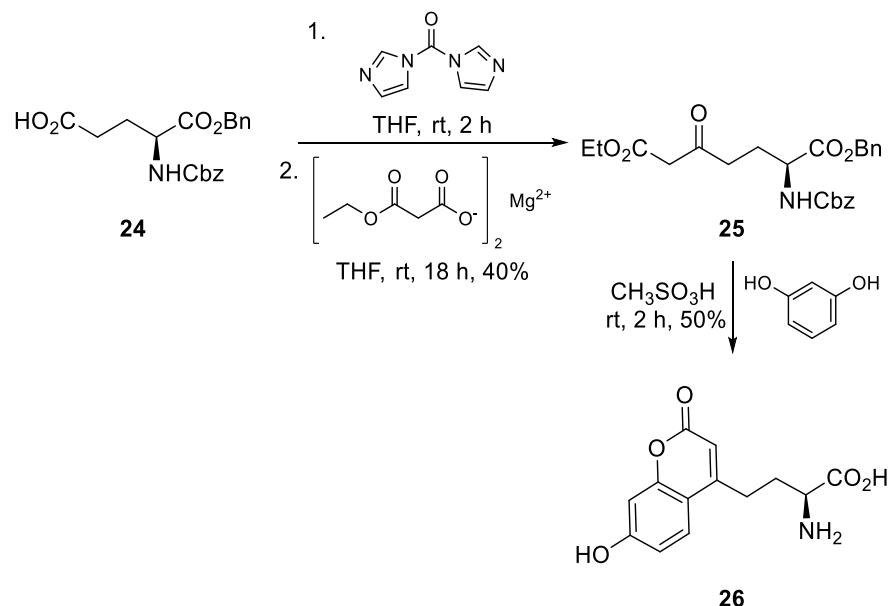
Scheme 10*: Synthesis of 7-hydroxycourmarin amino acid **26**.*

In 2021, novel coumarin derived amino acid **31** was synthesised, utilising a 7-dialkylaminocoumarin fluorophore (**Scheme 11**).[56] This amino acid showed strong environmental sensitivity, with an increase and blue-shift in fluorescence upon introduction to apolar environments. Through SPPS, this amino acid was incorporated into an analogue of a cyclic lipopeptide antibiotic. In the presence of liposomes, an increase in fluorescence was observed, and this peptide was used for the visualisation of bacteria. The synthesis of coumarin derived amino acid **31** began with commercially available coumarin **27**. Bromination with LiHMDS and *N*-bromosuccinimide (NBS) gave alkyl bromide **28**. The amino acid side-chain was next imparted through alkylation of the chiral nickel(II) glycine Schiff base complex **29** and subsequent decomposition of the complex through acidic hydrolysis gave free amino acid **30** in 97% enantiomeric excess. Finally, **30** was Fmoc-protected for compatibility with SPPS.
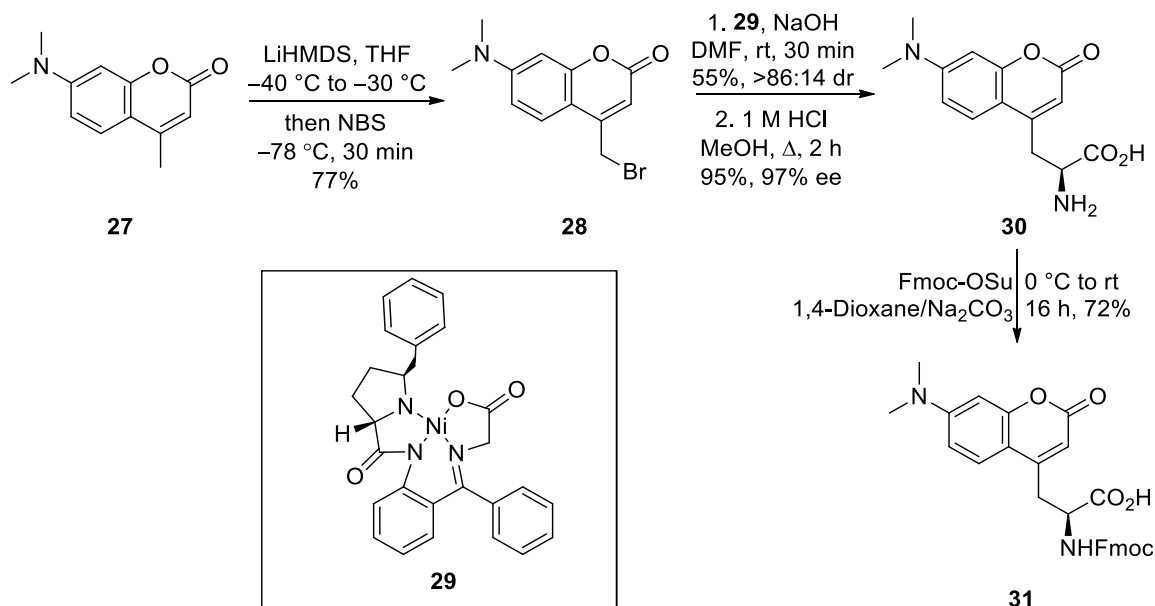
Scheme 11: *Synthesis of **31** using chiral nickel(II) glycine Schiff base complex **29**.*

In 2014, the synthesis of flavone based fluorescent amino acid **35** was described (**Scheme 12**), which demonstrated an absorbance maximum of 350 nm and dual emission bands at 440 nm and 520 nm in buffer solution.[57] The replacement of residues in an HIV-1 nucleocapsid peptide with this amino acid showed that peptide structure and function was preserved. In environments with restricted rotations, for example when stacked with nucleobases, long fluorescent lifetimes were observed, which were associated with an excited state intramolecular proton transfer. Two-photon fluorescence was used for imaging this fluorophore and allowed for the identification of the binding partners of the labelled peptides in living cells. The synthesis of this analogue was achieved in six steps starting with the acylation of tyrosine to give **32**. Subsequent Boc-protection gave **33**, and then aldol reaction with 4-methoxybenzaldehyde gave α,β-unsaturated ketone **34**. Finally, cyclisation under oxidising conditions followed by protecting group manipulation gave Fmoc-protected product **35**.
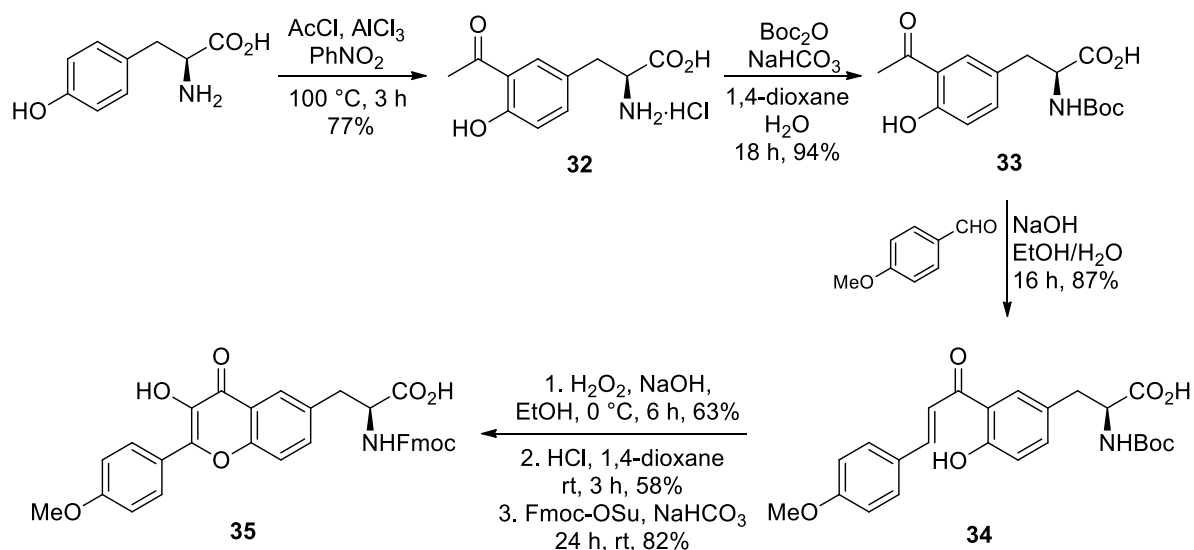
Scheme 12: *Synthesis of coumarin amino acid **35**.*

In addition to coumarins and flavones, BODIPY cores have been used as the side-chain of amino acids. The C-H activation of tryptophan has been shown as a viable method to attach BODIPY fluorophores to an amino acid scaffold (**Scheme 13**).[58] The reaction of iodinated BODIPY **36** with tryptophan in the presence of Pd(OAc)$_2$ and silver tetrafluoroborate under acidic conditions gave Trp-BODIPY **37** in 70% yield. This fluorophore demonstrated highly bathochromically shifted photophysical properties generally associated with BODIPY fluorophores (λ_{ab} = 500 nm, λ_{em} = 513 nm). Additionally, the incorporation of this fluorophore at the C2 position of tryptophan allowed for the amino acid to maintain the recognition features of the natural amino acid, including its hydrogen bonding pattern.
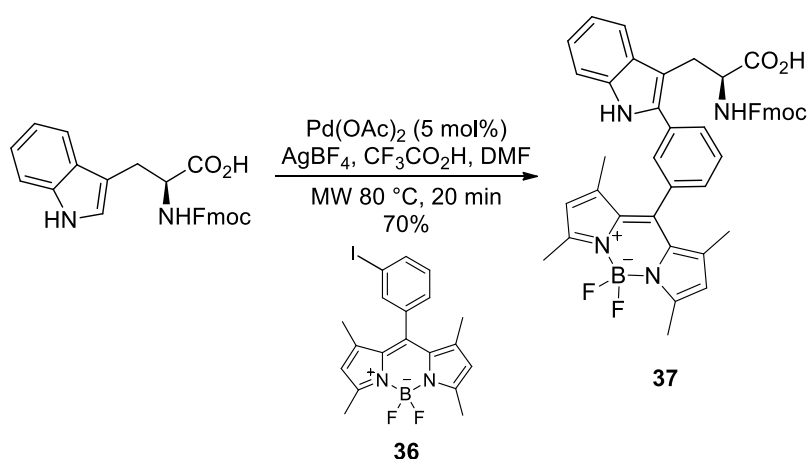
Scheme 13: *The C-H activation reaction of a BODIPY fluorophore with tryptophan.*

Building on this work, Vendrell and co-workers more recently produced the first tryptophan based red fluorogenic amino acid through the same method, using the C-H activation of tryptophan followed by attachment of red-BODIPY chromophore **38** at the C-2 position (**Scheme 14**).[59] This fluorescent amino acid was incorporated into a cyclic peptide, and it was shown that the photophysical properties of the red-BODIPY scaffold were maintained, with an absorption maximum of 520 nm and emission maximum of around 580 nm. This peptide was then used for live-cell and *ex vivo* imaging of KRT1+ cancer cells.
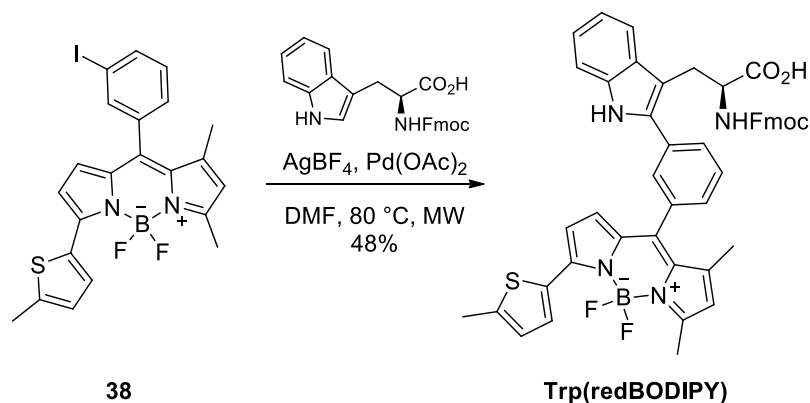
Scheme 14: *Synthesis of a red-BODIPY tryptophan amino acid.*

The fluorophore 6-propionyl-2-(dimethylamino)naphthalene (PRODAN), has been shown to be a suitable fluorophore for the monitoring of biological processes (**Figure 16**).[60–62] The fluorophore is highly environmentally sensitive and undergoes a large change in fluorescence intensity and emission wavelength upon environmental changes. Additionally, PRODAN can be excited at a higher wavelength than most biological chromophores and displays a large quantum yield. The favourable photophysical properties of PRODAN have made it a desirable target as an amino acid side-chain. Using the PRODAN scaffold in 2003, Imperali and co-workers described the synthesis of 6-(2-dimethylaminonaphthoyl) alanine (DANA).[63] Subsequently, in 2009, Schultz and co-workers described an alternative PRODAN type amino acid, 3-(6-acetylnaphthalen-2-ylamino)-2- aminopropanoic acid (ANAP).[64]
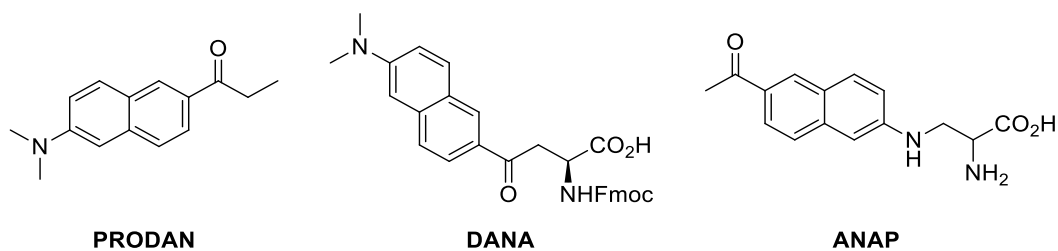
Figure 16: *PRODAN and fluorescent amino acids based on the PRODAN chromophore.*

The synthetic route to DANA began with commercially available 6-acetyl-2-methoxynaphthalene **39**, which was converted to alkyl bromide **40** via known methods (**Scheme 15**).[65] An enantioselective alkylation reaction then took place, which utilised phase transfer catalysis for the alkylation of **40** with glycine benzophenone imine **17**. This gave the desired benzophenone imine **41** in a good yield with high enantioselectivity. Acidic hydrolysis of imine **41** followed by Fmoc-protection gave protected the desired fluorescent amino acid, DANA. This amino acid was then successfully used for SPPS, and fluorescence measurements on the resulting short chain peptide incorporating this amino acid showed that the photophysical properties of DANA were retained within the peptide environment. Excitation of this analogue at 367 nm was possible, with a reported emission maximum of 525 nm. Incorporation of DANA into the S-peptide of RNase S was then achieved, and it was observed that large changes in fluorescence occurred upon peptide-protein interactions, with a blue-shifted emission maximum observed in a hydrophobic environment. These results were consistent with the environmental sensitivity of DANA.
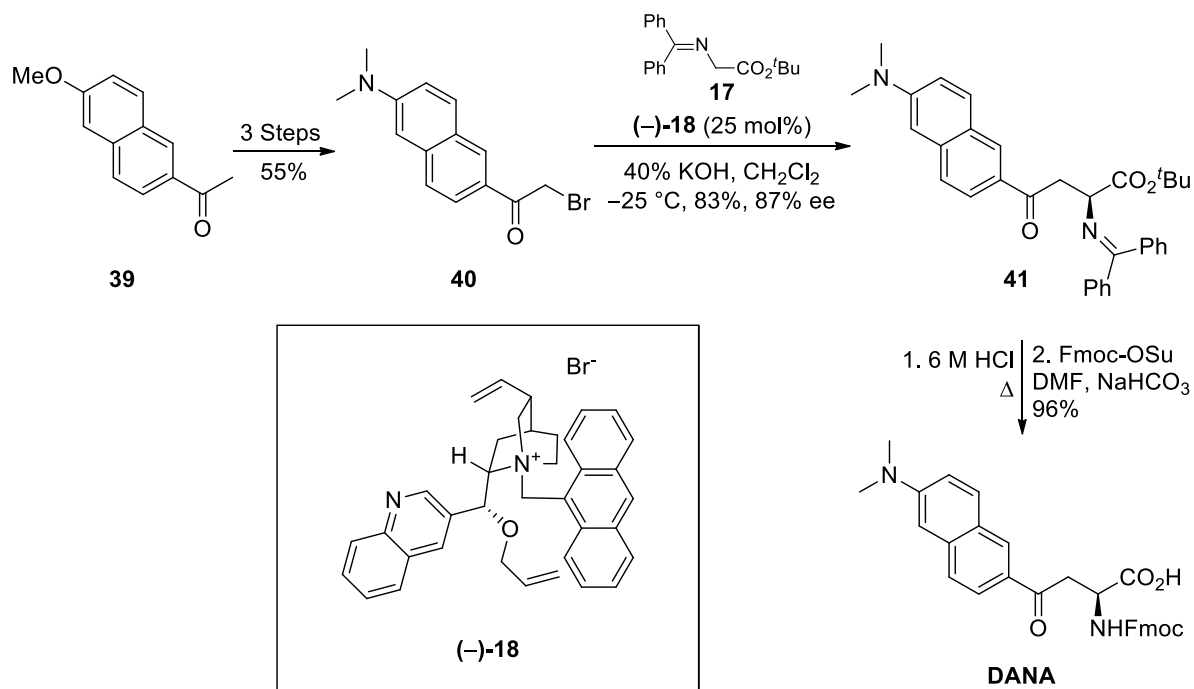
Scheme 15: *Synthesis of PRODAN based fluorescent amino acid, DANA.*

The amino acid ANAP was synthesised in six steps from 1-(6-hydroxynaphthalen-2-yl)ethanone (**Scheme 16**). The photophysical properties of ANAP were shown to be comparable to those of PRODAN, and additionally, the fluorophore showed significant environmental sensitivity.[64] Initially, naphthol starting material **42** was reacted with 2,4-dimethoxybenzylamine *via* a Bucherer reaction. Next, S_N2 substitution of the resulting naphthylamine with alkyl bromide **43** gave substitution product **44** in 26% overall yield. Subsequent reduction of the ketone and oxime moieties then gave amino ester **45**. The free amine was then Boc-protected, and the alcohol oxidised to give ketone **46**. Finally, removal of the protecting groups gave ANAP, which was site specifically incorporated into the *E. Coli* glutamine binding protein and used to probe structural changes induced by ligand binding. Following this initial report, Schultz and co-workers later showed that ANAP may also be site-specifically encoded and used to visualise the subcellular localisation of proteins in live mammalian cells.[66]
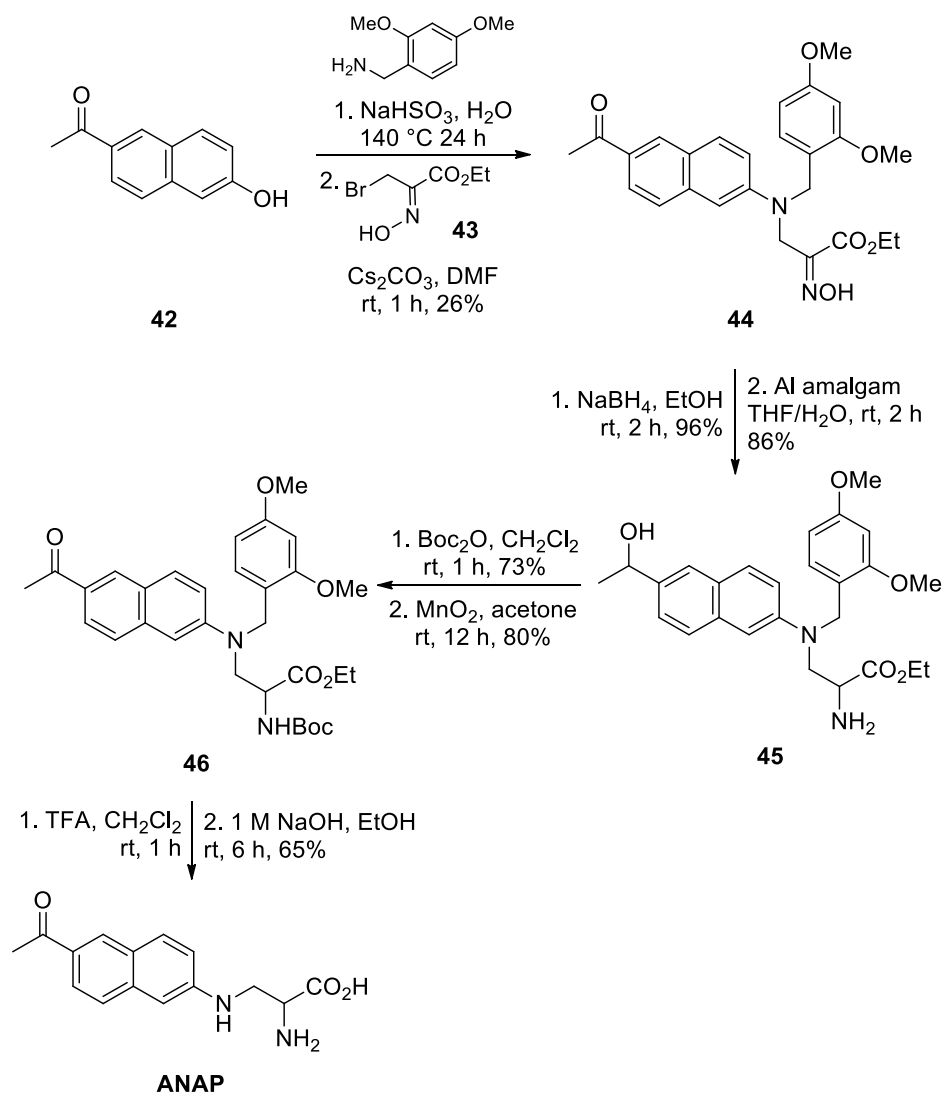
Scheme 16: *Synthesis of ANAP.*

The 4-(*N*,*N*-dimethylamino)phthalimide (4-DMAP) moiety has also been reported as a highly useful small molecule probe. This fluorophore exhibits high environmental sensitivity, with a large quantum yield in apolar environments when compared to aqueous solution, and is similar in size to the natural amino acid tryptophan.[67] The synthesis of an amino acid analogue of this fluorophore along with a more conjugated 6-*N*,*N*-dimethylamino-2,3-naphthalimide (6-DMN) amino acid were described by Imperiali and co-workers.[68,69] For the synthesis of these amino acids, the reaction of the respective anhydrides with allyl protected amino acid **48** was required.[70] The protection of commercially available amino acid **47** with allyl bromide was achieved in 78% yield and gave **48** (**Scheme 17**).
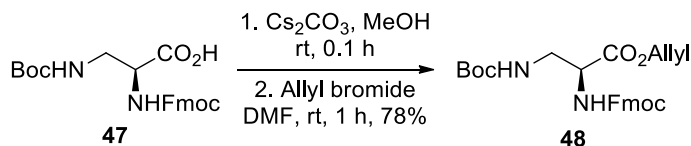
Scheme 17: Allyl protection of acid 47.

Anhydride **50** based on the 4-DMAP fluorescent scaffold was synthesised in two steps from 4-aminophthalic acid, starting with reductive amination of the amine to give **49** in quantitative yield (**Scheme 18**).[67] Next, sublimation of diacid **49** gave the desired anhydride **50**, also in excellent yield.
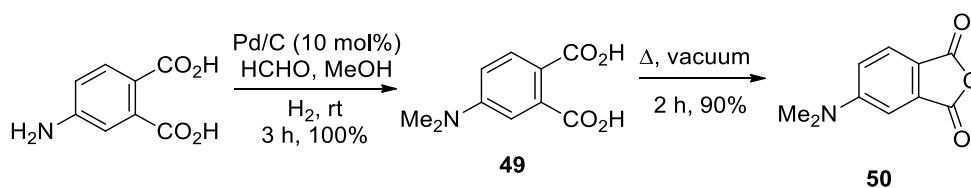
Scheme 18: Synthesis of anhydride 50 based on the 4-DMAP fluorescent scaffold.

The route to the more conjugated anhydride **55** began with the protection of the aldehyde of 2-nitrobenzaldehyde to give **51** (**Scheme 19**).[69] Reaction of this nitroarene with chloromethyl phenyl sulfone occurred through a vicarious nucleophilic substitution, in which a hydrogen of the arene was replaced by the sulfone group. A mixture of 1:1 isomers at the 2- and 4-positions were observed, and purification achieved through column chromatography. Deprotection then gave aldehyde **52**. The naphthalene moiety was next assembled. This was achieved through a multistep process which began with addition of the nucleophilic sulfone anion of **52** to diethyl maleate. Addition of the resulting anion to the electrophilic aldehyde and subsequent elimination of phenylsulfinic acid and water gave the desired naphthalene derivative **53**. Finally, in a similar procedure for the 4-DMAP analogue, the incorporation of a dimethylamino moiety was achieved through reductive amination of **53**, which gave **54** in 84% yield. Hydrolysis of **54** and then sublimation gave desired anhydride **55** in 77% yield.
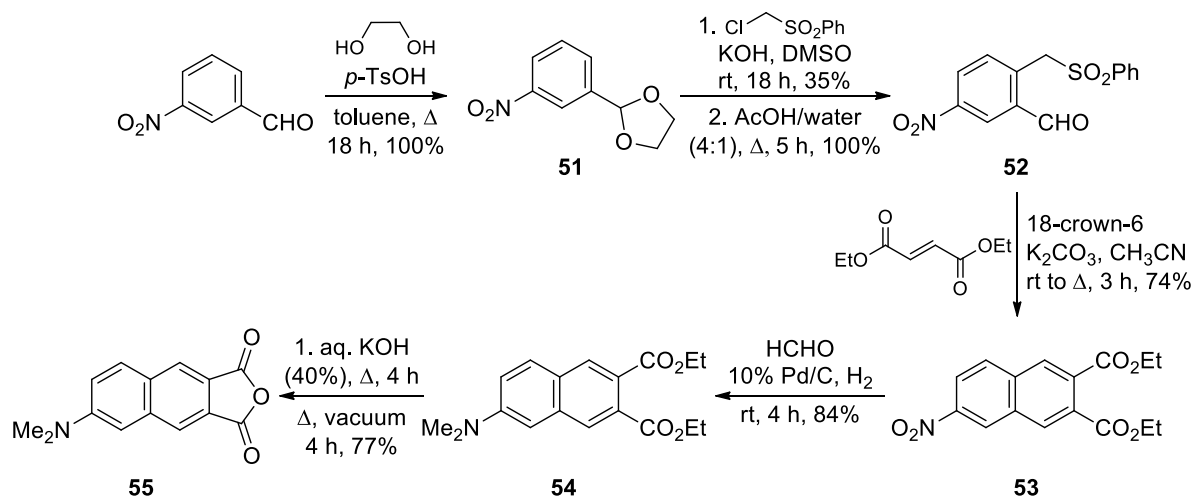
Scheme 19: *Synthesis of anhydride 55 based on 6-DMN scaffold.*

Coupling of these anhydrides with amine **56** formed from Boc-deprotection of 3-aminoalanine **48** was then possible (**Scheme 20**).[67] These reactions occurred smoothly, and were followed by activation of the acid intermediate using HBTU and HOBt for the subsequent ring closure to form the desired phthalimide amino acids **57** and **58**. Deprotection of the allyl groups was achieved using Pd(PPh$_3$)$_4$ and phenylsilane to give the Fmoc-protected amino acids for use in SPPS.
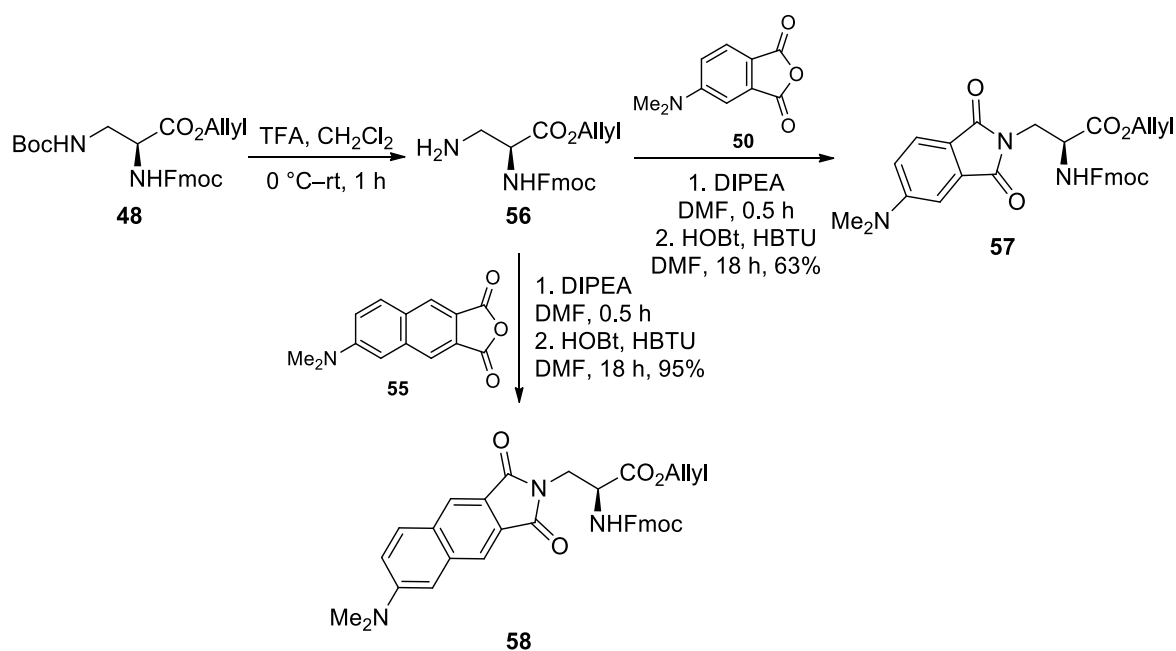
Scheme 20: *Coupling of anhydrides 50 and 55 with amine 56.*

Wagenknecht and co-workers have also recently reported amino acids incorporating the 4-aminophthalimide (4-AP) moiety, another small environment sensitive probe, similar in size to the indole of tryptophan.[71] This amino acid differed

from the 4-DMAP system by excluding the dimethylamino group in an attempt to produce probes with a higher quantum yield in polar environments.[68] As the dimethylamino group is known to contribute to non-radiative decay by a twisted intramolecular charge transfer state,[72] it was proposed that replacing this with an amine would give a brighter fluorophore. The amino acid building blocks were prepared as Fmoc-protected derivatives for solid phase peptide synthesis, and three different analogues were produced to test potential synthetic approaches and investigate linkers to attach the probe to the amino acid side chain. One of the amino acids produced involved direct attachment of 4-AP to the amino acid side chain (**Scheme 21**). This methodology used a similar approach as reported by Imperiali and co-workers.[67] Formation of the desired phthalimide was achieved by condensation of 3-aminoalanine derivative **56** with anhydride **59**. This was followed by allyl group removal by Pd^0 catalysis in the presence of phenylsilane as an allyl acceptor and gave phthalimide amino acid **60**. It was reported that the quantum yield of the synthesised 4-AP analogues demonstrated larger quantum yields than for 4-DMAP systems.
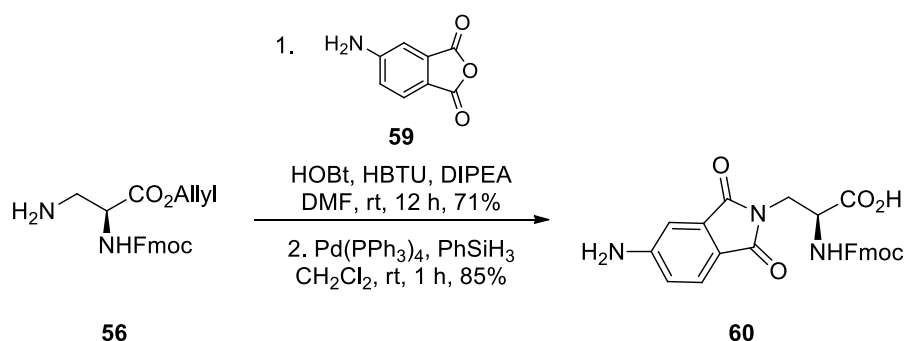
*Scheme 21: Formation of phthalimide amino acid **60**.*

Finally, the synthesis of fluorescent amino acids based on 7-nitrobenz-2-oxa-1,3-diazol-4-y (NBD) fluorophores have been reported (**Scheme 22**).[73] Reaction of the non-fluorescent NBD-chloride with Fmoc-protected 3-aminoalanine gave desired fluorescent amino acid **61**. The addition of the amino group into this compound allowed for the formation of the 'push-pull' system of NBD, resulting in fluorescent properties. For a small molecule, this analogue demonstrated a remarkably red-shifted absorption maximum of 480 nm, and an emission wavelength of 540 nm. The Fmoc-protected amino acid **61** was also incorporated into a peptide through a SPPS strategy.
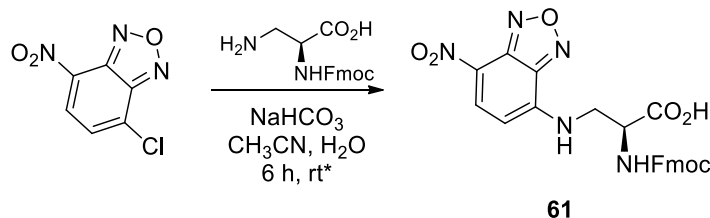
Scheme 22: *Synthesis of fluorescent amino acid based on the NBD fluorophore.*
*No reported yield.

1.2.3 Other Fluorescent Amino Acids

Fluorescent amino acids utilising less well known or novel fluorophores have also been described, particularly with extended polyaromatic fluorescent scaffolds. Fluorescent amino acids based on an azaindole structure were described by Hecht and co-workers in 2014 (**Figure 17**).[74] 1*H*-Pyrrolo[3,2-c]isoquinoline amino acid (**62**) and 1*H*-pyrrolo[2,3-f]quinoline amino acid (**63**) were synthesised, and it was found that of the two analogues, **62** demonstrated a larger quantum yield (0.10 *vs* 0.03)

62
λ_{abs} = 260 nm
λ_{em} = 420 nm
ϕ = 0.10

63
λ_{abs} = 272 nm
λ_{em} = 421 nm
ϕ = 0.03
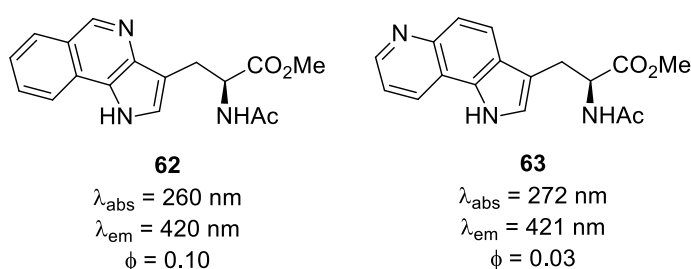
Figure 17: *Fluorescent amino acids based on an azaindole structure.*

The synthesis of brighter amino acid **62** began with preparation of pyrroloisoquinoline **64** using a previously described approach.[74] Synthesis of amino acid **69** then began with formylation of **64** under Duff reaction conditions,[75] followed by tosyl-protection of the indole nitrogen to give **65** (**Scheme 23**). Subsequent reduction of aldehyde **65** using sodium borohydride gave alcohol **66**. Chlorination with thionyl chloride in the presence of basic triethylamine gave alkyl chloride **67**. Reaction with the Schöllkopf chiral auxiliary, the (*R*)-bislactim ether, was then investigated. Regioselective lithiation of this chiral auxiliary occurred using *n*-BuLi to form the lithium enolate which reacted with alkyl chloride **67** and gave desired adduct **68**, with only one diastereomer visible by ^{1}H and ^{13}C NMR spectroscopy. Hydrolysis under mild conditions then gave amino acid **69**. Finally, acyl protection followed by deprotection of the *N*-tosylate gave protected amino acid **62** which was used for photophysical characterisation. The analogue was found to have similar

photophysical properties to tryptophan, however with a larger molar attenuation coefficient and more red-shifted emission maximum.
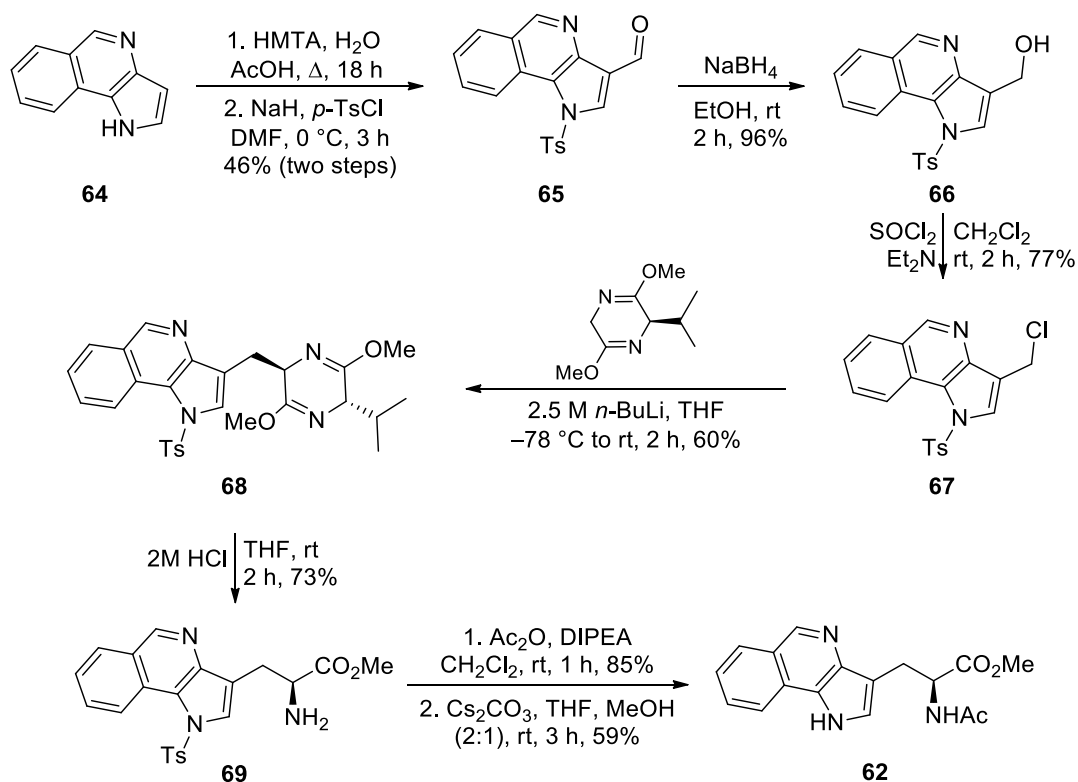
Scheme 23: *Synthesis of azaindole based fluorescent amino acid* **62**.

The Sutherland group have previously described the synthesis of 5-arylpyrazole-derived α-amino acids, such as **70**, with interesting fluorescent properties. However, these analogues demonstrated lower quantum yields than is often desirable for fluorescent probes. It has been reported that conformationally rigid chromophores allow for more efficient π overlap within a compound, and result in brighter chromophores.[21,76] As such, in a subsequent project, it was demonstrated that the photophysical properties of these analogues could be improved through the introduction of conformational restraint.[20] In this work, a new class of α-amino acid was described, bearing a planar pyrazoloquinazoline chromophore. The pyrazoloquinazolines demonstrated ten-fold increase in quantum yield compared with analogous 5-arylpyrazole-derived α-amino acids (**Figure 18**).
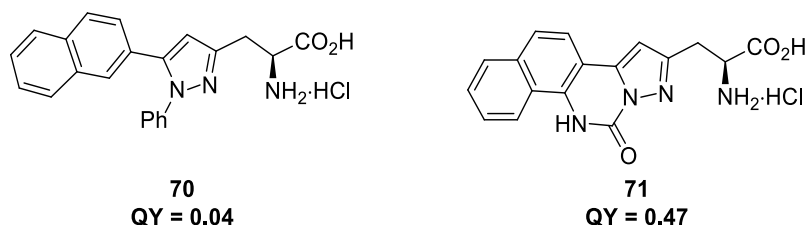
Figure 18: *Comparison of the quantum yields of amino acid 70 and more rigid amino acid 71.*

The synthetic route for the preparation of pyrazoloquinazoline containing α-amino acids was developed from L-aspartic acid.[17] A series of analogues were produced through the same synthetic route, which is demonstrated in **Scheme 24** for one of the lead analogues, dimethylamino compound **76**. Phosphonate ester **72** was initially produced in five steps from L-aspartic acid using methods previously described by the group.[77] Horner-Wadsworth-Emmons reaction between 4-dimethylamino-2-nitrobenzaldehyde and phosphonate ester **72** then gave enone **73**. Reaction with hydrazine in a one-pot condensation and aza-Michael process, followed by oxidation of the resulting 2-pyrazoline with DDQ was used to construct the pyrazole ring of analogue **74**. The final stage was then a two-step process involving reduction of the nitro-group, followed by reaction with triphosgene under basic conditions to give cyclised product **75**. A two-step deprotection strategy which used caesium carbonate for hydrolysis of the ester group, followed by acidic deprotection of the amino group gave amino acid **76**. Also reported was the excitation of pyrazoloquinazoline amino acid **76** using two photon induced fluorescence *via* near-IR excitation.[17]
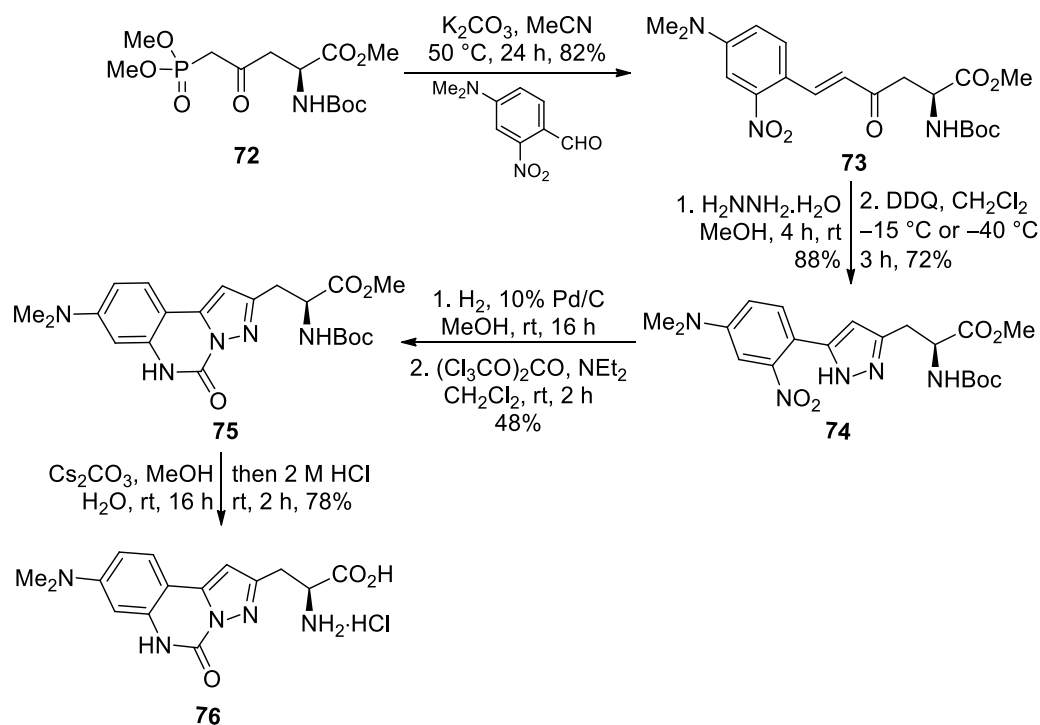
*Scheme 24: Synthesis of pyrazoloquinazoline amino acid **76**.*

1.3 Summary

Small organic molecules with fluorescent properties have proven to be useful biological imaging tools.[1] The modification of these fluorophores through rational design has allowed for the optimisation of photophysical properties such as absorption or emission wavelength, as well as the brightness of these fluorophores. Tuning of fluorophores for desired applications has also been possible, including in the design of compounds which show environmental sensitivity. Crucially, small molecule fluorophores may be used in the synthesis of fluorescent amino acids through modification of naturally occurring amino acids, or through the attachment of a fluorescent moiety to an amino acid side-chain.[4,78] Additionally, novel fluorophores may be incorporated as amino acid side-chains. These fluorescent amino acids have wide-reaching applications as chemical biology probes, owing to their ability to be incorporated into proteins and peptides through SPPS or genetic encoding.

1.4 Thesis Outline

The remainder of the thesis will discuss research completed during this PhD. Initially, pyridine derived amino acids previously developed in the Sutherland group will be discussed, followed by improvements to this series of compounds which were established in the duration of this research. In chapter three, a discussion of benzotriazole derived amino acids previously synthesised in the group occurs, followed by improvements and expansions which were made to this series during this PhD. Finally, a brief introduction to fluoroprolines is outlined in chapter four, followed by a discussion of research which led to the development of novel fluoroproline precursors.

2.0 Pyridine Derived Fluorescent Amino Acids

2.1 Previous Work

Previous work in the Sutherland group described the synthesis of a series of fluorescent β-pyridyl α-amino acids (**Scheme 25**).[36] The route to these analogues began from L-aspartic acid with the key step involving a highly regioselective hetero-Diels-Alder cyclisation of enones with ethyl vinyl ether. This was followed by a modified Knoevenagel-Stobbe reaction to form the desired pyridine heterocycle. Among the library synthesised were analogues containing various aromatic side-chains which featured both electron-withdrawing and electron-donating substituents.
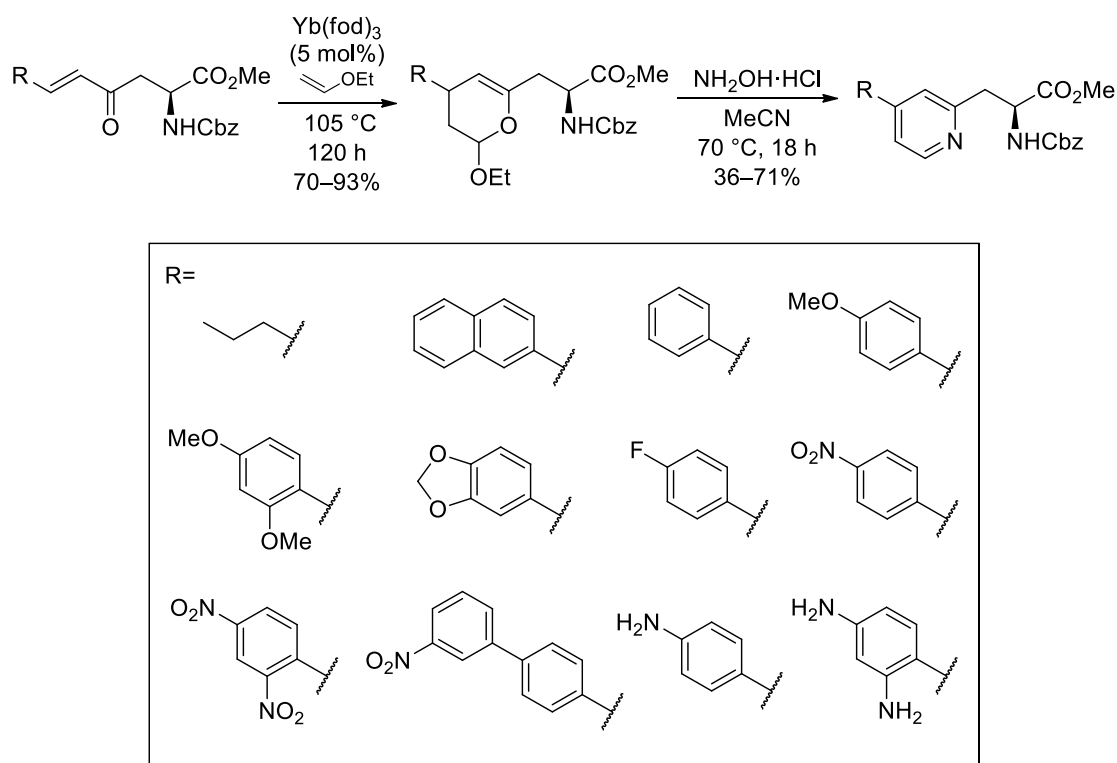
Scheme 25: *Diels-Alder cyclisation followed by modified Knoevenagel-Stobbe reaction to form β-pyridyl α-amino acids.*

It was shown that analogues in this series containing electron-rich groups exhibited the most favourable photophysical properties (**Figure 19**), resulting from the "push-pull" character between these electron rich groups and the electron-withdrawing pyridine ring. The 1,4-dimethoxy **77** and 4-amino **78** analogues showed red-shifted absorption maxima compared to other analogues, however both suffered from low brightness. While the naphthalene analogue **79** showed the most red-shifted

emission spectra and a MegaStokes shift of 193 nm, overall, the 4-methoxy analogue **80** was determined to have the most favourable properties for further investigation, owing to a good quantum yield and relatively high resulting brightness.

77
λ_{abs} = 275, 298 nm
λ_{em} = 384, 413 nm[a]
ϕ = 0.19
Brightness = 1634 cm^{-1} M^{-1}

78
λ_{abs} = 315 nm
λ_{em} = 433 nm[a]
ϕ = 0.04
Brightness = 464 cm^{-1} M^{-1}

79
λ_{abs} = 259 nm
λ_{em} = 380, 452 nm[b]
ϕ = 0.18
Brightness = 6185 cm^{-1} M^{-1}

80
λ_{abs} = 286 nm
λ_{em} = 366 nm[c]
ϕ = 0.46
Brightness = 11,923 cm^{-1} M^{-1}
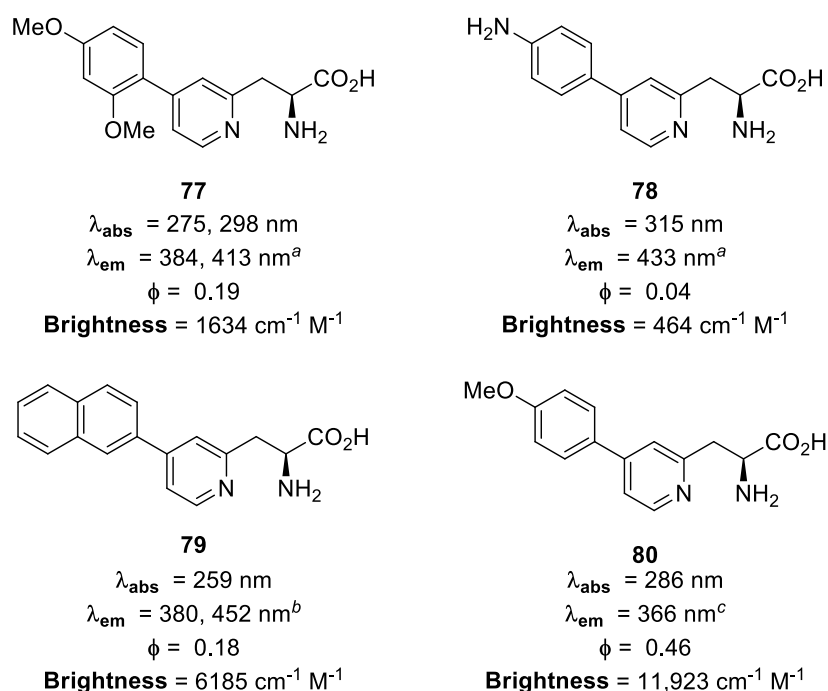
Figure 19: *β-Pyridyl α-amino acids bearing electron donating groups. Measured in MeOH at [a] 1 × 10^{-5} M, [b] 0.5 × 10^{-5} M or [c] 1 × 10^{-7} M.*

A solvatochromic study was undertaken with this analogue (**80**), which showed that the emission wavelength was solvent dependent (**Figure 20**). This analogue possessed an emission maximum of 308 nm in THF, and 423 nm in phosphonate-buffered saline.[36] The increased wavelength of emission in polar solvents suggested excited state stabilisation of the compound in polar environments, often observed in compounds which exhibit a dipole across the chromophore.[10] This amino acid was also incorporated into a hexapeptide using Fmoc-based SPPS methodology.
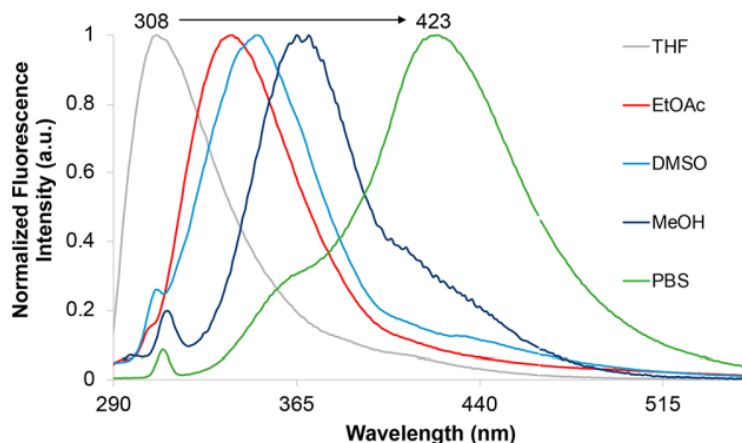
Figure 20: Solvatochromic study undertaken with 4-methoxy analogue 80.

2.2 Project Aims

The first aim of this project was to improve the synthetic route towards *β*-pyridyl *α*-amino acids through a change in protecting group strategy. The existing synthetic route to these compounds involved a change in protecting group after a key Horner-Wadsworth-Emmons reaction which branched the route to provide different analogues (**Scheme 26**). It was proposed that a change in the synthetic sequence whereby protecting group exchange occurred before the Horner-Wadsworth-Emmons reaction would allow for diversification at a later stage.
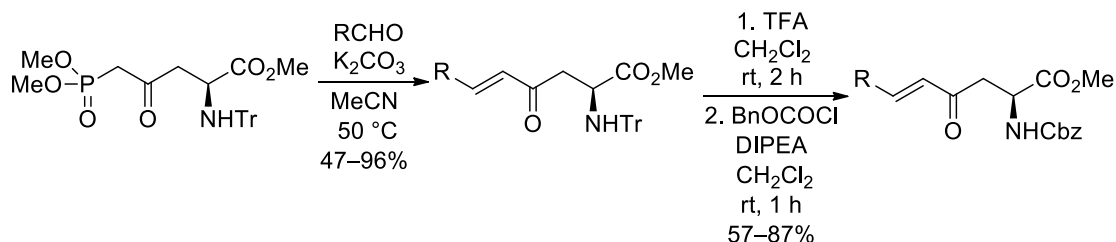
Scheme 26: Existing protecting group strategy for the synthesis of β-pyridyl α-amino acids.

This project then aimed to further investigate the properties of *β*-pyridyl *α*-amino acids. First of all, it was proposed that the 4-hydroxyl analogue **81** would be an interesting target as a potential pH probe (**Figure 21**). Secondly, as the 4-methoxy analogue **80** showed promising fluorescent properties, further derivatisation of this analogue was proposed. In methanol, this analogue demonstrated a λ_{abs} of 286 nm and a λ_{em} of 366 nm. As extended π systems have been shown to red-shift these values,[1] it was suggested that the synthesis of more conjugated pyridyl analogues

would be beneficial. These analogues would include an extra aromatic ring bearing electron donating substituents that would increase the charge transfer across the compound.
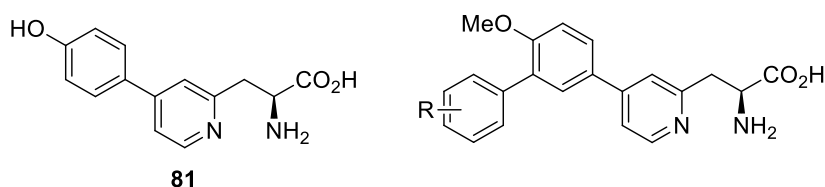
Figure 21: *Proposed β-pyridyl α-amino acid targets. Where R = electron donating group.*

Finally, the project aimed to further investigate the photophysical properties of 4-methoxy amino acid **80** and associated analogues, including investigations into the pH and environmental sensitivity of these compounds.

2.3 Modified Synthesis of Lead Pyridine Derived *α*-Amino Acid

Work began towards the synthesis of 4-methoxy amino acid **80** through the synthetic route previously described by the Sutherland group with modification of the order of the synthetic steps. Initially, the required phosphonate ester **83** was synthesised in three steps from commercially available L-aspartic acid (**Scheme 27**). Following protection of the acid and amine groups, the use of the bulky *N*-trityl protecting group allowed for the regioselective reaction of the anion of dimethyl methylphosphonate with the less hindered *β*-methyl ester of **82** to give phosphonate ester **83** in 70% yield.
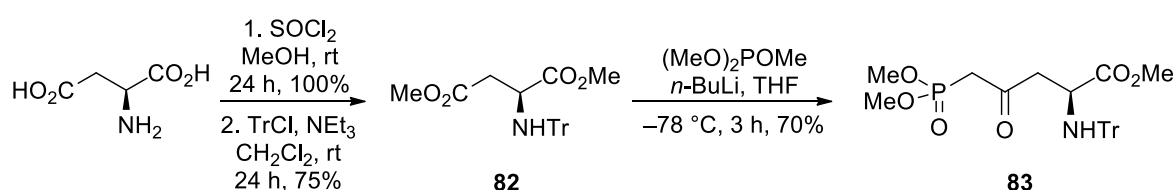
Scheme 27: *Synthesis of N-trityl protected phosphonate ester 83.*

Next, protecting group manipulation was undertaken in order to exchange the *N*-trityl for an *N*-carboxybenzyl (Cbz) group, before Horner-Wadsworth-Emmons reaction to provide enone **85** (**Scheme 28**). This protecting group manipulation was required as the *N*-trityl group would hinder any subsequent reactions of the enone moiety.[79] The protecting group exchange involved TFA-mediated removal of the

trityl group and reprotection of the resulting amine with benzyl chloroformate under basic conditions. This allowed the multigram synthesis of Cbz-protected phosphonate ester **84** in 91% yield. The Horner-Wadsworth-Emmons reaction of phosphonate ester **84** with 4-methoxybenzaldehyde, under mild basic conditions then proceeded smoothly, and gave the product enone **85** in 71% yield. The electron rich nature of the aldehyde resulted in an extended reaction time of 96 h. Synthesis of the *E*-enone was confirmed by ^{1}H NMR spectroscopy, as a doublet at 6.58 ppm was observed with a coupling constant value of 16.2 Hz, which was assigned as the H-5 alkenyl hydrogen atom
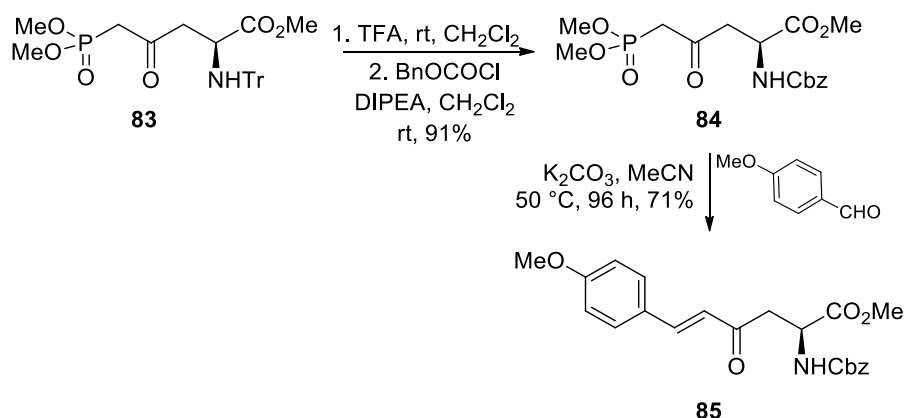
Scheme 28: *Protecting group manipulation and Horner-Wadsworth Emmons reaction to give enone **85**.*

Finally, two-stage pyridine ring formation was undertaken. The first step involved an inverse-demand hetero-Diels-Alder reaction as first described by Danishefsky and co-workers in 1984.[80] For this reaction, enone **85** was heated to 105 °C in neat ethyl vinyl ether and in the presence of the Lewis acid catalyst, tris(6,6,7,7,8,8,8-heptafluoro-2,2-dimethyl-3,5-octanedionato)ytterbium (Yb(fod)$_3$) (**Scheme 29**). Subsequent reaction with hydroxylamine hydrochloride through a modified Knoevenagel−Stobbe reaction gave pyridine **87** in 63% yield over two steps. The best yields for the two-step process were achieved using the dihydropyran intermediate without purification, as this was prone to decomposition. The use of an alternative, cheaper, Lewis acid catalyst, ytterbium(III) triflate was considered for this reaction. Using the same conditions, at 105 °C with ethyl vinyl ether, however, no reaction of starting material was observed and the reaction mixture became very viscous overnight. No reaction was observed after 196 h and the reaction was abandoned. As such, future reactions were completed with Yb(fod)$_3$.
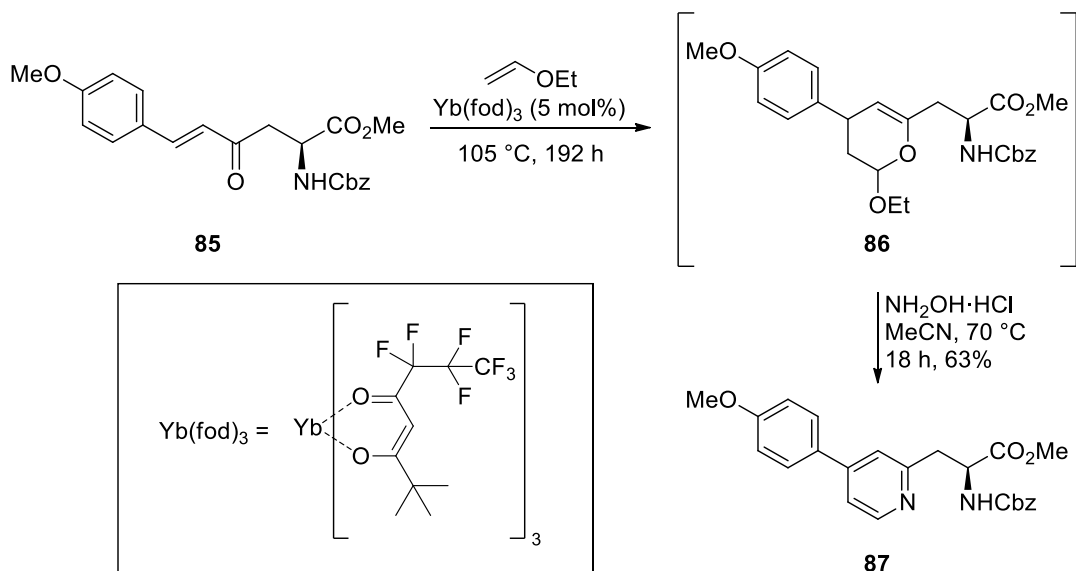
Scheme 29: *Two-step pyridine-forming process to give **87***.

In an inverse demand Diels-Alder reaction, an electron poor diene (here, enone **85**) reacts with an electron rich dienophile (ethyl vinyl ether). As such, the lowest occupied molecular orbital (LUMO) of the enone reacts with the highest occupied molecular orbital (HOMO) of ethyl vinyl ether (**Figure 22a**). In these reactions, an *endo* approach of the electron donating substituents on the dienophile is generally favoured. This allows for a favourable secondary orbital interaction between the carbonyl carbon of the enone and the oxygen of ethyl vinyl ether (**Figure 22b**). Coordination of the Lewis acid catalyst to the enone carbonyl lowers the LUMO energy, thus making the reaction faster and more regioselective. It is proposed that coordination of Yb(fod)$_3$ to the enone carbonyl may also result in some coordination to the nearby amino group in a six membered ring orientation. This coordination would block the top face of the molecule and encourage dienophile approach from the bottom face (**Figure 22c**). While it was likely that a major diastereomer was formed in this reaction, owing to the complexity of the crude ^{1}H NMR spectrum a diastereomeric ratio could not be determined. The stereochemistry established in the dihydropyran step was subsequently removed by aromatisation in the pyridine forming process.
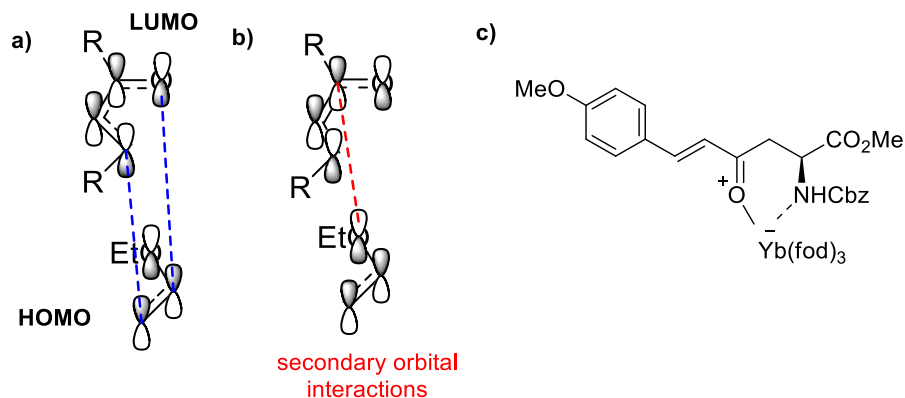
*Figure 22: Inverse demand Diels-Alder reaction of **85** with ethyl vinyl ether showing: a) HOMO-LUMO interactions, b) secondary orbital interactions and c) coordination of Yb(fod)₃ catalyst to the top face of enone **85**.*

Following the synthesis of pyridine **87**, deprotection was required to give the parent amino acid. Previously in the group, deprotection was achieved through heating the synthesised pyridines to 100 °C in 6 M HCl for a period of 48 h. In recent years, however, a milder method has been employed by the group for the deprotection of other amino acid libraries,[81] and this method was investigated as an alternative approach for deprotection here (**Scheme 30**). First, the methyl ester was subject to mild basic hydrolysis using caesium carbonate. Next, the Cbz-protecting group was removed by heating in 6 M HCl for just one hour. This gave deprotected amino acid **80** in an 88% yield over two-steps.
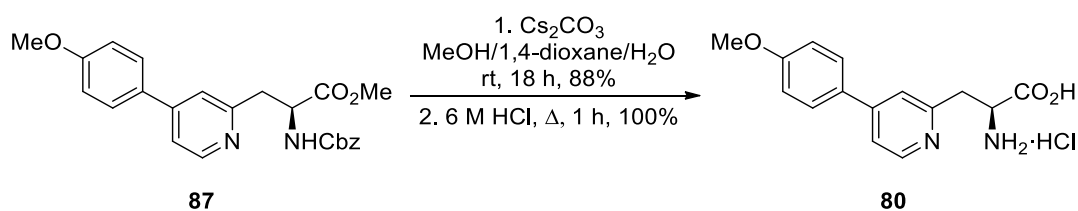
*Scheme 30: Two step deprotection of 4-methoxypyridyl amino acid **87** to give amino acid **80**.*

Following the successful synthesis of the 4-methoxy analogue **80** through a modified synthetic route, work was undertaken towards the synthesis of a novel pyridine derived amino acid analogue **81**, bearing a 4-hydroxy substituent. The hydroxyl group would still allow for strong push-pull character throughout the chromophore, with the additional benefit of the compound now containing two pH sensitive groups (**Figure 23**). It was proposed that under basic conditions, deprotonation of the

52

phenol would occur, leaving an alkoxide which would have additional electron-donating properties. This would increase the push-pull character and give a red-shift in absorption and emission maxima. Meanwhile, in an acidic environment, protonation of the pyridine moiety could occur which would give a stronger electron withdrawing substituent. This would have the same effect, increasing the dipole across the chromophore and giving a red-shifted absorption and emission maxima.
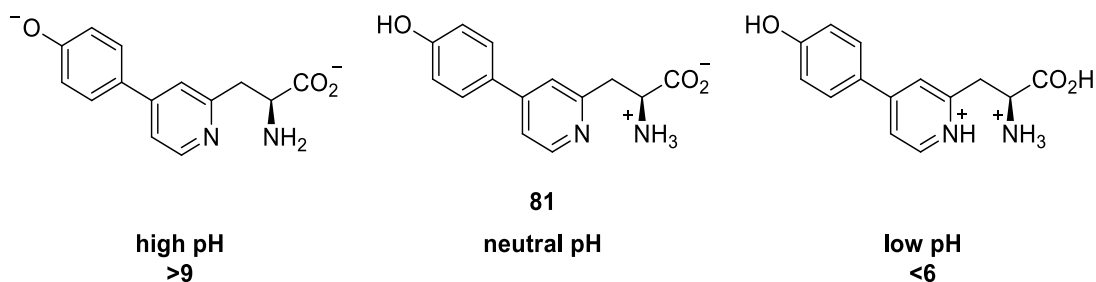
Figure 23: *Proposed phenol derived pyridine amino acid 81 and pH sensitivity.*

It was proposed that the synthesis of 4-hydroxyl analogue **81** could be achieved via a benzyl ether derivative, which would be deprotected at a later stage. The first step in the synthesis involved reaction of the previously synthesised Cbz-protected phosphonate ester **84** with 4-(benzyloxy)benzaldehyde in a Horner-Wadsworth Emmons reaction (**Scheme 31**). Under the same conditions as previously, enone **88** was isolated in 52% yield. Again, the *E*-alkene was confirmed by ^{1}H NMR spectroscopy, and long reaction times were required owing to the electron rich nature of the aldehyde. Enone **88** then underwent the two-step inverse-demand hetero-Diels-Alder reaction and modified Knoevenagel−Stobbe process to give pyridine **90** in 27% yield over the two steps. While benzyl ethers are generally stable, it was proposed that the low yield here could be a result of loss of the protecting group under the harsh conditions of the cyclisation, which required heating to 105 °C, in neat ethyl vinyl ether and in the presence of a Lewis acid catalyst for 192 h.[82]
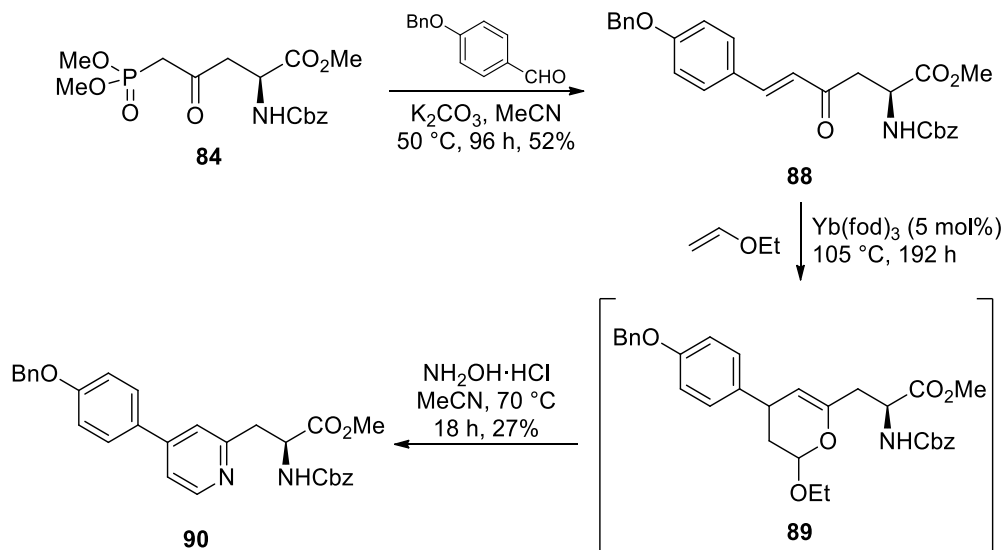
Scheme 31: Synthesis of O-benzyl protected hydroxypyridine amino acid **90**.

Finally, the deprotection of this analogue was required. It was proposed that the *N*-Cbz and the *O*-Benzyl groups could be simultaneously removed by hydrogenation. Following hydrolysis of the methyl ester to give acid **91**, indicated by the absence of the methyl ester peak by ^{1}H NMR spectroscopy, hydrogenation conditions were investigated (**Scheme 32**). Full characterisation of compound **91** could not be obtained owing to the small amount of material produced at this stage, and the insolubility of this compound. Unfortunately, an initial attempt at hydrogenation using 10% palladium on carbon at room temperature and atmospheric pressure gave none of the desired product. Upon increasing the pressure (6 bar), decomposition of the analogue was observed.
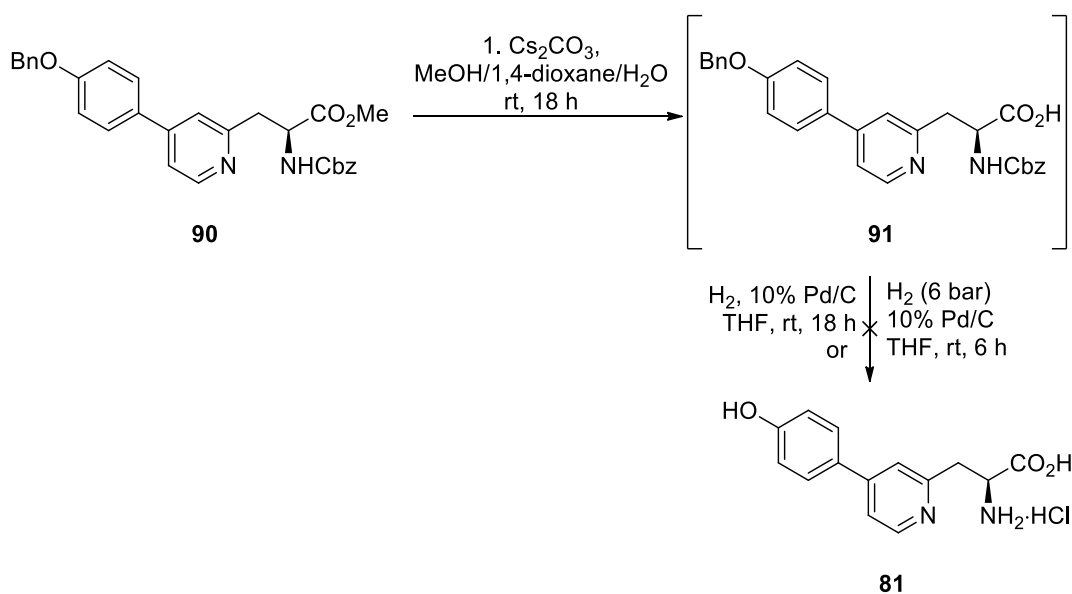
Scheme 32: Attempted deprotection of **90** to give amino acid **81**.

As it was not possible to produce the desired deprotected product through this synthesis, and owing to the low yielding key cyclisation step, work on this analogue was abandoned. Focus was shifted to investigate how 4-methoxy analogue **80** might be modified to produce novel fluorescent amino acids with improved properties.

2.4 Extending the Conjugation of Pyridine Derived *α*-Amino Acids

It was proposed that additional conjugation across the chromophore of lead compound **80** from the previously synthesised library of *β*-pyridyl *α*-amino acids, would red-shift the absorption and emission spectra of this compound.[1] The proposed targets would include an additional aryl ring (**Scheme 33**). A simple retrosynthetic analysis showed that compounds with this general structure could be synthesised through a Suzuki-Miyaura cross-coupling reaction with the 3-bromophenyl side-chain of amino acid **92** with aryl boronic acids.
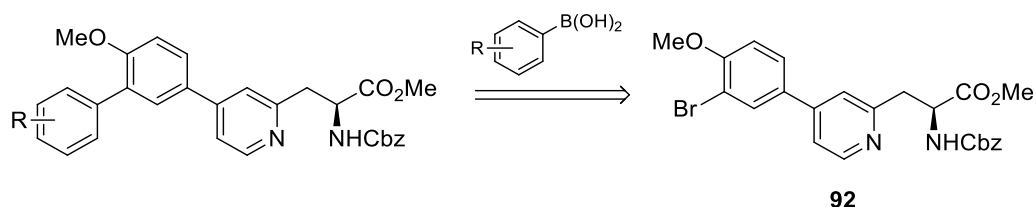
Scheme 33: *Retrosynthetic analysis of proposed target compounds.*

As such, the first step was to investigate the bromination of the 4-methoxyphenyl moiety of amino acid **80**. Previous work in the Sutherland group has developed a mild, efficient and regioselective method for the bromination of activated aryl rings (**Scheme 34**).[83] It was shown that a mixture of iron(III) chloride and the ionic liquid 1-butyl-3-methylimidazolium bis(trifluoromethylsulfonyl)imide, [BMIM]NTf$_2$ could be reacted in situ to give the powerful Lewis acid Fe(NTf$_2$)$_3$. This Lewis acid is particularly powerful due to the highly delocalised, weakly coordinating nature of the triflimide counterion. As a result, coordination of Fe(NTf$_2$)$_3$ to *N*-bromosuccinimide (NBS) increases the reactivity of the brominating agent.
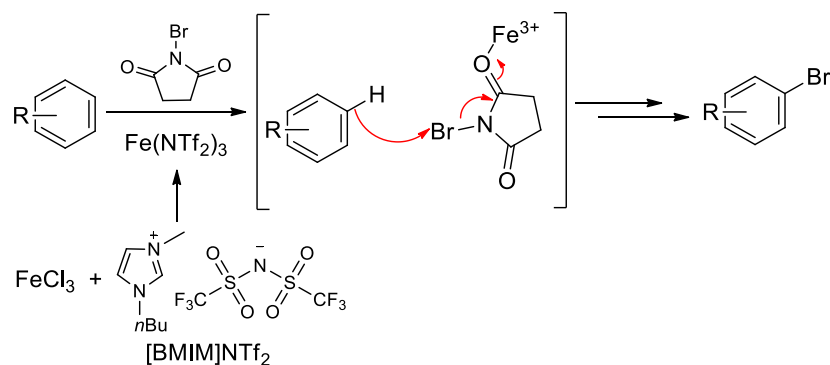
Scheme 34: *Iron(III) triflimide catalysed bromination of arenes.*

Bromination of **80** began using standard conditions developed within the group, involving iron(III) chloride (5 mol%) and a corresponding loading of [BMIM]NTf$_3$ (15 mol%) (**Table 1**, entry 1). This gave the desired product in a 37% isolated yield. An increase in catalyst loading to 8 mol% of iron(III) chloride along with an increase in the equivalents of NBS gave an increased isolated yield of 63% (entry 2). It was proposed that the requirements for increased loading here was a result of the electron withdrawing pyridine ring.
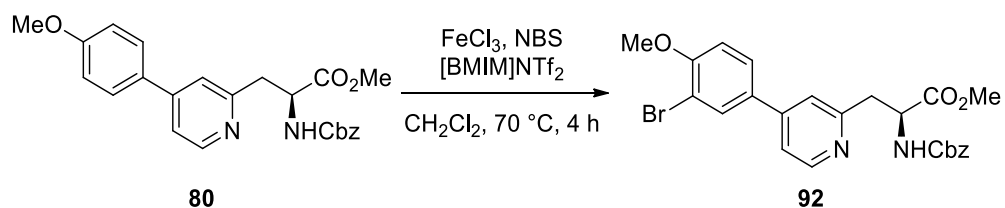
Entry	FeCl$_3$ (mol%)	[BMIM]NTf$_2$ (mol%)	NBS (equiv.)	Yield (%)
1	5	15	2	37
2	8	24	3.5	63

Table 1: *Conditions for the bromination of 80.*

Next, the Suzuki-Miyaura cross-coupling reaction of **92** with boronic acids was investigated. Conditions were chosen based on Suzuki-Miyaura reactions previously performed on similar aryl bromide *α*-amino acids within the group.[81] These involved the use of Pd(dppf)Cl$_2$ (7.5 mol%) as a catalyst, with potassium fluoride as the base, in a dioxane/water mixture (**Scheme 35**). Three analogues were synthesised; firstly the bis(methoxyphenyl) analogue **93a**. This was chosen as it was proposed that the extra electron donating group would help to increase the push-pull character of the fluorophore. Secondly, a naphthyl analogue **93b** was

chosen as it has been shown that these analogues generally have a high brightness due to their rigidity.[36,81] Finally, a trifluoromethyl analogue **93c** was synthesised to investigate the effect of an additional electron withdrawing group on the pyridine-based chromophore. Using the Suzuki-Miyaura reaction described, these analogues were synthesised in yields of 53–71%.
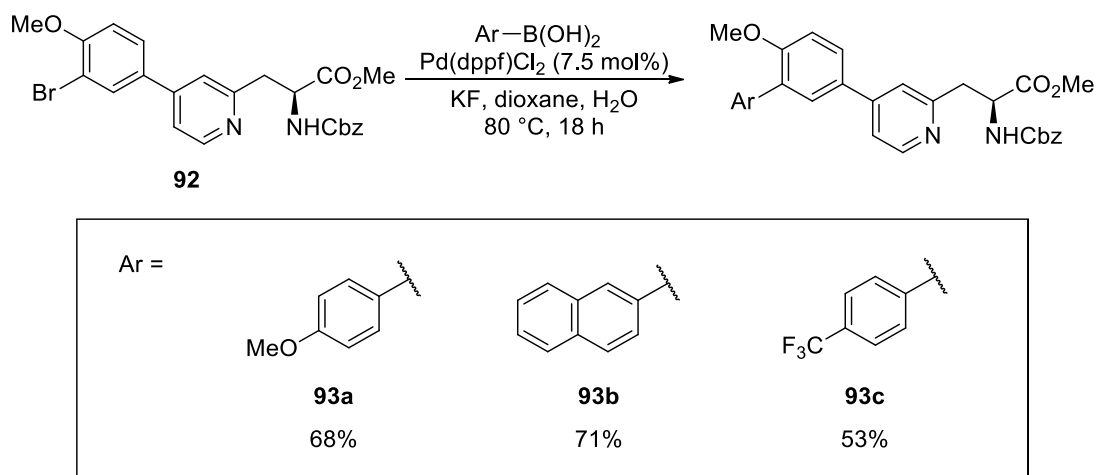
Scheme 35: *Suzuki-Miyaura cross coupling reaction of brominated **92** with aryl boronic acids.*

Finally, the deprotection of these analogues was investigated (**Scheme 36**). Ester hydrolysis with caesium carbonate in a co-solvent mixture gave the desired acids. Next, Cbz-deprotection was undertaken through reflux in acidic conditions for 1 h and gave the deprotected amino acids in moderate to high yields after recrystallisation.
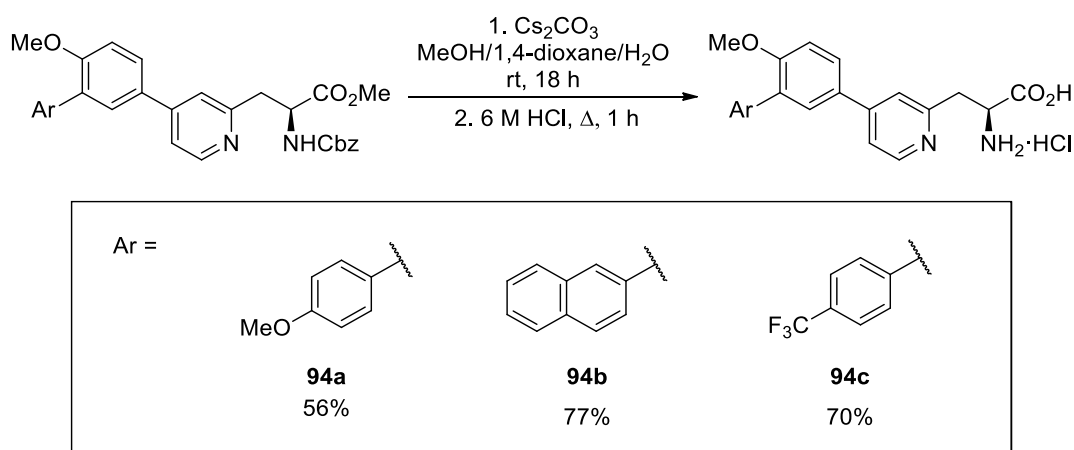
Scheme 36: *Deprotection of Suzuki-Miyaura cross coupling products.*

Following the successful Suzuki-Miyaura cross-coupling reactions of amino acid **92**, an additional analogue with extended conjugation was proposed. This could be achieved through the incorporation of an alkenyl group, as it has been reported that benzene-styryl analogues show red-shifted spectra when compared to simple biphenyl analogues.[84] Amino acid **95** was prepared from brominated analogue **92** through a Heck cross-coupling reaction with 4-methoxystyrene (**Scheme 37**). This styrene was chosen as it would install a second electron-donating group onto the chromophore. Conditions for the coupling used a stable palladium (II) pre-catalyst in the presence of *N,N*-diisopropylethylamine as a base and gave the product in 61% yield.
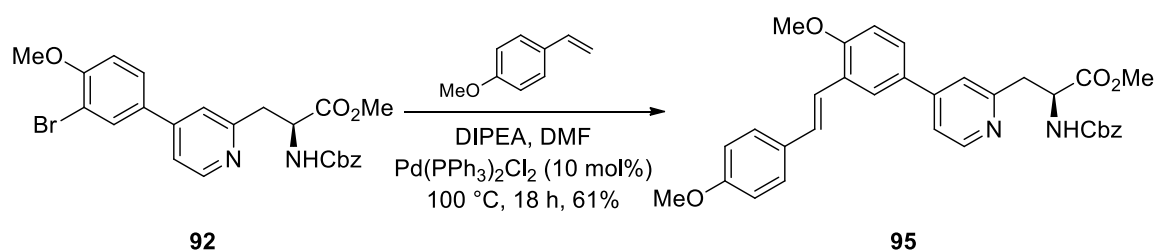
Scheme 37: Heck reaction of **92 to** give alkenyl analogue **95**.

Deprotection of amino acid **95** was then investigated. Ester hydrolysis using caesium carbonate, under standard conditions proceeded smoothly to give the corresponding carboxylic acid **96** in 71% yield (**Scheme 38**). However, attempted removal of the Cbz-protecting group with 6 M HCl at reflux led to a complex mixture by ^{1}H NMR spectroscopy. The same problem was observed upon multiple attempts, with a complex mixture observed after 0.5 h (partially deprotected) and 1.5 h (fully deprotected) reaction times. An attempt to aid this reaction by ensuring solubility from the reaction start time with the addition of 1,4-dioxane was unsuccessful, and attempts at recrystallisation did not yield clean product. It was proposed that the harsh acidic conditions were not compatible with the alkene moiety of this analogue.
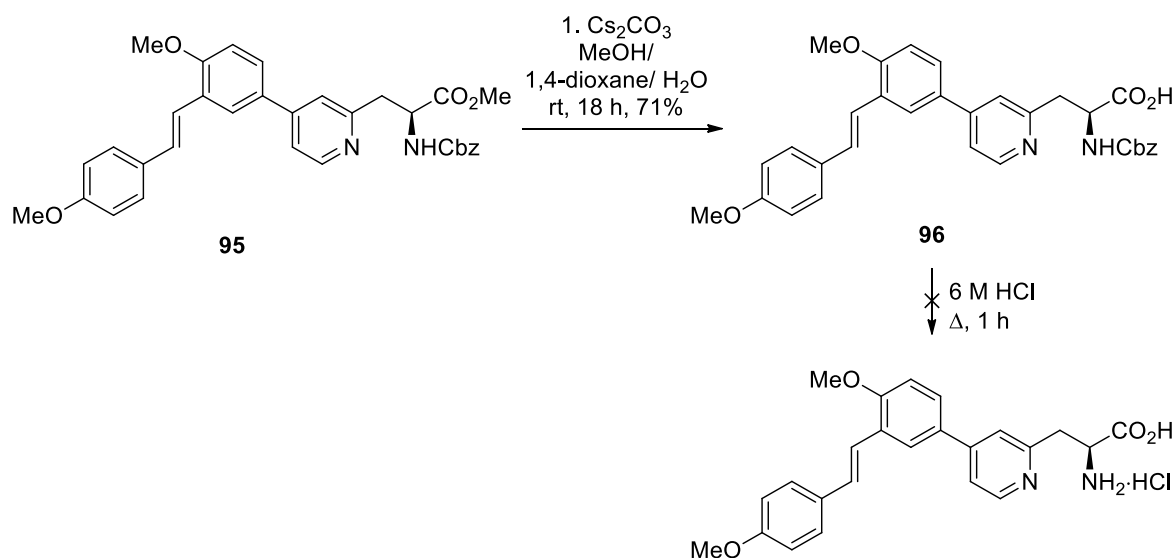
Scheme 38: *Ester hydrolysis of **95** and attempted Cbz-deprotection.*

As it was not possible to fully deprotect this analogue, it was suggested that partially deprotected compound **95** was used for simple fluorescence measurements. A comparison of this analogue to other pyridine analogues would help determine whether it was worth investigating other conditions to access the fully deprotected amino acid.

Finally, the deprotection of brominated analogue **92** was also pursued, so that an investigation of the impact of the halogen on the photophysical properties of this chromophore could be undertaken. This deprotection proceeded well, with ester hydrolysis at room temperature followed by Cbz-removal under acidic conditions. This gave deprotected amino acid **97** in an 80% yield over two steps (**Scheme 39**).
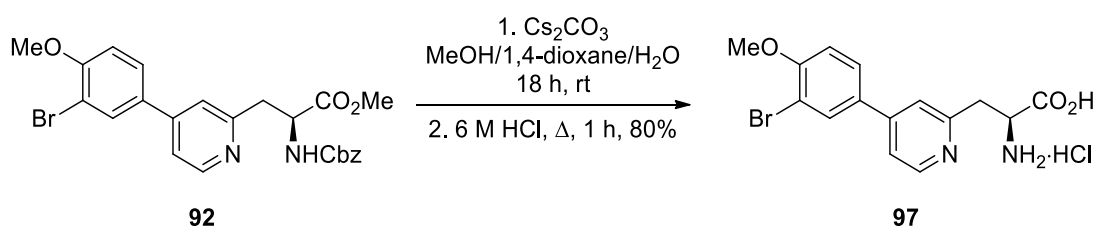
Scheme 39: *Deprotection of brominated pyridine derived amino acid **92**.*

2.5 Fluorescent Properties of Pyridine Derived *α*-Amino Acids

Following the synthesis of pyridine derived amino acid **80**, as well as the synthesis of several novel pyridine derived amino acids with extended conjugation, the photophysical properties of these analogues were investigated. First, the absorbance and emission spectra of biaryl amino acid **80** (**Figure 24**) were

59

compared to 4-methoxyphenyl extended analogue **94a** (**Figure 25**) and styryl analogue **96** (**Figure 26**). Although styryl analogue **96** still contained a Cbz-protecting group, it was proposed that this would not have a large impact on the photophysical properties of **96**, due to the absorption and emission of the Cbz-protecting group being more blue shifted and outwith the spectroscopic range of interest. In addition to this, having the amine of the amino acid protected mimics the environment of an amino acid in a peptide, and it has been shown that simple peptide incorporation does not drastically alter the fluorescence of amino acid residues (unless due to environmental sensitivity).[20]

Figure 24*: Absorbance and emission spectra of amino acid **80**. Measured in MeOH at 5 µM, excitation at 283 nm.*

Figure 25*: Absorbance and emission spectra of amino acid **94a**. Measured in MeOH at 5 µM, excitation at 264 nm.*
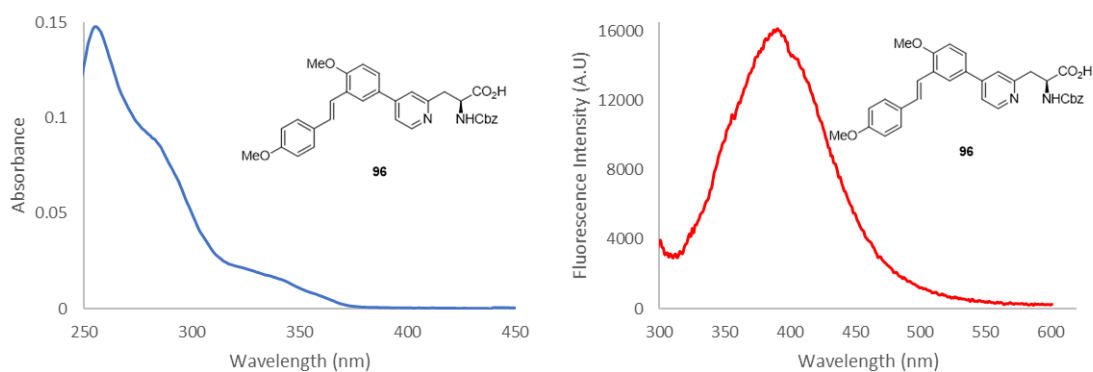
Figure 26: Absorbance and emission spectra of Cbz-protected amino acid 96. Measured in MeOH at 5 µM, excitation at 260 nm.

Comparing the normalised emission spectra of these three analogues, it is observed that both **94a** and **96** demonstrated a red-shifted emission in comparison to that of **80** (**Figure 27**). For simple biaryl **80**, an emission maxima of 366 nm was observed, whereas for the styryl analogue **96**, an emission maxima of 390 nm was observed. Most remarkable, however, was the emission of triaryl analogue **94a**, which demonstrated a largely red-shifted emission maxima of 450 nm. After considering the fluorescent properties of these analogues, it was decided that focus would be on further measurements of the photophysical properties of triaryl analogue **94a**, rather than styryl analogue **96**.
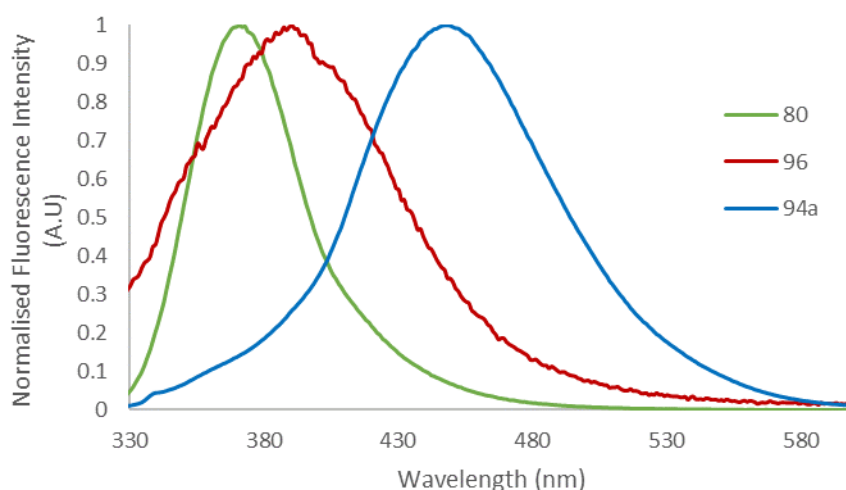
Figure 27: Normalised fluorescence intensity of three methoxy pyridine analogues, amino acid 80, Heck cross-coupling product 96 and Suzuki-Miyaura product 94a. Measured in MeOH.

The absorbance and emission spectra of brominated analogue **97** (**Figure 28**) and the other Suzuki-Miyaura coupled products (naphthyl analogue **94b** (**Figure 29**) and

trifluoromethyl analogue **94c** (**Figure 30**)) were also investigated. All three of these compounds exhibited similar absorption properties, with absorbance maxima stretching to 300 nm. Brominated analogue **97** displayed an emission maxima of 380 nm, which was not significantly different to the emission displayed by non-halogenated analogue **80**. Naphthyl analogue **94b** show two key peaks, one with an emission maxima of around 390 nm and a second red-shifted peak at 510 nm which stretches past 600 nm. It is proposed that these two bands are a result of locally excited and charge transfer bands respectively. For the trifluoromethylated analogue **94c**, two bands are again visible. Here, however, the locally excited state (360 nm) is much more prominent than the charge transfer (420 nm), likely as a result of a reduced charge transfer due to the electron withdrawing nature of the trifluoromethyl substituent.
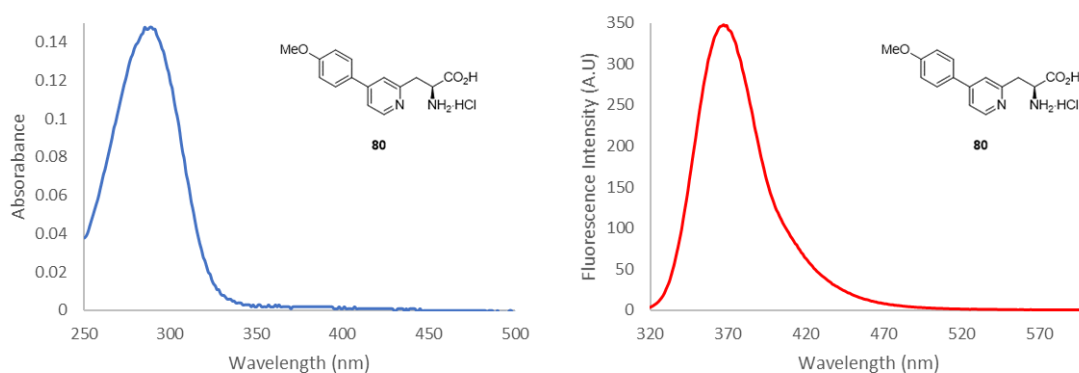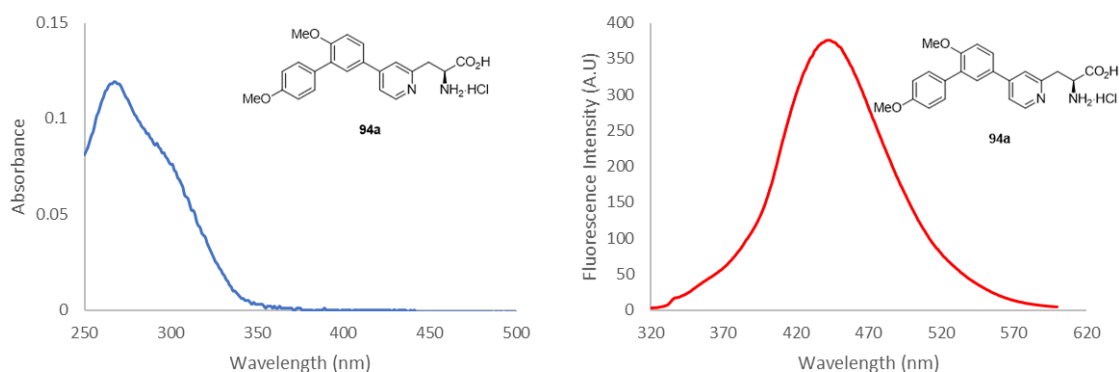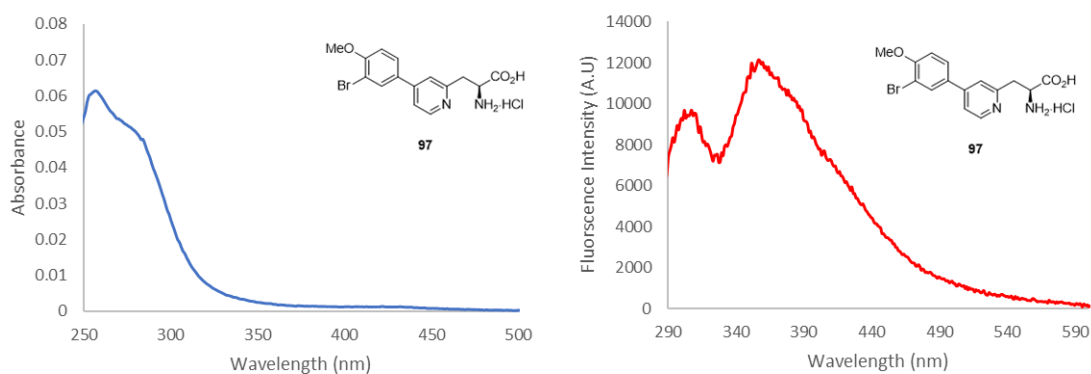

Figure 28: *Absorbance and emission spectra of amino acid* **97**. *Measured in MeOH at 5 µM, excitation at 260 nm.*
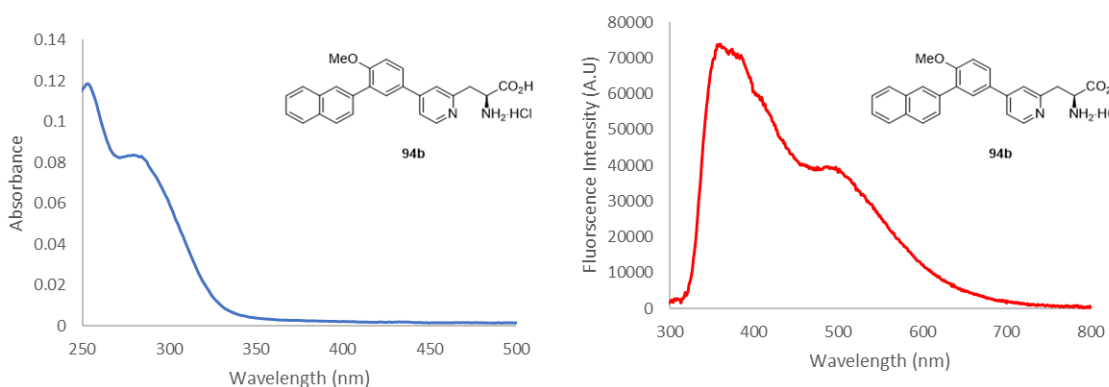
Figure 29: *Absorbance and emission spectra of amino acid* **94b**. *Measured in MeOH at 5 µM, excitation at 255 nm.*
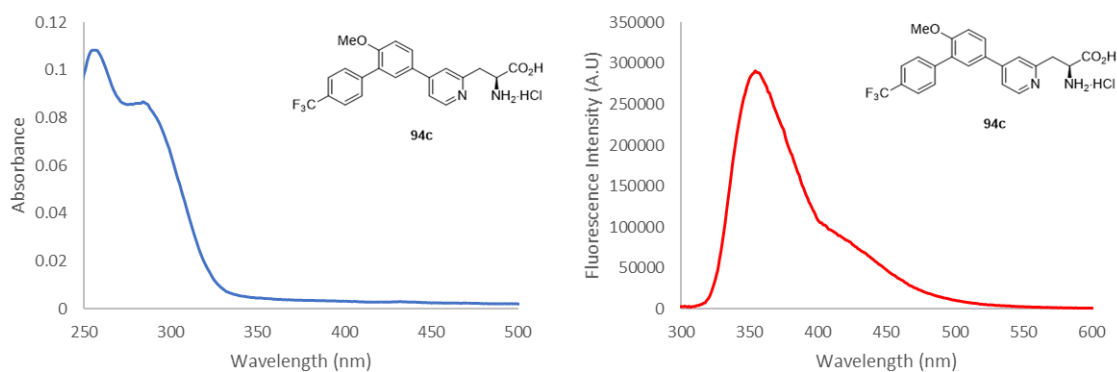
Figure 30*: Absorbance and emission spectra of amino acid **94c**. Measured in MeOH at 5 µM, excitation at 260 nm.*

Following the measurement of absorbance and emission for these analogues, further investigation of their photophysical properties was undertaken. Molar extinction coefficients (ε) and quantum yields (Φ) were measured in order to determine the brightness of these compounds. The molar extinction coefficient is a measure of how strongly a compound absorbs light, and was determined by plotting a straight line graph of the absorbance of each analogue *vs* the concentration at which the measurement was taken. Quantum yields were determined through a comparative method (using tryptophan and anthracence as standards), dependent upon the absorbance wavelength required for excitation. This was achieved by measuring each standard and sample at five known concentrations and then plotting a straight-line graph of their integrated fluorescence intensity *vs* absorbance. The gradient of these lines could then be compared using **Equation 3** to give a quantum yield for each analogue.

$$\phi_x = \phi_{ST}\left(\frac{Grad_{ST}}{Grad_x}\right)\left(\frac{\eta_x^2}{\eta_{ST}^2}\right)$$

Equation 3*: Equation for the comparative determination of quantum yield. ST = standard. X = novel compound. Grad = gradient. η = refractive index of the solvent. η = 1.333 for water, 1.361 for ethanol and 1.331 for methanol.*

Decreases in fluorescence quantum yields have been reported upon halogen substitution because of the "heavy halogen effect". This was observed for brominated analogue **97**, where a brightness could not be calculated owing to its weak emission intensity (**Table 2**). It was found that the new analogues were all less bright than biaryl **80**. This was unsurprising, as it has been frequently reported that

63

the addition of extra aryl rings may reduce quantum yield as a result of additional vibrational and rotational modes available to the compound.[1] Relaxation through these modes red-shifts the emission of fluorophores but also provides alternative pathways to the ground state through non-radiative processes, thus depleting the number of photons emitted by a compound. As such, fluorophore design is about compromise between the two properties and fluorophores must be chosen for specific applications. Of the three Suzuki-Miyaura coupling products, naphthyl analogue **94b** showed the most red-shifted emission spectra, however also demonstrated the lowest brightness. Trifluoromethyl analogue **94c** was the brightest, with a quantum yield of 0.2, however, this amino acid demonstrated the least red-shifted spectra. Finally, triaryl analogue **94a**, demonstrated an intermediate brightness between the other two analogues as well as an excellent red-shift in emission band. As such, it was decided that further experiments would be undertaken with this analogue (**94a**), as well as with the original amino acid **80**. These experiments would determine the impact of additional aryl rings on the environmental sensitivity of these fluorophores.
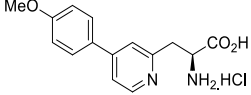
Amino Acid	Absorption Maximum (nm)	Emission Maximum (nm)	Stokes Shift (nm)	Molar Extinction Coefficient (cm^{-1} M^{-1})	Quantum Yield (Φ)	Brightness (cm^{-1} M^{-1})
80	283	366	83	25,920	0.46	11 923
97	260 (286)	360	100 (74)	-	-	-
94a	264 (304)	445	181	19,304	0.13	2590
94b	255 (295)	361 (495)	106 (200)	20,177	0.08	1614
94c	260 (288)	357	71	19,316	0.2	3863
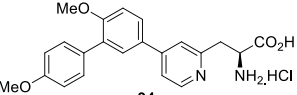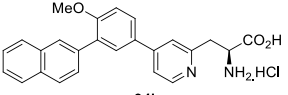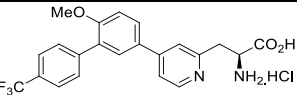
Table 2: *Photophysical properties of amino acids **80, 97** and **94a–94c**.*

Finally, computational studies were undertaken which confirmed the charge transfer nature of these analogues. The geometries of biaryl amino acid **80** and triaryl analogue **94a** were optimised in methanol using DFT calculations with the wB97XD functional[85] and def2-TZVP basis set.[86] Population analysis was performed at the same level of theory using Gaussian 16. This allowed for the visualisation of the HOMO and LUMO of each of these analogues using Avogadro software. For biaryl amino acid **80**, it was observed that the electron density of the HOMO is localised around the 4-methoxyphenyl ring, whereas in the LUMO significantly more electron density is localised around the pyridine ring (**Figure 31**). This supported the theory that the emission exhibited by this compound is a result of intramolecular charge transfer from the electron rich 4-methoxyphenyl ring to the electron deficient pyridine ring.[87]
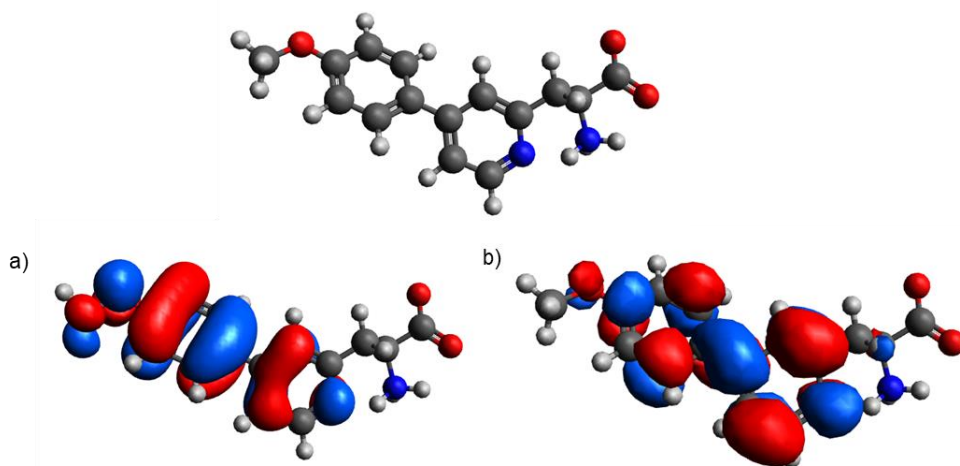
*Figure 31: Visualisation of the a) HOMO and b) LUMO of amino acid **80**.*

The visualisation of the HOMO and LUMO of triaryl amino acid **94a** showed similar results (**Figure 32**). Electron density in the HOMO was localised on the new 4-methoxyphenyl ring and across to the central phenyl ring, with almost no contribution from the pyridine ring. Electron density in the LUMO was mostly centred on the pyridine ring. Again, this suggested that a charge transfer between the electron rich aromatic rings and the electron poor pyridine moiety contributed to the emission of this analogue.
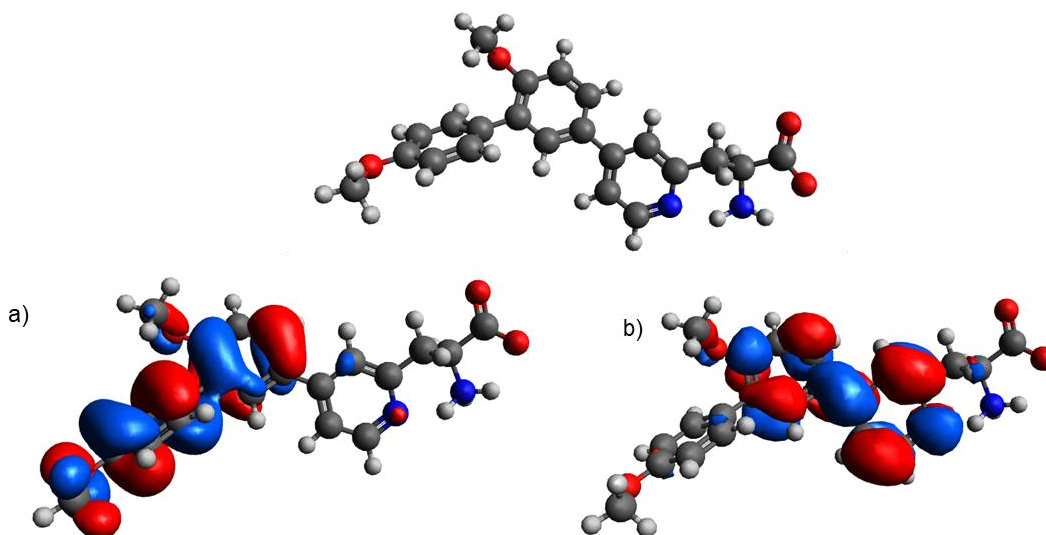
Figure 32: Visualisation of the a) HOMO and b) LUMO of biphenyl amino acid 94a.

2.6 Environmental Sensitivity of Pyridine Derived *α*-Amino Acids

Fluorophores which exhibit environmental sensitivity can be used to probe different environments, with a change in λ_{abs}, λ_{em} or Φ being used to report on information such as environmental polarity, acidity or viscosity. The simplest measure of a fluorophore's environmental sensitivity is an investigation into how the Stokes shift of the fluorophore changes in solvents of different polarity. More polar solvents tend to shift emission spectra to a longer wavelength owing to additional stabilisation of the excited state (**Figure 33**).[10] As most fluorophores contain some type of charge transfer system, they are often highly polar compounds and so stabilisation of the excited state can lead to large shifts in wavelength. Non-polar compounds tend to show much less sensitivity to solvent changes.
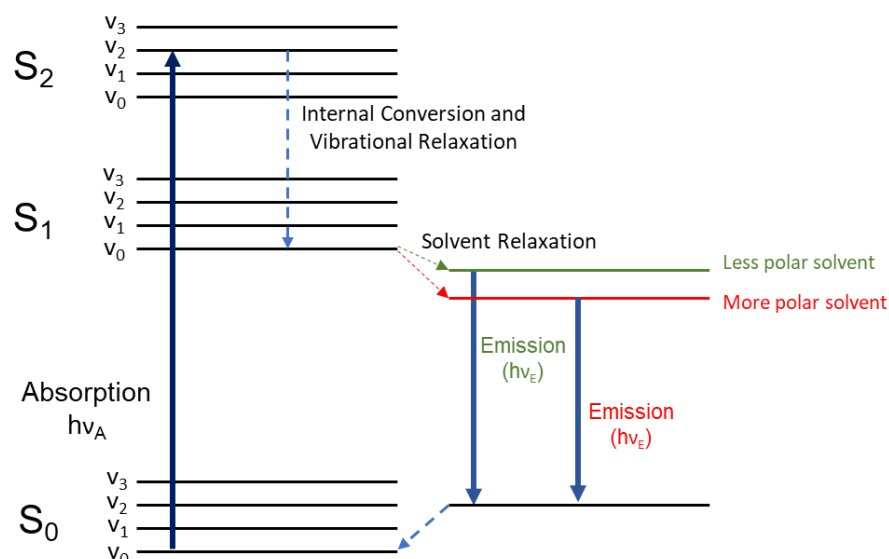
Figure 33: *Jablonski diagram showing solvent relaxation effects.*

Changes in emission wavelength that rely simply on a solvent dipole can be called "general" solvent effects and are described in basic terms by the Lippert-Mataga equation (**Equation 4**).[10] The solvent sensitivity of a fluorophore can thus be estimated by a Lippert-Mataga plot, which is a plot of Stokes shift verses the orientation polarisability of the solvent (Δf).[88–90] However, specific solvent effects can also impact on the wavelength of emission which can lead to deviations from a linear Lippert-Mataga plot. Such interactions include hydrogen bonding, preferential solvation, acid-base chemistry or charge-transfer interactions.[10] These must be taken into consideration when determining the suitability of a fluorophore to report on environmental polarity.

$$\dot{v}_A - \dot{v}_F = \frac{2\Delta f}{hca^3}(\mu_E - \mu_G)^2 + k$$

Equation 4: *Lippert-Mataga equation. Where h= Plancks constant (6.6256 × 10^{−34} m² kg s⁻¹), c = speed of light in a vacuum (2.997 × 10⁸ m s⁻¹), a is the radius of the cavity in which the fluorophore resides, $\bar{v}_A$ and $\bar{v}_F$ are the wavenumbers (cm⁻¹) of absorption and emission respectively. Δf is the orientation polarisability of the solvent.*

Previous work in the Sutherland group investigated the environmental sensitivity of amino acid **80** by placing the analogue in different solvents (**Figure 34**).[36] There was no shift in absorption maxima when placed in different solvents, showing the minimal

impact of solvation on the ground state energy. However, the emission maxima for the fluorophore was red-shifted with increasing solvent polarity.
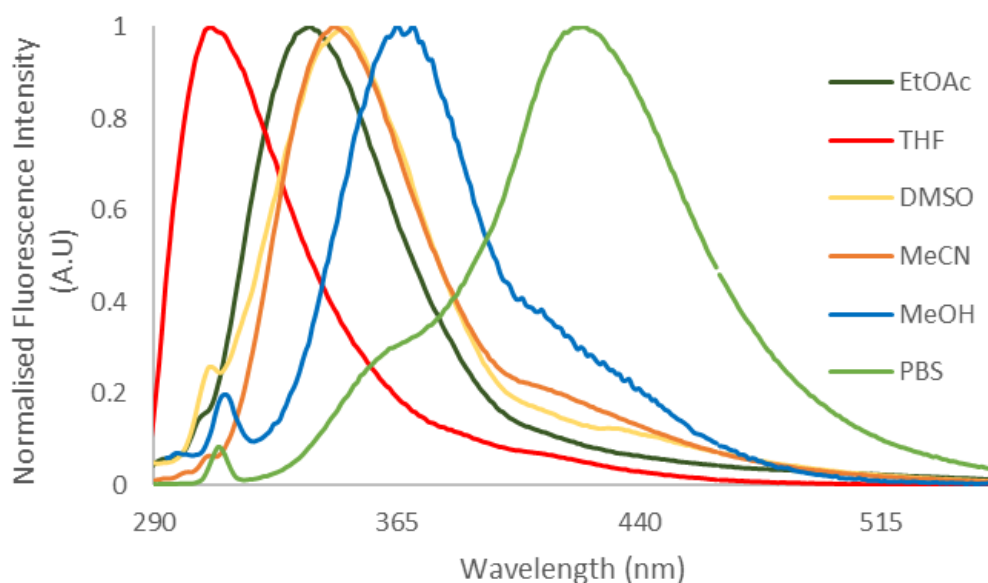
Figure 34: *Solvatochromic properties of β-pyridyl α-amino acid **80**, measured at 5µM. Measurements by Dr. Jonathan Bell.*

Narrow bands can be seen for less polar solvents such as ethyl acetate and tetrahydrofuran, while a second band around 420 nm started to become evident in more polar solvents – particularly visible in the emission spectra in methanol. In buffer solution, this second red-shifted band appears to become the more prominent state (430 nm), with a smaller blue-shifted band at 365 nm. It was proposed that these two bands are the locally excited (LE) and charge transfer (CT) states. The absorption maxima for most of the solvents measured had a good correlation when plotted in a Lippert-Mataga plot (**Figure 35**), indicating that shifts in their emission maxima were for the most part a result of general solvent effects. However, the emission maxima in phosphate-buffered saline (PBS) did not follow the general trend, which indicated it was a result of more specific solvent effects. Owing to the polar nature of the fluorophore and the presence of an electron-donating and electron-withdrawing group, it seemed plausible that this significant red-shift in the emission maxima observed in PBS could be a result of stabilisation of the charge-transfer state.
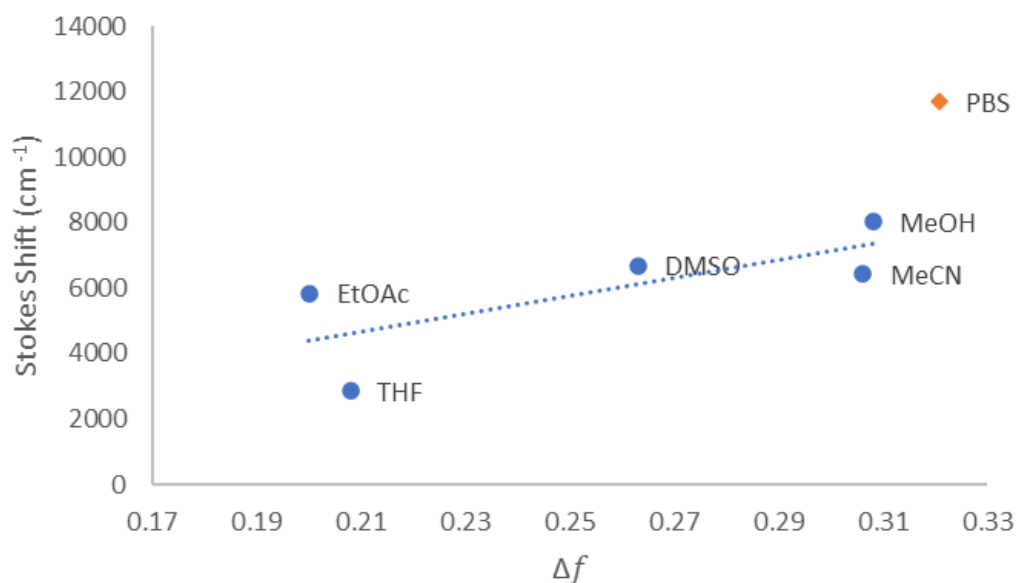
*Figure 35: Lippert-Mataga plot of Stokes Shift vs solvent polarizability factor for amino acid **80**.*

A similar experiment was performed with triaryl analogue **94a**. Again, absorption maxima were independent of solvent used, which suggested that the solvent choice had little effect on the fluorophore in the ground state. However, emission maxima were highly solvent sensitive which suggested that the compound was largely affected by solvent in the excited state (**Figure 36**).
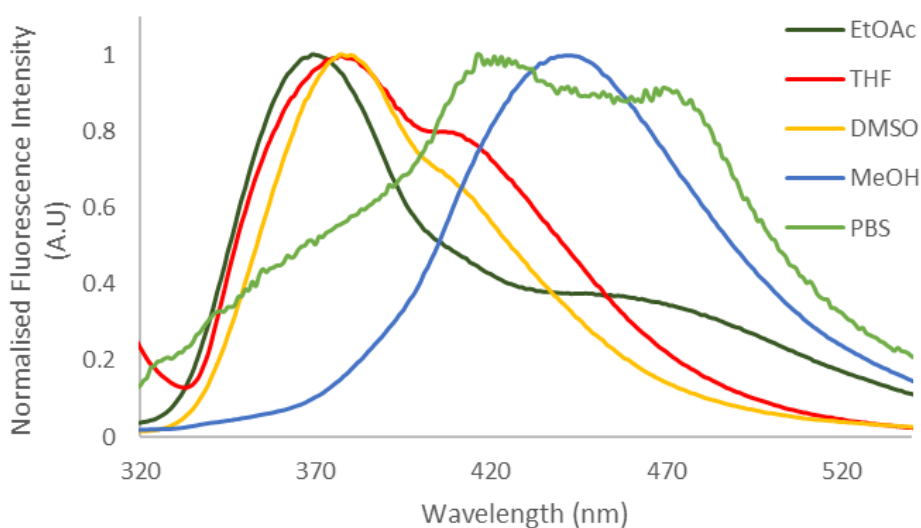
*Figure 36: Solvatochromic properties of amino acid **94a**. Measured at 5µM.*

Generally, triaryl analogue **94a** displayed a blue-shifted maxima in less polar solvents (ethyl acetate/tetrahydrofuran) and a more red-shifted emission in more polar solvents (methanol/phosphate-buffered saline). As can be seen from the Lippert plot for this compound (**Figure 37**), generally a good relationship between solvent polarity and compound dipole relaxation is seen. As such, this amino acid can be assumed to have potential as a solvatochromic probe. Not plotted, however, are the secondary (red-shifted) peaks observed which are proposed to be CT states. This is most evident in PBS where two distinct peaks are visible. Only in methanol is one band visible, however owing to the broadness of this peak it is proposed that this is a result of overlap between the LE and CT states.
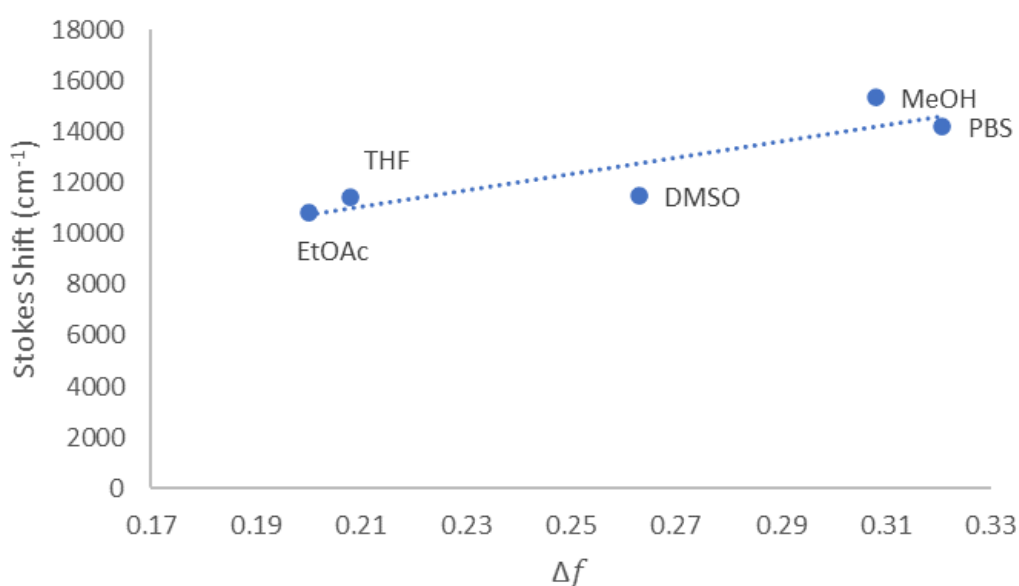
Figure 37: Lippert-Mataga plot for novel amino acid **94a**.

The pH dependency of the amino acids was next investigated. It was proposed that as each of these analogues contain a pyridine ring, they should be sensitive to acidic environments, whereby protonation of the pyridine nitrogen would increase the dipole across the chromophore (**Figure 38**).[91,92]
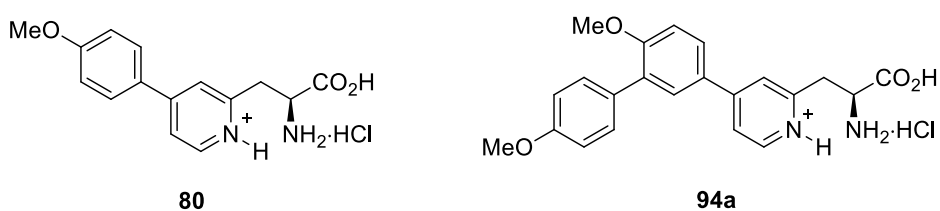
Figure 38: Proposed structure of protonated amino acids **80** and **94a**.

Previous work in the group showed that this was the case for amino acid **80**, with a red-shift in absorption and emission maxima observed at pH 1. Here, a more in-depth pH study was undertaken where the effect of varying concentrations of acid was analysed. It was observed that even a small addition of acid, to give a pH 6 solution was enough to red-shift the absorption maximum of this compound from 283 nm to 338 nm (**Figure 39**). These changes in absorption maxima were a result of changes to the molecules ground state energy due to the expected protonation. Pyridine has a pK$_a$H value of 5.2, while 4-methoxypyridine has been reported to have a pK$_a$H value of 6.5. It is proposed that the pyridine of amino acid **80** would have a pK$_a$H value similar to this, as the electron density across the system would be similar - which explained its tendency towards protonation at pH 6.
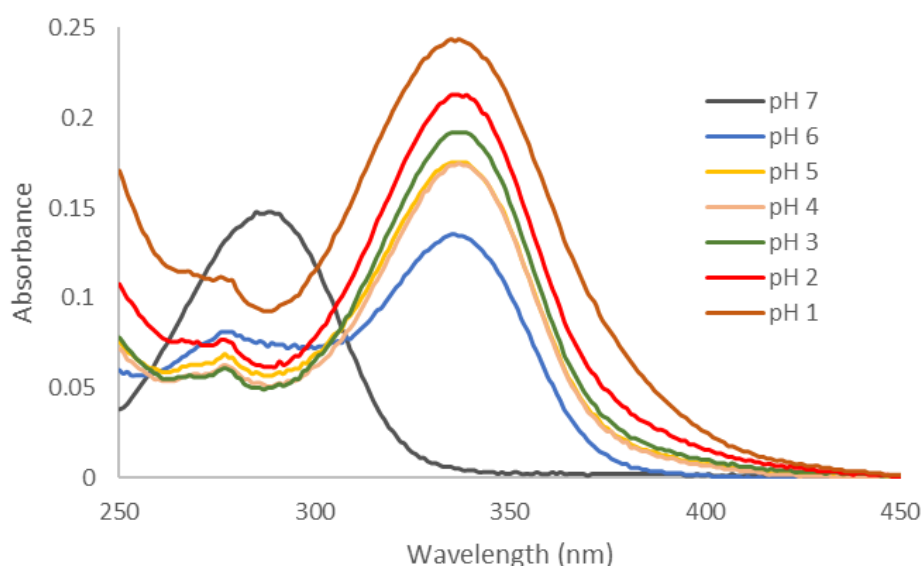
Figure 39: *Absorbance spectra of amino acid **80** between pH 7 and pH 1. Spectra measured in MeOH at 5 µM. 0.5 M HCl in MeOH used for acidification of solutions.*

A similar effect was observed in the emission spectra of this compound (**Figure 40**). Upon addition to a solution of pH 6, the emission maximum of analogue **80** was shifted from 365 nm to 420 nm. A decrease in fluorescence intensity was observed in acidic environments, but complete quenching was not observed.
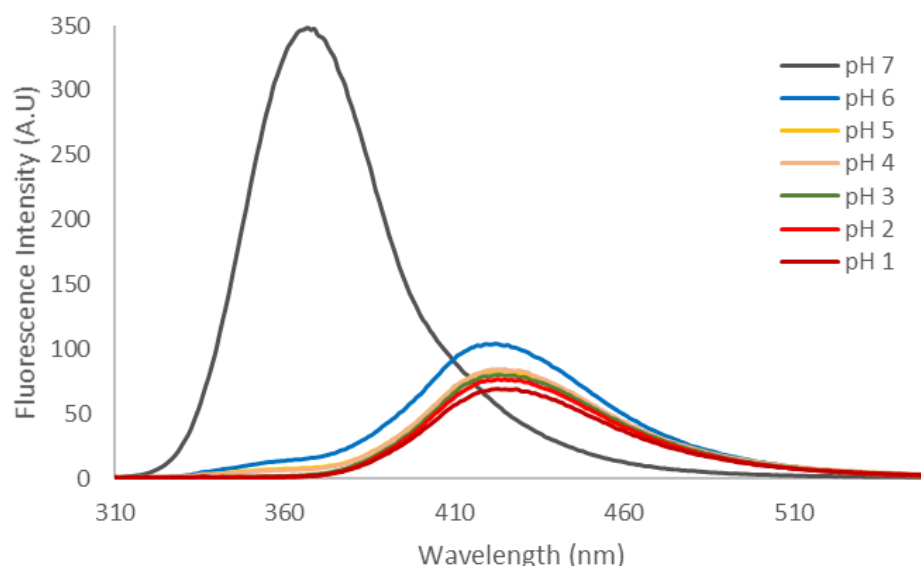
Figure 40*: Emission spectra of amino acid **80** between pH 7 and pH 1. Spectra measured in MeOH at 5 µM. 0.5 M HCl in MeOH used for acidification of solutions.*

The same experiment was repeated for triaryl pyridine analogue **94a**. Again, a red-shift in absorption maximum was observed (**Figure 41**). The main absorbance band peak shifted from 264 nm to 360 nm. Also evident was multiple absorption bands. These structural features were likely a result of the additional aryl ring leading to additional rotational bands when compared to the biaryl analogue.
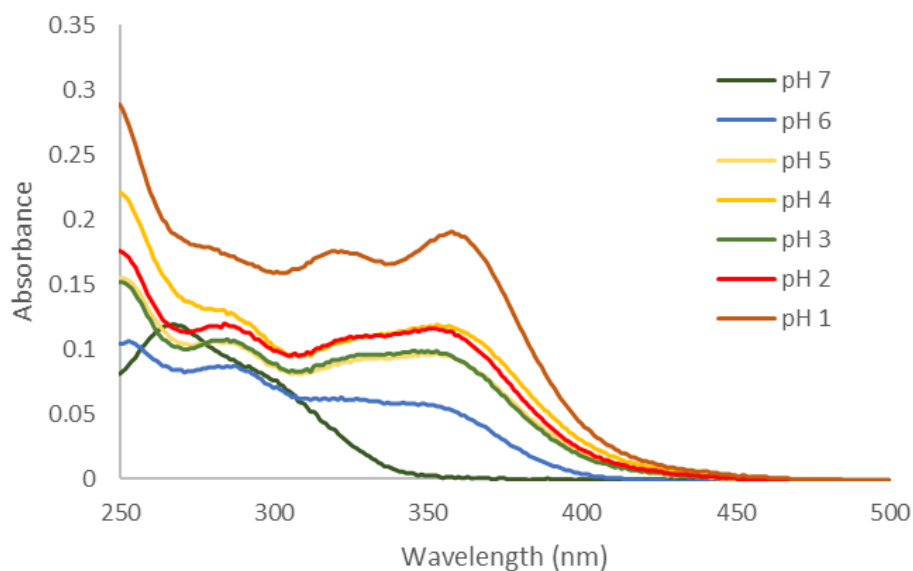
Figure 41*: Absorption spectra of novel pyridine amino acid **94a** between pH 7 and pH 1. Spectra measured in MeOH at 5 µM. 0.5 M HCl in MeOH used for acidification of solutions.*

In the emission spectra for this analogue, the fluorescence was strongly quenched upon the addition of acid (**Figure 42**). Unlike for the biaryl analogue, a red-shift in the emission maximum was not observed. Instead a slight blue shift to 426 nm was observed compared to 445 nm at pH 7. It was not clear why the two analogues demonstrated such different results in acidic environments, but one explanation could be that the additional aryl ring in triaryl analogue **94a** allows for a quenching mechanism to take place which was not observed in biaryl analogue **80**.[10]
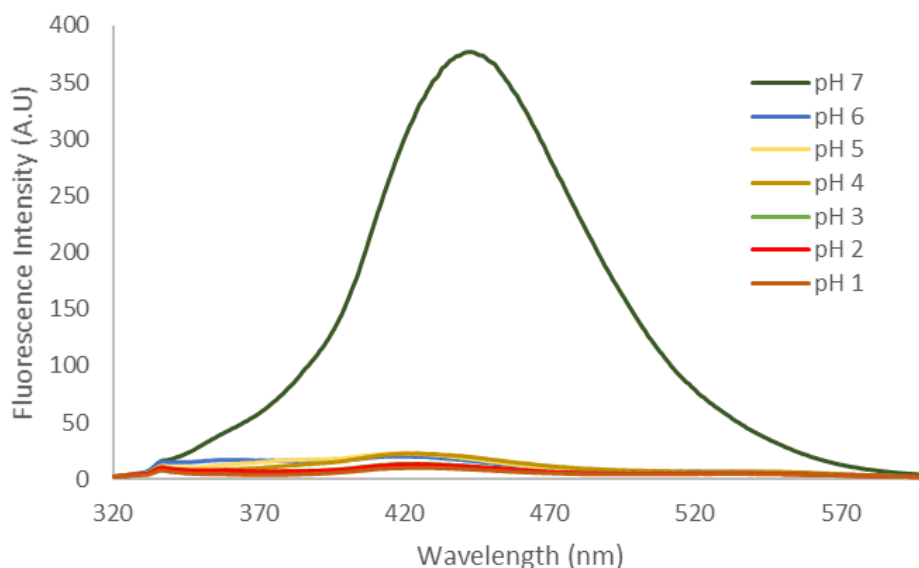
*Figure 42: Emission spectra of novel pyridine amino acid **94a** between pH 7 and pH 1. Spectra measured in MeOH at 5 µM. 0.5 M HCl in MeOH used for acidification of solutions.*

To investigate the degree of quenching present in acidic solutions for these analogues, the molar attenuation coefficient and quantum yield of each was measured at pH 2. A comparison of these analogues with their neutral counterparts is presented in **Table 3**. It was observed that the brightness of the protonated form of the simple pyridine **80** (5411 cm^{-1} M^{-1}) was approximately half that of the neutral analogue (11,923 cm^{-1} M^{-1}). It was, however, still a bright compound which could be useful for monitoring pH changes owing to a large shift in emission wavelength occurring upon a small change in pH. Literature reports show that fluorophores which respond to a change in acidity levels by a shift in absorption or emission maxima are limited, which makes this compound a potentially useful pH probe.[32]

Triaryl amino acid **94a** showed a large decrease in fluorescence intensity upon protonation, with a brightness of 374 cm^{-1} M^{-1}. This was almost ten times less bright

than the neutral form of compound **94a**. As a result, this probe would as such be more useful as an "on-off" sensing probe, where fluorescence is turned off in acidic environments.

Pyridine	Absorption Maximum (nm)	Emission Maximum (nm)	Stokes Shift (nm)	Molar Extinction Coefficient (cm⁻¹ M⁻¹)	Quantum Yield (Φ)	Brightness (cm⁻¹ M⁻¹)
80	283	366	83	25,920	0.46	11,923
80 (pH 2)	340	430	90	15,916	0.34	5411
94a	264	445	181	19,304	0.13	2590
94a (pH 2)	365	426	61	12,479	0.03	374
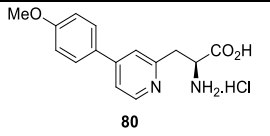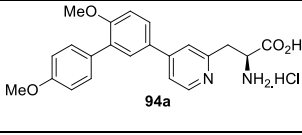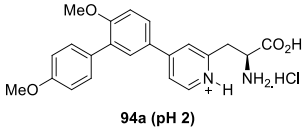
Table 3*: Comparison of the photophysical properties of amino acids **80** and **94a** in neutral and acidic (pH 2) environments.*

Finally, the amino acids were used in viscosity studies – to investigate how the fluorescence of each amino acid changed when placed in an environment where rotation is restricted. This was achieved by dissolution of biaryl amino acid **80** and triaryl amino acid **94a** in environments of increasing viscosity – a series of five solutions each with increasing percentages of ethylene glycol. As with the solvatochromism study, here no changes were observed in the absorption spectra of these compounds.

The emission spectrum of amino acid **80** in a solution of 20% ethylene glycol in methanol displayed a second band (**Figure 43a**). It could be observed from the normalised fluorescence spectra (**Figure 43b**), that this new band at 420 nm increased in intensity up to 60% glycol before reaching a maxima. At the same time, the band at 368 nm appeared to decrease in size. As methanol has a larger solvent orientation polarisability factor (0.31) than ethylene glycol (0.26), it was proposed that this change was a result of the viscosity change in solution rather than any solvent effects.
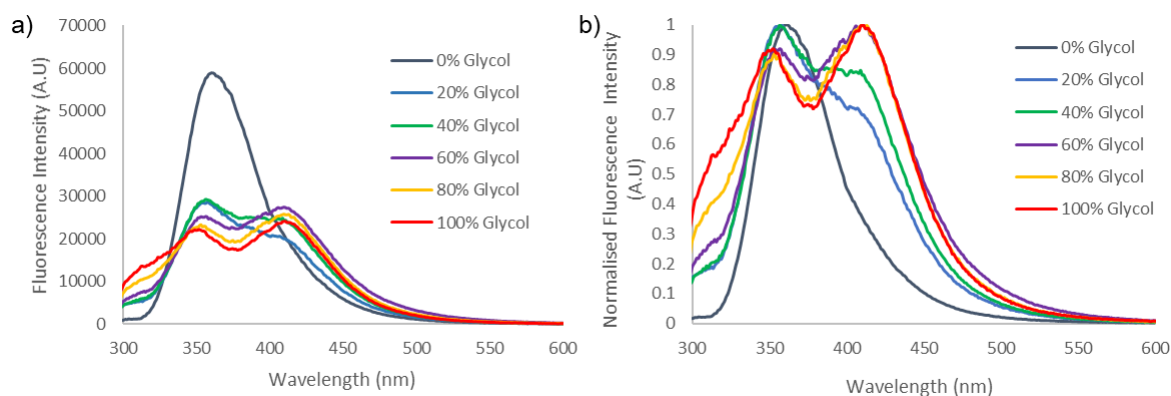
Figure 43*: The effect of solvent viscosity on the emission spectra of amino acid 80. a) measured emission spectra and b) normalised fluorescence intensity.*

The presence of two bands in an emission spectra is often used to indicate the existence of two excited states.[10] These are generally referred to as the locally excited (LE) or intramolecular charge transfer state (ICT). As it has been reported that ICT often results from the twisting of one group out of plane in order to facilitate electron transfer from a donor group to an acceptor group, this may also be described as twisted intramolecular charge-transfer (TICT).[24,33,34] A TICT state is often associated with a large red-shift in emission wavelength resulting from the increased polarity of this state. Upon excitation, a fluorophore which is free to rotate, relaxes into either the LE or TICT state, or a mixture of both. Emission from the LE state is usually bright, while emission from the TICT state often decays through non-radiative processes and is therefore either weaker in intensity or not observed in fluorescence spectra at all.

Upon placement of a fluorophore into a more viscous environment, rotation is slowed. It is proposed that here, as seen in methanol, upon excitation, the LE is generally favoured, where the molecule orients itself into a planar state. However, when solvent viscosity is increased, rotation around the central bond (**Figure 44**) is restricted and so some of the excited molecule population is found in both the LE and trapped TICT states (430 nm).
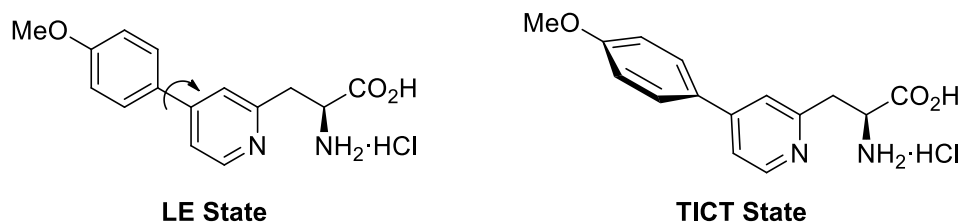
LE State   **TICT State**

Figure 44: Proposed locally excited (LE) and twisted-intramolecular charge transfer (TICT) states for amino acid 80.

Interestingly, for modified pyridine **94a**, a second peak was also observed in more viscous solutions, however in this case the peak was significantly blue-shifted (**Figure 45**). In general, it can be seen that as solvent viscosity was increased the peak at 442 nm decreases in intensity whereas the peak at 315 nm increases in intensity.
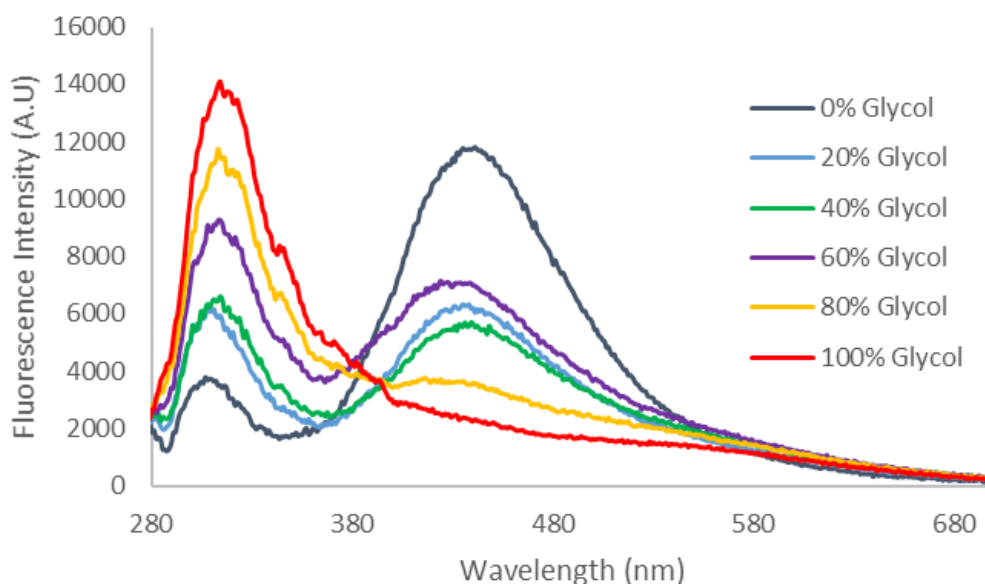
Figure 45: The effect of solvent viscosity on the emission spectra of amino acid 94a.

It was proposed that for this analogue, the reason for the large red-shift of emission maximum in methanol when compared to amino acid **80** is because the twisted triaryl fluorophore prefers to relax to a TICT state upon excitation. However, when the viscosity is increased, causing restricted rotation and a more planar conformation of the chromophore, this TICT state cannot be formed (e.g. 100% glycol) and so the fluorophore emits from the blue-shifted, LE state. This effect has been observed for other fluorophores in viscous solutions.[87]

Interestingly, the emission from glycol occurs at an even more blue-shifted wavelength than that in the less polar solvents tetrahydrofuran and ethyl acetate, which would not be expected in line with simple solvent effects (**Figure 46**). This far blue-shifted band also seems evident in the fluorescence of the compound in ethyl acetate and methanol, but not the other solvents. The causation of this peak is unclear. Further investigation is required to determine whether this is truly a LE state or a result of an alternative fluorescence effect. For example, far blue-shifted peaks have been reported as a result of aggregation induced emission.[93] Alternatively, it has been reported that solvent relaxation is much slower in viscous solvents such as ethylene glycol.[10] It is possible that emission here is a result of rapid emission from the locally excited state before solvent relaxation can occur.
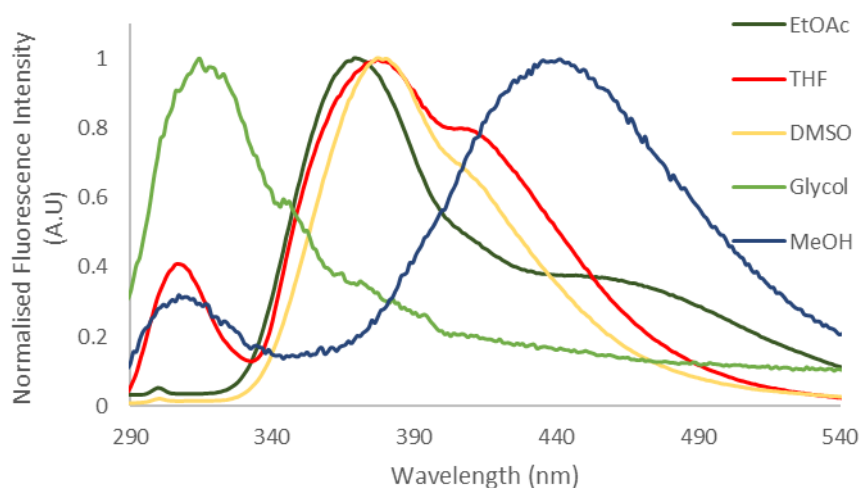
Figure 46*: The emission spectrum of amino acid **94a** in ethylene glycol compared to other less polar solvents (EtOAc, THF and DMSO).*

2.7 Summary

A route to fluorescent α-amino β-pyridyl amino acids was modified and optimised for the synthesis of lead compound **80**. Iron-catalysed bromination of this analogue, followed by Suzuki-Miyaura cross-coupling reactions allowed for the synthesis of a novel series of conjugated fluorescent amino acids. Their photophysical properties were analysed and it was decided that further investigation of biaryl amino acid **80** and triaryl amino acid **94a** was merited. Studies into the environmental sensitivity of these analogues were undertaken and showed that both exhibited sensitivity to solvent polarity, acidic environments and solvent viscosity.

2.8 Future Work

As biaryl amino acid **80** showed good sensitivity to pH, it is proposed that this probe could be used to image acidic environments. This could include the imaging of acidic environments within cells, including endosomes and lysosomes. For triaryl analogue **94a**, it is proposed that this analogue could find applications as a viscosity sensor owing to the drastic blue shift observed when this analogue is placed into ethylene glycol. First, however, it is proposed that an investigation into the cause of this blue shift should be undertaken. To determine whether this is a result of solvent viscosity or a possible aggregation effect, a study investigating the aggregation behaviour of this fluorophore is proposed. This would involve the placement of this fluorophore into a solvent such as THF while gradually increasing the concentration of a less polar solvent such as hexane.

For further investigations into the applications of these amino acids, the synthesis of larger quantities of these analogues would be required. The synthetic route discussed previously allowed for the late stage synthesis of a range of fluorescent amino acids and determination of the fluorescent properties of the lead compounds. As that has been achieved, it is proposed that an alternative synthesis to biaryl amino acid **80** and triaryl amino acid **94a** may be preferential. An alternative synthesis could allow for a shorter route to these analogues, and the late stage installation of the amino acid moiety, preventing any potential racemisation of the stereogenic centre during preparation. A suggested alternative route for the synthesis of biaryl amino acid **80** is shown below (**Scheme 40**). Suzuki-Miyaura cross-coupling reaction of 4-bromo-2-methylpyridine with 4-methoxyphenyl boronic acid would give the key fluorophore **98**.[94] Bromination would then give the alkyl bromide **99**.[95] Smith and co-workers recently described a novel synthesis of 4-cyanotryptophan through asymmetric phase-transfer catalysis,[45] based on early work by Lygo[96] and Corey.[97] In these early papers, a range of alkyl bromides are used for asymmetric C–C bond formation and so it is proposed that pyridine **99** be used as a potential substrate for this reaction. In the work by Smith and co-workers, this reaction was reported to proceed with >98% enantioselectivity on a large scale. If successful, hydrolysis and acid deprotection could then be undertaken on imine **100** to give desired amino acid **80** via a five-step route. Alternatively, selective hydrolysis of the imine followed by Fmoc-protection would give the amino acid suitably protected for peptide synthesis.
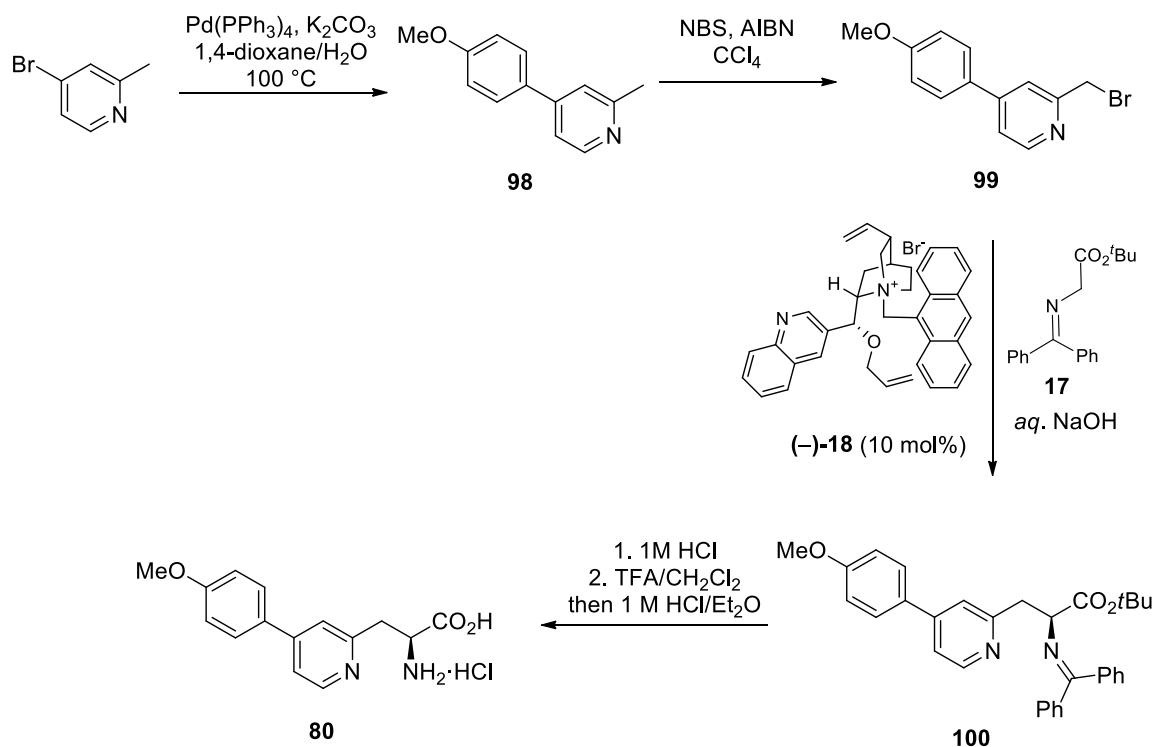
Scheme 40: *Alternative synthesis of fluorescent amino acid **80**.*

For the synthesis of triaryl amino acid **94a**, the same synthetic strategy described in **Scheme 40** could be applied. This would involve bromination of 4-(4-methoxyphenyl)-2-methylpyridine (**98**) using iron(III) triflimide, followed by Suzuki-Miyaura cross-coupling reaction, formation of the alkyl bromide and phase-transfer catalysis.

3.0 Benzotriazole Derived Fluorescent Amino Acids

3.1 Previous Work

Previous research in the Sutherland group described a simple and efficient route to benzotriazole derived α-amino acids.[81] The route began with the synthesis of protected L-3-aminoalanine **102** through Hofmann rearrangement[98] of *N*-Cbz-L-asparagine **101** and subsequent esterification (**Scheme 41**). A range of analogues were then prepared through the S$_N$Ar reaction of this amino acid with different 3-nitro-4-fluoroarene coupling partners. Reduction of the nitro group was followed by diazotisation,[99] utilising a polymer supported nitrite reagent and *p*-toluenesulfonic acid to form stable diazonium salt intermediates. Finally, intramolecular cyclisation gave a small library of amino acids bearing benzotriazole side-chains.[100]
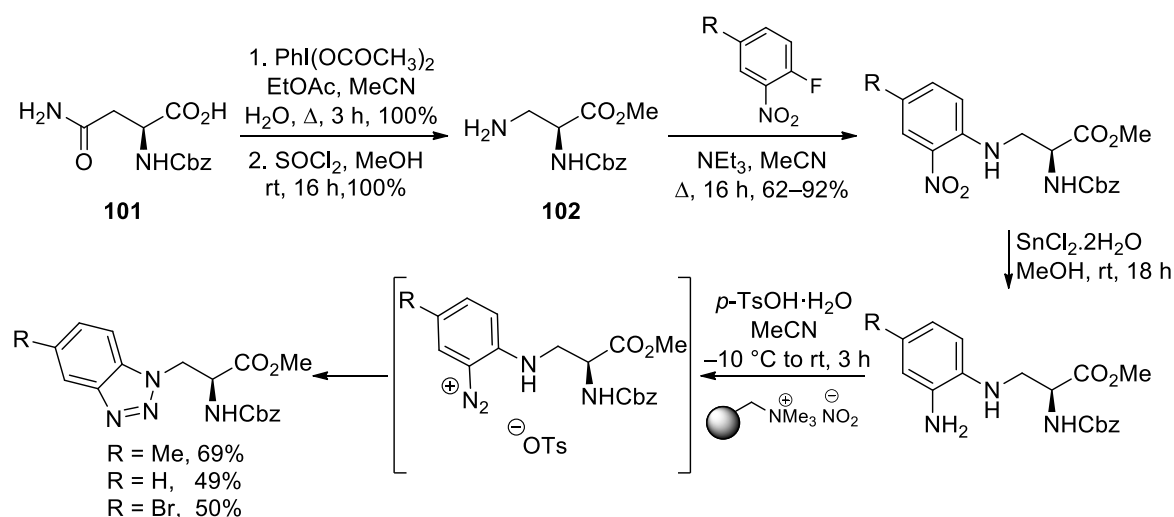
Scheme 41: Synthesis of benzotriazole derived α-amino acids.

The Suzuki-Miyaura cross-coupling of brominated analogue **103** with various aryl boronic acids was then investigated (**Scheme 42**), and this gave more conjugated systems with fluorescent properties.[81] These analogues demonstrated large Stokes shifts, with analysis after deprotection showing that methoxy analogue **104a** and naphthyl analogue **104b** displayed the most favourable photophysical properties. These compounds showed the largest quantum yields, and as a result, were the brightest fluorophores.
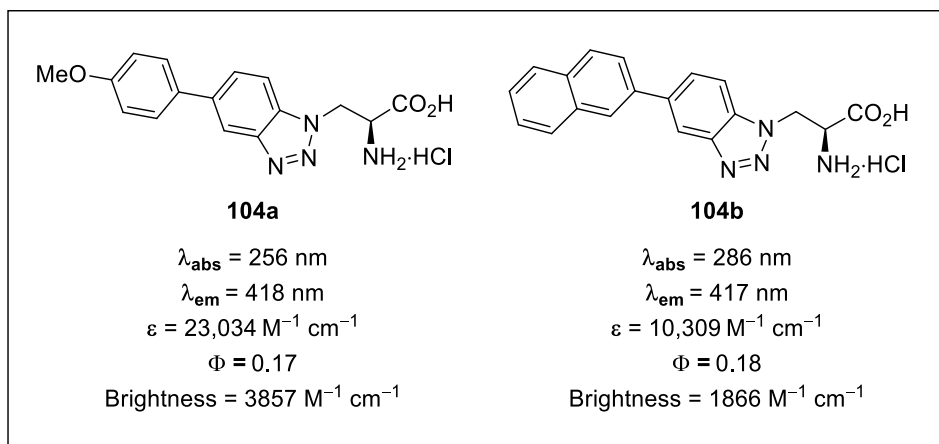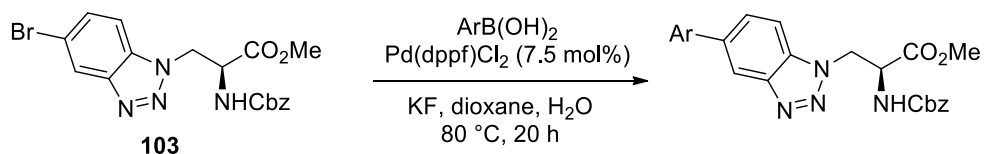
Scheme 42: *Suzuki-Miyaura cross-coupling of brominated benzotriazole **103** and brightest synthesised analogues **104a** and **104b** after deprotection.*

3.2 Project Aims

The aim of this project was to build on the design of previous fluorescent α-amino acids and synthesise analogues with extended (stretched) benzotriazole fluorophores. The lead compounds previously synthesised showed favourable photophysical properties in most regards, however it was proposed that increasing the conjugation across the fluorophore would red-shift the absorption and emission maxima for these analogues.[1] A red-shift in the absorption maxima was desirable to allow for imaging with these analogues to occur without the excitation of any naturally occuring fluorescent amino acids within a peptide or protein. To avoid drastic increases in the size of these compounds, which could disrupt peptide folding, it was proposed that this conjugation increase could be achieved through the synthesis of alkenyl or alkynyl analogues. The synthesis of similar extended analogues when compared to simple biaryl compounds has been shown to produce a red-shift in absorption and emission owing to extra conjugation across the fluorophore.[101] The synthesis of these compounds could be achieved from brominated analogue **103** through Heck or Sonogashira cross-coupling reactions (**Scheme 43**).
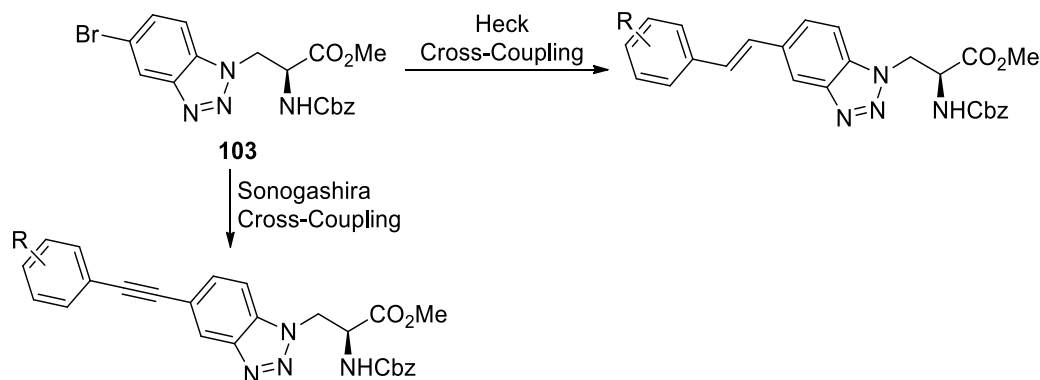
Scheme 43: *Proposed cross-coupling reactions of brominated benzotriazole **103***.

3.3 Synthesis of Alkynyl Benzotriazole Derived α-Amino Acids

Work on this project began with the synthesis of brominated benzotriazole **103**. Hofmann rearrangement of various *N*-protected L-asparagine derivatives to give *β*-amino L-alanine derivatives has been described by Yin and co-workers.[102] This procedure used the hypervalent iodine reagent (diacetoxyiodo)benzene (PIDA) and gave the desired products in short reaction times. This methodology was employed here for the large scale rearrangement of *N*-Cbz-L-asparagine **101** in a co-solvent mixture of ethyl acetate, acetonitrile and water (**Scheme 44**). Subsequent esterification with thionyl chloride in methanol proceeded smoothly, and allowed for the quantitative synthesis of protected L-3-aminoalanine **102** without the requirement for column chromatography.
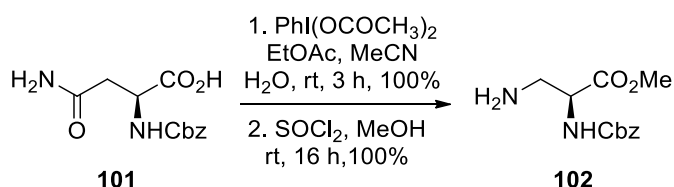
Scheme 44: *Hofmann rearrangement and esterification of N-Cbz-L-asparagine.*

Next, S_NAr reaction of **102** with 4-bromo-2-fluoro-nitroaniline was achieved and gave **105** in 92% yield (**Scheme 45**). This reaction proceeded with high selectivity for attack at the fluorine-substituted carbon and resulted in rapid reaction with full conversion observed overnight. In the next step, the nitro group was reduced using tin(II) dichloride and gave diamine **106** in 76% yield. Finally, diazotisation and cyclisation was required. The formation of stable aryl diazonium salts was described by Filimonov and co-workers in 2008 using a polymer supported nitrite reagent and *p*-toluenesulfonic acid.[99] These reactions occurred under mild conditions, avoiding

82

the use of sodium nitrite at elevated temperatures which can lead to the formation of toxic nitrogen oxides. In 2019 the Sutherland group reported the use of these stable diazonium salts in the formation of benzotriazoles through the diazotisation and intramolecular cyclisation of 1,2-aryldiamines.[100] This methodology was employed here to synthesise the diazonium intermediate **107**. In situ cyclisation of the amine moiety then gave benzotriazole **103** in 66% yield.
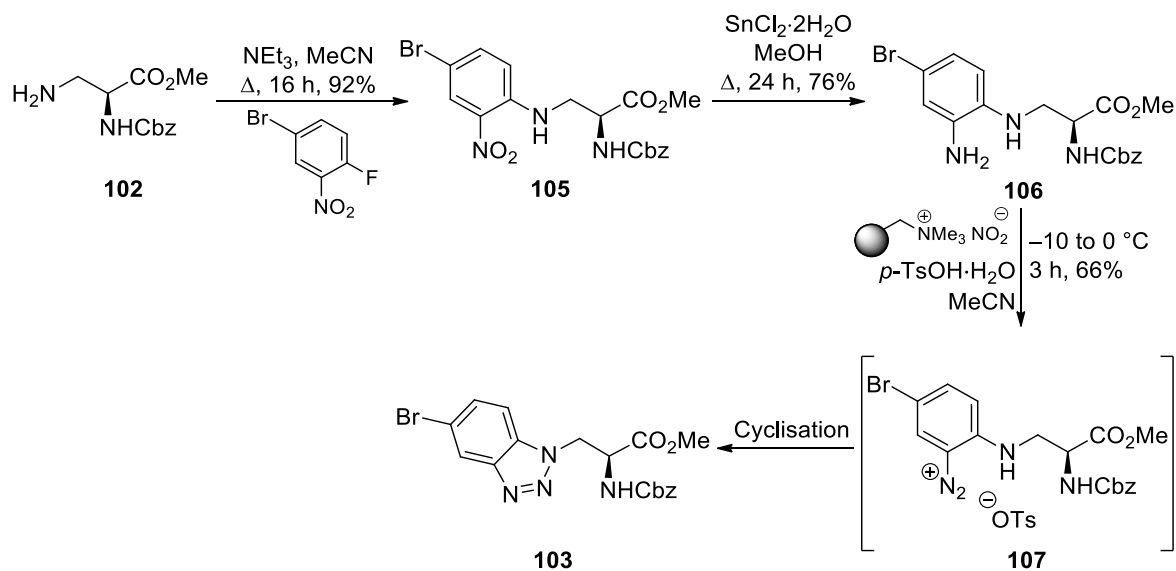
Scheme 45: Synthesis of brominated benzotriazole *103*.

Next, the Sonogashira cross-coupling of brominated analogue **103** with phenylacetylene was investigated. The use of PdCl2(PPh3)2 with copper(I) iodide was trialled (**Table 4**).[103,104] An initial attempt was made at room temperature, however no product was observed (entry 1). It was proposed that harsher conditions may be required for the coupling, however an increase in temperature also resulted in no observed product (entry 2). The catalyst loading of both the palladium pre-catalyst and copper(I) iodide were increased (entry 3) and the temperature was increased further (entry 4). However, under all of these conditions no product was detected. Only starting material and Glaser coupled alkyne product **109** were recovered from these reactions.

Table 4: *Attempted Sonogashira cross-coupling of brominated benzotriazole **103**.*
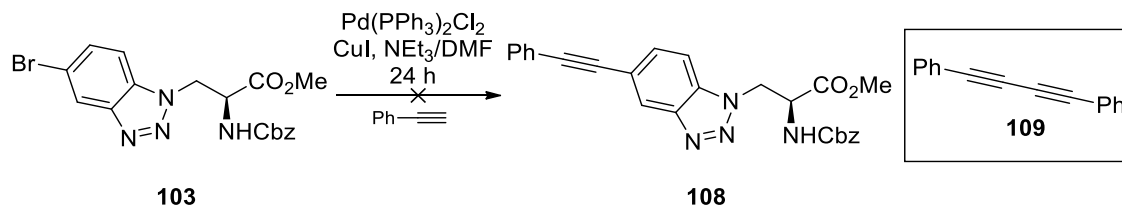
Entry	PdCl₂(PPh₃)₂ (mol%)	CuI (mol%)	Temperature (°C)	Yield of 108 (%)
1	5	10	rt	0
2	5	10	50	0
3	10	20	50	0
4	10	20	70	0

It was proposed that the use of an iodinated benzotriazole in place of the brominated analogue **103** would facilitate this cross-coupling owing to the weaker nature of the carbon-iodine bond which would allow for a more facile addition of Pd(0) into the carbon-halogen bond.[105] Many mild Sonogashira cross-couplings of aryl iodides have been reported at room temperature.[106] To synthesise this analogue, the same synthetic route as for the brominated analogue was proposed (**Scheme 46**). This would begin with an S$_N$Ar reaction of protected L-3-aminoalanine **102** with 4-iodo-2-nitrofluorobenzene to give **110** followed by reduction and benzotriazole formation. The first step, the S$_N$Ar reaction of **102** was successful and gave coupled product **110** in 89% yield.
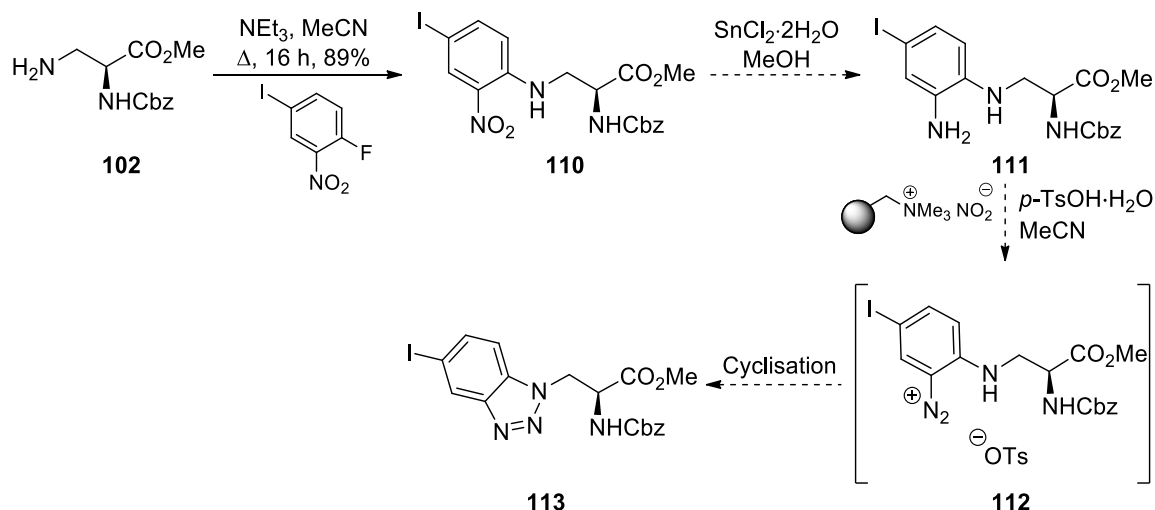
Scheme 46: S_NAr reaction of protected L-3-aminoalanine with 4-iodo-2-nitrofluorobenzene and proposed subsequent synthetic route to iodinated benzotriazole 113.

An initial attempt at reduction of the nitro group with tin(II) chloride gave diamine 111 in a moderate 48% yield (Table 5, entry 1). It was proposed that the carbon-iodine bond could be unstable under these conditions, and so a decrease of reaction temperature to 50 °C was investigated (entry 2). However, at the lower temperature, the reaction proceeded very slowly, resulting in a 10% yield for the same reaction time. As such, alternative reduction conditions were considered. The use of Pd/C with sodium borohydride resulted in no reaction (entry 3), whereas the use of zinc and acetic acid proved successful (entry 4). This gave aniline 111 in an excellent 85% yield after a 0.5 h reaction time.
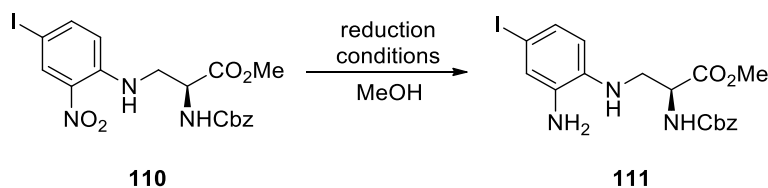
Entry	Reagents	Time (h)	Temperature (°C)	Yield (%)
1	SnCl$_2$·2H$_2$O	24	65	48
2	SnCl$_2$·2H$_2$O	24	50	10
3	Pd/C, NaBH$_4$	24	rt	N/A
4	Zn, AcOH	0.5	rt	85

Table 5: Reduction of nitro analogue 110 to 1,2-diamine 111.

Finally, application of the one-pot diazotisation and cyclisation methodology gave desired iodinated benzotriazole **113** in 65% yield, which was comparable to the yield for brominated analogue **103** (**Scheme 47**). This resulted in the development of a five-step synthesis of iodinated benzotriazole **113** in 49% overall yield.
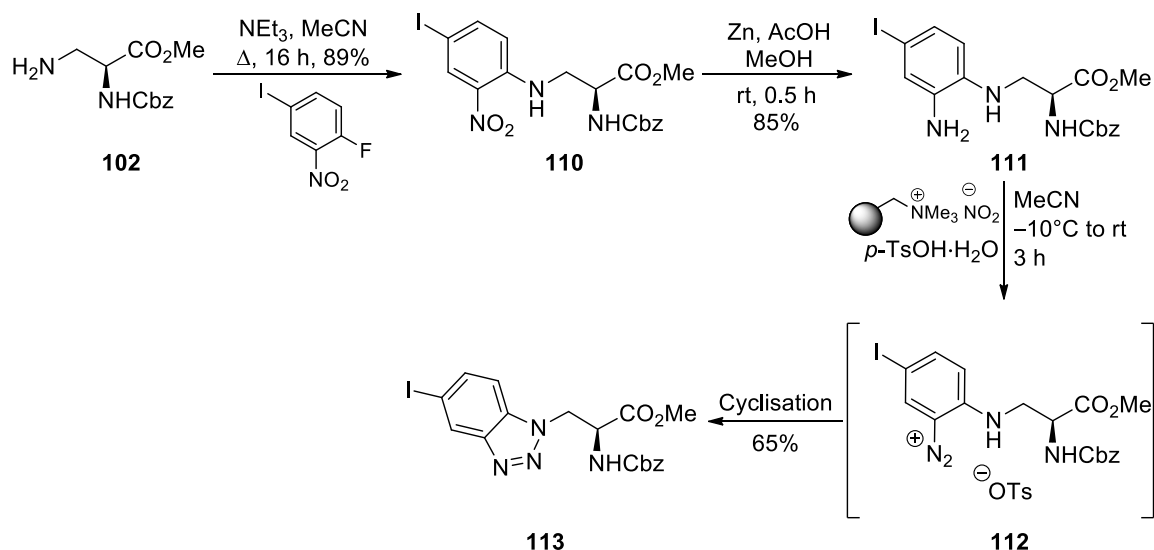
Scheme 47: Synthesis of iodinated benzotriazole 113.

The use of this benzotriazole for Sonogashira cross-couplings was next investigated, and with the weaker carbon-iodine bond these reactions proceeded smoothly (**Scheme 48**). The reaction was performed using $PdCl_2(PPh_3)_2$ (10 mol%), heating briefly (5 minutes) to 90 °C, followed by stirring at room temperature for 3 h.[103] It was proposed that this brief heating step was required to encourage formation of the active palladium(0) species from the pre-catalyst. Coupling with phenylacetylene and 4-fluorophenylacetylene gave the desired analogues **114a** and **114b** in 94% and 79% yields, respectively.
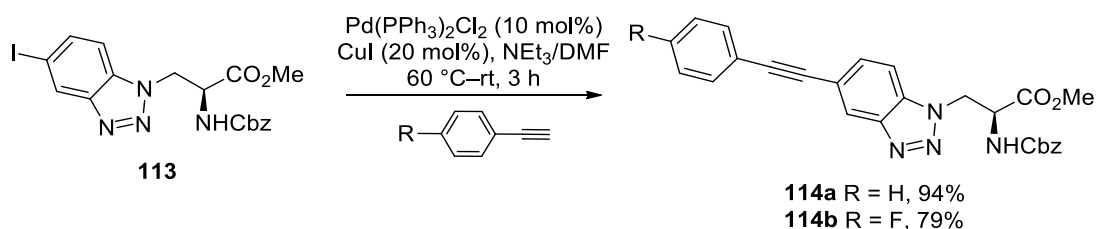
Scheme 48: Sonogashira cross-couplings of iodinated benzotriazole 113.

Before the synthesis of further analogues, the deprotection of these compounds was explored, using phenyl analogue **114a** (**Scheme 49**). A two-step deprotection method was considered, with ester hydrolysis followed by Cbz-protecting group

removal. The hydrolysis of the methyl ester was performed using caesium carbonate in a solvent mixture of methanol, dioxane and water, under mild basic conditions at room temperature. This gave carboxylic acid **115a** in 66% yield.
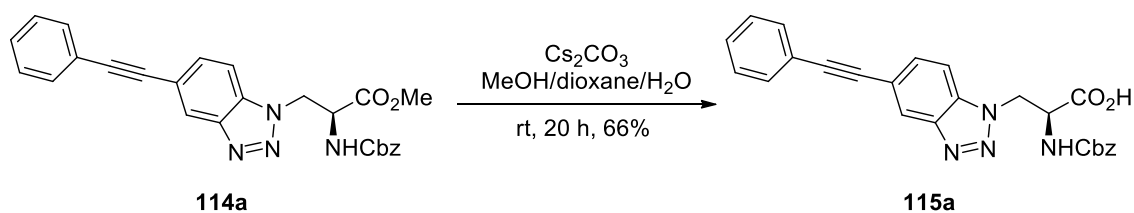
Scheme 49: Ester hydrolysis of 114a to give acid 115a.

Next, removal of the Cbz group using 6 M HCl was investigated. The initial attempt involved heating the reaction to 100 °C for 1 h.[36] However, under these conditions, decomposition of the starting material was observed (**Scheme 50**). The use of a shorter reaction time was explored, but decomposition was observed after just ten minutes. As such, it was proposed that the alkyne group was unstable under these strongly acidic conditions. It has been suggested that alkynes are stable under milder acidic conditions,[107] and so the deprotection was also trialled with 3 M HCl. However, under these conditions partial decomposition was observed, with no removal of the protecting group.
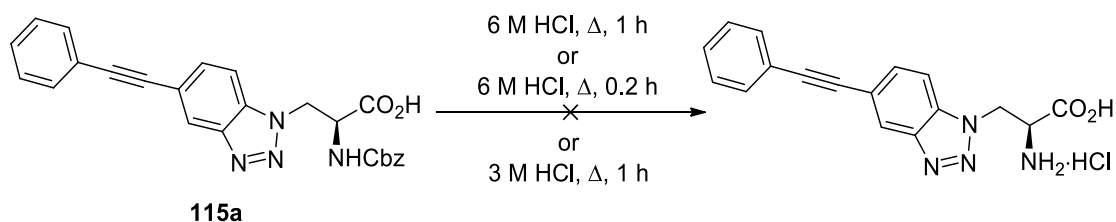
Scheme 50: Attempted acidic deprotection of Cbz-protecting group.

As traditional methods of Cbz-protecting group removal involving hydrogenation would be expected to result in reduction of the alkyne moiety, other methods for removal of the Cbz-protecting group were considered. The use of the Lewis acid, aluminium trichloride, with anisole as a scavenger as described by Williams and co-workers was investigated.[108] Under these conditions, no reaction at room temperature (**Table 6**, entry 1) or 40 °C (entry 2) was observed. A change in solvent to toluene allowed an increase of reaction temperature to 70 °C (entry 3). However, under these conditions, decomposition was observed – which could be explained by the poor solubility of **115a** in toluene. Therefore, a co-solvent mixture of

acetonitrile and 1,4-dioxane was trialled, resulting in no reaction at 60 °C (entry 4). As these solvents could coordinate to the Lewis acid and limit reactivity, two non-coordinating solvents, 1,2-dichloroethane and chlorobenzene were also investigated (entries 5 and 6). Both attempts led to decomposition of starting material.
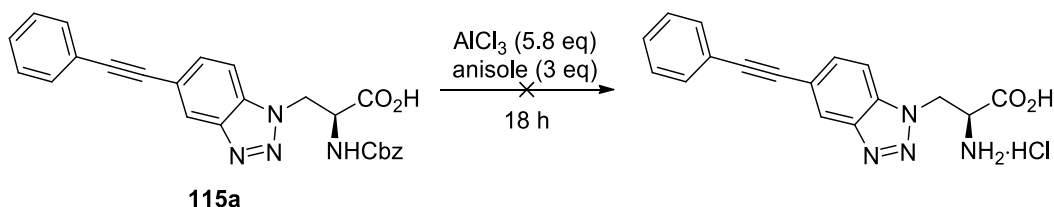
Entry	Solvent	Temperature (°C)	Comments
1	CH_2Cl_2	rt	no reaction
2	CH_2Cl_2	40	no reaction
3	toluene	70	decomposition
4	MeCN/1,4-dioxane	60	no reaction
5	1,2-dichloroethane	60	decomposition
6	chlorobenzene	60	decomposition

Table 6: *Attempted Cbz-deprotection of **115a** with a Lewis acid catalyst.*

The removal of Cbz groups has been reported under mild conditions using TFA in the presence of thioanisole at room temperature.[109,110] These conditions also led to decomposition of starting material (**Scheme 51**).
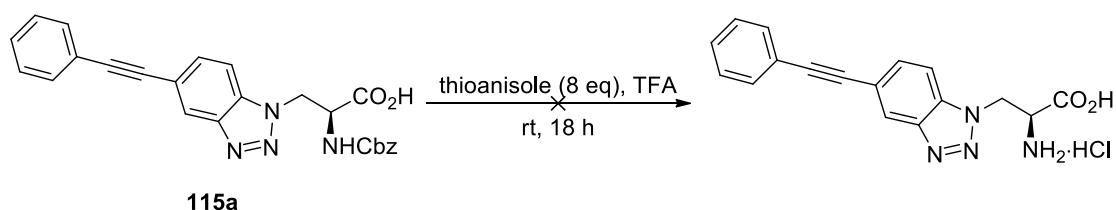
Scheme 51: *Attempted TFA deprotection of **115a**.*

Finally, barium hydroxide was considered as a reagent for Cbz-protecting group removal.[111] A co-solvent mixture of dimethoxyethane (DME) and water was used, under reflux for 24 h. Again, no product was isolated. Analysis of the crude reaction mixture by ^{1}H NMR spectroscopy suggested the loss of amino acid side-chain, which gave benzotriazole **116** (**Scheme 52**). These results suggested that under

basic conditions and high temperature, an elimination reaction was more facile than deprotection. At a lower temperature (60 °C), no reaction was observed.

Reaction conditions: BaOH$_2$·8H$_2$O, DME:H$_2$O (3:2), 100 °C, 24 h, converting **115a** to **116**.
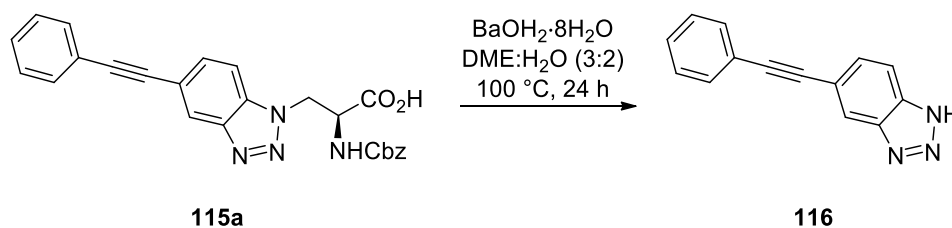
Scheme 52: Attempted Cbz-deprotection using barium hydroxide.

As a result of the inability to deprotect these amino acids, it was proposed that an alternative protecting group strategy was required. It was proposed that the use of the Boc-protecting group might allow facile deprotection at the end of a similar synthetic route, as these groups can be removed under much milder acidic conditions and several papers have reported Boc-protecting group removal in the presence of alkynes.[112–114] In addition, the Hofmann rearrangement of *N*-Boc protected asparagines has also been described.[98] Therefore, this route would begin from the Hofmann rearrangement of *N*-Boc protected asparagine **117** (**Scheme 53**). The reaction was successful and gave *N*-Boc-L-3-aminoalanine **118** in 84% yield. Following Cbz-protection of the free amine, esterification of **119** was achieved under literature conditions using methyl iodide.[115] Deprotection of the amine was then achieved through hydrogenation with 10% palladium on carbon and gave suitably protected L-3-aminoalanine analogue **121**. This multistep procedure involving amine protection and deprotection was required to avoid the use of thionyl chloride for the esterification step. It was predicted that the acidic conditions resulting from HCl formation in reaction with thionyl chloride would result in undesired deprotection of the Boc-protecting group.
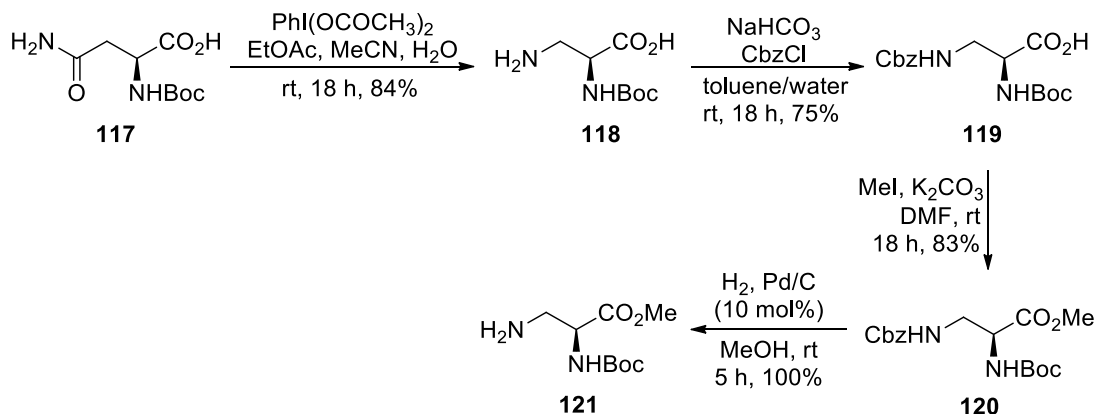
Scheme 53: *Synthesis of N-Boc L-3-aminoalanine **121**.*

The synthesis of Boc-protected amino acid **125** was then completed as for Cbz-protected analogue **113** (**Scheme 54**). The S_NAr reaction of amine **121** with 1-fluoro-4-iodonitrobenzene proceeded in 78% yield. This was followed by reduction with zinc and acetic acid and gave amine **123** in 91% yield. Diazotisation and cyclisation were then undertaken and gave *N*-Boc benzotriazole amino acid **125** in 70% yield. It should be noted that despite the acidic conditions required for the reduction and diazotisation steps, Boc-deprotection was generally avoided owing to the low temperatures and short reaction times.
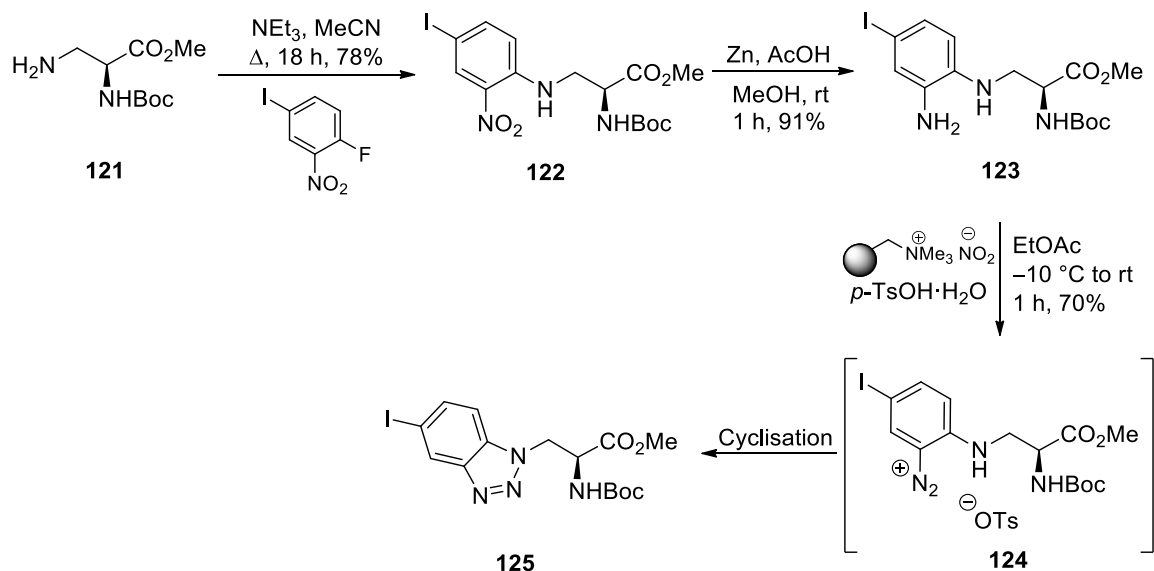
Scheme 54: *Synthesis of N-Boc protected benzotriazole **125**.*

Five alkynes were next synthesised through Sonogashira cross-coupling reactions of Boc-protected amino acid **125** with various phenylacetylenes. Again, these reactions utilised $PdCl_2(PPh_3)_2$ and copper(I) iodide in a DMF/triethylamine co-solvent mixture. This gave a series of benzotriazole derived amino acids, containing

extended chromophores (**Scheme 55**). An electronically neutral phenyl analogue **126a** was synthesised, along with two electron rich alkynes, methoxy analogue **126b** and dimethylamino analogue **126c**. Two electron poor alkynes were also synthesised, fluoro analogue **126d** and nitro analogue **126e**. Excellent yields of 78–97% were achieved for the cross-coupling reactions.

126a R = H, 85%
126b R = OMe, 97%
126c R = NMe$_2$, 83%
126d R = F, 80%
126e R = NO$_2$, 78%
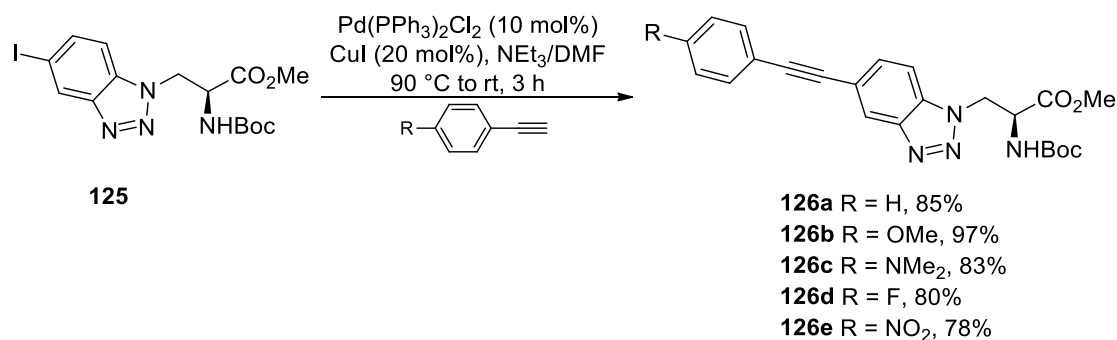
Scheme 55: Sonogashira cross-couplings of benzotriazole *125* to give extended chromophores.

Finally, the two step deprotection of these *N*-Boc protected analogues was investigated (**Scheme 56**). As described previously, ester hydrolysis was undertaken with caesium carbonate to give carboxylic acids **127a**–**127e**. Next, acidic removal of the Boc-protecting group in 2 M HCl for 3 h was explored. These conditions were suitable for phenyl analogue **127a**, fluoro analogue **127d** and nitro analogue **127e**. However, for electron rich analogues **127b** and **127c**, milder reaction conditions were required to avoid the formation of by-products. For dimethylamino analogue **127c**, deprotection was achieved with 1 M HCl after only 0.5 h. Deprotection of methoxy analogue **127b** required milder conditions and a longer reaction time (0.5 M HCl for 24 h). These mild conditions meant that the decomposition observed for the *N*-Cbz protected analogues was avoided. Final amino acids **128a**–**128e** were produced in moderate to good yields (51–76%).
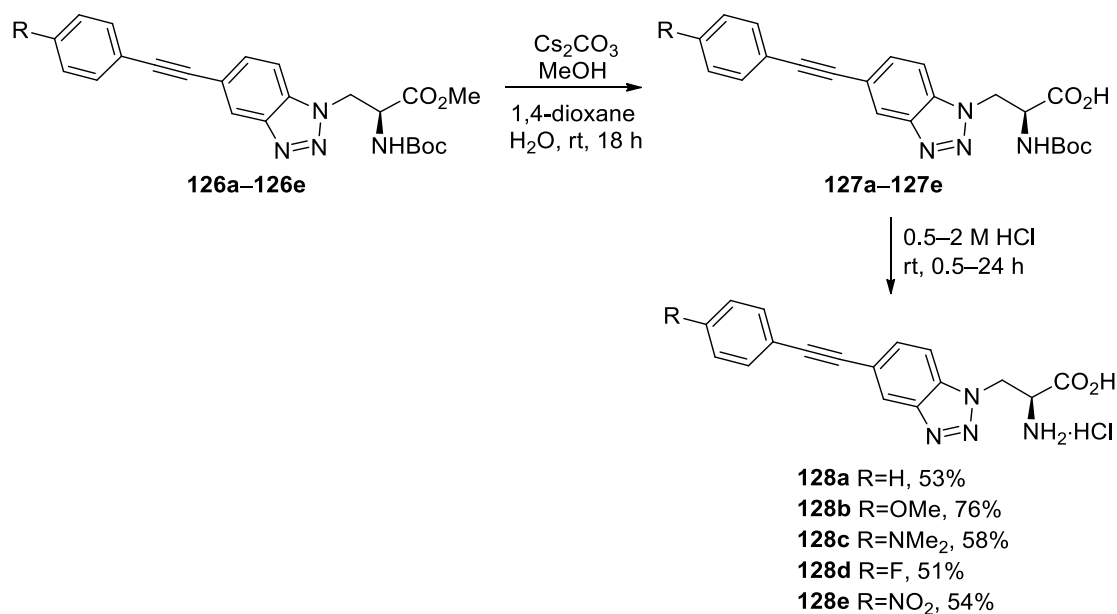
Scheme 56: *Two-step deprotection of alkyne benzotriazoles **126a–126e**.*

Upon the synthesis of this series of extended chromophores, the photophysical properties of each analogue were investigated. It was observed that all of these analogues showed absorption spectra above 300 nm, which is beneficial as this absorption is red-shifted when compared to the absorption of any naturally occurring amino acids. A red-shifted absorption peak at 320 nm could be observed for phenyl analogue **128a** (**Figure 47**), which showed an emission maximum at 370 nm. A similar absorption band was observed around 320 nm for the methoxy analogue **128b** (**Figure 48**), however the emission maxima for this compound was significantly shifted, demonstrating an emission maximum at 430 nm. As the benzotriazole unit is often used as an 'electron acceptor' in D-π-A systems, it was predicted that this red-shift was a result of the formation of a push-pull system.[116] This was proposed to be as a result of the electron-donating methoxy substituent, where the benzotriazole ring acts as an electron-withdrawing group. For fluoro analogue **128d** (**Figure 50**), the spectra were very similar to that of the unsubstitued compound. Particularly interesting were the dimethylamino (**128c**) (**Figure 49**) and nitro (**128e**) (**Figure 51**) analogues, which both showed absorption maxima above 350 nm. However, the emission spectra for both of these analogues displayed low intensity and fluorescent quenching was suspected.
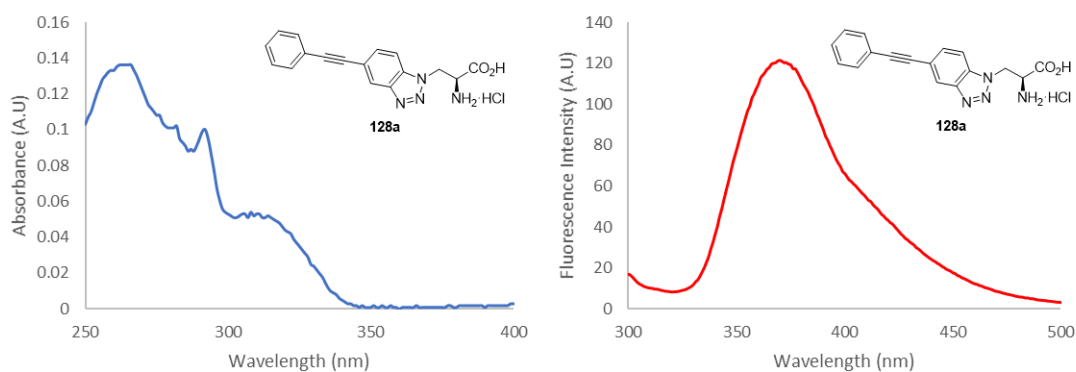
Figure 47: *Absorbance and emission spectra for amino acid* **128a** *measured at 5 μM in MeOH. Excitation at 275 nm.*
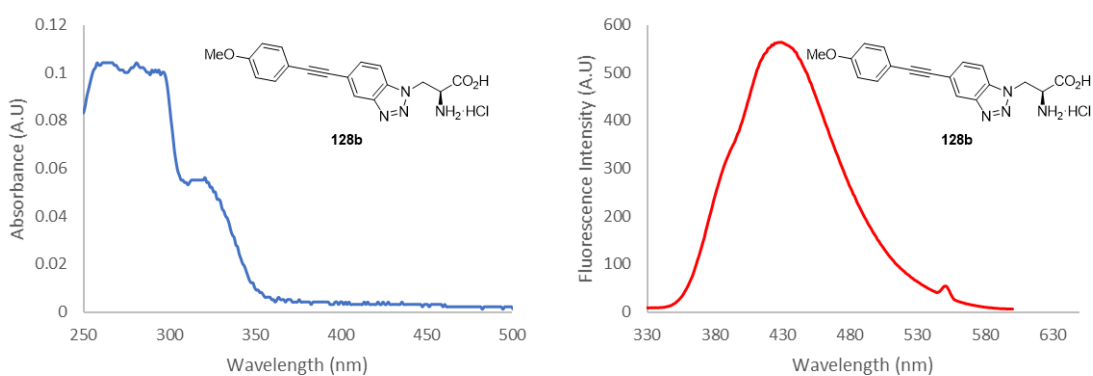
Figure 48: *Absorbance and emission spectra for amino acid* **128b** *measured at 5 μM in MeOH. Excitation at 275 nm.*
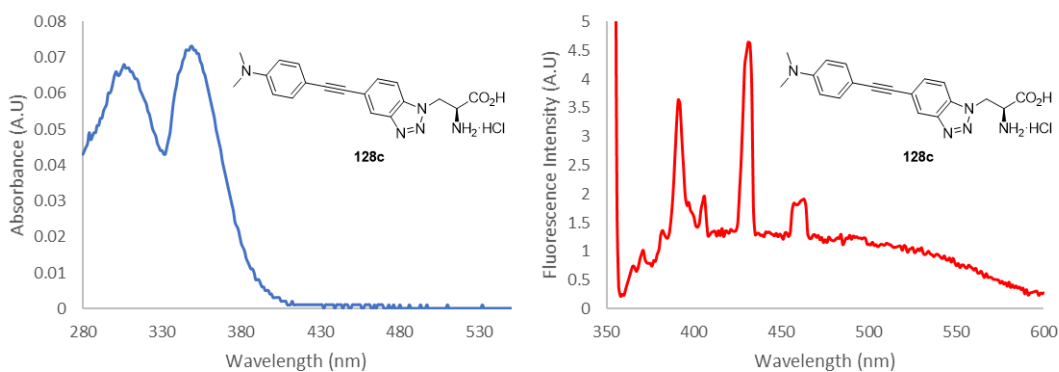
Figure 49: *Absorbance and emission spectra for amino acid* **128c** *at 5 μM in MeOH. Excitation at 350 nm.*
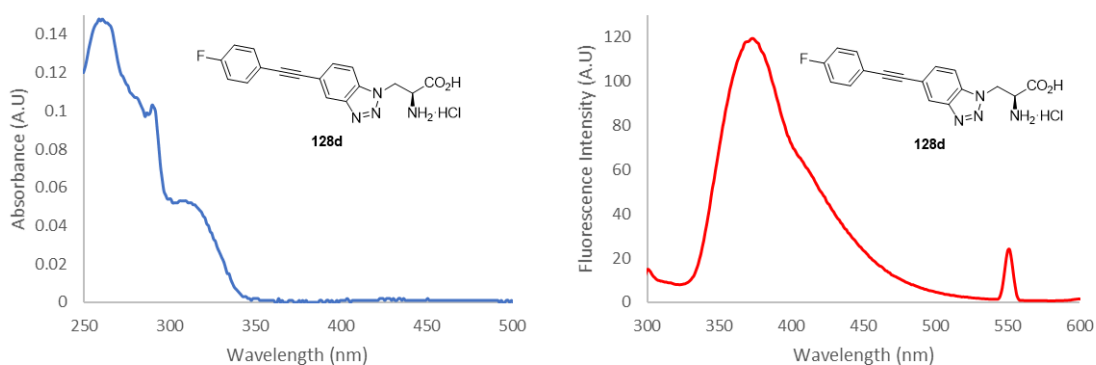
*Figure 50: Absorbance and emission spectra for amino acid **128d** measured at 5 µM in MeOH. Excitation at 275 nm.*
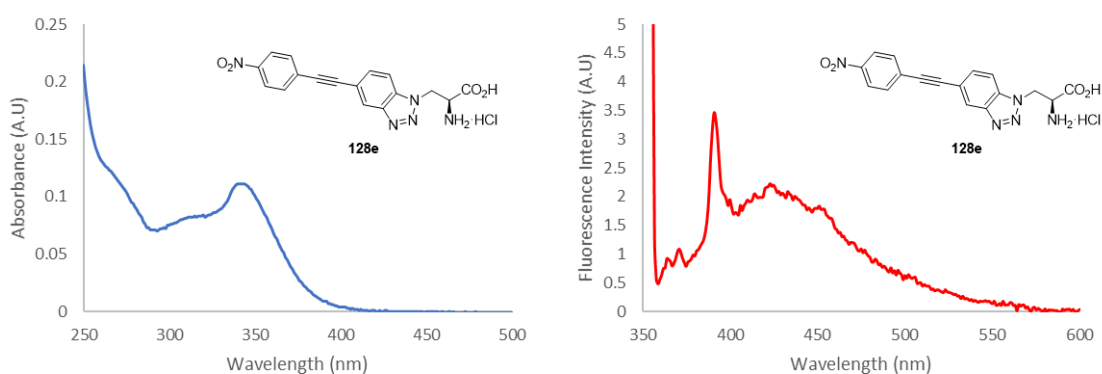
*Figure 51: Absorbance and emission spectra for amino acid **128e** at 10 µM in MeOH. Excitation at 350 nm.*

It was observed that these analogues had a red-shifted absorption and emission when compared to the previously synthesised aryl benzotriazole analogues, likely owing to the extra conjugation across the extended chromophore.[1] This is demonstrated by a comparison between 4-MeO-phenyl analogue **104a** and corresponding alkyne compound **128b** (**Figure 52**). While benzotriazole **104a** exhibited an absorption maximum of 260 nm, the absorption maximum of alkyne analogue **128b** extended to 300 nm, with a secondary peak at 320 nm. A slight red-shift in emission maximum was also observed, from 420 nm for **104a** to 430 nm for **128b**. It should be noted that the shift in absorption maximum for compounds such as **128b** is significant as it means that these compounds can be selectively excited in proteins containing other naturally-occurring amino acids.
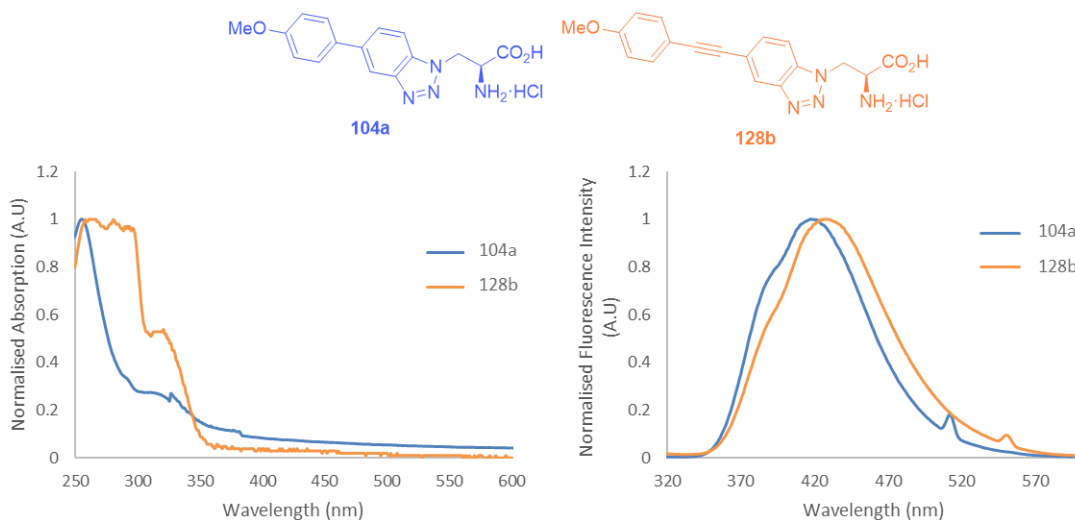
Figure 52: *Comparison of normalised absorption and emission spectra of amino acids **104a** and **128b**. Spectra for compound **104a** recorded by Dr. Jonathan Bell.*

Next, further photophysical properties of these analogues were determined. Stokes shifts, quantum yields, molar attenuation coefficient and brightness for each of the compounds in methanol were investigated and the results are presented in **Table 7**. Lead amino acid **104a** from the previously synthesised benzotriazole series is shown for comparison. Phenyl analogue **128a** and fluoro analogue **128d** showed similar photophysical properties with a brightness around 2000 cm^{-1} M^{-1}. The extended methoxy derivative **128b** in this series showed the strongest brightness (7240 M^{-1} cm^{-1}) as a result of a high quantum yield and good molar absorption coefficient, and was significantly brighter than biaryl amino acid **104a**. Unfortunately, the analogues which demonstrated the most red-shifted absorbances (dimethylamino analogue **128c** and nitro analogue **128e**) were the least bright, with no fluorescence observed from the nitro analogue **128e** and very little from the dimethylamino **128c** analogue. As methoxy analogue **128b** also demonstrated a large Stokes shift it was identified as the lead compound from this initial library.
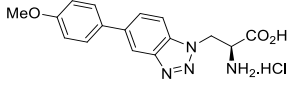
Amino Acid	Absorption Maximum (nm)	Emission Maximum (nm)	Stokes Shift (nm)	Molar Extinction Coefficient (cm^{-1} M^{-1})	Quantum Yield (Φ_F)	Brightness (cm^{-1} M^{-1})
104a	256	418	162	23,034	0.17	3857
128a	265 (310)	373	108 (63)	25,000	0.08	2030
128b	296 (321)	421	125 (100)	20,800	0.34	7240
128c	349	430	81	14,500	<0.01	10
128d	261 (310)	371	110 (61)	28,900	0.07	2110
128e	342	N/A	N/A	10,200	N/A	N/A
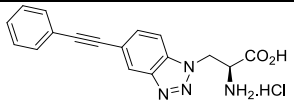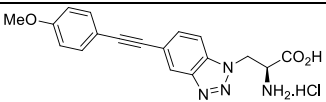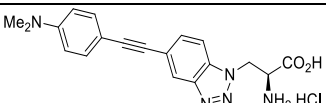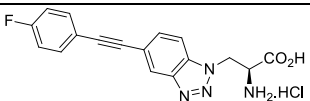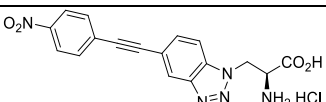
Table 7*: Photophysical properties of amino acids **128a–128e**.*

Using the information obtained from this study, a second series of analogues was proposed (**Figure 53**). Considering the red-shifted absorbance exhibited by dimethylamino analogue **128c**, it was determined that this analogue merited further investigation. It has been reported that fluorescence quenching by dimethylamino groups can occur through a TICT mechanism.[34] Suppression of this quenching by the inclusion of azetidine rings in the place of alkylamines has been observed. It has been proposed that azetidine rings experience less steric repulsion than alkylamines, and are thus less likely to adopt a TICT state. The inclusion of an azetidine ring in the place of dialkylamino groups in various fluorophore scaffolds has been reported, with an improvement in quantum yield.[117] As such, it was proposed that the synthesis of azetidine analogue **128f** would allow for an analogue which showed both red-shifted absorbance and good brightness. The red-shifted absorption of nitro analogue **128e** was also of interest. As it has been reported that nitro groups can quench fluorescence, the synthesis of an analogue with similar electronic properties but without a nitro group was desired. It was suggested that

the inclusion of an alternative electron-withdrawing group into the fluorophore should allow for the same red-shift without the quenching effect. As such, the synthesis of cyano analogue **128g** was proposed.

Finally, owing to the promising photophysical properties of methoxy analogue **128b**, the synthesis of further electron rich analogues was proposed. A dioxazole analogue **128h** was suggested as this analogue would have the electron rich character of the methoxy analogue **128b**, but restricted rotation which could increase the brightness of this compound. In addition, naphthyl analogue **128i** and methoxy naphthyl analogue **128j** were suggested as naphthyl amino acids within the Sutherland group previously have shown good photophysical properties.[36]
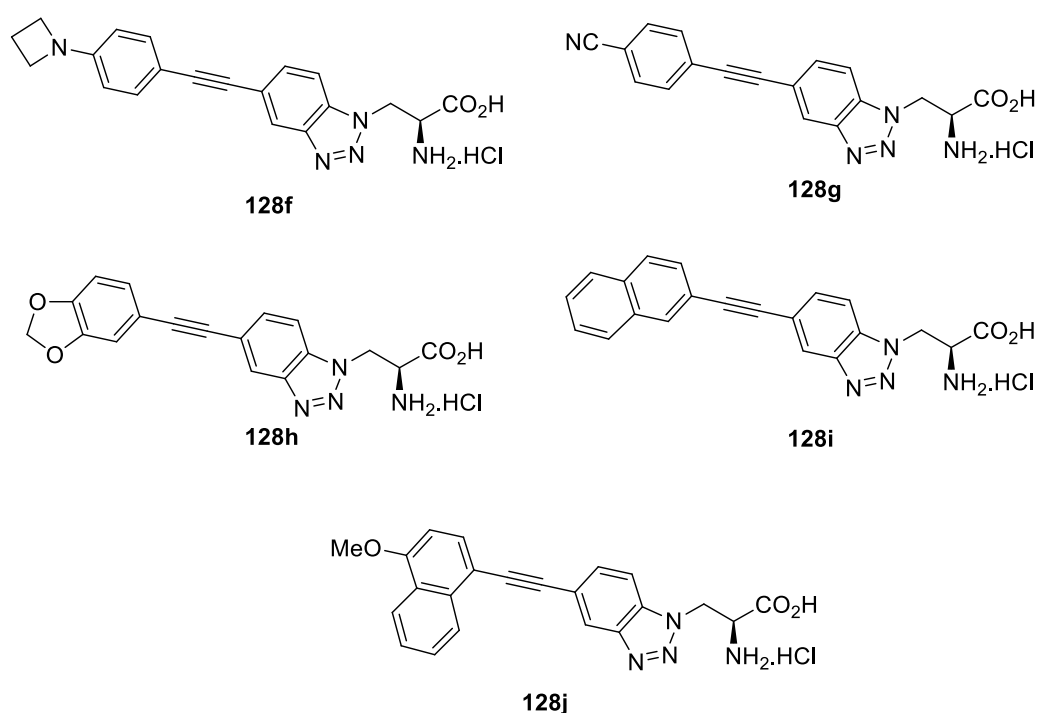
Figure 53: *Proposed derivatives of a second series of alkynyl benzotriazole amino acids.*

The cyano **128g** and naphthyl analogue **128i** could be synthesised from commercially available alkynes, however for the other analogues the synthesis of suitable acetylenes was first required. Benzodioxazole alkyne **130** was synthesised in two steps following literature precedent (**Scheme 57**).[118] First, a Sonogashira cross-coupling between 4-bromo-1,2-(methylenedioxy)benzene and trimethylsilylacetylene was undertaken with the use of catalytic $PdCl_2(PPh_3)_2$ and copper(I) iodide, which gave TMS-protected alkyne **129**. Removal of the TMS group

under mild basic conditions with potassium carbonate then gave alkyne **130** in 62% overall yield.
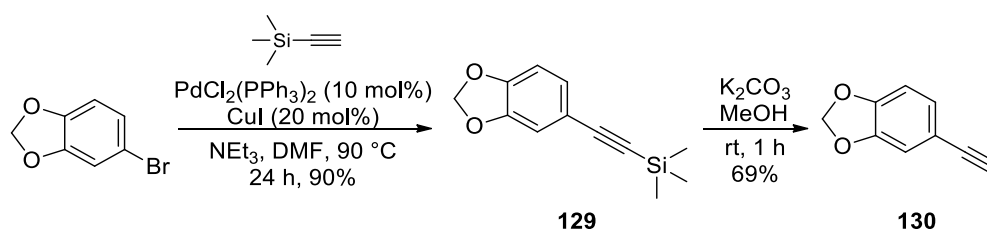
Scheme 57: Synthesis of benzodioxazole alkyne **130**.

Synthesis of an azetidine alkyne began with the Buchwald-Hartwig coupling of 1-bromo-4-iodobenzene with azetidine, under basic conditions, using tris(dibenzylideneacetone)dipalladium(0) (1 mol%) and *rac*-BINAP (3 mol%) (**Scheme 58**).[119] This gave coupled product **131** in 87% yield. Subsequently, the Sonogashira cross-coupling of **131** with trimethylsilylacetylene was attempted. However, for this analogue the reaction proceeded sluggishly. Using 10 mol% catalyst loading of $PdCl_2(PPh_3)_2$ gave only 10% conversion to the product overnight, and a repeat reaction with increased catalyst loading (20 mol%) only gave 20% conversion after 36 h.
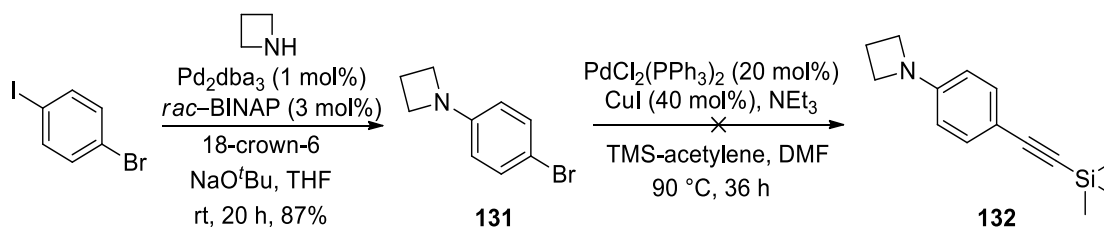
Scheme 58: Attempted synthesis of protected azetidine alkyne **132**.

It was proposed that swapping the order of the synthetic steps would allow for the Sonogashira reaction to proceed using a more reactive aryl iodide. This proved successful under mild conditions, at room temperature for 0.5 h, and gave **133** in 95% yield (**Scheme 59**). The Buchwald-Hartwig coupling of azetidine with aryl bromide **133** was next investigated. Initially, this reaction was trialled using the same conditions as for the coupling with the iodide but at a higher temperature (80 °C).[119] Under these conditions, some deprotection of the TMS-group was observed leading to a mixture of products. A change in solvent, from THF to toluene, gave 17% yield of deprotected product **134**. Finally, the reaction was trialled in the absence of 18-crown-6.[120] It was observed that in the absence of the crown ether the reaction

proceeded smoothly with an 83% yield of **132** and no TMS-deprotection was observed. The role of 18-crown-6 in this reaction was unclear, as this crown ether has a particular affinity for potassium ions which were not present in this reaction. However, as the removal of the crown ether from this reaction led to such a dramatic increase in yield, it was proposed that the crown ether possessed some ability to coordinate to the sodium cation of sodium *tert*-butoxide, increasing the reactivity of the base – and so with the removal of this crown ether, the base was reactive enough for deprotonation of the azetidine, but did not cause removal of the TMS-group. Finally, potassium carbonate mediated deprotection of the alkyne gave **134** in essentially quantitative yield.
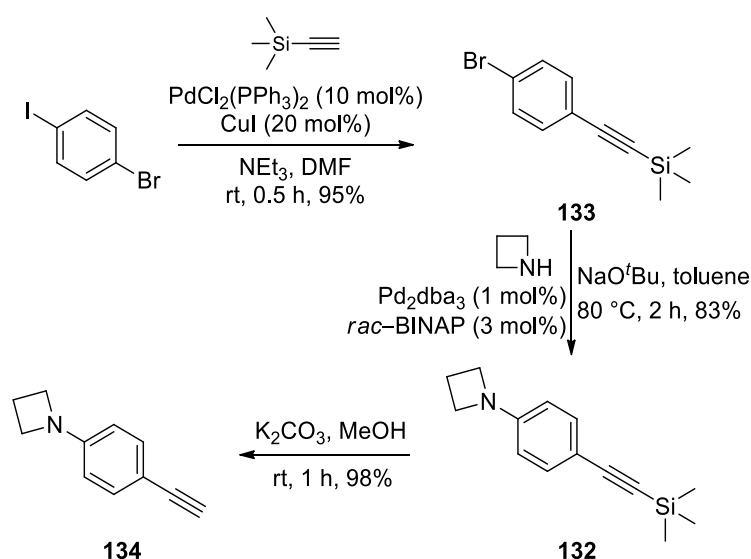
*Scheme 59: Synthesis of azetidine alkyne **134**.*

Finally, 4-methoxynaphthyl acetylene **138** was synthesised from 1-methoxynaphthalene in three steps. The first step used methodology developed within the group for regioselective iodination of arenes.[121] This methodology utilised *N*-iodosuccinimide which was activated by catalytic iron(III) triflimide (formed *in situ* from the ionic liquid [BMIM]NTf$_2$ and iron(III) chloride). The reaction, which was highly regioselective gave 1-iodo-4-methoxynaphthalene **136** in 97% yield (**Scheme 60**). Sonogashira reaction of **136** with trimethylsilylacetylene proceeded smoothly at room temperature in 4 h and gave coupled product **137** in 80% yield. Finally, deprotection was achieved with potassium carbonate at room temperature, which gave the desired alkyne **138** in 90% yield.
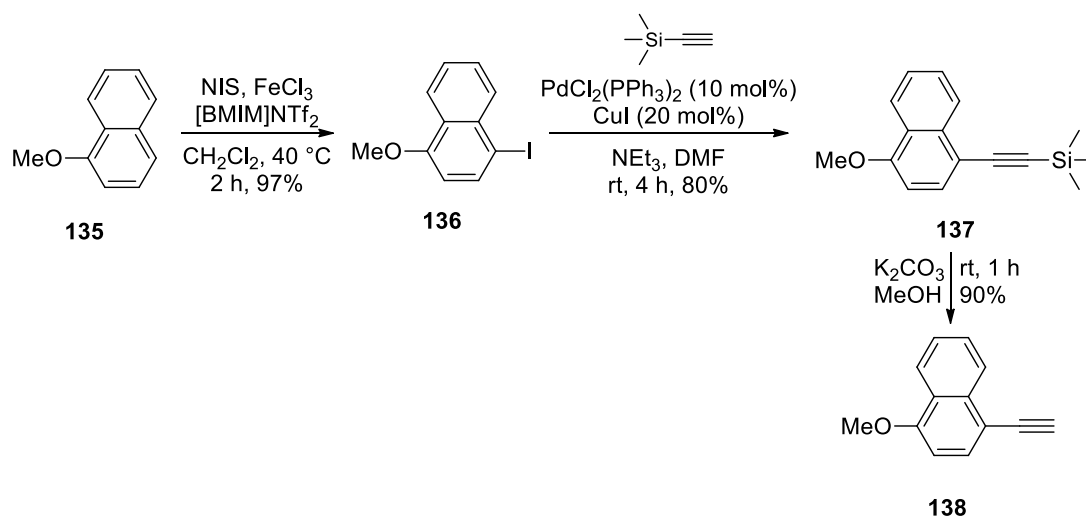
Scheme 60: Synthesis of 1-ethynyl-4-methoxynapthalene 138.

The Sonogashira cross-couplings of these alkynes with iodinated benzotriazole **125** was next investigated (**Scheme 61**). These reactions were performed under the same conditions as previously described, with catalytic PdCl₂(PPh₃)₂ and copper(I) iodide in a co-solvent mixture of triethylamine and DMF. This allowed the synthesis of a second series of protected analogues. Each reaction required only 3 h and gave the desired products in high to excellent yields (70–92%).
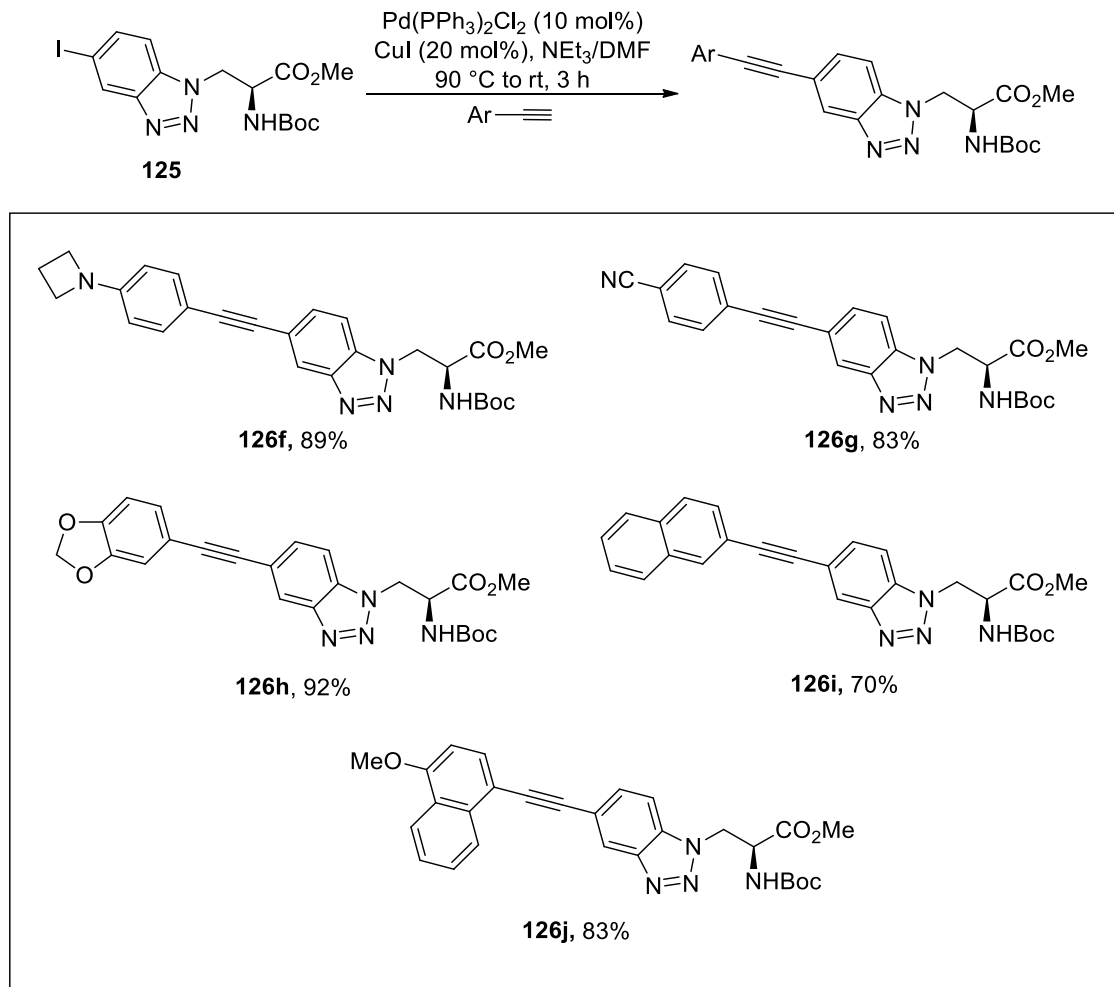
Scheme 61: *Synthesis of a second series of alkynyl benzotriazole analogues.*

The deprotection of these analogues was next investigated, using the two-step procedure of ester hydrolysis and acid mediated Boc-group deprotection previously described. For these analogues, ester hydrolysis using caesium carbonate at room temperature proceeded successfully to give the carboxylic acids **127f–127j** (**Scheme 62**).

127f Ar=4-Azetidine-C$_6$H$_4$, 83%
127g Ar=4-CNC$_6$H$_4$, 94%
127h Ar=1,3-benzodioxole, 70%
127i Ar=2-Napthyl, 91%
127j Ar=4-MeONapthyl, 85%
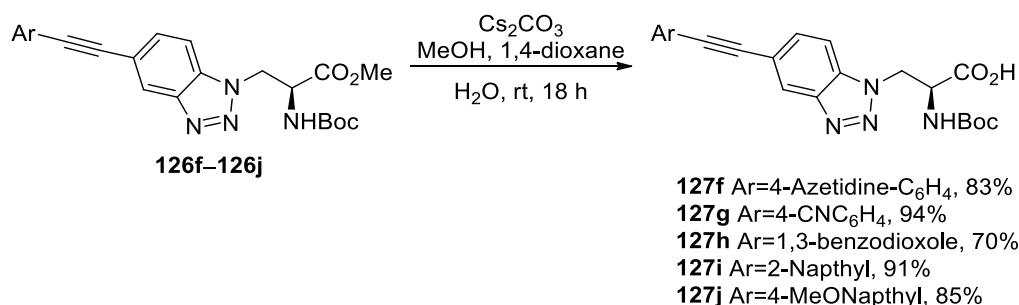
Scheme 62: *Ester hydrolysis of alkynyl benzotriazoles 126f–126j.*

Subsequent Boc-deprotection for cyano analogue **127g,** benzodioxazole analogue **127h** and naphthyl analogue **127i** was achieved by using 2 M HCl at room

temperature for 3 h (**Scheme 63**). Recrystallisation from methanol and diethyl ether gave the final deprotected amino acids **128g–128i**.

128g Ar=4-CNC$_6$H$_4$, 88%
128h Ar=1,3-benzodioxole, 70%
128i Ar=2-Napthyl, 80%
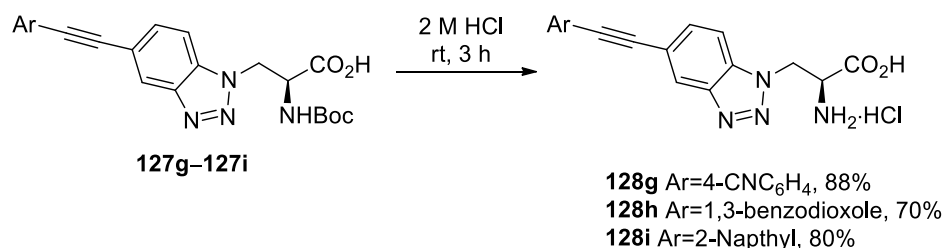
Scheme 63: *Boc-deprotection of amino acids* **127g**, **127h** *and* **127i**.

The Boc-deprotection of methoxynapthyl analogue **127j** was next explored. On reaction with 2 M HCl for 3 h, at room temperature, a mixture of starting material and two Boc-deprotected compounds were observed. Upon further stirring overnight, a single product was isolated, however analysis of this compound showed that it was not the desired product. Instead, it appeared that chlorinated analogue **139** was formed in 78% yield by addition of HCl across the alkyne bond (**Scheme 64**).
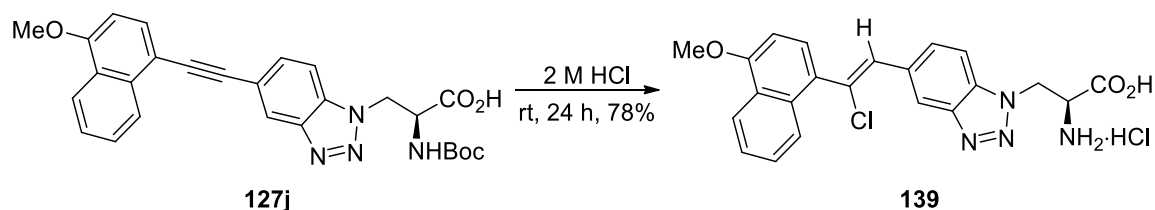
Scheme 64: *Attempted Boc-deprotection of analogue* **127j**.

This deviation from the expected structure was initially highlighted by the appearance of an additional singlet in the ^{1}H NMR spectrum for this compound (**Figure 54**). The formation of the *Z*-alkene **139** was suggested to be favoured due to the steric hindrance which would accompany the *E*-alkene. It was proposed that this may be confirmed by an NOE experiment, investigating the correlation observed between 1''-H and 2'''-H. Unfortunately, owing to the overlapping nature of these two signals in the 1H NMR spectrum, the precise geometry of this alkene could not be ascertained.
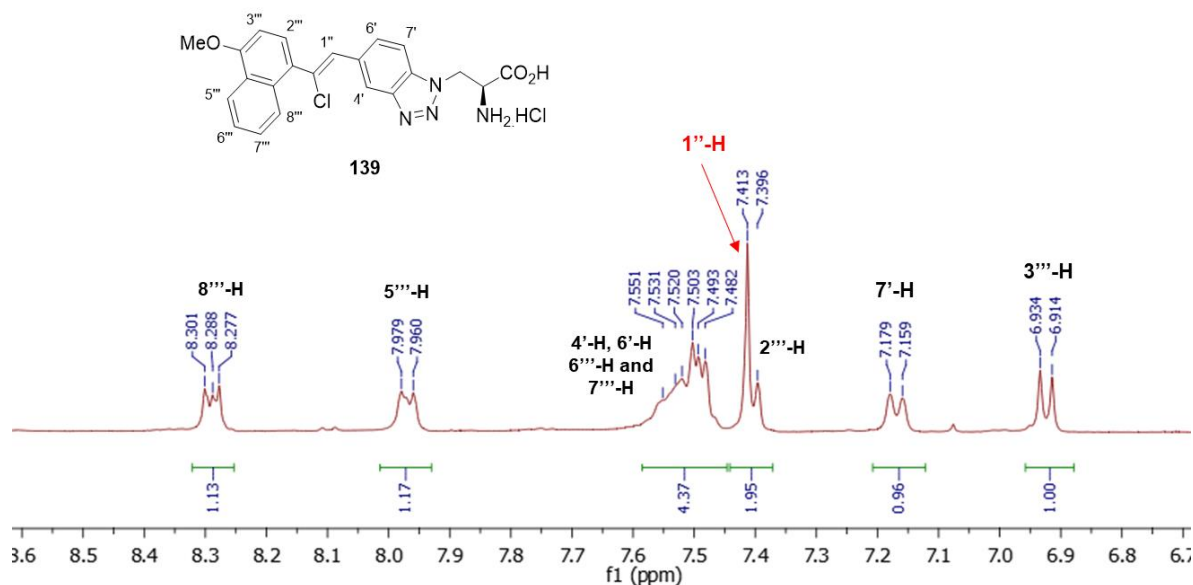
Figure 54: *¹H NMR Spectrum which is proposed to correspond to analogue **139**, measured in CD₃OD (region from 6.8–8.4 ppm).*

Upon further analysis it appeared that this addition product formed rapidly under acidic conditions. Using milder conditions (0.5 M HCl, 0.5 h), the formation of this compound was still observed, while some starting material remained. As such, it was determined that isolation of the desired product was unlikely to be achieved and this analogue was abandoned. It was proposed that this rapid addition of HCl across the alkyne was a result of the highly electron rich nature of the aryl ring, more so than any of the previously synthesised compounds.

Difficulties were also encountered with the deprotection of azetidine analogue **127f** (**Scheme 65**). Reaction of **127f** with 2 M HCl at room temperature for 3 h gave a mixture of two deprotected compounds. Reaction with 1 M HCl for just 0.1 h also led to the formation of the impurity at the same rate, indicating that the formation of the by-product was again too favourable to be avoided. In addition to this, the products obtained appeared to be unstable to longer reaction times (6 h), as decomposition was observed by ¹H NMR spectroscopy. As such the by-product could not be isolated, instead only a mixture of two compounds could be obtained, and so it was not possible to fully analyse the by-product. It was unclear whether the problems encountered were again due to addition of HCl across the alkyne bond. Alternatively, the side-product and subsequent decomposition may be due to ring opening of the azetidine ring under acidic conditions, as acid sensitivity was not observed for dimethylamino analogue **127c**.
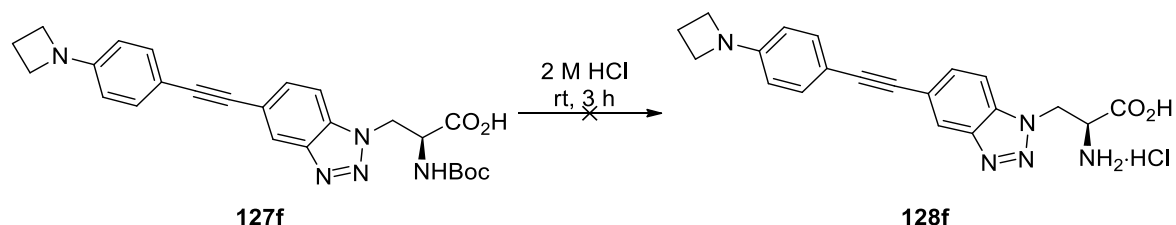
Scheme 65: *Attempted deprotection of azetidine analogue 127f.*

The absorbance and emission spectra for amino acids **128g**, **128h** and **128i** were next investigated, to observe how variation of the structures had affected these properties. The electron deficient cyano analogue **128g** showed a good red-shift in absorption with a strong absorbance up to 350 nm (**Figure 55**). However, this was less shifted than for the previously synthesised nitro analogue **128e**. In contrast to the nitro analogue, however, this compound showed a strong emission peak, with an emission maxima at 370 nm. The electron donating benzodioxazole analogue **128h** (**Figure 56**) showed absorbance up to 330 nm, and an emission maxima of 440 nm, which were slightly red-shifted when compared to the methoxy analogue – possibly due to the electron donating effect of the two ether groups. The second electron rich analogue, naphthyl **128i** (**Figure 57**), also showed a good red-shift in absorption (320 nm) but had a blue-shifted emission (380 nm) when compared to methoxy analogue **128b**. Finally, the absorbance and emission spectra of azetidine analogue **127f** were obtained. As Boc-deprotection was not possible for this compound, measurements were obtained of the Boc-protected analogue. As the Boc-protecting group does not contain strongly absorbent moieties, it was proposed that this was unlikely to cause complications. These measurements were undertaken to investigate whether an azetidine ring would help prevent fluorescence quenching, which can occur in the presence of a dimethylamino group. The compound showed good absorbance with a secondary peak at 340 nm (**Figure 58**), and a weak emission maxima of 440 nm, both of which were similar to dimethylamino analogue **128c**.
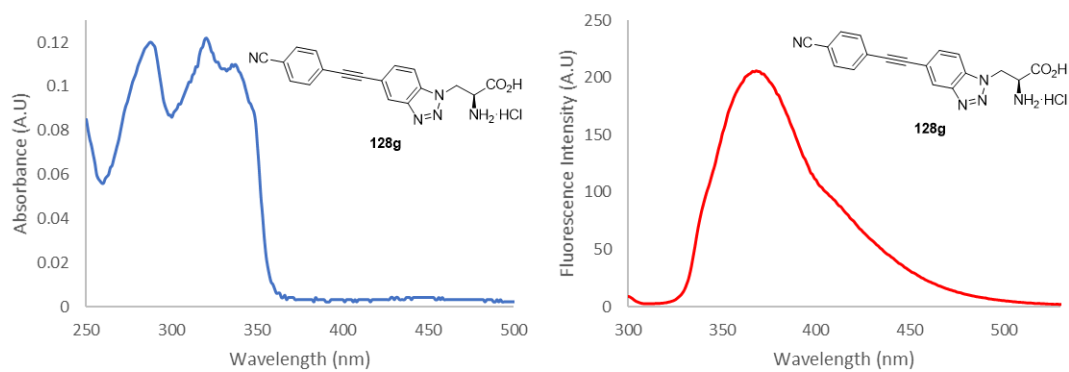
Figure 55: Absorbance and emission spectra of amino acid **128g**. Measured in MeOH at 5 µM, excitation at 320 nm.
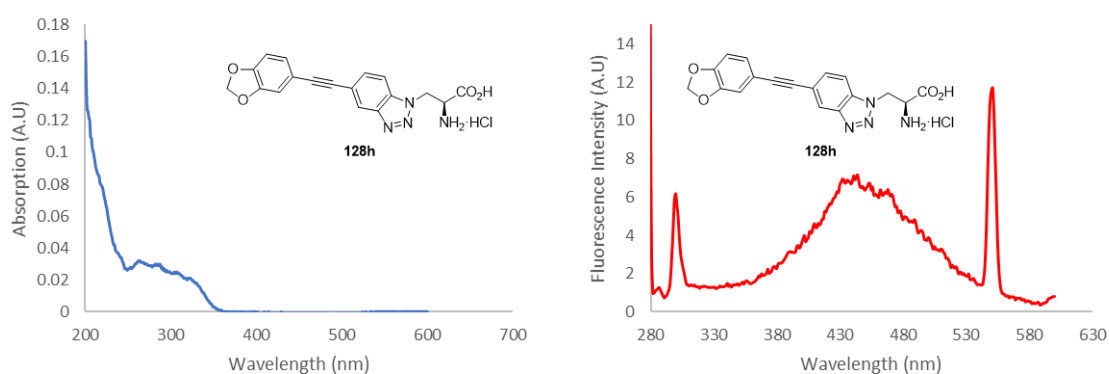
Figure 56: Absorbance and emission spectra of amino acid **128h**. Measured in MeOH at 5 µM, excitation at 275 nm.
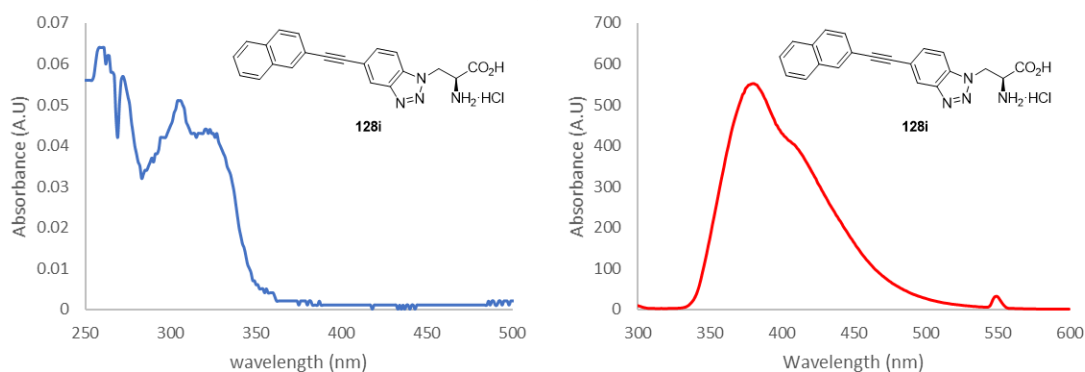
Figure 57: Absorbance and emission spectra of amino acid **128i**. Measured in MeOH at 5 µM, excitation at 275 nm.
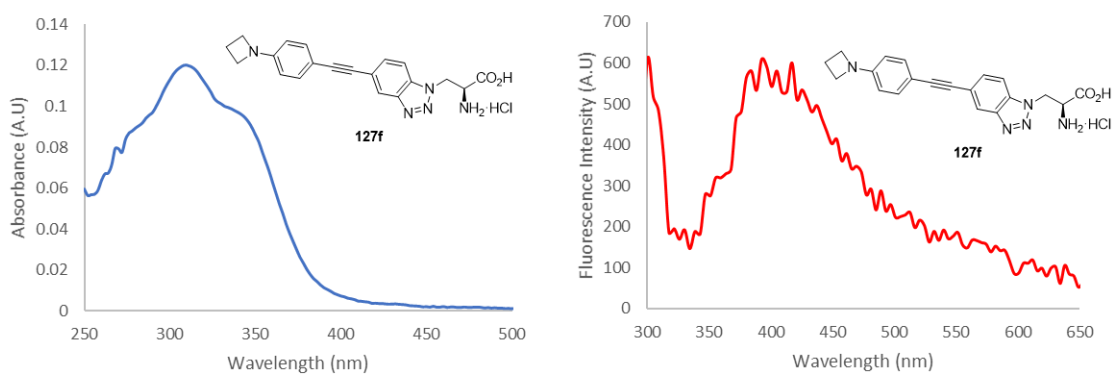
Figure 58*: Absorbance and emission spectra of amino acid **127f**. Measured in MeOH at 5 µM, excitation at 310 nm.*

Further photophysical properties of these compounds were next determined (**Table 8**). Cyano derivative **128g** had an excellent red-shifted absorption maxima but overall was limited by a small Stokes shift, and additionally, was not as bright as some of the other analogues synthesised. The benzodioxazole analogue **128h** had a low brightness, despite the increased rigidity of the structure, which has been observed in similar analogues produced by the group.[81] Naphthyl analogue **128i** showed excellent properties, with a red-shifted absorption maxima and large brightness. Finally, Boc-protected azetidine analogue **127f** was investigated. It was found that the inclusion of an azetidine ring into this compound did not prevent fluorescence quenching, and this analogue was too weakly emissive for a quantum yield and brightness to be measured. This result for **127f** show that the use of the azetidine ring was not able to prevent fluorescence quenching of an aniline side-chain in this fluorophore.
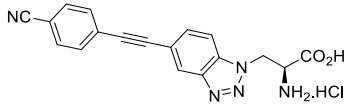
Amino Acid	Absorption Maximum (nm)	Emission Maximum (nm)	Stokes Shift (nm)	Molar Extinction Coefficient (cm^{-1} M^{-1})	Quantum Yield (Φ_F)	Brightness (cm^{-1} M^{-1})
128g	290 (341)	371	47 (30)	15000	0.17	2470
128h	262 (325)	450	188 (125)	7300	0.03	190
128i	304 (320)	382	78 (62)	12400	0.42	5200
127f	311 (343)	420	109 (77)	17900	<0.01	N/A
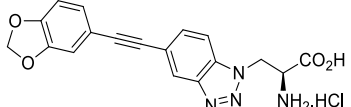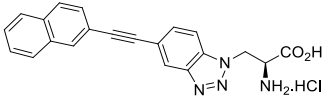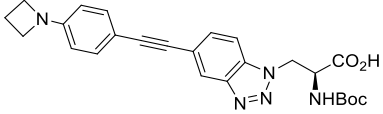
Table 8: *Photophysical properties of benzotriazole amino acids **128g**–**128i** and **127f**.*

The electron rich analogues in this series, amino acids **128b**, **128c**, and **128f**, generally showed red-shifted emission maxima when compared to electron deficient analogues. As such, it is proposed that the benzotriazole unit does offer some electron-withdrawing properties which allow for the stabilisation of these compounds in the excited state. However, it has also been reported that in some circumstances, the benzotriazole unit can act as more of an electron-neutral moiety.[122] This could explain why electron-deficient analogues such as amino acids **128e** and **128g** display red-shifted absorption spectra. For these analogues, conjugation with the nitro or cyano groups allows for red-shifted absorption properties, however, no dipole stabilisation occurs in the excited state and so these analogues display blue-shifted emission maxima.

3.4 Synthesis of Alkenyl Benzotriazole Derived α-Amino Acids

In addition to the synthesis of alkynyl benzotriazoles, the synthesis of alkenyl benzotriazoles through Heck cross-couplings was proposed. These analogues would also contain stretched chromophores, and the photophysical differences between alkenyl and alkynyl analogues could be compared.

Initially, the cross-coupling reaction of bromine-substituted benzotriazole **103** with styrene to form conjugated benzotriazole **140a** was explored. This was trialled with PdCl$_2$(PPh$_3$)$_2$ (5 mol%) in acetonitrile, with potassium carbonate as the base at 80 °C (**Table 9**, entry 1).[123] Under these conditions, however, elimination of the benzotriazole to give alkene **141** was observed. It was proposed that changing the base would minimise elimination and instead facilitate cross-coupling. With an initial change to diisopropylethylamine, no reaction occurred (entry 2). A change of solvent was then considered.[124] Although no reaction was observed in 1,4-dioxane (entry 3), some product was observed in DMF (entry 4). Based on this result, optimisation of this reaction in DMF was attempted. An increase of catalyst loading to 10 mol% led to no change in yield (entry 5). With a further increase in temperature, it was possible to improve the ratio of product produced (entry 6), while a study of the equivalents of base showed that fewer equivalents led to a sluggish reaction (entry 7), whereas more equivalents resulted in an increase in the formation of alkene **141** (entry 8). Finally, using the optimised conditions of entry 6, the catalyst was changed to palladium acetate but in the presence of this catalyst, full conversion of starting material was not observed (entry 9).[84]
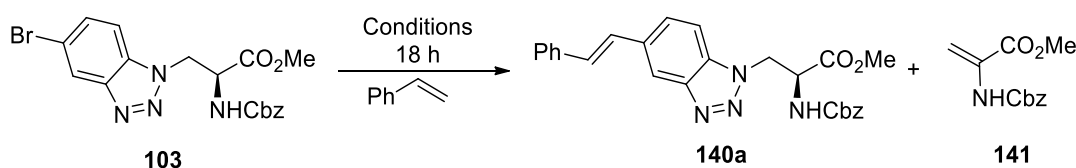
Entry	Solvent	Base	Base (equiv.)	Catalyst (5 mol%)	Temp. (° C)	Reaction Conversion (%)	140a:141[a]
1	MeCN	K$_2$CO$_3$	1.5	PdCl$_2$(PPh$_3$)$_2$	80	100	0:1
2	MeCN	DIPEA	3	PdCl$_2$(PPh$_3$)$_2$	80	0	N/A
3	Dioxane	DIPEA	3	PdCl$_2$(PPh$_3$)$_2$	80	0	N/A
4	DMF	DIPEA	3	PdCl$_2$(PPh$_3$)$_2$	80	32	1:2
5	DMF	DIPEA	3	PdCl$_2$(PPh$_3$)$_2$[b]	80	28	1:2
6	**DMF**	**DIPEA**	**3**	**PdCl$_2$(PPh$_3$)$_2$**	**100**	**100**	**1:0.25**
7	DMF	DIPEA	1	PdCl$_2$(PPh$_3$)$_2$	100	75	1:0.5
8	DMF	DIPEA	5	PdCl$_2$(PPh$_3$)$_2$	100	100	1:3
9	DMF	DIPEA	3	Pd(OAc)$_2$[c]	100	59	1:1.5

Table 9*: Optimisation of Heck reaction of benzotriazole **103**. a: relative ^{1}H NMR ratios determined from crude reaction mixture; b: 10 mol% catalyst loading; c: with P(o-CH$_3$C$_6$H$_4$)$_3$ ligand.*

Using the optimised conditions (**entry 6**) for this reaction, the synthesis of phenyl alkenyl benzotriazole **140a** was attempted (**Scheme 66**). However, the desired product was obtained in only a 23% yield. The *E*-stereochemistry of the alkene was confirmed by ^{1}H NMR spectroscopy, with two doublets present for the alkene hydrogens, at 7.14 ppm and 7.23 ppm, each with a coupling constant of 16.3 Hz.

Scheme 66: *Heck cross-coupling of benzotriazole **103** with styrene.*

As an alternative approach, the Suzuki-Miyaura reaction of bromine-substituted benzotriazole **103** with vinyl boronic acids was considered. Coupling with 4-methoxyphenyvinyl boronic acid was attempted, as it was proposed that methoxy analogue **140b** would display optimal photophysical properties for this series, and allow for the determination of whether alkenyl amino acids were worth pursuing. As Suzuki-Miyaura cross-couplings of brominated analogue **103** with aryl boronic acids had previously been succesful, these conditions were trialled for this transformation.[81] This reaction used catalytic Pd(dppf)Cl$_2$, with potassium fluoride as a mild base in a dioxane/water co-solvent mixture and gave the desired methoxy analogue **140b** in a 25% yield (**Scheme 67**). The lower yield observed in this reaction compared to the reaction with aryl boronic acids was likely a result of the instability of vinyl boronic acids.[125]

Scheme 67: *Suzuki-Miyaura cross-coupling of brominated amino acid **103** with 4-methoxyphenylvinyl boronic acid.*

The alkenyl benzotriazoles **140a** and **140b** were then subjected to a two-step deprotection using caesium carbonate for hydrolysis of the methyl ester, followed by heating in 6 M HCl for the removal of the *N*-Cbz protecting-group (**Scheme 68**). Purification by recrystallisation gave the desired deprotected alkenyl amino acids

142a and **142b** in good yields. Unlike the corresponding alkynes, these compounds appeared to be stable under these acidic conditions.

140a, R=H
140b, R=OMe

141a, R=H, 78%
141b, R=OMe, 74%

142a, R=H, 68%
142b, R=OMe, 60%

*Scheme 68: Two-step deprotection of alkenyl amino acids **142a** and **142b**.*

A brief investigation of the photophysical properties of these analogues was next undertaken, to determine how they compared to previously synthesised analogues. Phenyl derivative **142a** showed an absoption maximum of 266 nm and an emission of 384 nm (**Figure 59**), while methoxy derivative **142b** showed more red-shifted absorption (305 nm) and emission (450 nm) peaks (**Figure 60**). This was likely due to the extra "push-pull" character across this chromophore, when compared to the unsubstituted analogue.
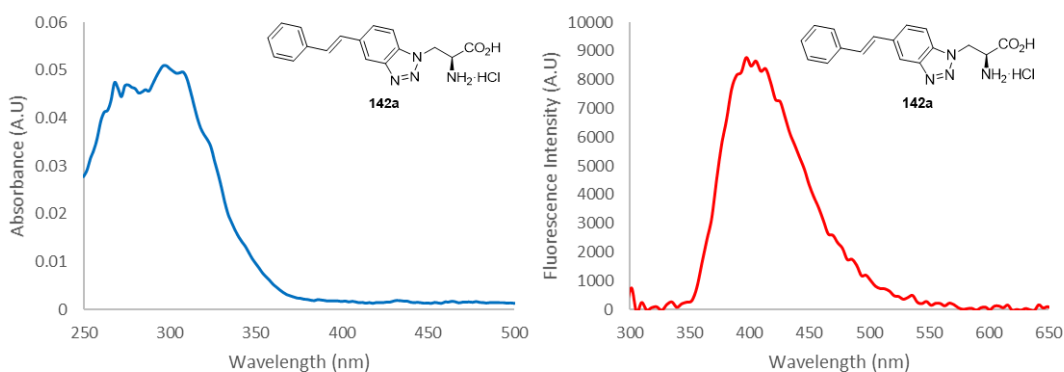
*Figure 59: Absorbance and emission spectra of amino acid **142a**. Measured at 5 µM in methanol. Excitation at 296 nm.*
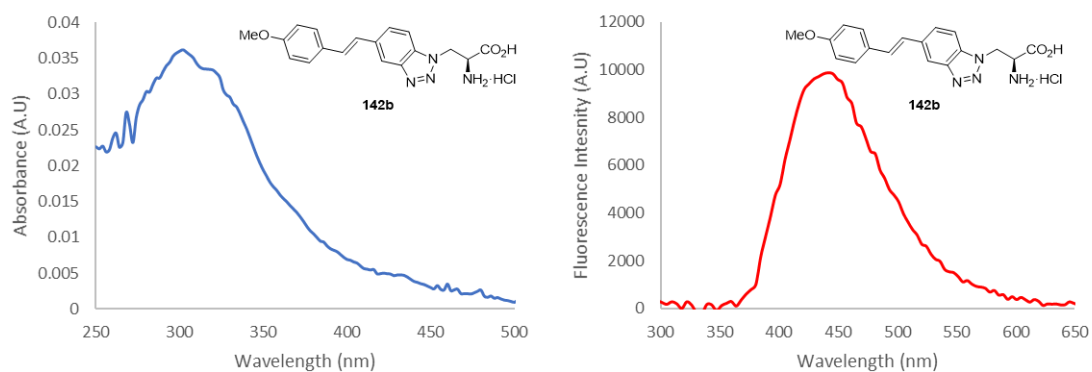
Figure 60: *Absorbance and emission spectra of amino acid **142b**. Measured at 5 µM in methanol. Excitation at 296 nm.*

It was observed that alkenyl analogues **142a** and **142b** showed red-shifted spectra when compared to amino acids with aryl-substituted benzotriazole side-chains **143a** and **104a** (**Table 10**). Due to the improved photophysical properties, it was decided to investigate an alternative, more efficient synthesis of these compounds. This would allow for the synthesis of additional material and other analogues for more detailed photophysical investigations.

Compound	Absorbance Maxima (nm)	Emission Maxima (nm)
143a	250	363
142a	**266**	**384**
104a	256	418
142b	**305**	**450**

Table 10: *Comparison of alkenyl amino acids **142a** and **142b** to previously synthesised amino acids **143a** and **143b**.*

Due to the low yield of the Suzuki-Miyaura reaction and the limited availability and stability of vinyl boronic acids, it was decided that further investigation for the synthesis of these compounds should revert to a Heck reaction. Following the

synthesis of iodinated benzotriazole **113** for Sonogashira cross-coupling reactions, it was proposed that this analogue could also be a better substrate for Heck cross-couplings. The weaker carbon-iodine bond would allow for reactions to occur at lower temperatures, whereby elimination reactions may be avoided.[126]

Using the optimal conditions for cross-coupling reactions of brominated benzotriazole **103**, the cross-coupling of iodinated benzotriazole **113** was explored, albeit at a lower temperature to minimise any elimination of the benzotriazole side-chain (**Table 11**). Under these conditions, the reaction was determined to have reached completion after 3 h by ^{1}H NMR spectroscopy. The desired product was formed in 23% yield, with an 18% yield of de-iodinated side-product **144** (entry 1), formed through protodepalladation. At a lower temperature (entry 2), no reaction was observed, whereas at a higher temperature there was no improvement in yield (entry 3). An increase in catalyst loading did not significantly improve the isolated yield (entry 4). The use of Pd(OAc)$_2$, a common choice of catalyst for Heck reactions,[126] resulted in similar yields to those observed with PdCl$_2$(PPh$_3$)$_2$ (entry 5). It was proposed that protodepalladation was more prominent in DMF than in other solvents[124] and so different solvents were considered. However, a screen involving acetonitrile, THF and 1,4-dioxane showed no reaction occurred in any of these solvents (entries 6−8). It was proposed that an increase of the rate of styrene addition to the active palladium(0) catalyst would be desirable to limit protodepalladation. This would be achieved by increasing the concentration of the reaction mixture and the number of styrene equivalents. Initially the previously optimised conditions were tested at double the concentration with an extra two equivalents of styrene (entry 9), and then at 10 times the concentration while also increasing catalyst loading (entry 10). However, these experiments only gave desired product **140a** in 32% yield.
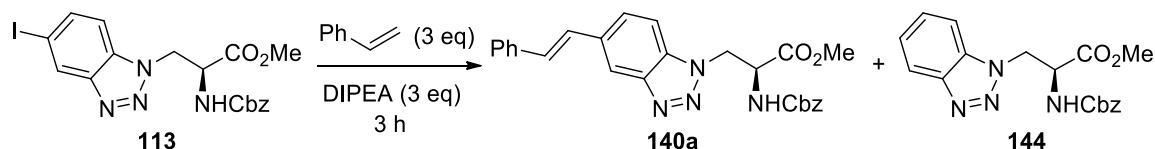
Entry	Catalyst	Conc. (M)	Catalyst Loading (mol%)	Solvent	Temp. (° C)	140a[*] (%)	144[*] (%)
1	PdCl$_2$(PPh$_3$)$_2$	0.1	5	DMF	75	23	18
2	PdCl$_2$(PPh$_3$)$_2$	0.1	5	DMF	60	-	-
3	PdCl$_2$(PPh$_3$)$_2$	0.1	5	DMF	90	22	18
4	PdCl$_2$(PPh$_3$)$_2$	0.1	10	DMF	75	25	16
5	Pd(OAc)$_2$, PPh$_3$	0.1	10	DMF	75	25	30
6	PdCl$_2$(PPh$_3$)$_2$	0.1	10	MeCN	75	-	-
7	PdCl$_2$(PPh$_3$)$_2$	0.1	10	THF	75	-	-
8	PdCl$_2$(PPh$_3$)$_2$	0.1	10	1,4-dioxane	75	-	-
9**	PdCl$_2$(PPh$_3$)$_2$	0.2	10	DMF	75	32	26
10**	PdCl$_2$(PPh$_3$)$_2$	1	15	DMF	75	32	26

*Table 11: Optimisation of the Heck-Miyaura cross-coupling reaction of benzotriazole 113. *Isolated yields. **5 Equivalents of styrene.*

It has been reported that the addition of tetraalkylammonium salts to Heck reactions can greatly enhance the selectivity and reactivity of reactions.[127] These conditions have been shown to be successful in the production of conjugated α-amino acid compounds where other conditions have failed.[127,128] The "Jeffery" conditions use catalytic amounts of Pd(OAc)$_2$ and have been shown to be effective with a range of inorganic and organic bases. The addition of tetra-*n*-butylammonium chloride to this reaction was investigated, however, under these conditions no reaction was observed (**Scheme 69**).

Scheme 69: *Attempted cross-coupling of iodinated benzotriazole* **113** *under "Jeffery" conditions.*

As Heck cross-couplings to form alkenyl benzotriazoles ultimately proved to be low yielding, an alternative method for their synthesis was considered. Generally, the synthesis of alkynyl analogues proceeded smoothly, and so it was envisioned that these compounds could be prepared by reduction of the alkyne to an alkene (**Scheme 70**). The production of the more stable *E*-alkene was desired, as this motif is common among fluorophores.[84,129]

Scheme 70: *Proposed reduction of alkynyl benzotriazoles to give alkenyl benzotriazoles.*

While the partial hydrogenation of alkynes to *Z*-alkenes can be achieved under a hydrogen atmosphere using heterogeneous catalysts such as Lindlar's catalyst,[130] reduction to *E*-alkenes has generally required harsher conditions. Typically, Birch-type conditions have been used for this reduction, and such methods often lack functional-group tolerance. In recent years, milder conditions for the partial hydrogenation of alkynes to *E*-alkenes have been developed, although require two steps, such as in a hydrosilylation/desilylation strategy,[131] require high pressures of hydrogen,[132] or use expensive transition metal catalysts.[133]

In 2018, Jackowski and co-workers described a catalytic partial hydrogenation of 1,2-disubstituted alkynes to *E*-alkenes using PdCl$_2$(PPh$_3$)$_2$ and stoichiometric zinc iodide, at room temperature, under an atmospheric pressure of hydrogen (**Scheme 71**).[134] This reaction proceeded by hydrogenation of the alkyne to the *Z*-alkene, followed by isomerisation to the *E*-alkene. Through mechanistic experiments, it was proposed that initially the zinc iodide reacted with the PdCl$_2$(PPh$_3$)$_2$ precatalyst to

give the more reactive PdI$_2$(PPh$_3$)$_2$. This was then reduced *in situ* by zinc(0) to give palladium(0). Following hydrogen addition to form the active palladium(II) catalyst, co-ordination to the alkyne and initial reduction to the *Z*-alkene occurred. The *Z*-alkene was then isomerised into the *E*-alkene, and mechanistic studies showed that both the palladium catalyst and zinc iodide were required for this alkene isomerisation. During similar reactions, over-reduction to the alkane is common. The authors proposed that in this case, the addition of zinc iodide was responsible for preventing over-reduction, as in the absence of zinc iodide full conversion to the alkane was observed.
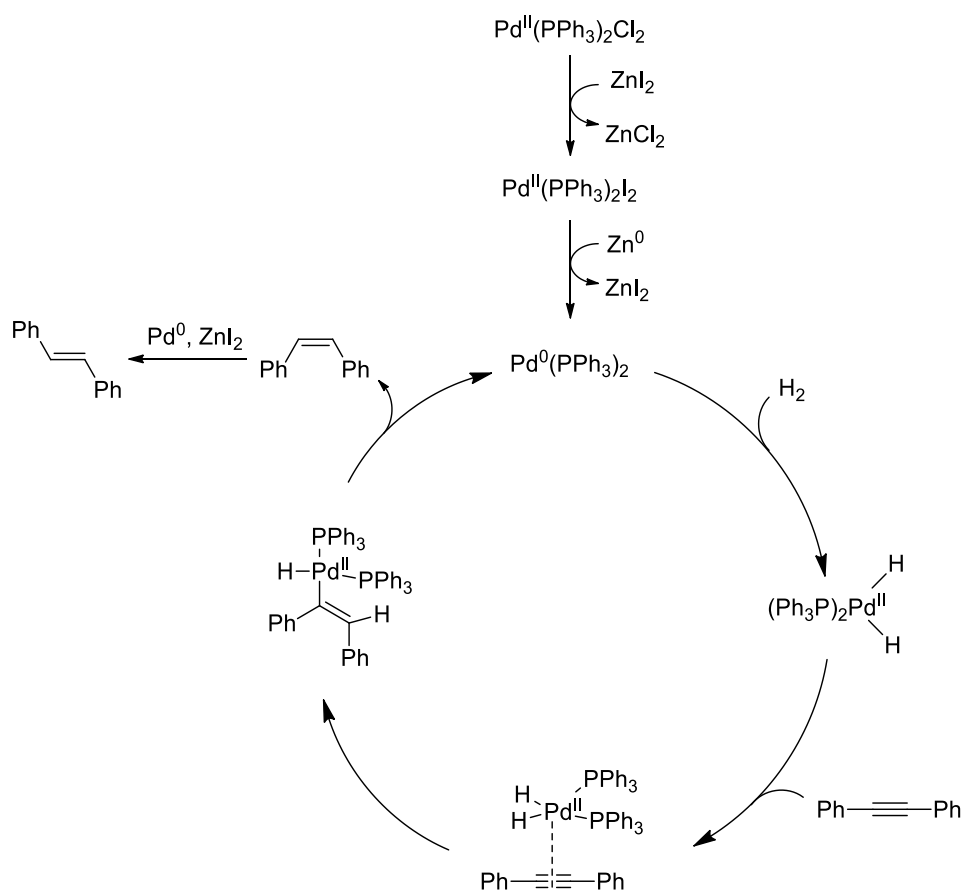
Scheme 71: *Catalytic semi-hydrogenation described by Jackowsi and co-workers.*

The conditions described by Jackowski and co-workers were trialled for the reduction of alkyne **126b** to *E*-alkene **145b**. The first attempt for this reaction proceeded very slowly (**Table 12**, entry 1). The reaction took 90 h to reach full conversion of starting material to a mixture of 1:1 *E:Z* alkenes. After 112 h, a 2:1 ratio of *E:Z* alkenes was observed and gave the desired *E*-alkene product in 17% yield. An increase in catalyst loading and temperature was considered to increase the rate of reaction (entry 2), and after 48 h at 30 °C with 20 mol% catalyst loading,

full conversion to the *E*-alkene was observed. This allowed for the isolation of **145b** in 43% yield as the sole product. A further increase in temperature to 40 °C (entry 3) allowed the isolation of **145b** in 64% yield, after a reaction time of 20 h.
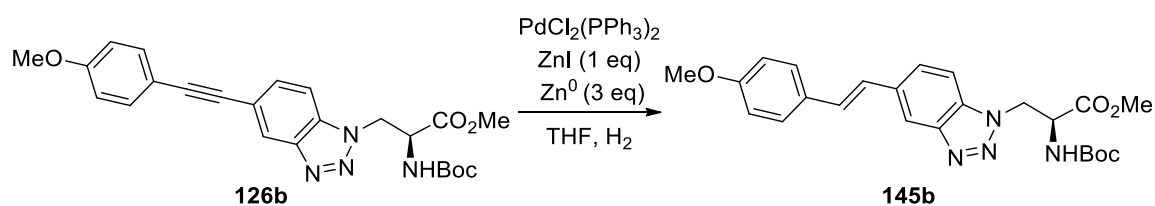
Entry	Catalyst Loading (mol %)	Temperature (° C)	Time (h)	*Z:E*	Yield (%)
1	5	25	112	1:2	17
2	20	30	48	0:1	43
3	20	40	20	0:1	64

Table 12: *Optimisation of the reduction of alkyne **126b** to alkene **145b**.*

Following optimisation, reproduction of the reaction was found difficult, with variation of the ratios of *E:Z* isomers. It was proposed that the hygroscopic nature of zinc iodide used in this reaction may result in the reagent becoming less reactive over time. Indeed, when subsequent reactions were performed using freshly prepared zinc iodide, rather than the commercially purchased reagent, the reaction became significantly more reproducible.

The reduction of phenyl analogue **126a** was next investigated, and the reaction proceeded in a similar manner to methoxy analogue **126b**. After 18 h, a 1:1 mixture of *E:Z* alkenes were present in the ^{1}H NMR spectrum of the crude reaction mixture (**Figure 61**). The alkene doublets for the *Z*-alkene were clearly visible at 6.65 and 6.72 ppm after 18 h, with a *J* value of 12.1 Hz. After 24 h, it was clear that isomerisation had taken place as the *Z*-alkene doublets were significantly reduced. Although the *E*-alkene hydrogens could not be clearly observed in the crude reaction mixture, after column chromatography it was clear that the *E*-alkene had been formed. This was confirmed by two doublets with *J* values of 16.3 Hz, and the *E*-alkene product was isolated in a 65% yield. It is proposed that these doublets were shifted in the crude reaction mixture owing to possible coordination to zinc or palladium metals.
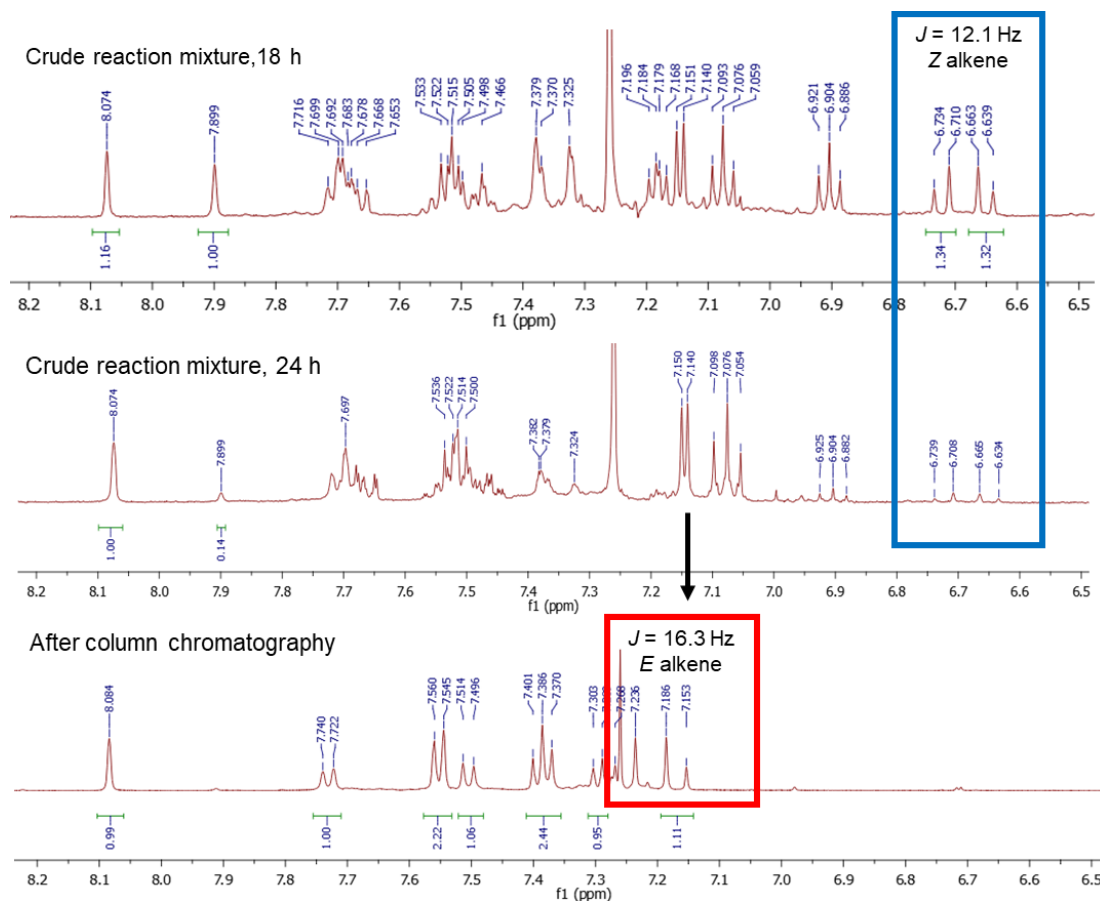
Figure 61*: ¹H NMR spectroscopy (region 6.5–8.2 ppm) showing reaction progress for reduction of phenyl alkyne **126a**. Crude reaction mixture after 18 h, 24 h and product ¹H NMR spectrum are displayed. Measured in CDCl₃ (18 h and column chromatography spectrum on 500 MHz spectrometer, 24 h spectrum ran on 400 MHz spectrometer).*

With an optimised and reproducible procedure in hand, the reduction of other alkynes was next investigated (**Scheme 72**). The reduction of fluoro analogue **126d** proceeded smoothly to give the desired *E*-alkene 57% yield. However, the reduction of cyano analogue **126g** and benzodioxazole analogue **126h** gave the desired products in low yields. These reactions proceeded slowly, with isomerisation of the *Z*-alkene to the *E*-alkene not complete after 20 h. However, when these reactions were left for extended reaction times, decomposition was observed and no improvement in yield could be achieved, and as such separation of isomers through column chromatography was required. In the case of naphthyl analogue **126i**, attempted reduction gave a complex, inseparable mixture of compounds. While Jackowski and co-workers reported that over-reduction of alkenes to give alkanes

was a common problem with their substrates, over-reduction was not observed in this study.
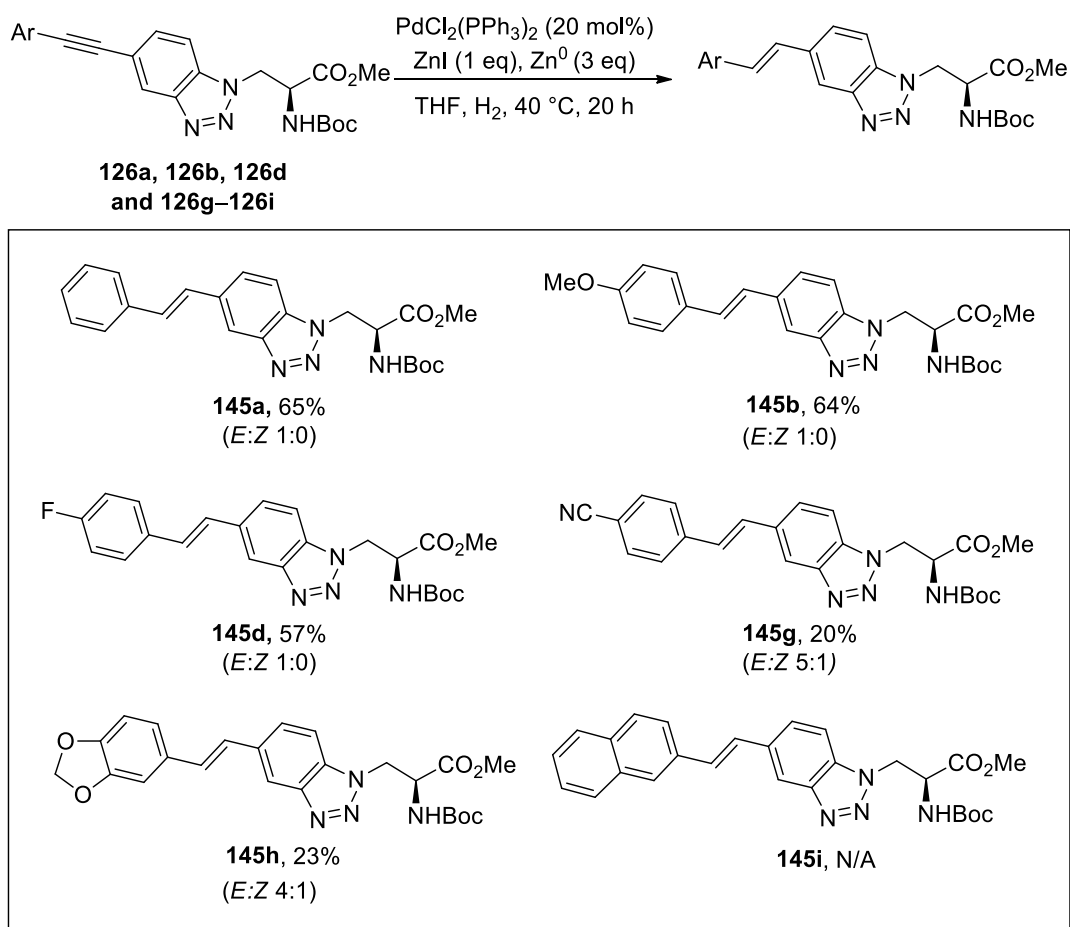
Scheme 72: *Reduction of alkynyl amino acids **126a**, **126b**, **126d** and **126g**–**126i** to give alkenes **145a**, **145b**, **145d**, and **145g**–**145i**. E:Z ratios are based on ^{1}H NMR spectroscopy of crude reaction mixtures. Yields are isolated yields of E-product.*

Following the synthesis of these alkenyl amino acids, it was decided that only the analogues produced in good yields would be deprotected, so that enough material could be generated for analysis of photophysical data. Deprotection of amino acids **145a**, **145b** and **145d** proceeded in good yields over two steps (**Scheme 73**). Ester hydrolysis using caesium carbonate was followed by mild Boc-protecting group removal with 2 M HCl at room temperature.
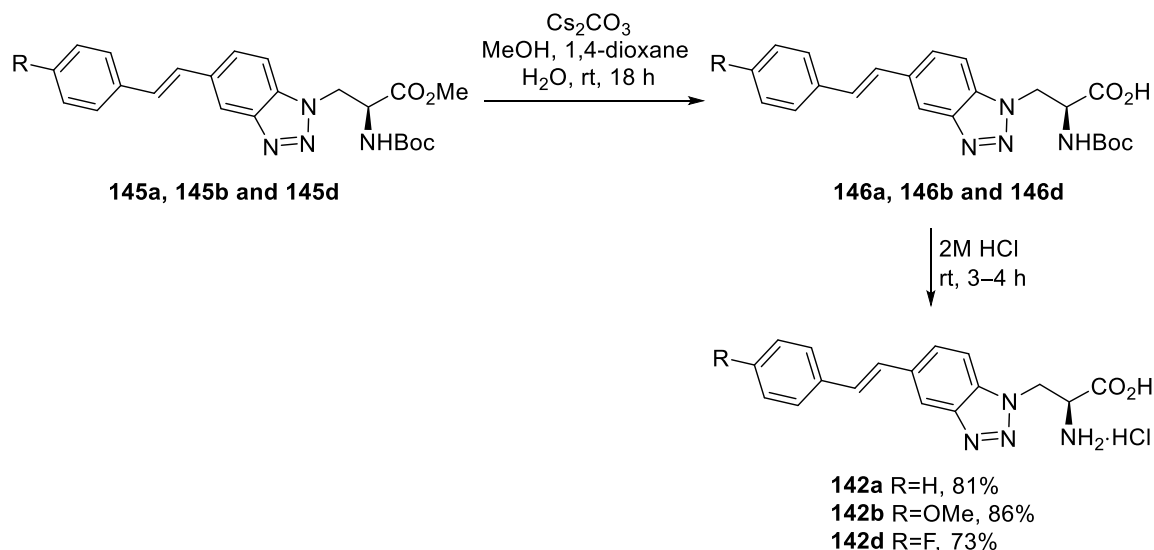
Scheme 73: *Deprotection of alkenyl amino acids* **145a, 145b** *and* **142d**.

As the absorption and emission spectra of methoxy analogue **142a** and phenyl analogue **142b** had been obtained previously, the corresponding spectra of fluorinated analogue **142d** were next obtained (**Figure 62**). This analogue displayed an absorption maxima of 263 nm, with an absorption peak which stretched to 330 nm, and an emission maxima of 408 nm.
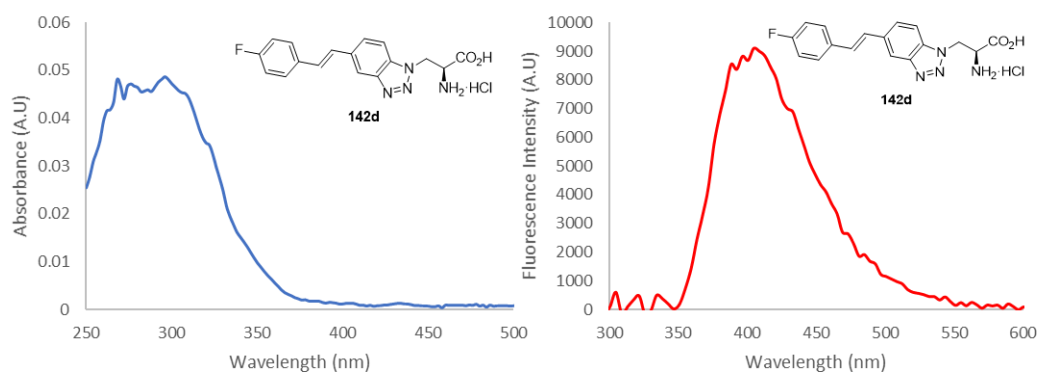
Figure 62: *Absorbance and emission spectra for amino acid* **142d**. *Measured at 5 µM in methanol. Excitation at 296 nm.*

Following the synthesis of sufficient quantities of the alkenyl fluorophores, extended photophysical characterisation of these compounds was undertaken (**Table 13**). All of the analogues had quantum yields of around 10%, with the overall brightness of amino acids **142a** and **142b** being very similar. Amino acid **142d** was the least bright of the series, as a result of a lower molar extinction coefficient than the other two analogues. As observed with the corresponding alkynes, the methoxy analogue

142b showed the most red-shifted absorption and emission values and the largest Stokes shift. Owing to this, amino acid **142b** was determined to be the most promising fluorophore from this small series.
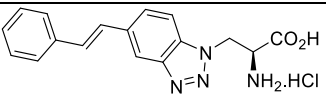
Amino Acid	Absorption Maximum (nm)	Emission Maximum (nm)	Stokes Shift (nm)	Molar Extinction Coefficient (cm^{-1} M^{-1})	Quantum Yield (Φ_F)	Brightness (cm^{-1} M^{-1})
142a	263 (307)	402	139 (95)	18000	0.09	1670
142b	304 (320)	443	139 (123)	12400	0.11	1410
142d	263 (303)	398	135 (95)	5900	0.09	550
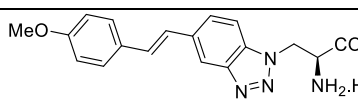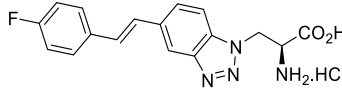
*Table 13: Photophysical properties of amino acids **142a, 142b and 142d**, measured in methanol.*

A direct comparison of alkene **142b** and alkyne-derived amino acid **128b** showed that the photophysical properties observed for the alkynyl series were generally more favourable than those for the alkenyl series (**Figure 63**). While alkenyl **142b** showed a more red-shifted emission spectra, this was outweighed by the significantly brighter fluorescence displayed by alkyne-derived amino acid **128b**. As fluorescence quantum yield is a measure of the number of photons emitted relative to those absorbed, it is generally lower if there are more non-radiative decay pathways available to a fluorophore. Owing to the quantum yield exhibited by alkenyl amino acid **142b** being lower than that for alkynyl analogue **128b**, it can be assumed that this fluorophore possesses more non-radiative decay pathways to the ground state. Such pathways may include extra rotational and vibrational modes of relaxation when compared to alkenyl amino acid **142b**. A similar result was observed by Perez-Inestrosa and co-workers in their synthesis of a series of di-alkenyl and alkynyl benzotriazoles.[135] For these analogues, quantum yields for the alkynyl series were generally higher than for the quantum yields of the alkenyl series. This was attributed to the fact that alkynyl derivatives cannot undergo photoisomerisation, which could be another consideration as to why the alkenyl series studied here demonstrate lower quantum yields.

142b
λ_{abs} = 304 nm, 320 nm
λ_{em} = 443 nm
ε = 12,400 M^{-1} cm^{-1}
Φ = 0.11
Brightness = 1400 M^{-1} cm^{-1}

128b
λ_{abs} = 296 nm, 321 nm
λ_{em} = 421 nm
ε = 20,800 M^{-1} cm^{-1}
Φ = 0.34
Brightness = 7072 M^{-1} cm^{-1}

128i
λ_{abs} = 304 nm, 320 nm
λ_{em} = 382 nm
ε = 12,400 M^{-1} cm^{-1}
Φ = 0.52
Brightness = 5200 M^{-1} cm^{-1}
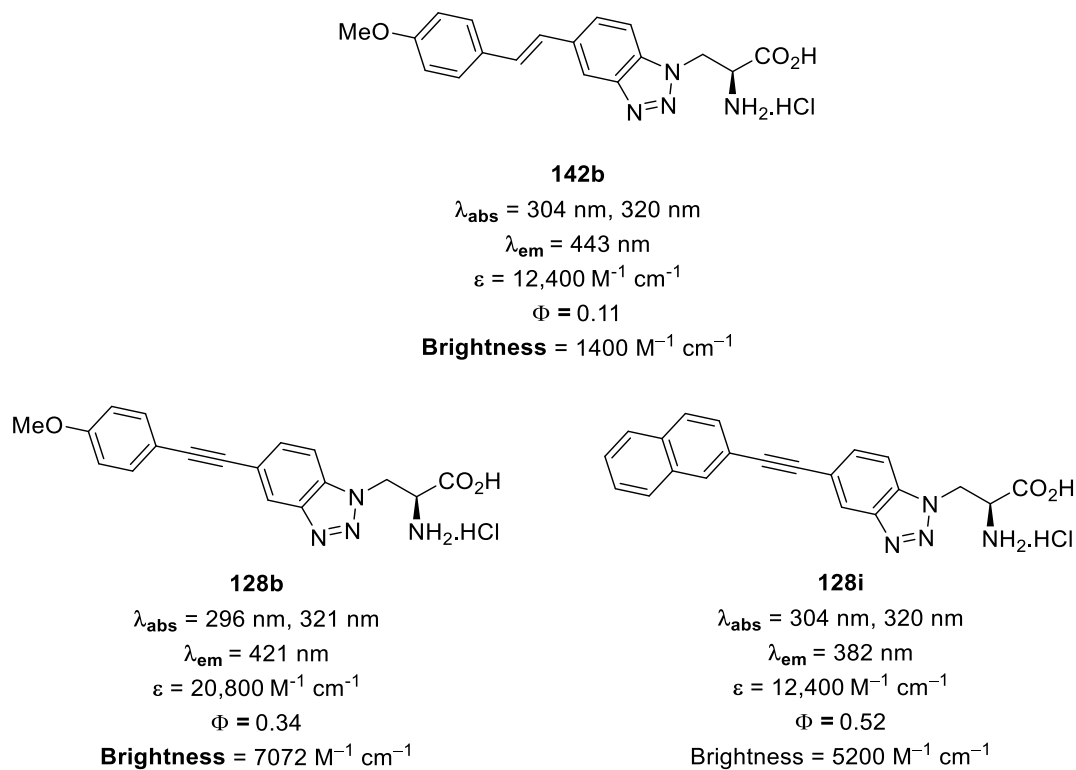
*Figure 63: Comparison of alkyne amino acids **128b** and **128i** alkenyl amino acid **142b**.*

3.5 Further Analysis of Lead Analogues

Overall, from all the amino acids synthesised, it was determined that methoxy analogue **128b** and naphthyl analogue **128i** had the best photophysical properties (**Figure 63**). Each of these analogues had a red-shifted absorption when compared to the aryl equivalent and were also brighter – highlighting the benefits of the inclusion of an alkyne to form a stretched chromophore.

The environmental sensitivities of these fluorophores were next studied through a solvatochromic study. Such a study is a good indicator of whether a fluorophore exhibits environmental sensitivity – with a change in emission maxima as solvent polarity increases indicating greater stabilisation of the fluorophore's excited state in more polar environments. While neither amino acid showed a significant shift in absorption maxima in solvents of different polarity, both showed a significant change in emission maxima (**Figure 64**). The emission maxima for amino acid **128b** varied from 367 nm in ethyl acetate to 460 nm in water, showing a difference of 107 nm in wavelength in the different solvents. Similarly, the emission maxima of amino acid **128i** varied from 348 nm to 426 nm from ethyl acetate to water, a difference of 78 nm across the different solvents.
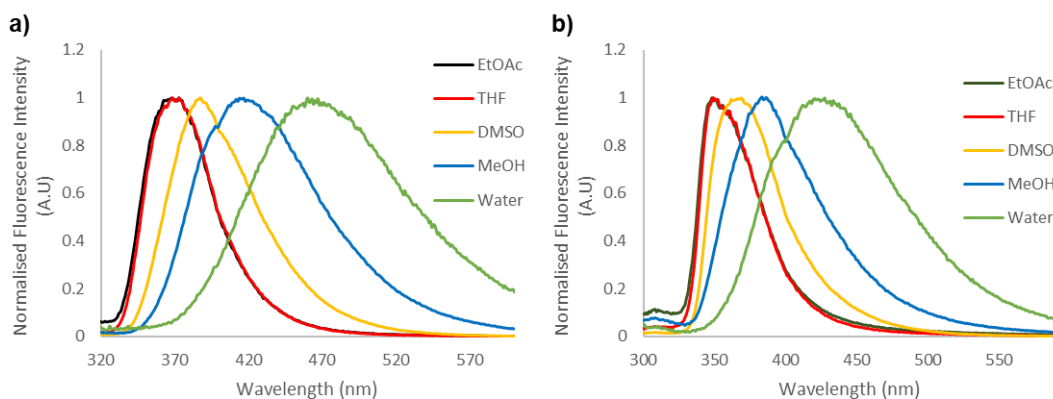
*Figure 64: Solvatochromic properties of a) amino acid **128b** and b) amino acid **128i**.*

As solvatochromism is a result of greater dipole stabilisation by more polar solvents, it is proposed that the larger shift in wavelength for amino acid **128b** is a result of a stronger dipole across the molecule. Lippart-Magata plots for each of these compounds showed a linear trend in emission maxima when compared to solvent polarity (**Figure 65**). This indicated that the change in emission wavelength was a result of excited state stabilisation resulting from the increasing polarity of each solvent.
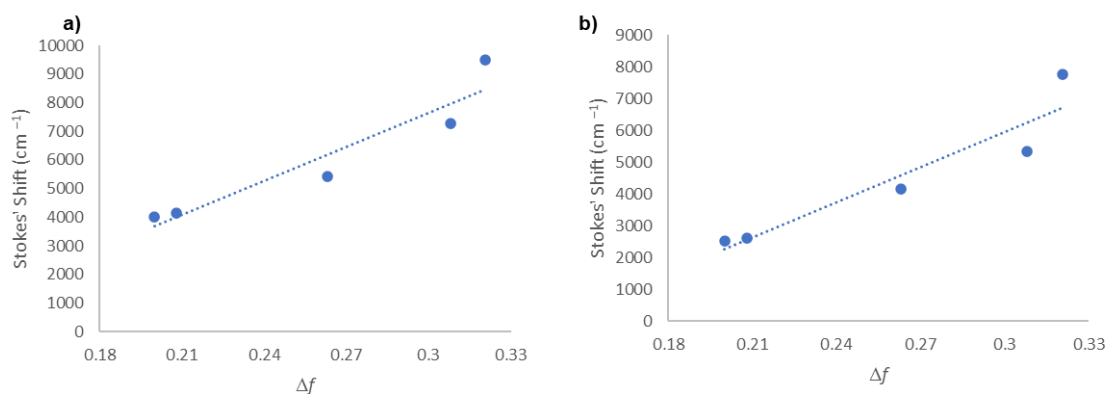
*Figure 65: Lippert-Magata graphs for a) amino acid **128b** and b) amino acid **128i**.*

As amino acid **128b** showed more environmental sensitivity, as well as being brighter with a more red-shifted emission maxima than amino acid **128i**, this was selected as the most promising candidate from this series of extended chromophores. Ultimately, the aim of this project was to synthesise a fluorophore with improved photophysical properties when compared to the previously synthesised library of benzotriazoles, and as this had been achieved, it was

122

subsequently proposed that it would be beneficial to investigate the use of this fluorophore for imaging as a component of a peptide. The incorporation of this amino acid into a peptide would confirm whether the improved photophysical properties were retained in a species that could be used as chemical biology tool. This investigation would require the synthesis of an Fmoc-protected analogue (**147**), to allow for peptide synthesis using a SPPS strategy. From amino acid **128b**, Fmoc-protection was achieved using *N*-(9-fluorenylmethoxycarbonyloxy)succinimide and sodium hydrogencarbonate as the base (**Scheme 74**). The reaction proceeded overnight at room temperature in a co-solvent mixture of 1,4-dioxane and water and gave desired Fmoc-protected amino acid **147** in 63% yield.
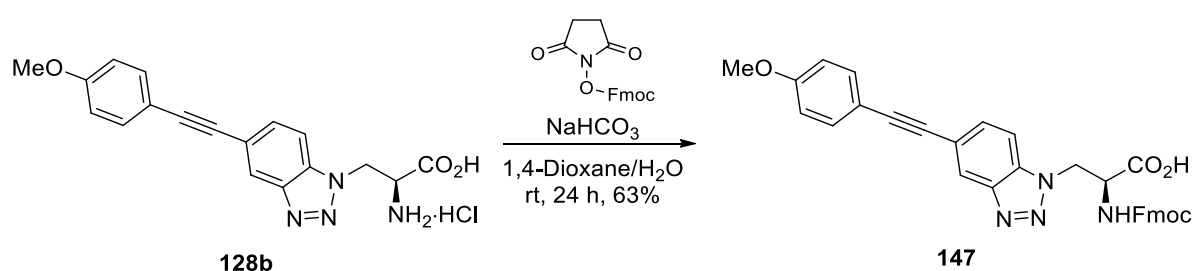
Scheme 74: Fmoc-protection of amino acid **147**.

3.6 Future Work

Prolonged exposure to UV light is known to cause cellular and tissue damage as a result of photobleaching.[136] As such, the use of small molecule fluorophores for cellular imaging applications is often limited, as generally these compounds absorb in the UV region owing to the limited degree of conjugation. One solution to this limitation is the use of two-photon or three-photon fluorescence microscopy whereby multiple photons of near-IR wavelength are used to excite the fluorophore.[137] The use of longer wavelengths for excitation can allow for cellular imaging over longer time periods, as well as deeper tissue penetration with minimal photo-bleaching and photo-toxicity. Such techniques have been used with fluorescent amino acids for the imaging of peptide-peptide interactions[57] as well as for the visualisation of fungal infections.[138] Recently, the Sutherland group showed that a two-photon excitation process was compatible with a pyrazoloquinazoline-derived α-amino acid, whereby a similar emission profiles were observed by one- and two-photon excitation.[20]

As the series of benzotriazole amino acids synthesised here show absorbances below 400 nm, it is proposed that future work will investigate the use of two-photon

or three-photon excitation of these amino acids. Two-photon excitation with photons of wavelength 700 nm, which is suitable for cellular imaging, would require a fluorophore with an absorption of half this wavelength (350 nm).[139,140] It is proposed that cyano-substituted amino acid **128g** which exhibited a suitable red-shifted absorption spectrum and acceptable brightness could be a suitable candidate for a two-photon excitation process. Meanwhile, for the use of three-photon excitation, which generally uses three photons of a longer wavelength (1300 nm or above), compounds with a more blue-shifted absorption spectrum may be used. As such, it is proposed that the brighter methoxy-substituted amino acid **128b** would be an appropriate candidate for three-photon excitation.

The incorporation of these amino acids into a peptide is also proposed, to allow for an investigation of their suitability for use in SPPS and whether the fluorescent properties of these compounds are consistent when incorporated into a peptide. The simple pentapeptide Val-Pro-Thr-Leu-Lys based on the Bax-binding domain of Ku70 has been shown to have low cytotoxicity and demonstrates good cell penetrating properties.[141] It is proposed that this peptide could be prepared using standard SPPS methodology, followed by incorporation of Fmoc-protected benzotriazole amino acid **147**, to give hexapeptide **148** (**Scheme 75**).[36] Following the synthesis of hexapeptide **148**, it is proposed that the fluorescent properties are determined, to examine how these change as part of a peptide.
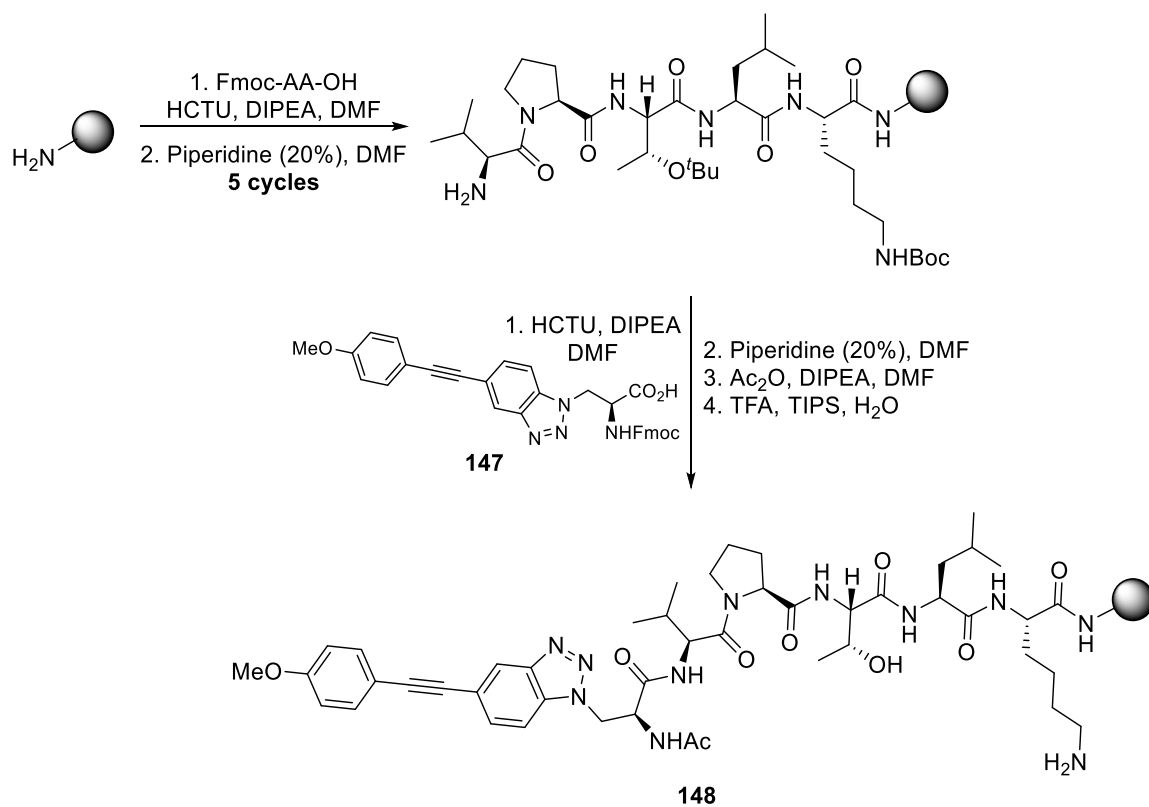
Scheme 75: *Proposed synthesis of hexapeptide* **148**.

4.0 Novel Synthesis of *cis*- and *trans*-4-Fluoroprolines

4.1 Introduction

Proline is unique among naturally occurring amino acids on account of containing a secondary amino group, as well as a conformationally restricted cyclic side chain (**Figure 66**).[142] Due to the conformational rigidity imposed by the cyclic ring, proline has a prominent role in determining protein secondary structure and is prevalent among structural proteins. In these proteins, proline has a tendency to act as a turn inducer as a result of the puckered conformation associated with the pyrrolidine ring.[143] The pyrrolidine ring exhibits two pucker modes, where C-4 is either *endo* or *exo* in the envelope conformation. In unsubstituted proline, the *endo* puckering mode is favoured.
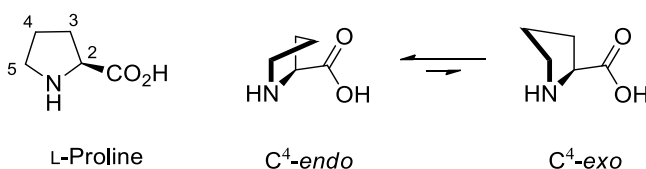
Figure 66: L-Proline, C4-endo and C4-exo conformers.

Large numbers of proline residues can be found in collagen, where these residues are oxidised during post-translational modification to yield 4-hydroxyproline.[144] Incorporation of the hydroxyl group by prolyl-4 hydroxylases occurs in the *R* configuration, to give *trans*-hydroxyproline. The electron withdrawing nature of the hydroxyl group stabilises a C^4-*exo* pucker through the gauche effect, which in turn enables an n→π * interaction, stabilising *trans* peptide bonds. It follows that inclusion of a more electronegative group at the C-4 position of the pyrrolidine ring would stabilise this pucker further, and this has been shown to be the case. Inclusion of the most electronegative element, fluorine, at the C-4 position in place of the hydroxyl group of *trans*-hydroxyproline greatly stabilises the C^4-*exo* pucker (**Figure 67**). Indeed, inclusion of *trans*-4-fluoroproline **149** into collagen in place of *trans*-4-hydroxyproline has been shown to further stabilise the triple helix conformation.[145]
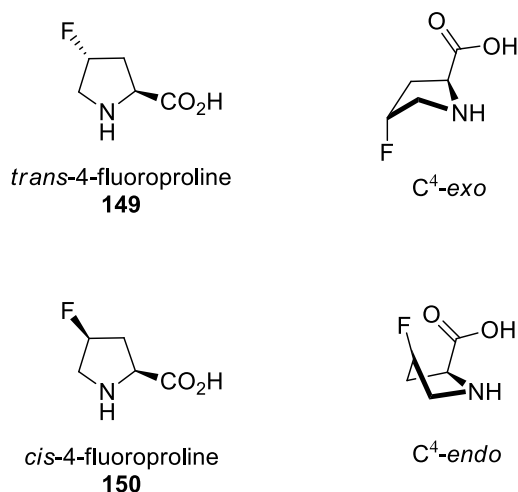
Figure 67: *Preferred ring puckers of trans-fluoroproline **149** and cis-fluoroproline **150**.*

The 4S-diastereomer of hydroxyproline, *cis*-hydroxyproline **150** has not been observed in natural proteins. While this diastereomer adopts the C^4-*endo* pucker, and consequently *cis* peptide bonds (usually imparted by an unsubstituted proline ring in collagen chains) would be expected to be favoured, it has been shown theoretically that hydrogen bonding between the hydroxyl group and carbonyl group results in this conformer preferring a *trans*-peptide bond.[144] As such, replacement of proline residues in collagen with *cis*-hydroxyproline does not impart more stable collagen folding. However, it has been shown that replacement in the same position with *cis*-fluoroproline *does* impart extra stability, as this has an even greater tendency towards a C^4-*endo* pucker and is unable to act as a hydrogen bond donor.[145] The ability of 4-fluoroprolines to stabilise (or destabilise) other proteins has also been noted, and ultimately these compounds have proven to be useful tools for investigating protein and peptide structures.[146]

4.1.1 4-Fluoroprolines Synthesis

As a prevalent component of collagen, *trans*-hydroxyproline is readily available and is frequently employed as a starting point in the synthesis toward fluoroprolines. Typical strategies to install fluorine in the C-4 position involve activation of the hydroxyl group, followed by S$_N$2 displacement by a fluoride anion. The first synthesis of 4-fluoroproline was reported in 1965 using this strategy[147] – with replacement of the *O*-toluenesulfonyl (*O*-tosyl) group of a *trans*-4-hydroxyproline derivative **151** using potassium fluoride at elevated temperatures (**Scheme 76a**). While this reaction proceeded mostly with the expected inversion of stereochemistry, some

127

retention was also observed. Subsequent deprotection steps allowed for the synthesis of *cis*-fluoroproline (**150**) in a 56% yield from the activated starting material. Using the analogous *O*-tosyl activated *cis*-hydroxyproline derivative **154**, *trans*-4-fluoroproline (**149**) was obtained in a 62% yield (**Scheme 76b**). No retention of stereochemistry was seen in the fluoride displacement step for this isomer.
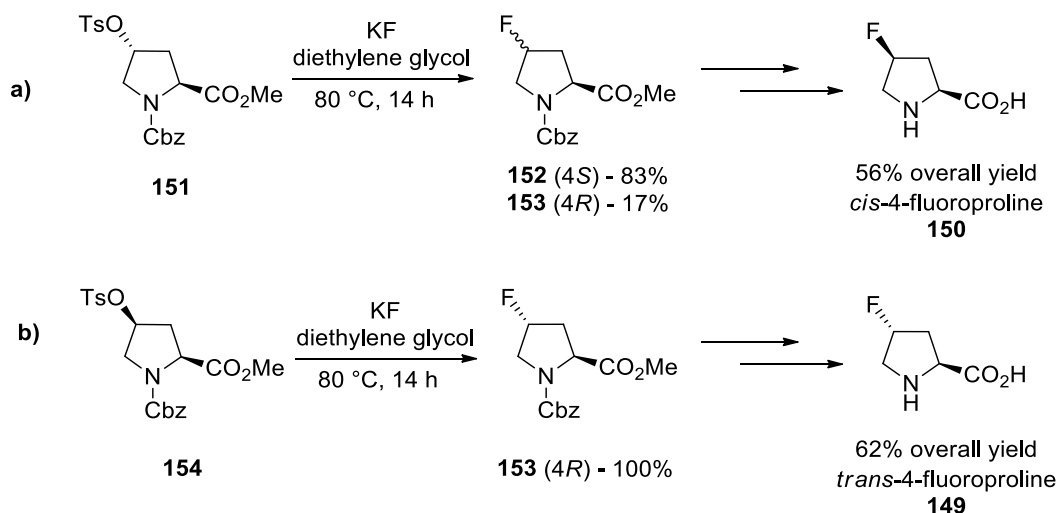
Scheme 76: First reported synthesis of a) cis-fluoroproline and b) trans-fluoroproline. Percentages of **152** and **153** describe relative isomer formations.

More recently, a scalable approach to the synthesis of *cis*-4-fluoroproline using a fluoride displacement strategy has been reported, where the displacement step occurred at a lower temperature.[148] In this route, the hydroxyl group of protected *trans*-4-hydroxyproline **155** was activated with trifluoromethanesulfonic anhydride, and tetra-*n*-butylammonium fluoride (TBAF) was used as a fluoride source for the substitution step to give protected *cis*-fluoroproline **156** in a 40% yield over the two steps (**Scheme 77**). Deprotection under reflux in acid conditions then gave the desired deprotected compound.
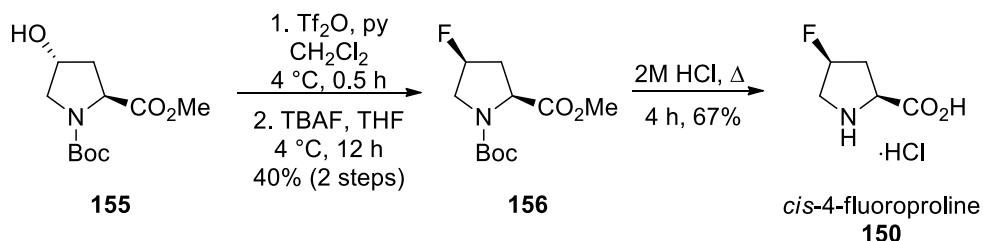
Scheme 77: Scalable synthesis of cis-4-fluoroproline.

While *trans*-4-hydroxyproline is a readily available starting material, its counterpart *cis*-4-hydroxyproline is considerably more expensive. As such, routes to *trans*-4-fluoroproline often also begin with the readily available *trans*-4-hydroxyproline and include extra steps to first invert the stereochemistry at the C-4 position. Raines and co-workers achieved this through initial activation of the hydroxyl group through mesylation to give **157**, followed by deprotonation and intramolecular cyclisation of the carboxylate to give lactone **158** (**Scheme 78**).[148] Ring opening with lithium hydroxide then gave protected *cis*-4-hydroxyproline **159** in a 78% yield over three steps. After methyl ester formation, synthesis towards *trans*-4-fluoroproline **149** was completed using the same S_N2 strategy shown above.
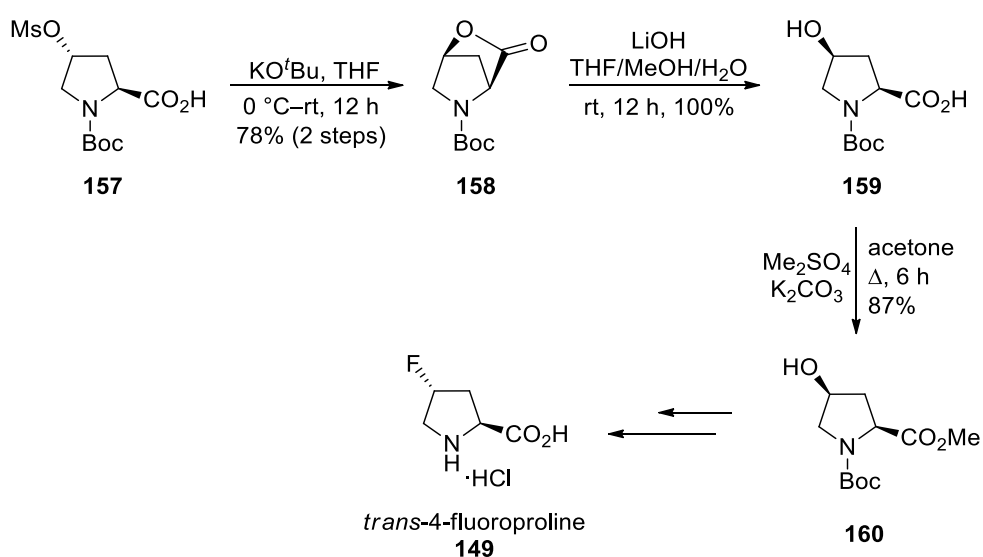
Scheme 78: *Inversion of stereochemistry of trans-4-hydroxyproline and subsequent synthesis of trans-fluoroproline.*

The use of organic fluorination reagents, such as diethylaminosulfur trifluoride (DAST) for the installation of fluorine at C-4 have also been reported.[142] These reagents for deoxyfluorination have the benefit of requiring only one step for the installation, as they provide both activation of the hydroxyl group and a fluoride source for displacement. In many early reports, the deoxyfluorination step was noted to occur with some epimerisation at the C-4 position, and formation of undesired alkenes were also reported. As a result, this approach was generally low yielding.[149–152] It has been proposed that the reason for epimerisation may be a result of intramolecular participation of the ester carbonyl group.[147] In 1998, the first successful synthesis using DAST was reported by Dugave and co-workers, where the deoxyfluorination step was carried out at –78 °C (**Scheme 79**).[153] Under these

conditions, no epimerisation was observed and an 81% yield was achieved for the synthesis of *cis*-fluoroproline **156** and a 63% yield for *trans*-fluoroproline **161**, although no reaction time was reported for these reactions. In subsequent years, other fluorinating reagents have shown to be effective for this transformation, including morph-DAST,[154] Fluolead,[155] PyFluor[156] and SulfoxFluor.[157]
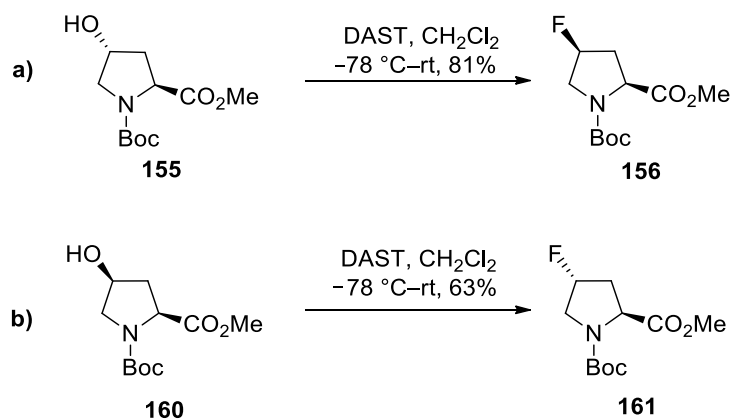
Scheme 79: *Synthesis of a) cis-4-fluoroproline **156** and b) trans-4-fluoroproline **161** using deoxyfluorination reagent DAST.*

In 1998, the synthesis of *trans*-4-fluoroproline by Dugave and co-workers was attempted using a Mitsunobu reaction.[153] This used *N*-Boc protected *trans*-4-hydroxyproline **155** to give the required *cis*-4-hydroxyproline **160** (**Scheme 80**). However, under these conditions, a mixture of *C*- and *N*- deprotected side-products were observed.
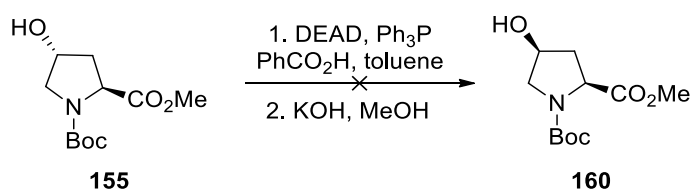
Scheme 80: *Attempted Mitsunobu inversion of C-4 stereochemistry with Boc-protected trans-4-hydroxyproline **155**.*

Instead, an alternative protecting group strategy was used. The trityl protected *trans*-4-hydroxyproline **162** was successfully transformed into *cis*-4-hydroxyproline **163** using a Mitsunobu procedure (**Scheme 81**). Protecting group manipulation gave *N*-Boc protected *cis*-4-hydroxyproline **160**, used for the subsequent deoxyfluorination step.
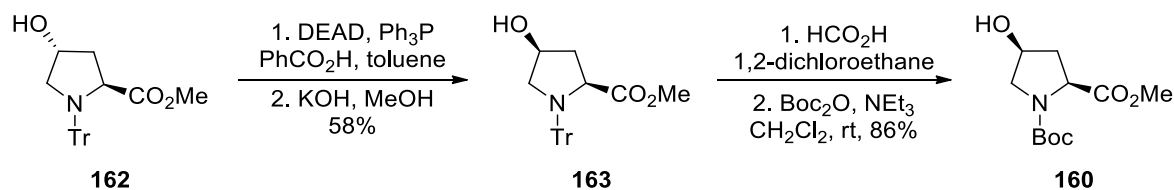
Scheme 81: *Inversion of stereochemistry using a Mitsunobu reaction.*

It has since been shown by Kobayashi and co-workers that the substitution of benzoic acid for formic acid in the Mitsunobu reaction allowed the efficient and direct conversion of **155** to **160** (**Scheme 82**).[154]
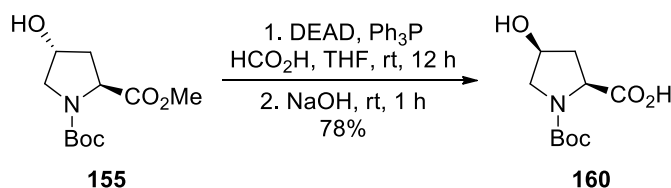
Scheme 82: *Mitsunobu reaction for the inversion of stereochemistry at C-4 of trans-4-hydroxyproline.*

4.1.2 4-[^{18}F]Fluoroproline

Radiolabelled compounds can be used as molecular imaging probes, providing a method for non-invasive visualisation of biological processes.[158] One such method for visualising these processes is Positron Emission Tomography (PET) imaging, which is one of the most sensitive techniques available for imaging function *in vivo*.[159] Radionuclides such as ^{11}C or ^{18}F decay through the emission of a positron, which on emission from the nucleus travels a short distance in surrounding tissue (**Figure 68**). This positron then combines with an electron (a process known as annihilation). During this process, the combined mass of the positron and electron is emitted as energy in the form of two γ-rays. These are emitted simultaneously at approximately 180° to each other and can be detected by surrounding detectors. Large numbers of these events can be recorded and combined to reconstruct the information into an image which provides information on the spatial distribution of radioactivity.
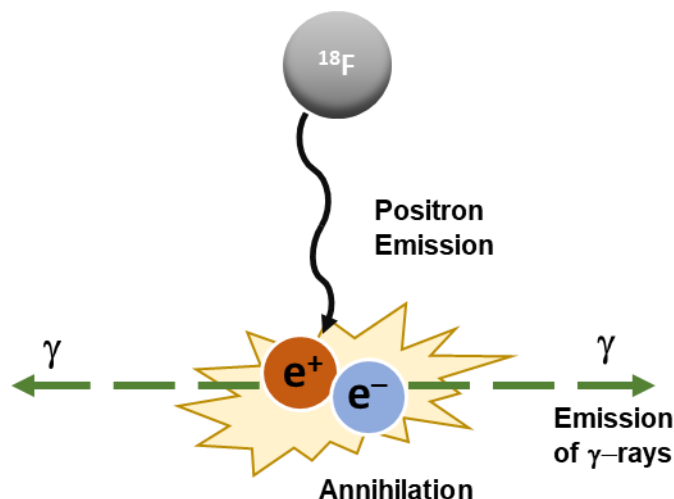
Figure 68: Emission and annihilation of a positron from ^{18}F.

The main isotopes used for PET imaging are ^{11}C and ^{18}F, however for the most part, compounds labelled with ^{18}F have more favourable properties.[159] The half-life of ^{18}F is 110 minutes, compared to 20 minutes for ^{11}C; this longer half-life allows time for more complex radiosynthesis and longer *in vivo* studies. Crucially, it also allows time for compounds to be transported to clinical PET centres which lack radiochemistry facilities.

Radiolabelling with ^{18}F typically occurs *via* a nucleophillic substitution strategy, employing an ^{18}[F]fluoride ion.[159,160] This can occur either as nucleophilic aromatic substitution on highly activated rings, or *via* an S_N2 mechanism at an aliphatic carbon. In the latter case, this generally involves displacement of a good leaving group such as a tosylate or triflate. As fluoride ions are poor nucleophiles, these reactions can be enhanced by adding alkali salts and cryptands. A commonly used cryptand is the aminopolyether Kryptofix (K222) (**Figure 69**), which complexes the cation to leave a more reactive fluoride source.
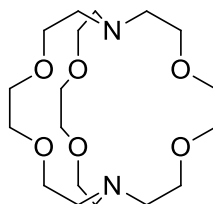
Kryptofix (K222)

Figure 69: Structure of Kryptofix (K222).

As the key building blocks of life, α-amino acids play an important role in biological processes. Thus, radiolabelled amino acids (**Figure 70**) are important targets for PET imaging, with potential applications in gaining non-invasive information on a range of diseases.[161] As amino acid transport and subsequent protein synthesis is upregulated in many tumour types, α-amino acids have proven important tools for imaging various forms of cancer.[162] Compounds including L-[11C]methionine ([11C]MET), and *O*-(2-[18F]fluoroethyl)-L-tyrosine ([18F]FET) have been selectively incorporated into tumours for PET imaging.[163,164] In addition to cancer imaging, compounds such as 6-[18F]fluoro-L-DOPA ([18F]FDOPA) have also been used in the investigation of neurodegenerative disorders.[165] Finally, studies involving radiolabelled 4-fluoroproline compounds, *trans*-4-[18F]fluoroproline (**[18F]149**) and *cis*-4-[18F]fluoroproline (**[18F]150**) have been undertaken to investigate the clinical application of these compounds in different diseases.[162] Potential applications include investigation of tumour growth and neurodegeneration, as well as the abnormal collagen biosynthesis which is present in diseases such as lung fibrosis. A number of biological studies using fluoroprolines have been carried out in animals,[166] cell cultures,[167] and humans.[168] Both *cis*- and *trans*-4-[18F]fluoroproline have been shown to be metabolically stable *in vivo*, and *cis*-4-[18F]fluoroproline has been shown to be incorporated into proteins.[162]
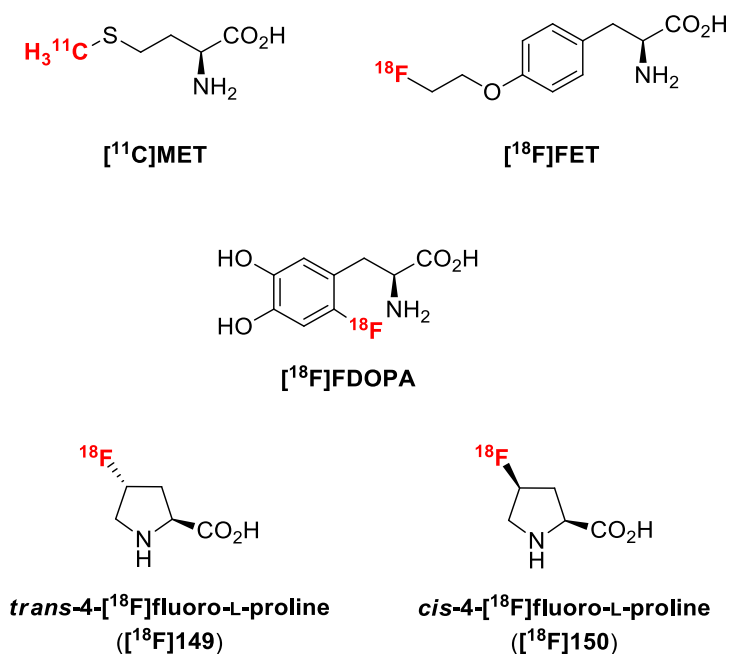
Figure 70: *Radiolabelled amino acids used in PET imaging.*

A stereoselective synthesis of both *cis*-4-[^{18}F]fluoroproline and *trans*-4-[^{18}F]fluoroproline was achieved in 1999, using diastereomerically pure precursors **164** and **165** (**Scheme 83**).[169] The synthesis used a cryptate mediated ^{18}F-fluorination step to give the [^{18}F]-fluorinated products **[^{18}F]156** and **[^{18}F]161** in radiochemical yields of approximately 36%. Radiochemical yield is defined as the amount of activity in the product expressed as a percentage of starting activity used, and is generally reported as a decay corrected number.[170]
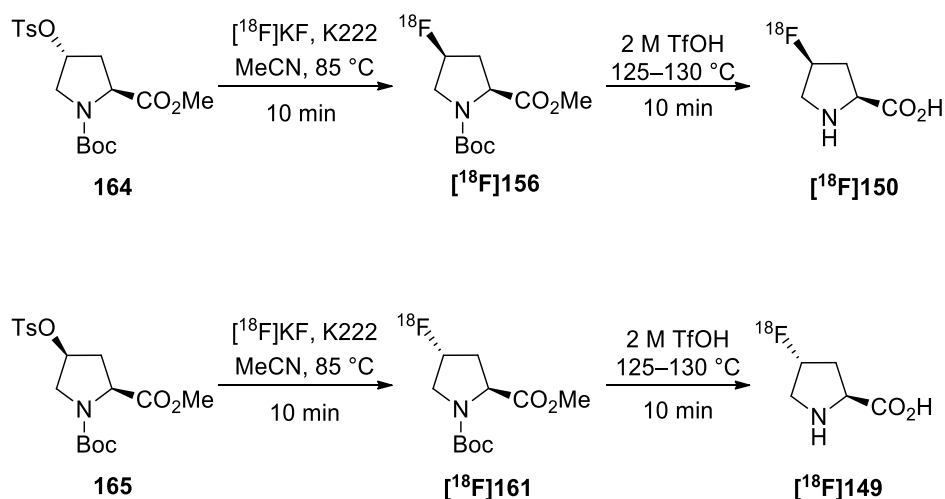
Scheme 83: *First radiosynthesis of cis-4-[^{18}F]fluoroproline* **[^{18}F]150** *and trans-4-[^{18}F]fluoroproline* **[^{18}F]149.**

After radiofluorination, **[^{18}F]156** and **[^{18}F]161** were subjected to deprotection using trifluoromethanesulfonic acid at high temperatures to give the desired fluoroprolines. It was noted that between 7 and 29% of the undesired diastereomer was formed in each case, indicating that something more complex than a simple S_N2 substitution with [^{18}F]fluoride occurred in this step. It was suggested that this could be due to both S_N1 and S_N2 pathways being present, or alternatively a result of intramolecular participation of the adjacent carbonyl group. This intramolecular participation of the carbonyl group was previously suggested by Gottlieb and co-workers when formation of the undesired diastereomer was observed in their cold synthesis of fluoroprolines using potassium fluoride as a nucleophile at 80 °C.[147]

While this method for the synthesis of [^{18}F]fluoroprolines is still in practice, it has since been updated with the development of automatic methodology for the radiofluorination step. In 2011, Chirakal and co-workers reported the automated synthesis of *cis*-4-[^{18}F]fluoroproline, with a 65% radiochemical yield of the

fluorinated intermediate, and a 38% radiochemical yield at the end of a 90-minute synthesis (**Scheme 84**).[171] In this work the authors note that diastereomerically pure fluoroproline is obtained at lower temperatures (85–100 °C), while at higher temperatures (130 °C) for the radiofluorination step, both diastereomers are formed. The lower temperatures used were comparable to those used by Hamacher and co-workers. It was proposed that the radiofluorination step was achieved diastereoselectively, and that the difference in product purity seen by the two groups may be a result of the purification of the fluorinated intermediate prior to the harsh deprotection conditions. It was proposed that the epimerisation observed by Hamacher and co-workers may have occurred during this step.

Following purification of the fluorinated intermediate, Chirakal and co-workers investigated an alternative deprotection method.[171] The use of trifluoromethanesulfonic acid at high temperatures in the deprotection step proved to be a major disadvantage in the synthesis of fluoroprolines. This acid is classified as a super acid, and as well as being extremely corrosive requires special care and equipment for storage and handling as a result of its hygroscopic nature. To circumnavigate the requirement for harsh acidic conditions, a manual two-step strategy using dilute aqueous hydrochloric acid for removal of the *N*-Boc protecting group followed by sodium hydroxide at room temperature for ester hydrolysis was investigated. It was reported that the use of these basic conditions resulted in some epimerisation, giving 5% formation of the undesired diastereomer.
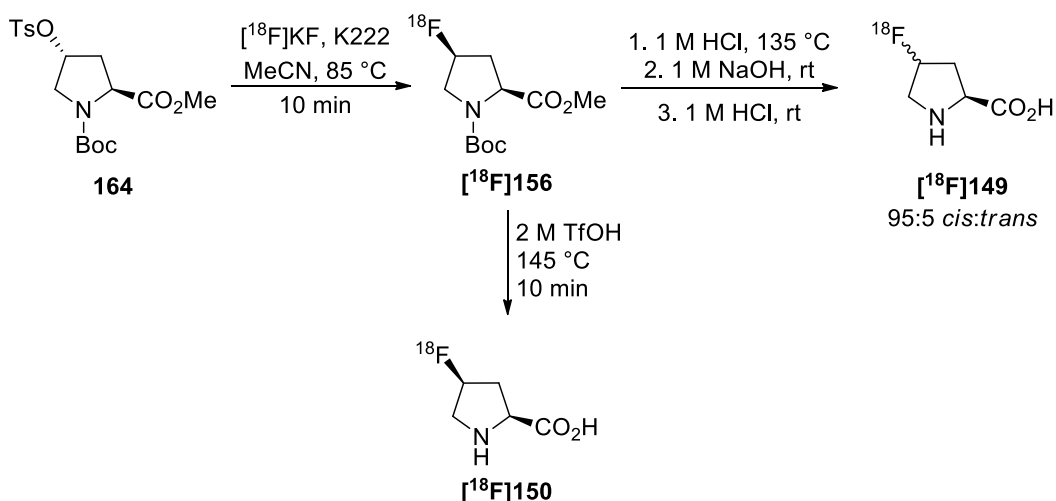
Scheme 84: *Alternative deprotection strategies in the radiosynthesis of 4-fluoroproline.*

4.2 Project Aims

Existing routes to radiolabelled *cis*- and *trans*-4-fluoroproline are limited by the conditions required for deprotection of the precursors used. For a one-step deprotection of the methyl ester and *N*-Boc group of **156** harsh acid conditions were required, using trifluoromethanesulfonic acid. Alternatively, a two-step deprotection method has been reported, which utilised a milder acidic deprotection followed by basic hydrolysis. Unfortunately, in this case, some epimerisation at C-4 was observed. In addition to this, these conditions aren't amenable to automation and require manual handling of radioactive intermediates. As such, the aim of this project was to produce a route to the radiolabelled compounds whereby the deprotection was mild enough to reproduce in an automated manner. Another reported problem with the synthesis of fluoroproline is the fluorination step involving an S_N2 controlled inversion of stereochemistry at the C-4 position. It has been proposed that interaction of the carbonyl carbon of the methyl ester may result in some retention of stereochemistry, requiring the difficult separation of the two isomers. It was proposed that a solution to both these issues would be to use a *tert*-butyl ester, in place of the methyl ester commonly used in these syntheses (**Figure 71**). This would allow for a mild acid deprotection, and it was proposed that the bulky *tert*-butyl group would minimise any risk of carbonyl interaction in the inversion step.

Figure 71: *Commonly used protecting group strategy in the synthesis of 4-fluoroprolines (**156**) and proposed alternative strategy (**166**).*

A route to the *tert*-butyl ester described was proposed starting from the readily available *N*-Boc-ʟ-4-hydroxyproline (**Scheme 85**), with esterification of the acid, followed by tosyl activation of the alcohol. This would provide a good leaving group for nucleophilic substitution with a fluoride source, and would be the precursor used for radiosynthesis with ^{18}F. In a non-radioactive route to *cis*-4-fluoroproline, it was proposed that a fluoride source such as TBAF could be used to give the desired inversion of stereochemistry and install fluorine at the C-4 position. Finally, a milder acidic deprotection at room temperature was proposed using aqueous hydrochloric

136

acid to simultaneously deprotect both protecting groups. This would give the non-radioactive *cis*-4-fluoroproline required as a standard to optimise the ^{18}F-radiofluorination reaction.
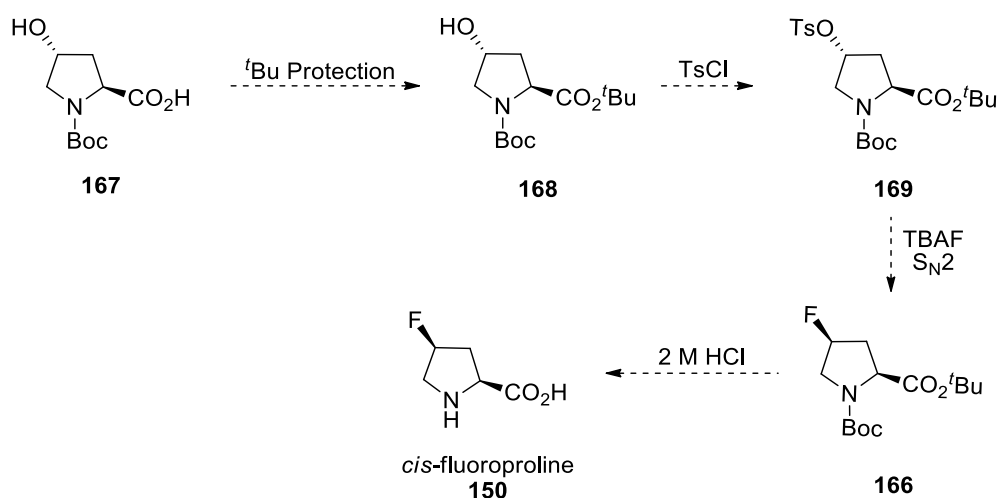
Scheme 85: *Proposed synthesis of cis-fluoroproline.*

A similar route to synthesise *trans*-4-fluoroproline was required, and it was proposed that the same steps could be undertaken starting from *N*-Boc-*cis*-4-hydroxyproline (**167**) to give *trans*-4-fluoroproline (**149**) and radiochemical precursor (**172**) (**Scheme 86**). As **170** was not commerically available, it was proposed that this could be produced from *N*-Boc-*trans*-4-hydroxyproline (**167**) in two steps following literature precedent.[148]
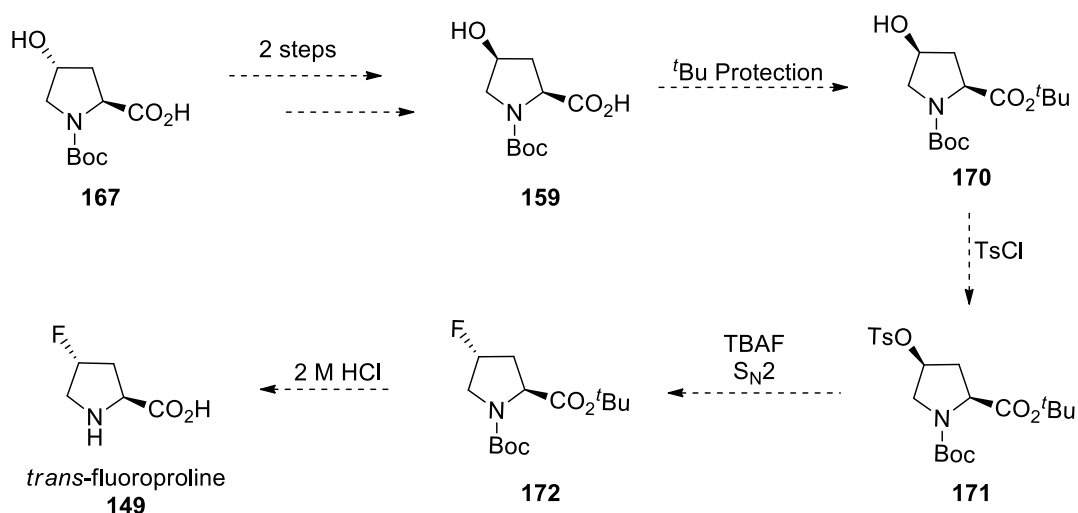
Scheme 86: *Proposed synthesis of trans-4-fluoroproline.*

4.3 Synthesis of *cis*-4-fluoroproline

Initial investigation into the *tert*-butyl protection of the carboxylic acid moiety of **167** began with the use of *O-tert*-butyl-*N,N'*-diisopropylisourea in dichloromethane at 40 °C for 24 h (**Table 14**).[172] Initial reaction conditions gave the desired product in a 40% yield (entry 1); an increase in reaction time to 48 h resulted in an improved yield of 60% (entry 2), while a further increase in reaction time led to no significant improvement (entry 3). It was proposed that an increase in temperature would allow this reaction to proceed more rapidly. Replacing dichloromethane with tetrahydrofuran as the reaction solvent allowed the temperature of reaction to be increased to 60 °C (entry 4). Under these conditions, the reaction proceeded to completion in 24 h. These optimised conditions were used to produce the desired *tert*-butyl ester (**168**) in a 68% isolated yield.
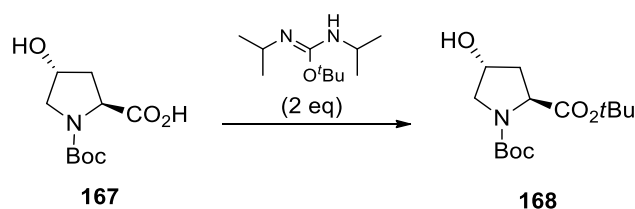
Entry	Solvent	Temperature (°C)	Time (h)	Yield (%)
1	CH$_2$Cl$_2$	40	24	40
2	CH$_2$Cl$_2$	40	48	60
3	CH$_2$Cl$_2$	40	60	61
4	THF	60	24	68

*Table 14: Optimisation of the tert-butyl esterification of **167**.*

Following the successful *tert*-butyl esterification, activation of the alcohol group of **168** was investigated. The alcohol group was converted into a good leaving group by reaction with 4-toluenesulfonyl chloride in the presence of pyridine at 40 °C in order to give the toluenesulfonate **169** with retention of stereochemistry. These conditions resulted in a successful reaction, with a 60% yield over 96 h. It was proposed that the addition of dimethylaminopyridine (DMAP) (10 mol%) could increase the rate of reaction[173] – and over the same 96 h time period, a slight improvement in yield (65%) was observed. Upon scale up, this reaction proceeded with a much improved yield and gave the desired product (**169**) in 81% yield (**Scheme 87**). The synthesis of the radiochemical precursor was then complete, which possessed a suitable leaving group for replacement with a nucleophilic

fluoride source. The purity of this compound was determined to be 98% by HPLC at 254 nm (**Appendix A**) and was passed to collaborators for radiolabelling experiments.
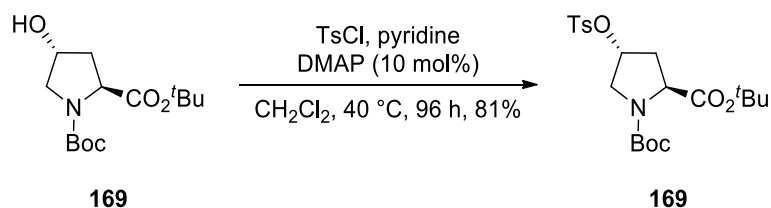
Scheme 87: *Reaction of alcohol **168** with 4-toluenesulfonyl chloride in the presence of catalytic DMAP.*

Installation of fluorine at the C-4 position was next investigated in the synthesis of a cold standard. The proposed method for this step involved using TBAF as a fluoride source to allow for an S_N2 displacement of the toluenesulfonate leaving group.[148] It was proposed that the large *tert*-butyl group of the ester would minimise interaction of the carbonyl group and allow for this reaction to proceed with complete inversion of stereochemistry. Instead of the desired substitution reaction, however, an elimination reaction was observed. The basicity of the fluoride source resulted in hydrogen atom extraction and elimination of the toluenesulfonate group and gave alkene **173** as the major product in 40% yield (**Scheme 88**).[174]
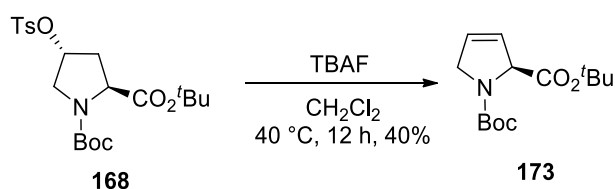
Scheme 88: *Elimination reaction to give alkene **173**.*

An alternative method for installation of the fluorine at C-4 was considered, which proceeded directly from alcohol **168**. The use of organic reagents for fluorination at this position have been reported, including the use of DAST,[153] and morpholinosulfur trifluoride (morph-DAST)[154] (**Figure 72**). As the first dialkylaminosulfur trifluoride reagent to be commercially available, significant studies have been performed using DAST. Unfortunately, this reagent has the potential to decompose violently when heated, and explosions have been reported in its use.[175] Thus, it was decided to pursue morph-DAST as a fluorinating agent for this step, which has been reported to be more stable. The use of a deoxyfluorination reagent had the added advantage

of producing the fluorinated product in one-step, by providing both activation and a fluoride source for the substitution reaction.
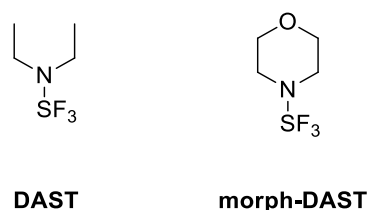
DAST   **morph-DAST**

Figure 72: *Structures of organic fluorinating agents DAST and morph-DAST.*

The deoxyfluorination of **168** with morph-DAST was successful, and gave the desired product in a 63% yield (**Scheme 89**). The addition of the fluorinating agent was carried out at −78 °C, and as reported by Kobayashi and co-workers, proceeded with complete inversion of stereochemistry.[154] No trace of the undesired diastereomer was present in the NMR spectrum of the crude reaction mixture, which allowed for simple column chromatography purification of this compound.
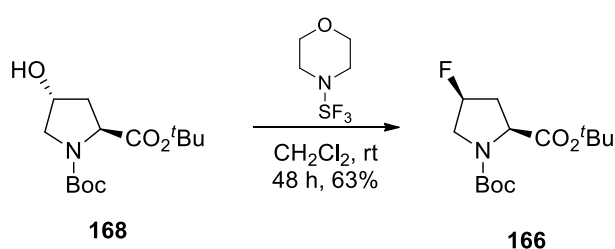
Scheme 89: *Deoxyfluorination of 168 using morph-DAST.*

In peptides, prolines can be present in a *cis* or *trans* conformation, due to the existence of two amide rotamers (**Figure 73**).[176] The *trans*-rotamer is favoured due to an n→π* interaction which involves the donation of electron density from the oxygen lone pair into the π* orbital of the adjacent carbonyl group.[177] This rotamer can be further favoured by an electron-withdrawing substituent in the 4*R* position, which encourages *exo* ring puckering and thus strengthens this n→π* interaction. Alternatively, this preference for a *trans*-rotamer can be weakened by an electron-withdrawing substituent in the 4*S* position, which encourages an *endo* ring puckering and weakens the n→π* interaction.[178]
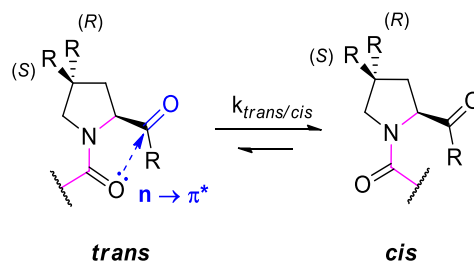
Figure 73: *cis- and trans-Amide bond proline rotamers.*

The existence of *cis-* and *trans*-rotamers is mimicked in prolines with an *N*-acyl protecting group, and as such all of the prolines discussed so far were visible as two rotamers by ^{1}H NMR spectroscopy. These rotamers were especially evident in the ^{19}F NMR spectrum of compound **166**, where two clear signals could be observed in a ratio of 1.86:1 (**Figure 74**). These peaks corresponded to the *trans* and *cis* isomers, respectively. This ratio of peaks gave a $K_{cis/trans}$ value of 1.86, which is in close agreement with values for the methyl ester found in literature ($K_{cis/trans}$ = 1.63).[178] This indicated that the presence of the bulky *tert*-butyl ester did not have a significant impact on the rotamer ratio of **166**.
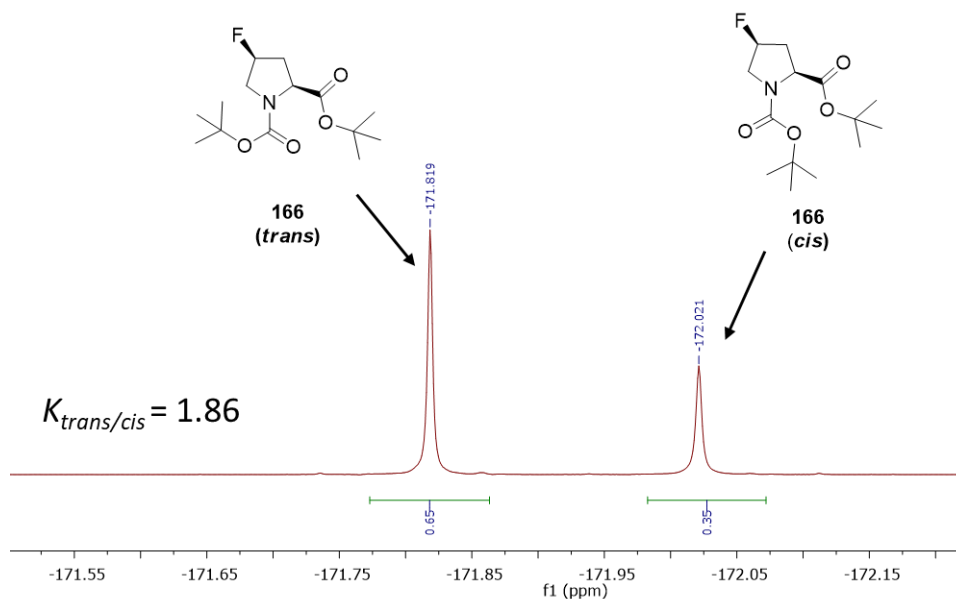
Figure 74: *Rotamers of N-Boc fluoroproline **166** as observed by ^{19}F NMR spectroscopy (measured in CDCl₃).*

Finally, the deprotection of **166** was required. A one step, room temperature acidic deprotection was successful in removing the labile protecting groups, using 2 M aqueous hydrochloric acid and acetonitrile as a co-solvent (**Scheme 90**). This

completed the synthesis of a non-radioactive standard of *cis*-4-fluoroproline. Crucially, the required conditions for the deprotection of the *tert*-butyl ester were considerably milder than required for the methyl ester frequently reported in literature.[171] It was proposed that the use of these milder conditions would allow this reaction to be reproduced successfully on an automated system. This would permit the synthesis of radiolabelled fluoroproline without the manual handling required for a two-step deprotection, or the use of highly corrosive trifluoromethanesulfonic acid. The production of *cis*-4-fluoroproline was clean as observed by NMR spectroscopy, however the exact purity could not be identified by HPLC analysis as the molecule was not visible by UV light.
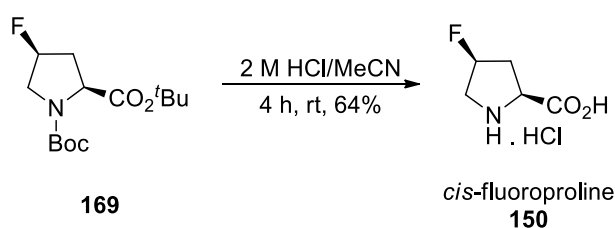
Scheme 90: *Acidic deprotection to give cis-4-fluoroproline.*

Overall, a two-step synthesis of the desired precursor **169** starting from readily available *N*-Boc-4-hydroxyproline was achieved (**Scheme 91**). From common intermediate **168**, deoxyfluorination and deprotection was possible, giving deprotected *cis*-4-fluoroproline in three steps.
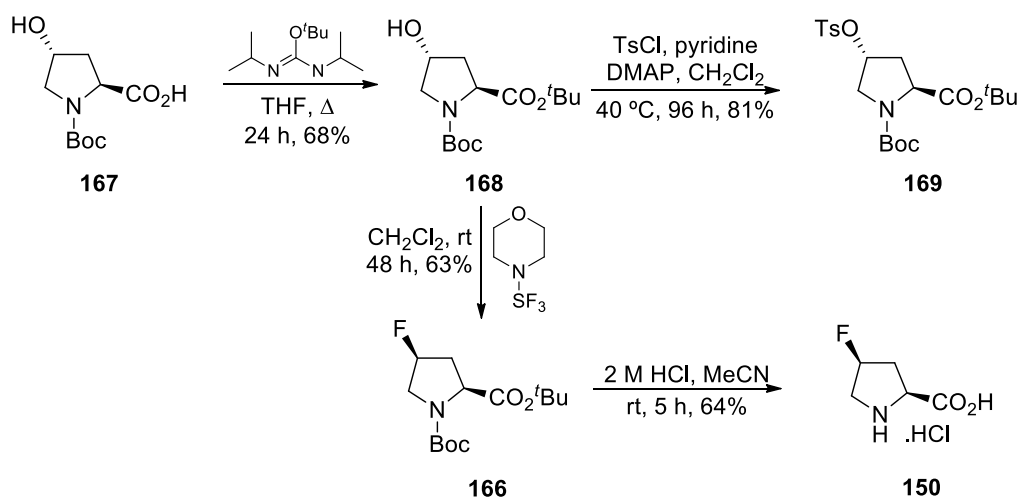
Scheme 91: *Final synthesis of precursor 169 and non-radioactive standard 150.*

4.4 Synthesis of *trans*-4-fluoroproline

Work towards the synthesis of *trans*-4-fluoroproline began with the investigation of inversion of stereochemistry at C4 of commercially available *N*-Boc-*trans*-4-hydroxyproline **167** to give the desired *N*-Boc-*cis*-4-hydroxyproline **159**. Initial exploration studied the use of methanesulfonyl chloride for mesylation of the hydroxyl group which would then be displaced by intramolecular attack from the carboxylic acid under basic conditions to give lactone **158**.[148] Hydrolysis of this compound would give the desired *N*-Boc-*cis*-4-hydoxyproline **159** (**Scheme 92**). Unfortunately, the protection with mesyl chloride, followed by use of potassium *tert*-butoxide to allow for the intramolecular cyclisation, led to a complex mixture which could not be separated to give any of the desired product.
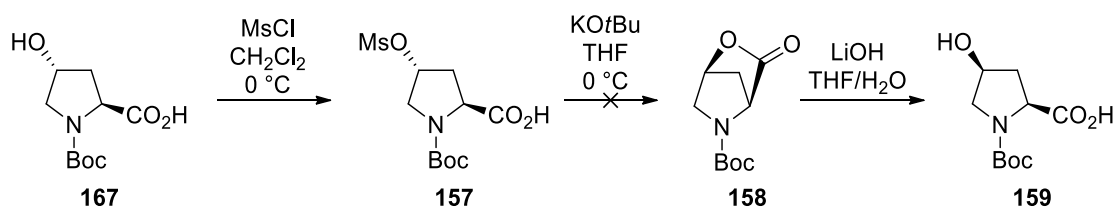
Scheme 92: Attempted inversion of C4 stereochemistry of N-Boc-trans-hydroxyproline.

An intramolecular Mitsunobu reaction was considered as an alternative method for the synthesis of the desired lactone **158** (**Scheme 93**). Reaction of the C-4 alcohol with a phosphonium intermediate generated through reaction of triphenylphoshine and diisopropyl azodicarboxylate (DIAD) provided a good leaving group. Intramolecular attack of the carboxylate would then occur, with elimination of triphenylphosphine oxide. In the event, this worked well and generated the desired lactone in a 77% yield.
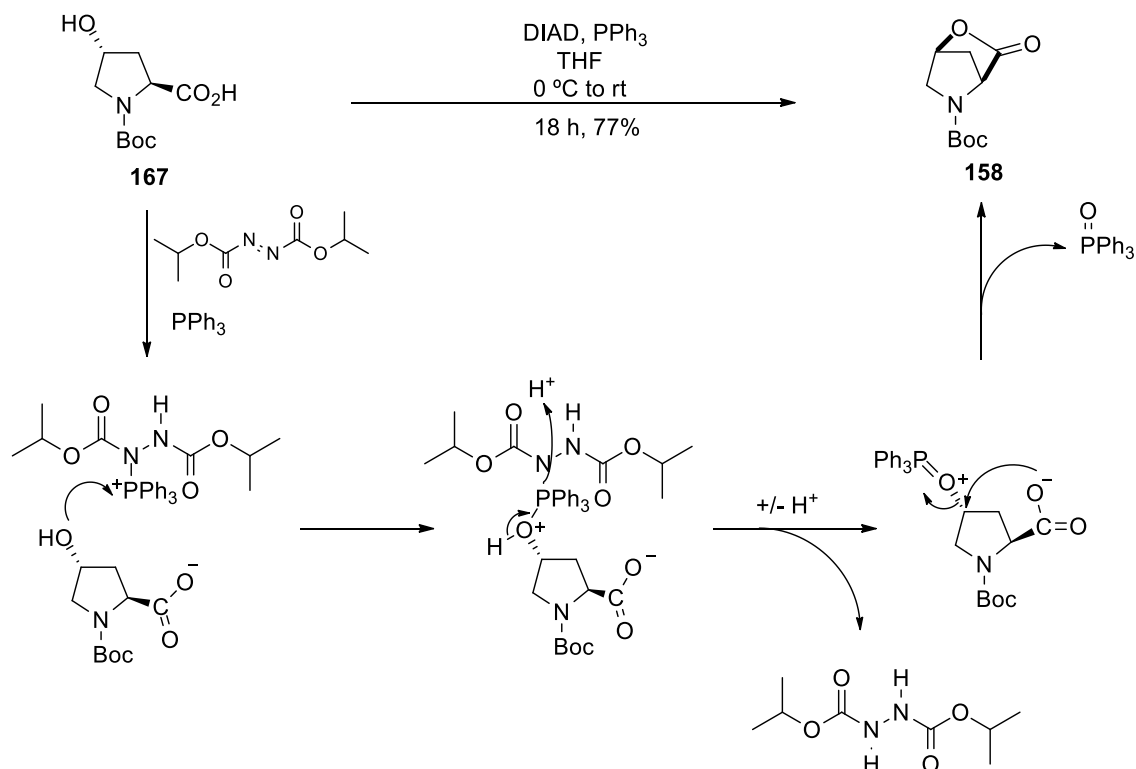
Scheme 93: *Synthesis of lactone **158** via intramolecular Mitsunobu reaction.*

While in literature this step is frequently followed by methanolysis to produce the methyl ester,[179] here a simple hydrolysis was used to yield the carboxylic acid of *cis*-hydroxyproline (**Scheme 94**). Protection as the *tert*-butyl ester was subsequently achieved using the same conditions as for the protection of *trans*-4-hydroxyproline, in an 87% yield.
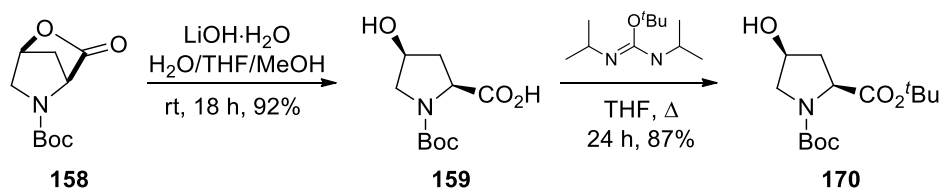
Scheme 94: *Ring opening of lactone **158** followed by tert-butyl esterification to give protected cis-4-hydroxyproline.*

Activation of the alcohol was subsequently performed using the same conditions as previously (**Scheme 95**), which provided the desired *trans*-4-fluoroproline precursor **171**. This precursor was passed to collaborators for radiolabelling, and purity was determined by HPLC to be 98% at 254 nm (**Appendix A**).
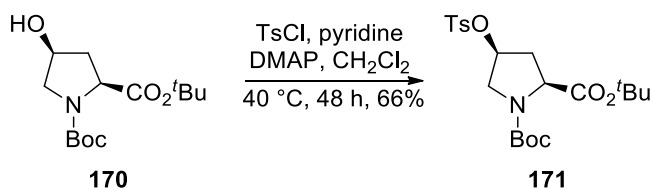
Scheme 95: *Activation of* **170** *using toluenesulfonyl chloride.*

Interestingly, this step was consistently lower yielding than the analogous step for the *trans*-analogue at this stage (66% *vs* 81% respectively), with no improvement in yield observed upon an increase in reaction time. It was proposed that this could be a result of the *cis* stereochemistry of the proline analogue, as described by Kobayashi and co-workers.[154] In an infrared study, it was shown that additional bands are present in the case of *cis*-hydroxyl group when compared to the *trans*-hydroxyl group. It is suggested that these extra bands indicate the presence of hydrogen bonding between the hydroxyl moiety and the carbonyl group of the ester moiety. This hydrogen bonding would in turn make this isomer less reactive, possibly explaining consistently lower yields observed. It is proposed this hydrogen bonding may be present for the *cis*-4-hydroxyl analogue **170** owing to its preference for an *endo* conformation, but not for the *trans*-4-hydroxyl analogue **168** as this has a larger preference for the *exo* conformation (**Figure 75**).
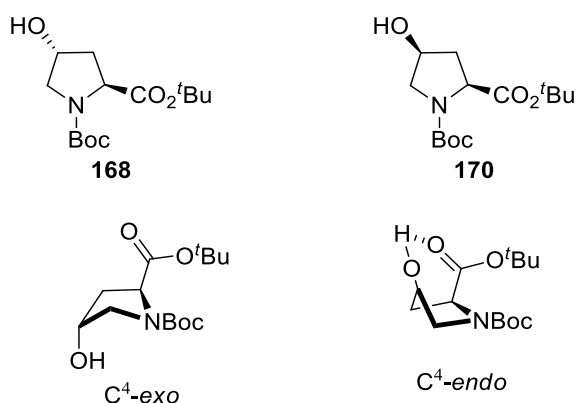
Figure 75: *Hydrogen bonding between the hydroxyl moiety and carbonyl ester of cis-4-hydroxyproline* **170**.

From the suitably protected *cis*-4-hydroxyproline **170**, synthesis of a non-radioactive *trans*-fluoroproline standard was then completed. The first step was inversion of stereochemistry at the C-4 position of **170** using morph-DAST, to give the protected *trans*-4-fluoroproline analogue **172** in a 57% yield (**Scheme 96**). This step also

145

proceeded with a slightly lower yield than for the other isomer, (57% vs 63%) which could be a result of hydrogen bonding making this compound less reactive.
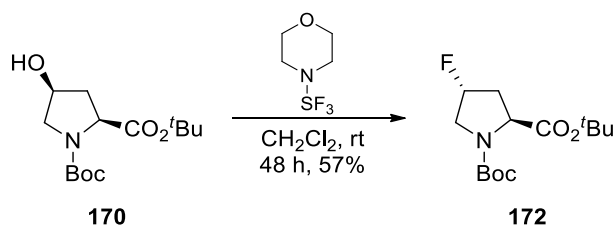
Scheme 96: *Completion of the synthesis of a non-radioactive trans-4-fluoroproline standard.*

Again, this step proceeded cleanly with inversion of stereochemistry with the *trans*-isomer being obtained cleanly by column chromatography. Upon isolation of both *cis* and *trans* analogues it was clear by ^{1}H NMR spectroscopy that despite the spectra being complicated by rotamers, single isomers of product had been obtained in each case. This is demonstrated in **Figure 76** where the ^{1}H NMR peaks corresponding to the diastereotopic hydrogens at C3 are highlighted. These are visible as two distinct peaks for protected *trans*-4-fluoroproline **172** compared to overlapping peaks for *cis*-4-fluoroproline **166**.
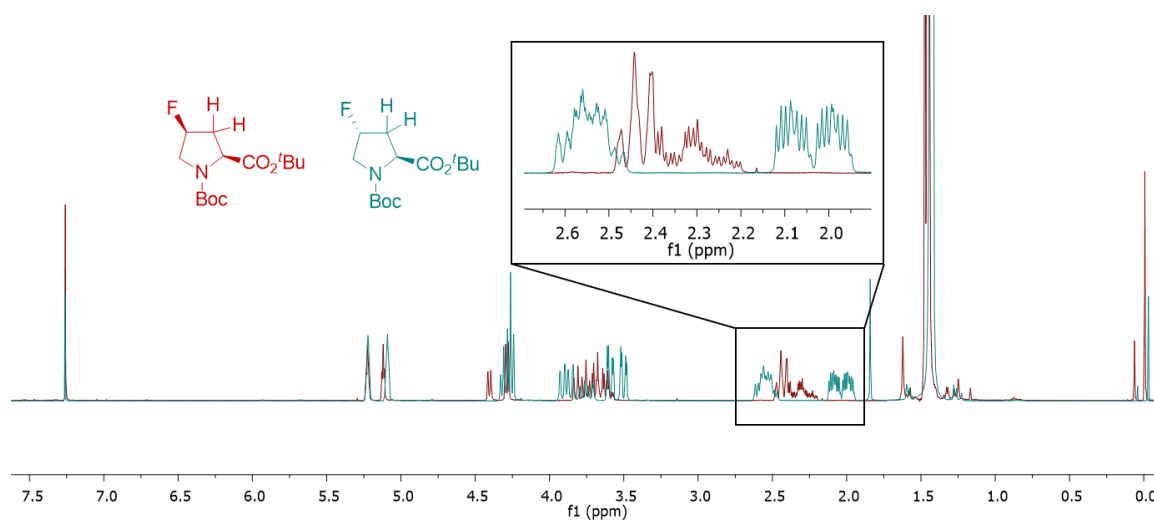
Figure 76: *Distinct ^{1}H NMR spectra of protected cis-4-fluoroproline **166** (red) and trans-4-fluoroproline **172** (blue). The region 2.00-2.60 ppm is highlighted, showing the 3-HH diastereotopic protons.*

As for the *cis*-4-fluoroproline analogue, two distinct peaks were observed in the ^{19}F NMR for the protected *trans*-4-fluoroproline (**Figure 77**). These peaks corresponded

to the two rotamers around the amide bond, with a ratio of 4.88:1 of the *trans* to the *cis* rotamer. This gave a $K_{trans/cis} = 4.88$ which was in close agreement with literature values ($K_{trans/cis} = 4.27$).
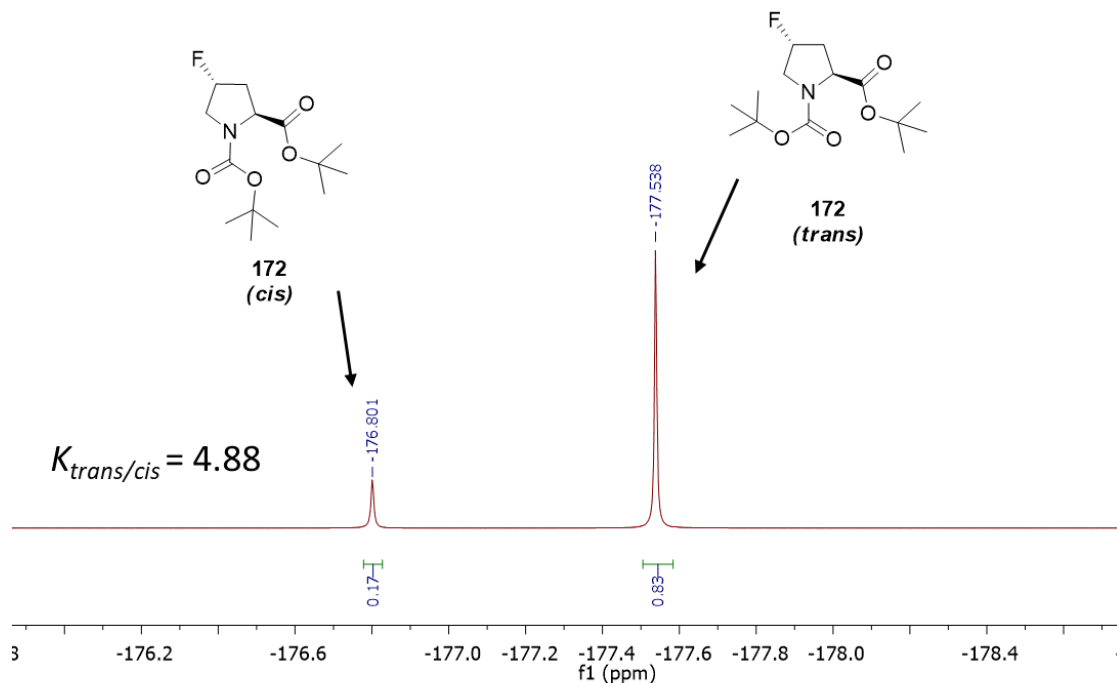
Figure 77: *Rotamers of N-Boc-4-fluoroproline **172** as observed by ^{19}F NMR spectroscopy (measured in CDCl₃).*

This is a larger $K_{trans/cis}$ ratio than is observed for *cis*-fluoroproline, as a result of the fluorine being in the 4*R* position. In this isomer, the preferred gauche conformer stabilises the C4-*exo* ring pucker (**Figure 78**). This ring pucker promotes the n→π* interaction, as the distance between donor and acceptor groups in this pucker is shorter, and ultimately further stabilises the *trans* amide bond.[180]
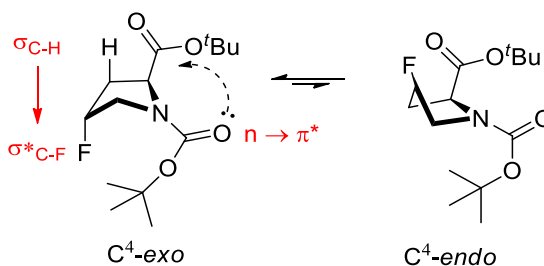
Figure 78: *Gauche effect of trans-fluoroproline and preferred exo ring pucker.*

The final step in the synthesis of non-radioactive *trans*-4-fluoroproline was deprotection. A mild deprotection using 2 M aqueous hydrochloric acid allowed for the synthesis of *trans*-4-fluoroproline **149** in 70% yield (**Scheme 97**).
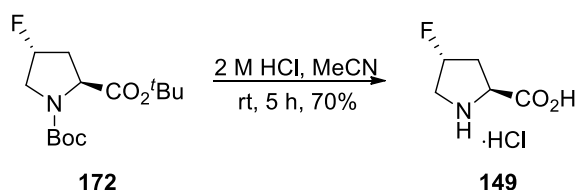
**Scheme 97**: *Deprotection to give trans-4-fluoroproline **149**.*

Overall, a four-step synthesis of the desired precursor **171** starting from readily available *N*-Boc-*trans*-4-hydroxyproline **167** was achieved, starting with a two-step inversion of stereochemistry at C4 to give *N*-Boc-*cis*-4-hydroxyproline **159** (**Scheme 98**). From common intermediate **170**, deoxyfluorination and deprotection was possible, giving *trans*-4-fluoroproline in five steps overall.
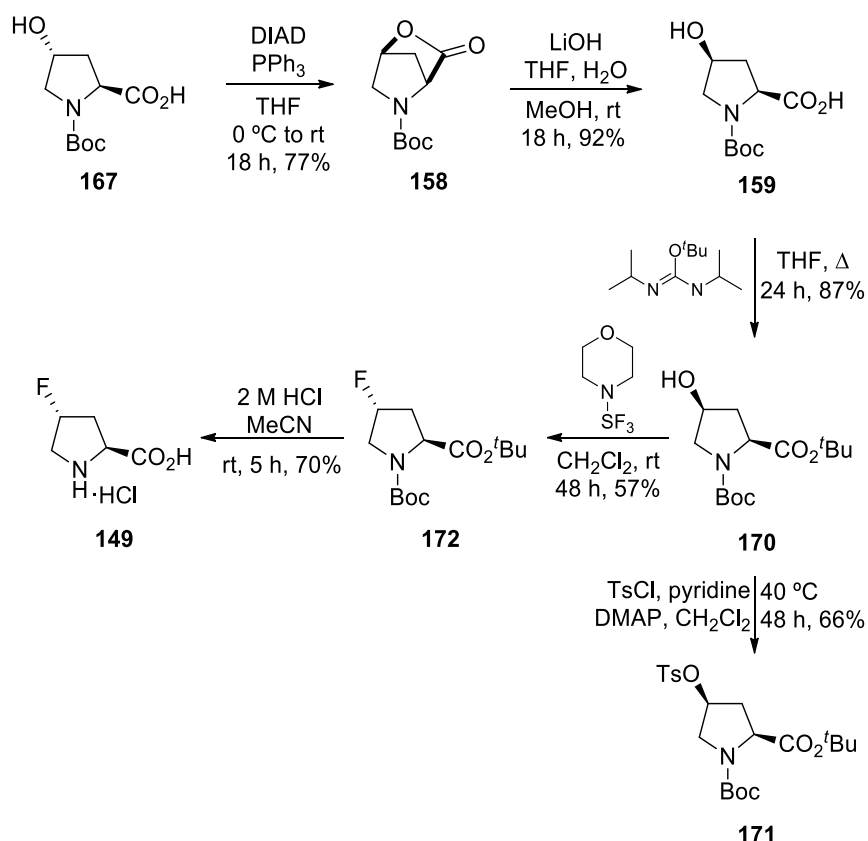
Scheme 98: *Final synthetic route to trans-4-fluoroproline precursor **171** and non-radioactive trans-4-fluoroproline **149**.*

4.5 Radiosynthesis

Radiochemistry experiments for the synthesis of *cis*-4-[^{18}F]fluoroproline and *trans*-4-[^{18}F]fluoroproline were next carried out by Dr Tim Morgan at the University of Edinburgh. The syntheses were carried out using a TRACERlab FX$_{FN}$ automated synthesiser, and work began by investigating previous methods published for the syntheses of these compounds (**Scheme 99**), so that a comparison between the effectiveness of alternative precursors and the novel precursors could be established. Initially, [^{18}F]fluoride was reacted with the commercially available methyl ester **164** under literature conditions, at 110 °C for 10 minutes. Deprotection was then carried out with 2M trifluoromethanesulfonic acid at 127 °C for 10 minutes. Radio-HPLC analysis showed high conversion to the *cis*-isomer **[^{18}F]150**, however both the *trans*-isomer **[^{18}F]149** (4.6%) and unreacted [^{18}F] fluoride (10.9%) were also detected. Crucially, using trifluoromethanesulfonic acid on the synthesiser caused damage to both tubing and valves, which ultimately resulted in failed syntheses.
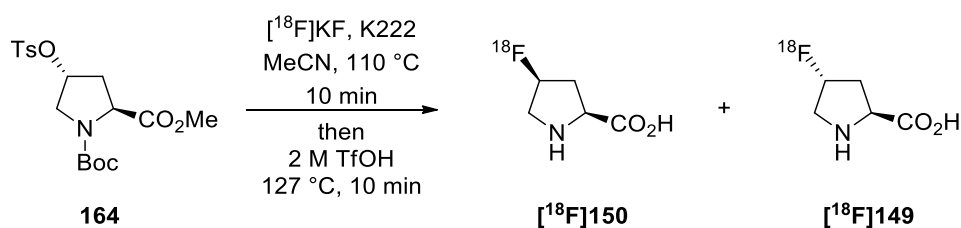
Scheme 99: *Automated synthesis of cis-4-[^{18}F]fluoroproline **[^{18}F]150** under literature conditions using precursor **164**.*

Next, similar conditions for the radiofluorination and deprotection of the novel *tert*-butyl ester **169** were investigated, replacing trifluoromethanesulfonic acid with 2 M aqueous hydrochloric acid and increasing the time for radiofluorination to ensure full conversion of [^{18}F]fluoride (**Table 15**). The initial reaction, where the deprotection step occurred at 127 °C (entry 1) gave the desired product in a 42% radiochemical yield (RCY) after a 15 minute fluorination step, followed by a 10 minute deprotection step. Using milder conditions for the deprotection step initially led to a decrease in radiochemical yield (entry 2), however it was proposed that this could be partly due to the strong cation exchange cartridge (SCX) used in the final formulation stage. Swapping this cartridge for a mixed-mode cation exchange cartridge (MCX) during the formulation stage (entry 3) led to an increase in RCY to 42%, with both the lower

temperature of 60 °C and a shorter deprotection time (5 minutes). Finally, it was shown that the evaporation step after fluorination could be omitted to decrease the total reaction time to just 63 minutes, with only a small impact on the overall radiochemical yield (entry 4). Radio-HPLC analysis showed that the synthesis of cis-4-[^{18}F]fluoroproline was clean, containing 98.8% cis-4-[^{18}F]fluoroproline and <0.4% of the trans isomer.
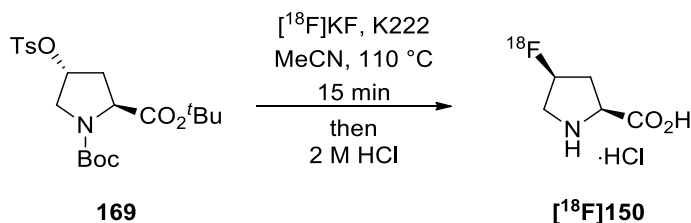
Entry	Deprotection Temperature (°C)	Deprotection Time (min)	Formulation Cartridge	Total Time (min)	Radiochemical Yield (%)
1	127	10	SCX	74	42
2	60	10	SCX	66	19
3	60	5	MCX	71	42
4*	60	5	MCX	63	36

*Table 15: Optimisation of the automated radiosynthesis of cis-4-fluoroproline using novel precursor 169. Radiochemical yields are decay corrected. *Evaporation not performed after the fluorination step.*

These optimised conditions were used to produce cis-4-[^{18}F]fluoroproline **[^{18}F]150** in an automated manner, including isolation and purification (**Scheme 100**). After a synthesis time of 59 minutes, cis-4-[^{18}F]fluoroproline **[^{18}F]150** was obtained in 41 ± 3% RCY yield (n = 9) with >99% radiochemical purity.

RCY: 41 ± 3% (n = 9)
Radiochemical Purity: >99%
Total Synthesis Time: 59 ± 1.9 min (n = 9)
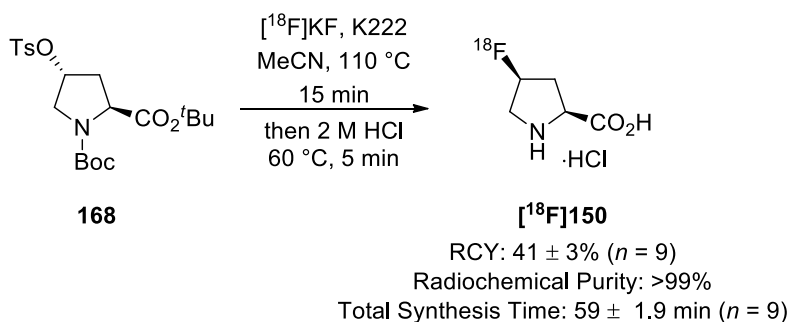
*Scheme 100: Radiochemical synthesis of cis-4-[^{18}F]fluoroproline **[^{18}F]150**.*

Next, the synthesis of *trans*-4-[^{18}F]fluoroproline **[^{18}F]149** was completed under the same conditions (**Scheme 101**) which gave the desired compound in a RCY of 34 ± 4.3% (n=11) and in >99% radiochemical purity. Analysis of the products **[^{18}F]149** and **[^{18}F]150** at 2 h and 11 h after completion of synthesis showed that within this timeframe these compounds are stable to decomposition pathways.
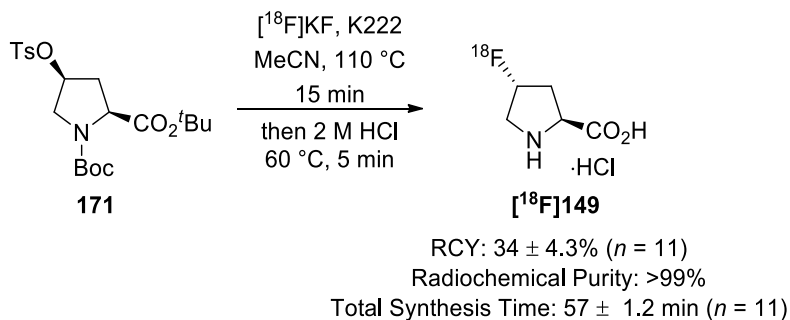
Scheme 101: *Radiochemical synthesis of trans-4-[^{18}F]fluoroproline [^{18}F]149.*

Ultimately, the development of *tert*-butyl ester precursors allowed for the fully automated synthesis of *cis*-4-[^{18}F]fluoroproline and *trans*-4-[^{18}F]fluoroproline. This was achieved using a milder acid than previously reported in literature, meaning that damage to important instruments and equipment was avoided. The alternative of manual handling of radioactive intermediates was also avoided, and the desired products were reproducibly synthesised in good radiochemical yields and excellent purity. The *cis*-4-fluoroproline synthesised by this method was subsequently used in imaging experiments by collaborators at the University of Edinburgh (**Figure 79**). It was shown through initial imaging, that distribution of this radiotracer in a rat model proceeded as anticipated, with high uptake in the kidneys and liver.
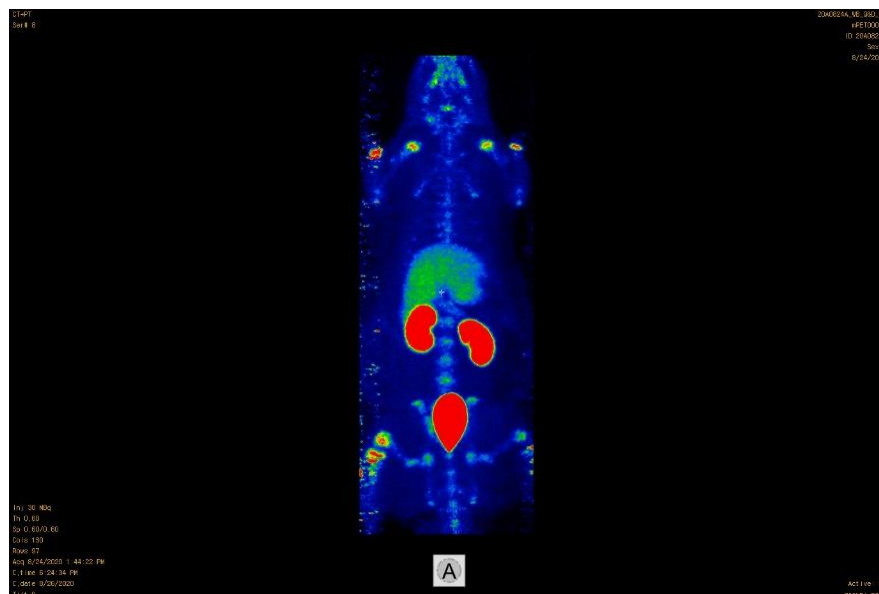
Figure 79: Distribution of cis-4-[¹⁸F]fluoroproline *[¹⁸F]150* in a rat model.

4.6 Future Work

Future experiments from an imaging perspective are expected to focus on the potential use of fluoroprolines in myocardial infarction and heart failure models. From a synthetic perspective, it is proposed that the work here could be expanded towards the synthesis of *cis*-D-4-fluoroproline (**174**) and *trans*-D-4-fluoroproline (**175**) (**Figure 80**).

cis-D-4-fluoroproline
174

trans-D-4-fluoroproline
175
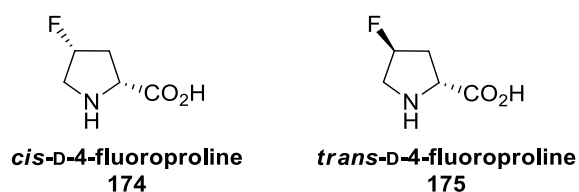
Figure 80: Structures of cis-D-4-fluoroproline and trans-D-4-fluoroproline.

It has been shown that there is a preference for D-proline to be transported into the brain,[181] and [¹⁸F]-*cis*-D-4-fluoroproline uptake in brain areas with secondary neurodegeneration has been observed.[182] It is proposed that novel synthetic routes to precursors for these analogues and their cold standards would allow for further investigations into the lesser explored D-isomers of 4-fluoroprolines.

The commercially available *N*-Boc-*cis*-D-4-hydroxyproline **176** could be used as a starting point for the synthesis of *cis*-D-4-fluoroproline (**174**) using the same series of steps as for *trans*-L-4-fluoroproline (**Scheme 102**). Protection of the acid as the

tert-butyl ester **177** would allow for mild deprotection steps later. Activation of the alcohol of **177** with toluenesulfonyl chloride would give precursor **178** which could be used for labelling with [^{18}F]fluoride. In a route to the non-radioactive standard, **177** could be fluorinated using morph-DAST to give **179** which would undergo mild deprotection to give *cis*-D-4-fluoroproline (**174**).
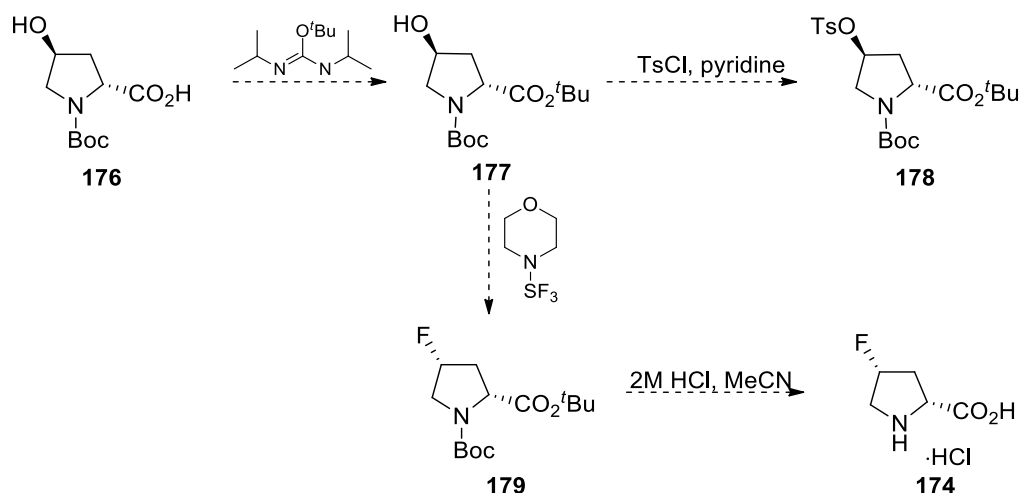
Scheme 102: *Proposed synthesis of cis-D-4-fluoroproline.*

The synthesis of *trans*-D-4-fluoroproline (**175**) could be achieved using the same strategy as previously, beginning with inversion of stereochemistry (**Scheme 103**), required as *N*-Boc-*trans*-D-4-hydroxyproline **181** is considerably more expensive than the *cis*-analogue. This route would begin with commercially available *N*-Boc-*cis*-D-4-hydroxyproline (**176**) undergoing a Mitsunobu reaction, followed by hydrolysis of the resulting lactone **180**, to give *N*-Boc-*trans*-D-4-hydroxyproline **181**. From this point, the same series of reactions as above could be performed to synthesise precursor **183** and non-radioactive *trans*-D-4-fluoroproline **175**.
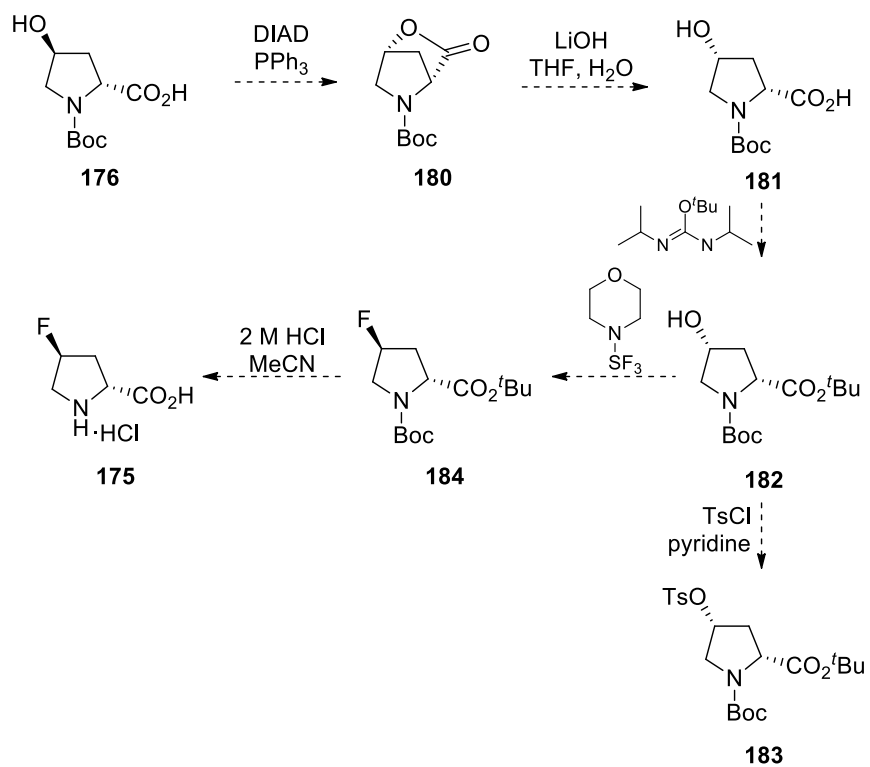
***Scheme 103**: Proposed synthetic route to trans-D-4-fluoroproline.*

5.0 Experimental

5.1 General Experimental

All reagents and starting materials were obtained from commercial sources and used as received. Dry solvents were purified using a PureSolv 500 MD solvent purification system. All reactions were performed under an atmosphere of argon unless otherwise mentioned. Brine refers to a saturated solution of sodium chloride. Flash column chromatography was carried out using Merck Millipore matrix silicagel 60 (40–63 μM). Merck aluminium-backed plates pre-coated with silica gel 60 (UV254) were used for thin-layer chromatography and visualised by staining with $KMnO_4$, vanillin or ninhydrin. ^1H NMR and ^{13}C NMR spectra were recorded on a Bruker DPX 400 or 500 spectrometer, with chemical shift values in ppm relative to tetramethylsilane (δ_H 0.00 and δ_C 0.00), or for ^1H NMR, relative to residual chloroform (δ_H 7.26), dimethylsulfoxide (δ_H 2.50) or methanol (δ_H 3.31) as standard. For ^{13}C NMR the chemical shifts are reported relative to the central resonance of $CDCl_3$ (δ_C 77.2), DMSO-d_6 (δ_C 39.5) or CD_3OD (δ_C 49.0) as standard. Proton and carbon assignments are based on two-dimensional COSY, HSQC, HMBC and DEPT experiments. Mass spectra were obtained either using a JEOL JMS-700 spectrometer for EI and CI, and Bruker Microtof-q or Agilent 6125B for ESI. Infrared spectra were obtained neat using a Shimadzu IR Prestige-21 spectrometer or Shimadzu 8400S spectrometer. Melting points were determined on either a Reichert platform melting point apparatus or Stuart Scientific melting point apparatus. Optical rotations were determined as solutions irradiating with the sodium D line (λ = 589 nm) using an Autopol V polarimeter. $[\alpha]_D$ values are given in units 10^{-1} deg cm^{-1} g^{-1}.

Absorption and emission data were recorded on one of two instruments:

1. UV-Vis spectra were recorded on a Pekin Elmer Lamda 25 instrument. Fluorescence spectra were recorded on a Shimadzu RF-5301PC spectrofluorophotometer. Emission data were measured using excitation and emission bandpass filters of 3 nm.

2. Both UV-Vis spectra and fluorescence spectra were recorded on a Horiba Duetta Fluorescence and Absorbance spectrometer. Absorbance spectra were recorded with an integration time of 0.05 s, and a band pass of 5 nm. Fluorescence spectra for benzotriazole derived amino acids were recorded with

and excitation and emission band pass of 5 nm, an integration time of 2 s, and with detector accumulations set to 1. Fluorescence spectra for pyridyl derived amino acids were recorded with excitation and emission band pass of 5 nm, an integration time of 0.1 s, and with detector accumulations set to 1. Respective standard samples were recorded with the same parameters.

Quantum yields were determined using a comparative method against two standards. Anthracene (Φ = 0.27, in ethanol) and L-tryptophan (Φ = 0.14 in water) were used as standard references. The integrated fluorescence intensity of each compound was determined from the emission spectra given. Measurements were performed at five different concentrations. Concentrations were chosen to ensure the absorption value was below 0.1 to avoid re-absorption effects. Integrated fluorescence intensity was plotted as a function of the measured absorbance and a linear fit was calculated. The resultant gradient was then used to calculate the quantum yield, using the equation below:

$$\phi_x = \phi_{ST} \left(\frac{Grad_{ST}}{Grad_x} \right) \left(\frac{\eta_x^2}{\eta_{ST}^2} \right)$$

Subscript *ST* signifies the quantities associated with the quantum yield standard. Subscript X signifies the quantities associated with the novel compound. $Grad_x$ is the determined gradient associated with the novel compound. $Grad_{ST}$ is the determined gradient associated with quantum yield standard. η is the refractive index of the solvent used in the fluorescence measurements. η = 1.333 for water, 1.361 for ethanol and 1.331 for methanol.

5.2 Pyridine Derived Amino Acids Experimental

Dimethyl (2*S*)-2-aminobutandioate hydrochloride [183]

$$\text{MeO}_2\text{C} \overset{3}{\diagdown} \overset{2}{\diagdown} \text{CO}_2\text{Me}$$
$$\underset{\text{NH}_2 \cdot \text{HCl}}{|}$$
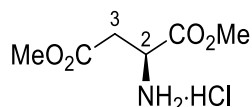
To a suspension of L-aspartic acid (5.00 g, 37.6 mmol) in methanol (100 mL) at 0 °C under argon was added thionyl chloride (3.80 mL, 52.6 mmol). The mixture was warmed to room temperature and stirred under reflux for 3 h. The solution was cooled to room temperature and concentrated *in vacuo* to give dimethyl (2*S*)-2-aminobutandioate hydrochloride as a white solid (7.41 g, 100%). Mp 115–116 °C (lit.[183] Mp 114–115 °C); $[\alpha]_D^{24}$ +22.0 (*c* 1.0, MeOH); δ_H (400 MHz, DMSO-d$_6$) 2.99 (1H, dd, *J* 18.0, 5.5 Hz, 3-*H*H), 3.05 (1H, dd, *J* 18.0, 5.5 Hz, 3-H*H*), 3.66 (3H, s, OCH$_3$), 3.74 (3H, s, OCH$_3$), 4.35 (1H, t, *J* 5.5 Hz, 2-H), 8.72 (3H, s, CHN*H*$_3^+$); δ_C (100 MHz, DMSO-d$_6$) 34.0 (CH$_2$), 48.4 (CH), 52.2 (CH$_3$), 53.0 (CH$_3$), 168.7 (C), 169.6 (C); *m/z* (CI) 162 (MH$^+$. 100%), 148 (5), 102 (20).

Dimethyl (2*S*)-2-(tritylamino)butandioate (82)[184]

$$\text{MeO}_2\text{C} \overset{3}{\diagdown} \overset{2}{\diagdown} \text{CO}_2\text{Me}$$
$$\underset{\text{NHTr}}{|}$$
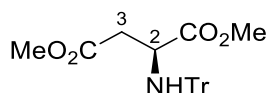
To a solution of dimethyl (2*S*)-2-aminobutandioate hydrochloride (6.00 g, 32.7 mmol) in dichloromethane (150 mL) at 0 °C was added dropwise triethylamine (9.20 mL, 75.4 mmol) and triphenylmethyl chloride (9.11 g, 32.7 mmol). The reaction mixture was allowed to warm to room temperature and stirred for 24 h. The reaction mixture was washed with 2 M citric acid (100 mL), water (100 mL), brine (100 mL), then dried (MgSO$_4$) and concentrated *in vacuo* to give a colourless oil. Purification by flash column chromatography, eluting with 50% diethyl ether in petroleum ether gave dimethyl (2*S*)-2-(tritylamino)butandioate (**82**) as a colourless solid (9.9 g, 75%). Mp 71–72 °C (lit.[184] 70–71 °C); $[\alpha]_D^{21}$ +36.6 (*c* 1.0, CHCl$_3$); δ_H (400 MHz, CDCl$_3$) 2.51 (1H, dd, *J* 14.7, 7.0 Hz, 3-*H*H), 2.66 (1H, dd, *J* 14.7, 5.4 Hz, 3-H*H*), 2.93 (1H, d, *J* 10.1 Hz, NH), 3.25 (3H, s, OMe), 3.67 (3H, s, OMe), 3.68–3.73 (1H, m, 2-H), 7.15–7.20 (3H, m, ArH), 7.23–7.28 (6H, m, ArH), 7.46–7.51 (6H, m, ArH); δ_C (101 MHz, CDCl$_3$) 39.0 (CH$_2$), 50.5 (CH), 50.7 (CH$_3$), 52.4 (CH$_3$), 69.9 (C), 125.2 (3

× CH), 126.6 (6 × CH), 127.5 (6 × CH), 144.4 (3 × C), 169.7 (C), 172.6 (C); *m/z* (EI) 403 (M$^+$. 1%), 326 (35), 243 (100), 165 (30), 83 (70).

Methyl (2*S*)-5-(dimethoxyphosphoryl)-4-oxo-2-(tritylamino)pentanoate (83)[185]
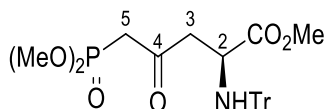
A solution of dimethyl methylphosphonate (2.95 mL, 27.3 mmol) in tetrahydrofuran (50 mL) was cooled to −78 °C under an argon atmosphere. *n*-Butyl lithium (2.5 M in hexane, 11.4 mL, 28.5 mmol) was added dropwise and the reaction mixture stirred for 1 h. In a separate reaction vessel, a solution of dimethyl (2*S*)-2-(tritylamino)butandioate (**82**) (5.00 g, 12.4 mmol) in tetrahydrofuran (100 mL) was cooled to −78 °C and then the dimethyl methylphosphonate/*n*-butyl lithium solution was cannulated into the flask and the reaction mixture stirred at −78 °C for 2 h to give a yellow solution. The reaction was quenched with a saturated solution of ammonium chloride (3 mL) and allowed to warm to room temperature. The mixture was concentrated *in vacuo*. The resulting residue was diluted with ethyl acetate (100 mL), washed with water (2 × 100 mL), brine (100 mL) then dried (MgSO$_4$) and concentrated *in vacuo*. Purification by flash column chromatography, eluting with 75% ethyl acetate in petroleum ether gave methyl (2*S*)-5-(dimethoxyphosphoryl)-4-oxo-2-(tritylamino)pentanoate (**83**) as a colourless solid (4.27 g, 70%). Mp 117–118 °C (lit.[185] 117–118.5 °C); $[\alpha]_D^{24}$ +31.1 (*c* 1.0, CHCl$_3$); δ_H (400 MHz, CDCl$_3$) 2.78 (1H, dd, *J* 16.7, 6.9 Hz, 3-H*H*), 2.85–2.95 (2H, m, 3-H*H* and NH), 3.06 (2H, d, *J*$_{H–C–P}$ 22.7 Hz, 5-H$_2$), 3.29 (3H, s, OMe), 3.65–3.73 (1H, m, 2-H), 3.76 (3H, s, OMe), 3.79 (3H, s, OMe), 7.15–7.21 (3H, m, ArH), 7.26 (6H, t, *J* 7.7 Hz, ArH), 7.47 (6H, d, *J* 7.7 Hz, ArH); δ_C (101 MHz, CDCl$_3$) 41.8 (d, *J*$_{C–P}$ 128 Hz, CH$_2$), 48.8 (CH$_2$), 52.0 (CH$_3$), 52.9 (CH$_3$), 53.0 (CH$_3$), 53.1 (CH), 71.3 (C), 126.6 (3 × CH), 127.9 (6 × CH), 128.8 (6 × CH), 145.7 (3 × C), 174.0 (C), 199.3 (C); *m/z* (CI) 496 (MH$^+$. 1%), 301 (5), 254 (90), 243 (100), 237 (55), 167 (45).

Methyl (2*S*)-2-[(benzyloxycarbonyl)amino]-5-(dimethoxyphosphoryl)-4-oxopentanoate (84)
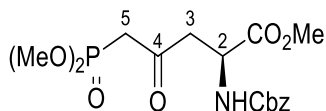
To a solution of methyl (2*S*)-5-(dimethoxyphosphoryl)-4-oxo-2-(tritylamino)pentanoate (**83**) (4.7 g, 9.50 mmol) in dichloromethane (150 mL) was added trifluoroacetic acid (1.5 mL, 19.0 mmol). The reaction mixture was stirred at room temperature for 1 h before concentrating *in vacuo*. The resulting residue was dissolved in chloroform (5 mL) and petroleum ether (40–60) was added until an orange oil formed, at which point the solvent was decanted off. The resulting oil was dissolved in dichloromethane (150 mL) and *N*,*N*-diisopropylethylamine (4.2 mL, 23.8 mmol) was added, followed by benzyl chloroformate (2.0 mL, 14.3 mmol). The reaction mixture was stirred at room temperature for 3 h, before diluting with water (50 mL). The mixture was then extracted with dichloromethane (3 × 50 mL), dried (MgSO$_4$) and concentrated *in vacuo*. The crude product was purified *via* flash column chromatography, eluting with 3% methanol in dichloromethane to produce methyl (2*S*)-2-[(benzyloxycarbonyl)amino]-5-(dimethoxyphosphoryl)-4-oxopentanoate (**84**) as an orange oil (3.28 g, 91%). ν_{max}/cm^{-1} (neat) 3265 (NH), 2924 (CH), 1716 (C=O), 1526, 1252, 1213, 1024, 810, 742, 700; [α]$_D^{24}$ +22.5 (*c* 1.0, CHCl$_3$); δ$_H$ (400 MHz, CDCl$_3$) 3.09 (2H, d, *J*$_{H–C–P}$ 22.7 Hz, 5-H$_2$), 3.17 (1H, dd, *J* 18.5, 4.3 Hz, 3-*H*H), 3.35 (1H, dd, *J* 18.5, 4.7 Hz, 3-H*H*), 3.73–3.74 (6H, m, 2 × OCH$_3$), 3.77 (3H, d, *J*$_{H–O–C–P}$ 0.6 Hz, OCH$_3$), 4.59 (1H, ddd, *J* 4.3, 4.7, 8.5 Hz, 2-H), 5.11 (2H, s, CH$_2$), 5.74 (1H, d, *J* 8.5 Hz, NH), 7.31-7.37 (5H, m, Ph); δ$_C$ (101 MHz, CDCl$_3$) 41.5 (d, J$_{C–P}$ 128 Hz, CH$_2$), 45.6 (CH$_2$), 49.8 (CH), 52.7 (CH$_3$), 53.1 (d, J$_{C–P}$ 7.2 Hz, CH$_3$), 53.2 (d, J$_{C–P}$ 7.2 Hz, CH$_3$), 67.0 (CH$_2$), 128.1 (2 × CH), 128.2 (2 × CH), 128.5 (CH), 136.2 (C), 156.0 (C), 171.2 (C), 199.7 (d, J$_{C–P}$ 6.0 Hz, C); *m/z* (ESI) 410.0966 (MNa$^+$. C$_{16}$H$_{22}$NNaO$_8$P requires 410.0975).

Methyl (2*S*,5*E*)-2-[(benzyloxycarbonyl)amino]-6-(4'-methoxyphenyl)-4-oxohex-5-enoate (85)[79]
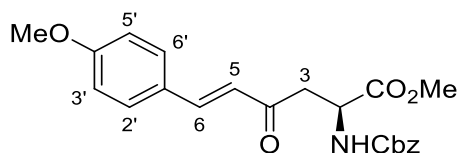
Methyl (2*S*)-2-[(benzyloxycarbonyl)amino]-5-(dimethoxyphosphoryl)-4-oxopentanoate (**84**) (0.500 g, 1.29 mmol) was dissolved in anhydrous acetonitrile (10 mL) and potassium carbonate (0.196 g, 1.42 mmol) was added. The mixture was stirred at room temperature for 0.5 h followed by addition of 4-methoxybenzaldehyde (0.340 mL, 2.58 mmol). The temperature was increased to 50 °C and the mixture was stirred for 72 h. Once the reaction was complete, the solution was concentrated *in vacuo* and the resulting residue was dissolved in ethyl acetate (20 mL) and washed with water (2 × 15 mL), brine (15 mL), dried (MgSO$_4$) and concentrated *in vacuo*. Purification by flash column chromatography, eluting with 50% diethyl ether in petroleum ether (40–60) gave methyl (2*S*,5*E*)-2-[(benzyloxycarbonyl)amino]-6-(4'-methoxyphenyl)-4-oxohex-5-enoate (**85**) as a yellow oil (0.368 g, 71%). Spectroscopic data were consistent with the literature.[79] ν_{max}/cm^{-1} (neat) 3347 (NH), 2953 (CH), 1717 (C=O), 1655 (C=O), 1597 (C=C), 1510 (C=C), 1248, 1208, 1169, 1026, 816; [α]$_D^{29}$ +30.3 (*c* 1.0, CHCl$_3$); δ$_H$ (400 MHz, CDCl$_3$) 3.23 (1H, dd, *J* 17.9, 4.2 Hz, 3-*H*H), 3.47 (1H, dd, *J* 17.9, 4.2 Hz, 3-H*H*), 3.75 (3H, s, OCH$_3$), 3.85 (3H, s, OCH$_3$), 4.67 (1H, dt, *J* 8.5, 4.2 Hz, 2-H), 5.12 (2H, s, OC*H*$_2$Ph), 5.88 (1H, d, *J* 8.5 Hz, NH), 6.58 (1H, d, *J* 16.2 Hz, 5-H), 6.92 (2H, d, *J* 8.8 Hz, 3'-H and 5'-H), 7.27−7.38 (5H, m, Ph), 7.49 (2H, d, *J* 8.8 Hz, 2'-H and 6'-H), 7.52 (1H, d, *J* 16.2 Hz, 6-H); δ$_C$ (101 MHz, CDCl$_3$) 42.3 (CH$_2$), 50.3 (CH), 52.8 (CH$_3$), 55.6 (CH$_3$), 67.1 (CH$_2$), 114.6 (2 × CH), 123.4 (CH), 126.9 (C), 128.1 (2 × CH), 128.2 (CH), 128.6 (2 × CH), 130.4 (2 × CH), 136.4 (C), 144.0 (CH), 156.2 (C), 162.1 (C), 171.8 (C), 197.4 (C); *m/z* (EI) 397.1526 (M$^+$. C$_{22}$H$_{23}$NO$_6$ requires 397.1525), 336 (10%), 289 (19), 262 (19), 243 (45), 182 (34), 161 (100), 91 (32).

Methyl (2S,5E)-2-[(benzyloxycarbonyl)amino]-6-(4'-benzyloxyphenyl)-4-oxohex-5-enoate (88)
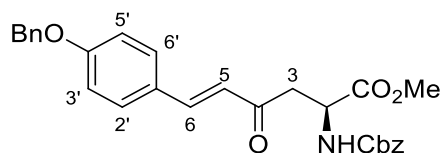
The reaction was carried out according to the above procedure for the synthesis of methyl (2S,5E)-2-[(benzyloxycarbonyl)amino]-6-(4'-methoxyphenyl)-4-oxohex-5-enoate (**85**) using methyl (2S)-2-[(benzyloxycarbonyl)amino]-5-(dimethoxyphosphoryl)-4-oxopentanoate (**84**) (0.200 g, 0.516 mmol) and 4-benzyloxybenzaldehyde (0.218 g, 1.03 mmol). Purification by flash column chromatography, eluting with 20% ethyl acetate in petroleum ether (40–60) gave methyl (2S,5E)-2-[(benzyloxycarbonyl)amino]-6-(4'-benzyloxyphenyl)-4-oxohex-5-enoate (**88**) as a yellow oil (0.115 g, 52%). ν_{max}/cm^{-1} (neat) 3375 (NH), 2951 (CH), 1722 (C=O), 1597 (C=C), 1510, 1250, 1173, 1094, 1026, 739; $[\alpha]_D^{19}$ +11.4 (c 1.0, CHCl$_3$); δ_H (400 MHz, CDCl$_3$) 3.23 (1H, dd, J 17.9, 4.2 Hz, 3-HH), 3.45 (1H, dd, J 17.9, 4.2 Hz, 3-HH), 3.74 (3H, s, OCH$_3$), 4.67 (1H, dt, J 8.6, 4.2 Hz, 2-H), 5.10 (2H, s, OCH$_2$Ph), 5.11 (2H, s, OCH$_2$Ph), 5.87 (1H, d, J 8.6 Hz, NH), 6.57 (1H, d, J 16.2 Hz, 5-H), 6.98 (2H, d, J 8.8 Hz, 3'-H and 5'-H), 7.26–7.50 (13H, m, 6-H, 2'-H, 6'-H and 2 × Ph); δ_C (101 MHz, CDCl$_3$) 42.2 (CH$_2$), 50.1 (CH), 52.7 (CH$_3$), 67.0 (CH$_2$), 70.1 (CH$_2$), 115.4 (2 × CH), 123.4 (CH), 127.0 (C), 127.5 (2 × CH), 128.0 (2 × CH), 128.1 (CH), 128.2 (CH), 128.5 (2 × CH), 128.7 (2 × CH), 130.3 (2 × CH), 136.3 (C), 136.3 (C), 143.8 (CH), 156.1 (C), 161.1 (C), 171.7 (C), 197.3 (C); m/z (ESI) 496.1720 (MNa$^+$. C$_{28}$H$_{27}$NNaO$_6$ requires 496.1731).

Methyl (2*S*)-2-[(benzyloxycarbonyl)amino]-3-[4'-(4''-methoxyphenyl)pyridin-2'-yl]propanoate (87)
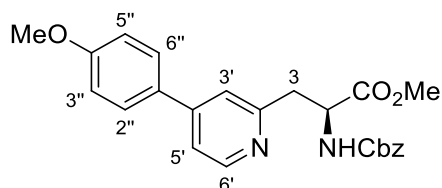
To a solution of methyl (2*S*,5*E*)-2-[(benzyloxycarbonyl)amino]-6-(4'-methoxyphenyl)-4-oxohex-5-enoate (**85**) (1.00 g, 2.52 mmol) in ethyl vinyl ether (12 mL) was added tris(6,6,7,7,8,8,8-heptafluoro-2,2-dimethyl-3,5-octanedionato)ytterbium (0.134 g, 0.126 mmol) in a sealed tube. The tube was then purged with argon, sealed and the reaction mixture was stirred at 110 °C for 168 h. The mixture was then allowed to cool to room temperature and concentrated *in vacuo*. The reaction mixture was washed through a silica plug eluting with 20% ethyl acetate in petroleum ether (40–60) and gave dihydropyran **86**. This was used for the next step without further purification. Dihydropyran **86** was then reacted with hydroxylamine hydrochloride (0.740 g, 10.7 mmol) in acetonitrile (80 mL) at 70 °C for 16 h. Purification by flash column chromatography, eluting with 1% methanol in dichloromethane gave methyl (2*S*)-2-[(benzyloxycarbonyl)amino]-3-[4'-(4''-methoxyphenyl)pyridin-2'-yl]propanoate (**87**) (0.576 g, 63%) as a yellow oil. ν_{max}/cm^{-1} (neat) 3341 (NH), 2953 (CH), 1718 (C=O), 1603, 1516 (C=C), 1251, 1180, 1026, 826, 698; $[\alpha]_D^{25}$ +23.0 (*c* 0.8, CHCl$_3$); δ_H (500 MHz, CDCl$_3$) 3.33 (1H, dd, *J* 14.9, 5.2 Hz, 3-*H*H), 3.42 (1H, dd, *J* 14.9, 5.2 Hz, 3-H*H*), 3.70 (3H, s, OCH$_3$), 3.86 (3H, s, OCH$_3$), 4.80 (1H, dt, *J* 8.2, 5.2 Hz, 2-H), 5.09 (1H, d, *J* 12.3 Hz, OC*H*HPh), 5.13 (1H, d, *J* 12.3 Hz, OCH*H*Ph), 6.36 (1H, d, *J* 8.2 Hz, NH), 6.99 (2H, d, *J* 8.7 Hz, 3''-H and 5''-H), 7.29–7.35 (7H, m, 3'-H, 5'-H and Ph), 7.55 (2H, d, *J* 8.7 Hz, 2''-H and 6''-H), 8.47 (1H, d, *J* 5.2 Hz, 6'-H); δ_C (126 MHz, CDCl$_3$) 39.2 (CH$_2$), 52.5 (CH$_3$), 53.6 (CH), 55.6 (CH$_3$), 67.0 (CH$_2$), 114.7 (2 × CH$_2$), 119.6 (CH), 121.2 (CH), 128.2 (3 × CH), 128.3 (2 × CH), 128.6 (2 × CH), 130.4 (C), 136.6 (C), 148.8 (C), 149.6 (CH), 156.3 (C), 157.5 (C), 160.8 (C), 172.3 (C); *m/z* (ESI) 443.1556 (MNa$^+$. C$_{24}$H$_{24}$N$_2$NaO$_5$ requires 443.1577).

Methyl (2*S*)-2-[(benzyloxycarbonyl)amino]-3-[4'-(4''-benzyloxyphenyl)pyridin-2'-yl]propanoate (90)
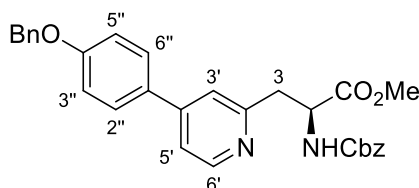
Methyl (2*S*)-2-[(benzyloxycarbonyl)amino]-3-[4'-(4''-benzyloxyphenyl)pyridin-2'-yl]propanoate (**90**) was synthesised as described for methyl (2*S*)-2-[(benzyloxycarbonyl)amino]-3-[4'-(4''-methoxyphenyl)pyridin-2'-yl]propanoate (**87**) using methyl (2*S*,5*E*)-2-[(benzyloxycarbonyl)amino]-6-(4'-benzyloxyphenyl)-4-oxohex-5-enoate (**88**) (0.500 g, 1.06 mmol) and gave dihydropyran (**89**) (0.400 g, 73%). The subsequent reaction was carried out with dihydropyran **89** (0.400 g, 0.7309 mmol) and hydroxylamine hydrochloride (0.255 g, 3.67 mmol). Purification by flash column chromatography, eluting with 10% acetonitrile in dichloromethane gave methyl (2*S*)-2-[(benzyloxycarbonyl)amino]-3-[4'-(4''-benzyloxyphenyl)pyridin-2'-yl]propanoate (**90**) (0.133 g, 27%) as a yellow oil. ν_{max}/cm^{-1} (neat) 3348 (NH), 2953 (CH), 1721 (C=O), 1603 (C=C), 1516, 1454, 1250, 1180, 1061, 824; $[\alpha]_D^{23}$ +13.2 (*c* 0.5, CHCl$_3$); δ_H (500 MHz, CDCl$_3$) 3.32 (1H, dd, *J* 14.9, 5.2 Hz, 3-*H*H), 3.42 (1H, dd, *J* 14.9, 5.2 Hz, 3-H*H*), 3.69 (3H, s, OCH$_3$), 4.79 (1H, dt, *J* 8.4, 5.2 Hz, 2-H), 5.07–5.14 (4H, m, 2 × OCH$_2$Ph), 6.34 (1H, d, *J* 8.4 Hz, NH), 7.06 (2H, d, *J* 8.8 Hz, 3''-H and 5''-H), 7.27–7.48 (12H, m, 3'-H, 5'-H and 2 × Ph), 7.54 (2H, d, *J* 8.8 Hz, 2''-H and 6''-H), 8.47 (1H, d, *J* 5.2 Hz, 6'-H); δ_C (101 MHz, CDCl$_3$) 39.1 (CH$_2$), 52.4 (CH$_3$), 53.4 (CH), 66.9 (CH$_2$), 70.2 (CH$_2$), 115.5 (2 × CH), 119.4 (2 × CH), 121.0 (CH), 127.5 (2 × CH), 128.1 (2 × CH), 128.1 (CH), 128.2 (2 × CH), 128.5 (2 × CH), 128.7 (2 × CH), 136.4 (C), 136.6 (2 × C), 148.5 (C), 149.6 (CH), 156.1 (C), 157.4 (C), 159.8 (C), 172.1 (C); *m/z* (ESI) 519.1892 (MNa$^+$. C$_{30}$H$_{28}$N$_2$NaO$_5$ requires 519.1890).

Methyl (2*S*)-2-[(benzyloxycarbonyl)amino]-3-[4'-(3''-bromo-4''-methoxyphenyl)pyridin-2'-yl]propanoate (92)
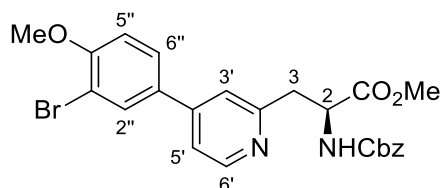
Iron(III) chloride (0.00250 g, 0.0156 mmol) in 1-butyl-3-methylimidazolium bis-(trifluoromethanesulfonyl)imide (0.0140 mL, 0.0468 mmol) was stirred for 0.5 h at room temperature. This was added to a solution of *N*-bromosuccinimide (0.118 g, 0.663 mmol) and methyl (2*S*)-2-[(benzyloxycarbonyl)amino]-3-[4'-(4''-methoxyphenyl)pyridin-2'-yl]propanoate (**80**) (0.0820 g, 0.195 mmol) in dichloromethane (0.3 mL). The reaction mixture was heated to 70 °C for 4 h. Upon completion, the reaction mixture was filtered through Celite® and concentrated *in vacuo*. Purification by flash column chromatography, eluting with 10% acetonitrile in dichloromethane gave methyl (2*S*)-2-[(benzyloxycarbonyl)amino]-3-[4'-(3''-bromo-4''-methoxyphenyl)pyridin-2'-yl]propanoate (**92**) (0.0610 g, 63%) as a yellow oil. ν_{max}/cm^{-1} (neat) 3345 (NH), 2953 (CH), 1717 (C=O), 1600 (C=C), 1504, 1454, 1287, 1213, 1053, 812; $[\alpha]_D^{19}$ +11.1 (*c* 1.0, CHCl$_3$); δ_H (500 MHz, CDCl$_3$) 3.33 (1H, dd, *J* 14.9, 5.2 Hz, 3-*H*H), 3.42 (1H, dd, *J* 14.9, 5.2 Hz, 3-H*H*), 3.70 (3H, s, OCH$_3$), 3.94 (3H, s, OCH$_3$), 4.80 (1H, dt, *J* 8.3, 5.2 Hz, 2-H), 5.09 (1H, d, *J* 12.5 Hz, OC*H*HPh), 5.12 (1H, d, *J* 12.5 Hz, OCH*H*Ph), 6.35 (1H, d, *J* 8.3 Hz, NH), 6.97 (1H, d, *J* 8.6 Hz, 5''-H), 7.26–7.35 (7H, m, 3'-H, 5'-H and Ph), 7.51 (1H, dd, *J* 8.6, 2.2 Hz, 6''-H), 7.80 (1H, d, *J* 2.2 Hz, 2''-H), 8.48 (1H, *J* 5.2 Hz, 6'-H); δ_C (126 MHz, CDCl$_3$) 39.1 (CH$_2$), 52.5 (CH$_3$), 53.4 (CH), 56.5 (CH$_3$), 67.0 (CH$_2$), 112.3 (CH), 112.5 (C), 119.4 (CH), 121.0 (CH), 127.2 (CH), 128.2 (2 × CH and CH), 128.6 (2 × CH), 131.6 (C), 131.9 (CH), 136.4 (C), 147.3 (C), 149.7 (CH), 156.2 (C), 156.8 (C), 157.7 (C), 172.2 (C); *m/z* (ESI) 521.0682 (MNa$^+$. C$_{24}$H$_{23}$^{79}BrN$_2$NaO$_5$ requires 521.0683).

Methyl (2*S*)-2-[(benzyloxycarbonyl)amino]-3-[4'-(4'',4'''-dimethoxy-[1'',1'''-biphenyl]-3''-yl)pyridin-2'-yl]propanoate (93a)
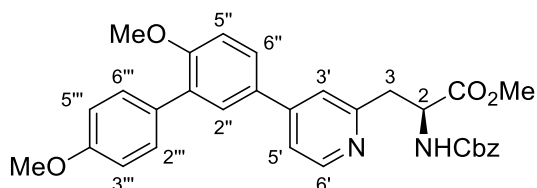
To a microwave vial containing 4-methoxyphenylboronic acid (0.0780 g, 0.510 mmol), potassium fluoride (0.0600 g, 1.02 mmol) and [1,1'-bis(diphenylphosphino)ferrocene]palladium(II) dichloride-dichloromethane complex (0.0255 g, 0.0210 mmol) was added a solution of methyl (2*S*)-2-[(benzyloxycarbonyl)amino]-3-[4'-(3''-bromo-4''-methoxyphenyl)pyridin-2'-yl]propanoate (**92**) (0.170 g, 0.340 mmol) in 1,4-dioxane (3.0 mL) and water (0.4 mL). The reaction mixture was degassed, and then stirred at 80 °C for 20 h. The reaction mixture was filtered through Celite® and washed with ethyl acetate (50 mL). The filtrate was washed with water (50 mL) and brine (50 mL), dried (MgSO₄) and concentrated *in vacuo* to give the crude product. Purification by flash column chromatography, eluting with 20% acetonitrile in dichloromethane gave methyl (2*S*)-2-[(benzyloxycarbonyl)amino]-3-[4'-(4'',4'''-dimethoxy-[1'',1'''-biphenyl]-3''-yl)pyridin-2'-yl]propanoate (**93a**) as a yellow oil (0.122 g, 68%). ν_{max}/cm^{-1} (neat) 3304 (NH), 2951 (CH), 1715 (C=O), 1600 (C=C), 1499, 1455, 1243, 1023, 831; $[\alpha]_D^{22}$ +16.7 (*c* 1.0, CHCl₃); δ_H (500 MHz, CDCl₃) 3.33 (1H, dd, *J* 14.9, 5.1 Hz, 3-*H*H), 3.42 (1H, dd, *J* 14.9, 5.1 Hz, 3-H*H*), 3.69 (3H, s, OCH₃), 3.85 (3H, s, OCH₃), 3.86 (3H, s, OCH₃), 4.80 (1H, dt, *J* 8.3, 5.1 Hz, 2-H), 5.10 (2H, s, OC*H*₂Ph), 6.38 (1H, d, *J* 8.3 Hz, NH), 6.98 (2H, d, *J* 8.8 Hz, 3'''-H and 5'''-H), 7.04 (1H, d, *J* 9.2 Hz, 5''-H), 7.25–7.36 (7H, m, 3'-H, 5'-H and Ph), 7.49 (2H, d, *J* 8.8 Hz, 2'''-H and 6'''-H), 7.52–7.56 (2H, m, 2''-H and 6''-H), 8.47 (1H, d, *J* 5.1 Hz, 6'-H); δ_C (126 MHz, CDCl₃) 39.0 (CH₂), 52.4 (CH₃), 53.4 (CH), 55.3 (CH₃), 55.8 (CH₃), 66.9 (CH₂), 111.7 (CH), 113.7 (2 × CH), 119.5 (CH), 121.1 (2 × CH), 126.8 (CH), 128.1 (CH), 128.1 (CH), 128.5 (2 × CH), 129.3 (CH), 130.2 (C), 130.3 (C), 130.6 (2 × CH), 131.1 (C), 136.4 (C), 148.6 (C), 149.6 (CH), 156.1 (C), 157.4 (C), 157.5 (C), 159.0 (C), 172.2 (C); *m/z* (ESI) 527.2168 (MH⁺. C₃₁H₃₁N₂O₆ requires 527.2177).

Methyl (2*S*)-2-[(benzyloxycarbonyl)amino]-3-[4'-(3''-(napthalen-2'''-yl)-4''-methoxyphenyl)pyridin-2'-yl]propanoate (93b)
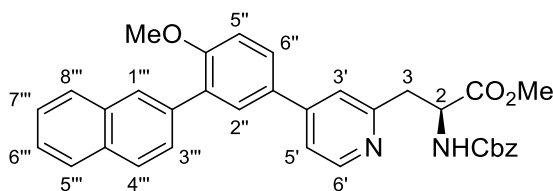
Methyl (2*S*)-2-[(benzyloxycarbonyl)amino]-3-[4'-(3''-(napthalen-2'''-yl)-4''-methoxyphenyl)pyridin-2'-yl]propanoate (**93b**) was synthesised as described for methyl (2*S*)-2-[(benzyloxycarbonyl)amino]-3-[4'-(4'',4'''-dimethoxy-[1'',1'''-biphenyl]-3''-yl)pyridin-2'-yl]propanoate (**93a**) using 2-napthylboronic acid (0.0770 g, 0.451 mmol), potassium fluoride (0.0523 g, 0.900 mmol), [1,1'-bis(diphenylphosphino)ferrocene]palladium(II) dichloride-dichloromethane complex (0.0184 g, 0.0225 mmol) and methyl (2*S*)-2-[(benzyloxycarbonyl)amino]-3-[4'-(3''-bromo-4''-methoxyphenyl)pyridin-2'-yl]propanoate (**92**) (0.150 g, 0.300 mmol) in 1,4-dioxane (2.0 mL) and water (0.24 mL). Purification by flash column chromatography, eluting with 10% acetonitrile in dichloromethane gave methyl (2*S*)-2-[(benzyloxycarbonyl)amino]-3-[4'-(3''-(napthalen-2'''-yl)-4''-methoxyphenyl)pyridin-2'-yl]propanoate (**93b**) as a yellow solid (0.116 g, 71%). Mp 100−103 °C; ν_{max}/cm^{-1} (neat) 3024 (NH), 2951 (CH), 1717 (C=O), 1601 (C=C), 1504, 1439, 1250, 752; $[\alpha]_D^{20}$ +12.4 (*c* 1.0, CHCl$_3$); δ_H (400 MHz, CDCl$_3$) 3.35 (1H, dd, *J* 14.9, 5.1 Hz, 3-*H*H), 3.44 (1H, dd, *J* 14.9, 5.1 Hz, 3-H*H*), 3.71 (3H, s, OCH$_3$), 3.90 (3H, s, OCH$_3$), 4.81 (1H, dt, *J* 8.1, 5.1 Hz, 2-H), 5.11 (2H, s, OC*H$_2$*Ph), 6.37 (1H, d, *J* 8.1 Hz, NH), 7.11 (1H, d, *J* 8.5 Hz, 5''-H), 7.27–7.42 (7H, m, 3'-H, 5'-H and Ph), 7.48–7.53 (2H, m, 5'''-H and 8'''-H), 7.62 (2H, dd, *J* 8.5, 2.1 Hz, 6''-H), 7.67–7.73 (2H, m, 2''-H and 3'''-H), 7.85–7.93 (3H, m, 4'''-H, 6'''-H and 7'''-H), 7.99 (1H, br s, 1'''-H), 8.50 (1H, d, *J* 5.1 Hz, 6'-H); δ_C (101 MHz, CDCl$_3$) 39.0 (CH$_2$), 52.4 (CH$_3$), 53.4 (CH), 55.9 (CH$_3$), 66.9 (CH$_2$), 111.8 (CH), 119.5 (CH), 121.1 (CH), 126.1 (CH), 126.1 (CH), 127.3 (CH), 127.4 (CH), 127.7 (2 × CH), 127.8 (CH), 128.1 (2 × CH), 128.2 (CH), 128.2 (CH), 128.5 (2 × CH), 129.8 (CH), 130.4 (C), 131.5 (C), 132.6 (C), 133.4 (C), 135.6 (C), 136.4 (C), 148.5 (C), 149.6 (CH), 156.1 (C), 157.5 (C), 157.7 (C), 172.2 (C); *m/z* (ESI) 547.2224 (MH$^+$. C$_{34}$H$_{30}$N$_2$O$_5$ requires 547.2227).

Methyl (2S)-2-[(benzyloxycarbonyl)amino]-3-[4'-(3''-(4'''-trifluoromethylphenyl)-4''-methoxyphenyl)pyridin-2'-yl]propanoate (93c)
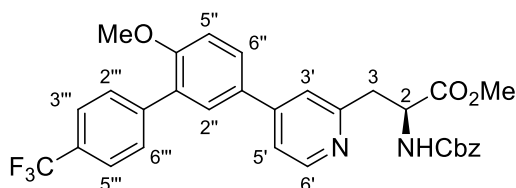
Methyl (2S)-2-[(benzyloxycarbonyl)amino]-3-[4'-(3''-(4'''-trifluoromethylphenyl)-4''-methoxyphenyl)pyridin-2'-yl]propanoate (**93c**) was synthesised as described for methyl (2S)-2-[(benzyloxycarbonyl)amino]-3-[4'-(4'',4'''-dimethoxy-[1'',1'''-biphenyl]-3''-yl)pyridin-2'-yl]propanoate (**93a**) using 4-(trifluoromethyl)phenylboronic acid (0.0850 g, 0.450 mmol), potassium fluoride (0.0523 g, 0.900 mmol), [1,1'-bis(diphenylphosphino)ferrocene]palladium(II) dichloride-dichloromethane complex (0.0184 g, 0.0225 mmol) and methyl (2S)-2-[(benzyloxycarbonyl)amino]-3-[4'-(3''-bromo-4''-methoxyphenyl)pyridin-2'-yl]propanoate (**92**) (0.150 g, 0.300 mmol) in 1,4-dioxane (2.0 mL) and water (0.24 mL). Purification by flash column chromatography, eluting with 10% acetonitrile in dichloromethane gave methyl (2S)-2-[(benzyloxycarbonyl)amino]-3-[4'-(3''-(4'''-trifluoromethylphenyl)-4''-methoxyphenyl)pyridin-2'-yl]propanoate (**93c**) as an off-white solid (0.0900 g, 53%). Mp 127−129 °C; ν_{max}/cm^{-1} (neat) 3333 (NH), 2951 (CH), 1721 (C=O), 1605 (C=C), 1505, 1327, 1265, 1068, 756; $[\alpha]_D^{19}$ +6.4 (c 1.0, CHCl$_3$); δ_H (400 MHz, CDCl$_3$) 3.34 (1H, dd, J 14.9, 5.1 Hz, 3-HH), 3.43 (1H, dd, J 14.9, 5.1 Hz, 3-HH), 3.70 (3H, s, OCH$_3$), 3.89 (3H, s, OCH$_3$), 4.81 (1H, dt, J 8.4, 5.1 Hz, 2-H), 5.11 (2H, s, OCH$_2$Ph), 6.34 (1H, d, J 8.4 Hz, NH), 7.09 (1H, d, J 8.6 Hz, 5''-H), 7.28–7.39 (7H, m, 3'-H, 5'-H and Ph), 7.56 (1H, d, J 2.3 Hz, 2''-H), 7.60–7.75 (5H, m, 6''-H, 2'''-H, 3'''-H, 5'''-H and 6'''-H), 8.49 (1H, d, J 4.9 Hz, 6'-H); δ_C (101 MHz, CDCl$_3$) 39.1 (CH$_2$), 52.4 (CH$_3$), 53.4 (CH), 55.8 (CH$_3$), 66.9 (CH$_2$), 111.8 (CH), 119.5 (CH), 121.0 (CH), 124.3 (q, $^1J_{C-F}$ 272.0 Hz, C), 126.1 (q, $^3J_{C-F}$ 3.7 Hz, 2 × CH), 128.0 (CH), 128.1 (2 × CH), 128.1 (CH), 128.5 (2 × CH), 129.4 (CH), 129.4 (q, $^2J_{C-F}$ 36.3 Hz, C), 129.9 (2 × CH), 130.0 (C), 130.6 (C), 136.4 (C), 141.6 (C), 148.2 (C), 149.6 (CH), 156.1 (C), 157.4 (C), 157.6 (C), 172.1 (C); m/z (ESI) 565.1942 (MH$^+$. C$_{31}$H$_{27}$F$_3$N$_2$O$_5$ requires 565.1945).

Methyl (2*S*)-2-[(benzyloxycarbonyl)amino]-3-[4'-(3''-(4''''-methoxystyryl)-4''-methoxyphenyl)pyridin-2'-yl]propanoate (95)
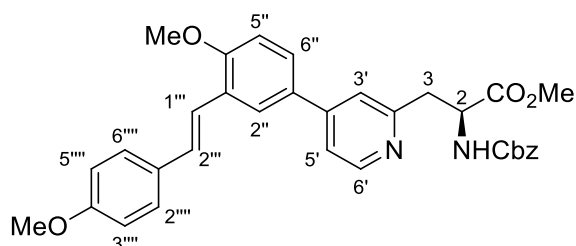
To a solution of methyl (2*S*)-2-[(benzyloxycarbonyl)amino]-3-[4'-(3''-bromo-4''-methoxyphenyl)pyridin-2'-yl]propanoate (**92**) (0.060 g, 0.12 mmol) in *N,N'*-dimethylformamide (1.6 mL) was added 4-methoxystyrene (0.040 g, 0.30 mmol), *N,N'*-diisopropylethylamine (0.060 mL, 0.36 mmol), and bis(triphenylphosphine)palladium(II) dichloride (0.0080 g, 0.012 mmol). The reaction mixture was degassed with argon for 0.15 h, and then stirred at 100 °C for 18 h. The reaction mixture was diluted with ethyl acetate (50 mL), washed with water (25 mL) and brine (25 mL), dried (MgSO$_4$) and concentrated *in vacuo* to give the crude product. Purification by flash column chromatography, eluting with 30% diethyl ether in dichloromethane gave methyl (2*S*)-2-[(benzyloxycarbonyl)amino]-3-[4'-(3''-(4''''-methoxystyryl)-4''-methoxyphenyl)pyridin-2'-yl]propanoate (**95**) as a yellow oil (0.040 g, 61%). ν_{max}/cm^{-1} (neat) 3340 (NH), 2897 (CH), 1721 (C=O), 1601, 1508, 1250, 1177, 968; [α]$_D^{24}$ +10.8 (*c* 0.2, CHCl$_3$); δ$_H$ (400 MHz, CDCl$_3$) 3.36 (1H, dd, *J* 14.8, 5.1 Hz, 3-*H*H), 3.45 (1H, dd, *J* 14.8, 5.1 Hz, 3-H*H*), 3.71 (3H, s, OCH$_3$), 3.84 (3H, s, OCH$_3$), 3.94 (3H, s, OCH$_3$), 4.82 (1H, dt, *J* 8.0, 5.1 Hz, 2-H), 5.12 (2H, s, OC*H*$_2$Ph), 6.38 (1H, d, *J* 8.0 Hz, NH), 6.91 (2H, d, *J* 8.6 Hz, 3''''-H and 5''''-H), 6.97 (1H, d, *J* 8.5 Hz, 5''-H), 7.15 (1H, d, *J* 16.4 Hz, 2'''-H), 7.27–7.41 (8H, m, 3'-H, 5'-H, 1'''-H and Ph), 7.47 (1H, dd, *J* 8.5, 1.7 Hz, 6''-H), 7.51 (2H, d, *J* 8.6 Hz, 2''''-H and 4''''-H), 7.90 (1H, d, *J* 1.7 Hz, 2''-H), 8.49 (1H, d, *J* 5.2 Hz, 6'-H); δ$_C$ (101 MHz, CDCl$_3$) 39.0 (CH$_2$), 52.4 (CH$_3$), 53.4 (CH), 55.3 (CH$_3$), 55.7 (CH$_3$), 66.9 (CH$_2$), 111.3 (CH), 114.1 (2 × CH), 119.6 (CH), 120.8 (CH), 121.1 (CH), 124.8 (CH), 126.8 (CH), 127.5 (C), 127.9 (2 × CH), 128.1 (2 × CH and CH), 128.5 (2 × CH), 129.6 (CH), 130.3 (C), 130.4 (C), 136.4 (C), 148.8 (C), 149.5 (CH), 156.1 (C), 157.4 (C), 157.6 (C), 159.4 (C), 172.2 (C); *m/z* (ESI) 553.2344 (MH$^+$. C$_{33}$H$_{32}$N$_2$O$_6$ requires 553.2339).

(2*S*)-2-Amino-3-[4'-(4''-methoxyphenyl)pyridin-2'-yl]propanoic acid hydrochloride (80)
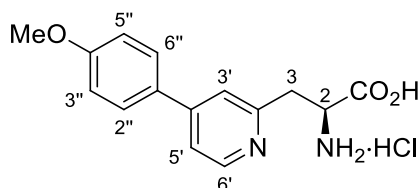
To a solution of methyl (2*S*)-2-[(benzyloxycarbonyl)amino]-3-[4'-(4''-methoxyphenyl)pyridin-2'-yl]propanoate (**87**) (0.0800 g, 0.190 mmol) in a mixture of methanol (5 mL) and 1,4-dioxane (5 mL) was added a solution of caesium carbonate (0.0810 g, 0.250 mmol) in water (2.5 mL). The reaction mixture was stirred at room temperature for 20 h and then concentrated *in vacuo.* The resulting residue was dissolved in water (10 mL) and acidified to pH 1 with 2 M aqueous hydrochloric acid. The aqueous layer was extracted with dichloromethane (3 × 30 mL) and the combined organic layers were dried (MgSO₄) and concentrated *in vacuo* to give (2*S*)-2-[(benzyloxycarbonyl)amino]-3-[4'-(4''-methoxyphenyl)pyridin-2'-yl]propanoic acid as a yellow solid (0.0680g, 88%). This was used for the next reaction without any further purification. (2*S*)-2-[(Benzyloxycarbonyl)amino]-3-[4'-(4''-methoxyphenyl)pyridin-2'-yl]propanoic acid (0.0500 g, 0.120 mmol) was suspended in 6 M aqueous hydrochloric acid (5 mL) and heated under reflux for 1 h. The reaction mixture was cooled to room temperature and concentrated *in vacuo.* Trituration with diethyl ether gave (2*S*)-2-amino-3-[4'-(4''-methoxyphenyl)pyridin-2'-yl]propanoic acid hydrochloride (**80**) as a yellow solid (0.0370 g, 100%). Mp 165−167 °C; ν_{max}/cm⁻¹ (neat) 3340 (NH), 2926 (CH), 1737 (C=O), 1369, 1224, 823; $[\alpha]_D^{21}$ +34.0 (*c* 0.8, MeOH); δ_H (500 MHz, CD₃OD) 3.70 (1H, dd, *J* 15.0, 9.5 Hz, 3-*H*H), 3.74 (1H, dd, *J* 15.0, 7.3 Hz, 3-H*H*), 3.91 (3H, s, OCH₃), 4.68−4.74 (1H, m, 2-H), 7.17 (2H, d, *J* 8.9 Hz, 3''-H and 5''-H), 8.04 (2H, d, *J* 8.9 Hz, 2''-H and 6''-H), 8.22 (1H, dd, *J* 6.3, 1.3 Hz, 5'-H), 8.39 (1H, d, *J* 1.3 Hz, 3'-H), 8.70 (1H, d, *J* 6.3 Hz, 6'-H); δ_C (126 MHz, CD₃OD) 35.1 (CH₂), 52.9 (CH), 56.2 (CH₃), 116.4 (2 × CH), 122.8 (CH), 125.0 (CH), 127.6 (C), 131.1 (2 × CH), 143.1 (CH), 152.1 (C), 158.3 (C), 164.8 (C), 170.0 (C); *m/z* (ESI) 307.0847 ([M−H]⁻. C₁₅H₁₆³⁵ClN₂O₃ requires 307.0855).

(2S)-2-Amino-3-[4'-(3''-bromo-4''-methoxyphenyl)pyridin-2'-yl]propanoic acid hydrochloride (97)
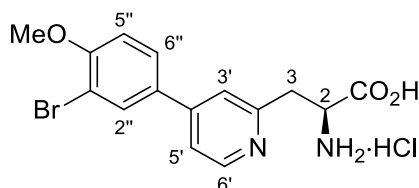
(2S)-2-[(Benzyloxycarbonyl)amino]-3-[4'-(3''-bromo-4''-methoxyphenyl)pyridin-2'-yl]propanoic acid (**97**) was synthesised as for (2S)-2-[(benzyloxycarbonyl)amino]-3-[4'-(4''-methoxyphenyl)pyridin-2'-yl]propanoic acid (**80**) using methyl (2S)-2-[(benzyloxycarbonyl)amino]-3-[4'-(3''-bromo-4''-methoxyphenyl)pyridin-2'-yl]propanoate (**92**) (0.100 g, 0.200 mmol), methanol (4 mL), 1,4-dioxane (4 mL), caesium carbonate (0.0850 g, 0.260 mmol) and water (2 mL). This gave (2S)-2-[(benzyloxycarbonyl)amino]-3-[4'-(3''-bromo-4''-methoxyphenyl)pyridin-2'-yl]propanoic acid as a yellow solid (0.0950 g, 95%) which was used for the next reaction without any further purification. (2S)-2-[(Benzyloxycarbonyl)amino]-3-[4'-(3''-bromo-4''-methoxyphenyl)pyridin-2'-yl]propanoic acid (0.0500 g, 0.103 mmol) was suspended in 6 M aqueous hydrochloric acid (5 mL) and heated under reflux for 1 h. The reaction mixture was cooled to room temperature and concentrated *in vacuo*. Purification by recrystallisation from a mixture of methanol and diethyl ether gave (2S)-2-amino-3-[4'-(3''-bromo-4''-methoxyphenyl)pyridin-2'-yl]propanoic acid hydrochloride (**97**) as a yellow solid (0.0320 g, 80%). Mp 225−227 °C (decomposition); v_{max}/cm^{-1} (neat) 3402 (NH), 2769 (CH), 1735 (C=O), 1628, 1589, 1477, 1281, 1184, 1049, 1010, 810; $[\alpha]_D^{18}$ +4.2 (*c* 0.2, MeOH); δ_H (400 MHz, CD$_3$OD) 3.70 (2H, d, *J* 6.5 Hz, 3-H$_2$), 4.00 (3H, s, OCH$_3$), 4.69 (1H, t, *J* 6.5 Hz, 2-H), 7.28 (1H, d, *J* 8.6 Hz, 5''-H), 8.03 (1H, dd, *J* 8.6, 1.3 Hz, 6''-H), 8.15 (1H, br d, *J* 5.7 Hz, 5'-H), 8.24 (1H, d, *J* 1.3 Hz, 2''-H), 8.30 (1H, br s, 3'-H), 8.71 (1H, d, *J* 5.7 Hz, 6'-H); δ_C (101 MHz, CD$_3$OD) 33.9 (CH$_2$), 51.6 (CH), 55.8 (CH$_3$), 112.5 (C), 112.6 (CH), 121.7 (CH), 123.8 (CH), 127.9 (C), 128.9 (CH), 132.5 (CH), 142.5 (CH), 151.4 (C), 155.0 (C), 159.1 (C), 168.7 (C); *m/z* (ESI) 351.0334 (MH$^+$. C$_{22}$H$_{23}$N$_2$O$_4$ requires 351.0339).

(2S)-2-Amino-3-[4'-(4'',4'''-dimethoxy-[1'',1'''-biphenyl]-3''-yl)pyridin-2'-yl]propanoic acid hydrochloride (94a)
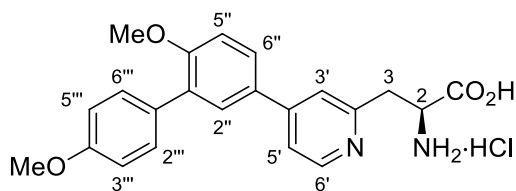
(2S)-2-[(Benzyloxycarbonyl)amino]-3-[4'-(4'',4'''-dimethoxy-[1'',1'''-biphenyl]-3''-yl)pyridin-2'-yl]propanoic acid (**94a**) was synthesised as described for (2S)-2-[(benzyloxycarbonyl)amino]-3-[4'-(4''-methoxyphenyl)pyridin-2'-yl]propanoic acid (**80**) using methyl (2S)-2-[(benzyloxycarbonyl)amino]-3-[4'-(4'',4'''-dimethoxy-[1'',1'''-biphenyl]-3''-yl)pyridin-2'-yl]propanoate (**93a**) (0.100 g, 0.200 mmol), methanol (4 mL), 1,4-dioxane (4 mL), caesium carbonate (0.0850 g, 0.260 mmol) and water (2 mL). This gave (2S)-2-[(benzyloxycarbonyl)amino]-3-[4'-(4'',4'''-dimethoxy-[1'',1'''-biphenyl]-3''-yl)pyridin-2'-yl]propanoic acid as a yellow solid (0.0830g, 66%) which was used for the next reaction without any further purification. (2S)-2-[(Benzyloxycarbonyl)amino]-3-[4'-(4'',4'''-dimethoxy-[1'',1'''-biphenyl]-3''-yl)pyridin-2'-yl]propanoic acid (0.0500 g, 0.103 mmol) was suspended in 6 M aqueous hydrochloric acid (5 mL) and heated under reflux for 1 h. The reaction mixture was cooled to room temperature and concentrated *in vacuo*. Purification by recrystallisation from a mixture of methanol and diethyl ether gave (2S)-2-amino-3-[4'-(4'',4'''-dimethoxy-[1'',1'''-biphenyl]-3''-yl)pyridin-2'-yl]propanoic acid hydrochloride (**94a**) as a yellow solid (0.0350 g, 85%). Mp 175−180 °C (decomposition); v_{max}/cm^{-1} (neat) 3389 (NH), 2835 (CH), 1742 (C=O), 1632 (C=C), 1596, 1502, 1479, 1268, 1245, 1180, 1021, 833; $[\alpha]_D^{22}$ +18.9 (c 0.2, MeOH); δ_H (400 MHz, CD$_3$OD) 3.65–3.79 (2H, m, 3-H$_2$), 3.84 (3H, s, OCH$_3$), 3.93 (3H, s, OCH$_3$), 4.74 (1H, dd, J 8.2, 6.6 Hz, 2-H), 6.99 (2H, d, J 8.8 Hz, 3'''-H and 5'''-H), 7.31 (1H, d, J 8.7 Hz, 5''-H), 7.51 (2H, d, J 8.8 Hz, 2'''-H and 6'''-H), 7.95 (1H, d, J 2.3 Hz, 2''-H), 8.05 (1H, dd, J 8.7, 2.3 Hz, 6''-H), 8.29 (1H, dd, J 6.2, 1.0 Hz, 5'-H), 8.46 (1H, d, J 1.0 Hz, 3'-H), 8.71 (1H, d, J 6.2 Hz, 6'-H); δ_C (101 MHz, CD$_3$OD) 35.1 (CH$_2$), 52.9 (CH), 55.8 (CH$_3$), 56.5 (CH$_3$), 113.6 (CH), 114.6 (2 × CH), 123.1 (CH), 125.3 (CH), 127.6 (C), 130.0 (CH), 130.9 (C), 131.3 (CH), 131.8 (2 × CH), 133.3 (C), 142.7 (CH), 151.7 (C), 158.8 (C), 160.7 (C), 161.7 (C), 169.9 (C); *m/z* (ESI) 379.1654 (MH$^+$. C$_{22}$H$_{23}$N$_2$O$_4$ requires 379.1652).

(2S)-2-Amino-3-[4'-(3''-(napthalen-2'''-yl)-4''-methoxyphenyl)pyridin-2'-yl]propanoic acid hydrochloride (94b)
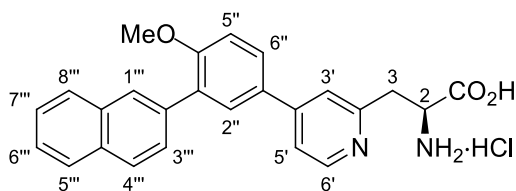
(2S)-2-[(Benzyloxycarbonyl)amino]-3-[4'-(3''-(napthalen-2'''-yl)-4''-methoxyphenyl)pyridin-2'-yl]propanoic acid (**94b**) was synthesised as described for (2S)-2-[(benzyloxycarbonyl)amino]-3-[4'-(4''-methoxyphenyl)pyridin-2'-yl]propanoic acid (**80**) using methyl (2S)-2-[(benzyloxycarbonyl)amino]-3-[4'-(3''-(napthalen-2'''-yl)-4''-methoxyphenyl)pyridin-2'-yl]propanoate (**93b**) (0.0800 g, 0.150 mmol), methanol (3 mL), 1,4-dioxane (3 mL), caesium carbonate (0.062 g, 0.190 mmol) and water (1.5 mL). This gave (2S)-2-[(benzyloxycarbonyl)amino]-3-[4'-(3''-(napthalen-2'''-yl)-4''-methoxyphenyl)pyridin-2'-yl]propanoic acid as a yellow solid (0.0750 g, 94%) which was used for the next reaction without any further purification. (2S)-2-[(benzyloxycarbonyl)amino]-3-[4'-(3''-(napthalen-2'''-yl)-4''-methoxyphenyl)pyridin-2'-yl]propanoic acid (0.0500 g, 0.0940 mmol) was suspended in 6 M aquous hydrochloric acid (5 mL) and heated under reflux for 1 h. The reaction mixture was cooled to room temperature and concentrated *in vacuo*. Purification by recrystallisation from a mixture of methanol and diethyl ether gave (2S)-2-amino-3-[4'-(3''-(napthalen-2'''-yl)-4''-methoxyphenyl)pyridin-2'-yl]propanoic acid hydrochloride (**94b**) as a yellow solid (0.0337 g, 82%). Mp 110−115 °C (decomposition); v_{max}/cm^{-1} (neat) 3371 (NH), 2924 (CH), 1732 (C=O), 1631 (C=C), 1593, 1481, 1265, 1242, 1153, 1014, 814; $[\alpha]_D^{19}$ −4.8 (c 0.2, MeOH); δ_H (400 MHz, CD$_3$OD) 3.67 (2H, d, J 6.7 Hz, 3-H$_2$), 3.95 (3H, s, OCH$_3$), 4.68 (1H, t, J 6.7 Hz, 2-H), 7.36 (1H, d, J 8.4 Hz, 5''-H), 7.47−7.55 (2H, m, 5'''-H and 8'''-H), 7.70 (1H, dd, J 8.5, 1.4 Hz, 3'''-H), 7.86−7.95 (3H, m, 2''-H, 6'''-H and 7'''-H), 7.99−8.09 (3H, m, 6''-H, 1'''-H and 4'''-H), 8.18 (1H, br d, J 5.8 Hz, 5'-H), 8.31 (1H, br s, 3'-H), 8.68 (1H, d, J 5.8 Hz, 6'-H); δ_C (101 MHz, CD$_3$OD) 35.3 (CH$_2$), 53.0 (CH), 56.6 (CH$_3$), 113.7 (CH), 122.9 (CH), 124.9 (CH), 127.2 (CH), 127.2 (CH), 128.2 (CH), 128.4 (CH), 128.6 (CH), 128.9 (CH), 129.2 (CH), 129.4 (C), 130.4 (CH), 131.7 (CH), 133.5 (C), 134.2 (C), 134.8 (C), 136.4 (C), 143.7 (CH), 152.6 (C), 157.7 (C), 161.6 (C), 170.1 (C); m/z (ESI) 399.1706 (MH$^+$. C$_{25}$H$_{22}$N$_2$O$_3$ requires 399.1703).

(2S)-2-Amino-3-[4'-(3''-(4'''-trifluoromethylphenyl)-4''-methoxyphenyl)pyridin-2'-yl]propanoic acid hydrochloride (94c)
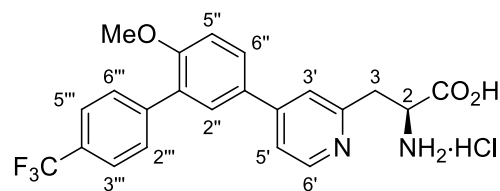
(2S)-2-[(Benzyloxycarbonyl)amino]-3-[4'-(3''-(4'''-trifluoromethylphenyl)-4''-methoxyphenyl)pyridin-2'-yl]propanoic acid (**94c**) was synthesised as described for (2S)-2-[(benzyloxycarbonyl)amino]-3-[4'-(4''-methoxyphenyl)pyridin-2'-yl]propanoic acid (**80**) using methyl (2S)-2-[(benzyloxycarbonyl)amino]-3-[4'-(3''-(4'''-trifluoromethylphenyl)-4''-methoxyphenyl)pyridin-2'-yl]propanoate (**93c**) (0.0700 g, 0.124 mmol), methanol (3 mL), 1,4-dioxane (3 mL), caesium carbonate (0.0530 g, 0.160 mmol) and water (1.5 mL). This gave (2S)-2-[(benzyloxycarbonyl)amino]-3-[4'-(3''-(4'''-trifluoromethylphenyl)-4''-methoxyphenyl)pyridin-2'-yl]propanoic acid as a yellow solid (0.0620 g, 91%) which was used for the next reaction without any further purification. (2S)-2-[(Benzyloxycarbonyl)amino]-3-[4'-(3''-(4'''-trifluoromethylphenyl)-4''-methoxyphenyl)pyridin-2'-yl]propanoic acid (0.0500 g, 0.0910 mmol) was suspended in 6 M aquous hydrochloric acid (5 mL) and heated under reflux for 1 h. The reaction mixture was cooled to room temperature and concentrated *in vacuo*. Purification by recrystallisation from a mixture of methanol and diethyl ether gave (2S)-2-amino-3-[4'-(3''-(4'''-trifluoromethylphenyl)-4''-methoxyphenyl)pyridin-2'-yl]propanoic acid hydrochloride (**94c**) as a yellow solid (0.0770 g, 77%). ν_{max}/cm^{-1} (neat) 3252 (NH), 2750 (CH), 1736 (C=O), 1632 (C=C), 1597, 1481, 1323, 1269, 1161, 1107, 840, 813; Mp (decomposition) 234−236 °C; $[\alpha]_D^{19}$ +3.5 (*c* 0.2, MeOH); δ_H (400 MHz, CD$_3$OD) 3.71 (2H, d, *J* 6.7 Hz, 3-H$_2$), 3.95 (3H, s, OCH$_3$), 4.69 (1H, t, *J* 6.7 Hz, 2-H), 7.37 (1H, d, *J* 8.7 Hz, 5''-H), 7.69−7.82 (4H, m, 2'''-H, 3'''-H, 5'''-H and 6'''-H), 8.00 (1H, d, *J* 2.0 Hz, 2''-H), 8.10 (1H, dd, *J* 8.7, 2.0 Hz, 6''-H), 8.22 (1H, br d, *J* 5.9 Hz, 5'-H), 8.39 (1H, br s, 3'-H), 8.70 (1H, d, *J* 5.9 Hz, 6'-H); δ_C (101 MHz, CD$_3$OD) 35.3 (CH$_2$), 53.0 (CH), 56.6 (CH$_3$), 113.8 (CH), 122.9 (CH), 124.5 (CH) 125.8 (q, $^1J_{C\text{-}F}$ 271.0 Hz, C), 126.0 (q, $^3J_{C\text{-}F}$ 3.7 Hz, 2 × CH), 128.4 (C), 130.5 (q, $^2J_{C\text{-}F}$ 32.2 Hz, C), 131.0 (CH), 131.4 (2 × CH), 131.4 (CH), 131.8 (C), 142.8 (C), 143.9 (CH), 152.8 (C), 157.3 (C), 161.2 (C), 170.1 (C); *m/z* (ESI) 417.1423 (MH$^+$. C$_{22}$H$_{19}$F$_3$N$_2$O$_3$ requires 417.1421).

(2S)-2-[(Benzyloxycarbonyl)amino]-3-[4'-(3''-(4''''-methoxystyryl)-4''-methoxyphenyl)pyridin-2'-yl]propanoic acid (96)
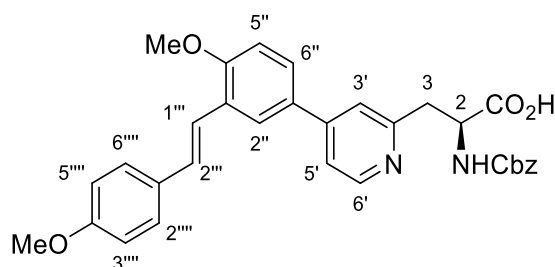
To a solution of methyl (2S)-2-[(benzyloxycarbonyl)amino]-3-[4'-(3''-(4''''-methoxystyryl)-4''-methoxyphenyl)pyridin-2'-yl]propanoate (**95**) (0.0800 g, 0.0700 mmol) in a mixture of methanol (3 mL) and 1,4-dioxane (3 mL) was added a solution of caesium carbonate (0.0680 g, 0.105 mmol) in water (1.5 mL). The reaction mixture was stirred at room temperature for 20 h and then concentrated *in vacuo.* The resulting residue was dissolved in water (10 mL) and acidified to pH 1 with 2 M aqueous hydrochloric acid. The aqueous layer was extracted with dichloromethane (3 × 30 mL) and the combined organic layers were dried (MgSO₄) and concentrated *in vacuo* to give (2S)-2-[(benzyloxycarbonyl)amino]-3-[4'-(3''-(4''''-methoxystyryl)-4''-methoxyphenyl)pyridin-2'-yl]propanoic acid (**96**) as a yellow solid (0.0530 g, 71%). Mp 153−157 °C; v_{max}/cm^{-1} (neat) 3349 (OH), 1717 (C=O), 1628, 1604 (C=C), 1512, 1250, 1026; $[\alpha]_D^{19}$ +60.0 (*c* 0.2, MeOH); δ_H (500 MHz, CD₃OD) 3.44–3.59 (2H, m, 3-H₂), 3.84 (3H, s, OCH₃), 3.96 (3H, s, OCH₃)*,* 4.52–4.61 (1H, m, 2-H), 5.12 (2H, d, *J* 3.3 Hz, OC*H*₂Ph), 6.28 (1H, d, *J* 4.0 Hz, NH), 6.91 (2H, d, *J* 8.6 Hz, 3''''-H and 5''''-H), 6.99 (1H, d, *J* 8.6 Hz, 5''-H), 7.17 (1H, d, *J* 16.4 Hz, 2'''-H), 7.27–7.40 (6H, m, 1'''-H and Ph), 7.48–7.57 (3H, m, 6''-H, 2''''-H and 4''''-H), 7.63 (1H, br d, *J* 5.6 Hz, 5'-H), 7.68 (1H, br s, 2''-H), 7.87 (1H, br s, 3'-H), 8.51 (1H, d, *J* 5.6 Hz, 6'-H); δ_C (101 MHz, CDCl₃) 38.4 (CH₂), 53.1 (CH), 55.4 (CH₃), 55.8 (CH₃), 66.9 (CH₂), 111.6 (CH), 114.2 (2 × CH), 120.5 (CH), 120.6 (CH), 122.6 (CH), 125.1 (CH), 127.3 (CH), 127.3 (C), 128.1 (2 × CH), 128.1 (2 × CH), 128.1 (C), 128.3 (CH), 128.6 (CH), 128.7 (2 × CH), 130.3 (C), 130.4 (C), 136.4 (C), 145.0 (CH), 152.8 (C), 155.9 (C), 158.7 (C), 159.6 (C), 172.7 (C); *m/z* (ESI) 539.2184 (MH⁺. C₃₂H₃₁N₂O₆ requires 539.2177).

5.3 Benzotriazole Derived Amino Acids Experimental

General procedure for the preparation of polymer-supported nitrite.[99] The polymer-supported nitrite reagent was prepared by the addition of Amberlyst® A26 hydroxide form resin (10.0 g, 40.0 mmol) to a solution of sodium nitrite (5.50 g, 80.0 mmol) in water (200 mL). The mixture was stirred at room temperature for 0.5 h. The polymer-supported nitrite was filtered and washed with water until the pH of the filtrate became neutral. The content of the polymer-supported nitrite was 3.5 mmol of NO_2^- per g.[99]

(2*S*)-2-[(Benzyloxycarbonyl)amino]-3-aminopropanoic acid [98]

A suspension of N_α-[(benzyloxycarbonyl)amino-L-asparagine (5.00 g, 18.8 mmol) and (diacetoxyiodo)benzene (7.26 g, 22.5 mmol) in acetonitrile (24 mL), ethyl acetate (24 mL) and water (12 mL) was stirred at 10 °C for 0.5 h. The reaction mixture was then stirred at room temperature for 3 h. The reaction mixture was filtered and the filtrate was washed with cold ethyl acetate (50 mL) and diethyl ether (50 mL) to give (2*S*)-2-[(benzyloxycarbonyl)amino]-3-aminopropionic acid (4.48 g, 100%) as a white solid. Mp 208–211 °C (lit.[188] 212 °C); $[\alpha]_D^{23}$ −7.9 (*c* 1.2, 1 M NaOH); δ_H (400 MHz, DMSO-d_6/TFA) 2.99–3.06 (1H, m, 3-*H*H), 3.21–3.28 (1H, m, 3-H*H*), 4.30 (1H, td, *J* 8.9, 4.6 Hz, 2-H), 5.07 (2H, s, OC*H*$_2$Ph), 7.28–7.37 (5H, m, Ph), 7.70 (1H, d, *J* 8.9 Hz, NH), 7.91 (2H, s, NH$_2$); δ_C (101 MHz, DMSO-d_6/TFA) 40.4 (CH$_2$), 51.9 (CH), 66.0 (CH$_2$), 128.0 (2 × CH), 128.0 (CH), 128.5 (2 × CH), 136.8 (C), 156.4 (C), 170.9 (C); *m/z* (ESI) 261 (MNa$^+$. 100%).

Methyl (2*S*)-2-[(benzyloxycarbonyl)amino]-3-aminopropanoate hydrochloride (102)[189]

To a suspension of (2*S*)-2-[(benzyloxycarbonyl)amino]-3-aminopropionic acid (4.48 g, 18.8 mmol) in methanol (30 mL) at 0 °C under argon was added dropwise thionyl chloride (1.78 mL, 24.4 mmol). The reaction mixture was warmed to room temperature and stirred for 16 h. The solution was concentrated *in vacuo* and triturated with diethyl ether to give methyl (2*S*)-2-[(benzyloxycarbonyl)amino]-3-aminopropanoate hydrochloride (**102**) (4.74 g, 100%) as a white solid. Mp 165–168 °C (lit.[189] 169–171 °C); $[\alpha]_D^{22}$ −41.4 (*c* 1.1, MeOH); δ_H (400 MHz, CD$_3$OD) 3.23 (1H, dd, *J* 13.2, 8.8 Hz, 3-*H*H), 3.45 (1H, dd, *J* 13.2, 5.1 Hz, 3-H*H*), 3.78 (3H, s, OCH$_3$), 4.51 (1H, dd, *J* 8.8, 5.1 Hz, 2-H), 5.14 (2H, s, OC*H*$_2$Ph), 7.30–7.40 (5H, m, Ph); δ_C (101 MHz, CD$_3$OD) 41.3 (CH$_2$), 53.1 (CH), 53.4 (CH$_3$), 68.2 (CH$_2$), 129.0 (2 × CH), 129.2 (CH), 129.5 (2 × CH), 137.8 (C), 158.7 (C), 170.9 (C); *m/z* (ESI) 275 (MNa$^+$. 100%).

Methyl (2*S*)-2-[(benzyloxycarbonyl)amino]-3-[(4'-bromo-2'-nitrophenyl)amino]propanoate (105)
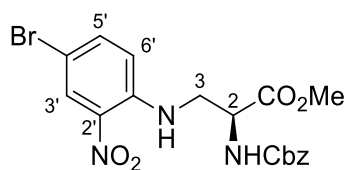
To a solution of methyl (2*S*)-3-amino-2-[(benzyloxycarbonyl)amino]propanoate hydrochloride (**102**) (3.97 g, 13.8 mmol) in acetonitrile (50 mL) under argon was added 5-bromo-2-fluoro-1-nitrobenzene (5.10 mL, 41.3 mmol) and triethylamine (5.90 mL, 41.3 mmol). The reaction mixture was stirred under reflux for 16 h. After cooling the reaction to ambient temperature, the solvent was removed *in vacuo*. The resulting residue was dissolved in ethyl acetate (50 mL), washed with water (3 × 50 mL) and brine (50 mL). The organic layer was dried (MgSO$_4$), filtered and concentrated *in vacuo*. Purification by flash column chromatography, eluting with 0–

20% ethyl acetate in dichloromethane gave methyl (2*S*)-2-[(benzyloxycarbonyl)amino]-3-[(4'-bromo-2'-nitrophenyl)amino]propanoate (**105**) as a yellow solid (5.75 g, 92%). Mp 86–89 °C; v_{max}/cm^{-1} (neat) 3364 (NH), 2955 (CH), 1721 (C=O), 1612 (C=O), 1504, 1227, 1065 cm^{-1}; [α]$_D^{25}$ +14.3 (*c* 1.1, CHCl$_3$); $δ_H$ (400 MHz, CDCl$_3$) 3.60–3.76 (5H, m, 3-H$_2$ and OCH$_3$), 4.60 (1H, dt, *J* 6.9, 5.8 Hz, 2-H), 5.06 (1H, d, *J* 12.2 Hz, OC*H*HPh), 5.11 (1H, d, *J* 12.2 Hz, OCH*H*Ph), 6.06 (1H, d, *J* 6.9 Hz, NH), 6.81 (1H, d, *J* 9.1 Hz, 6'-H), 7.20–7.30 (5H, m, Ph), 7.36 (1H, dd, *J* 9.1, 1.5 Hz, 5'-H), 8.16 (1H, d, *J* 1.5 Hz, 3'-H), 8.19 (1H, t, *J* 6.0 Hz, NH); $δ_C$ (101 MHz, CDCl$_3$) 44.2 (CH$_2$), 52.8 (CH$_3$), 53.2 (CH), 67.0 (CH$_2$), 107.0 (C) 115.3 (CH), 127.9 (2 × CH), 128.1 (CH), 128.3 (2 × CH), 128.6 (CH), 132.5 (C), 135.8 (C), 138.7 (CH), 143.6 (C), 155.9 (C), 170.4 (C); *m/z* (ESI) 474.0276 (MNa$^+$. C$_{18}$H$_{18}^{79}$BrN$_3$NaO$_6$ requires 474.0271).

Methyl (2*S*)-2-[(benzyloxycarbonyl)amino]-3-(5'-bromo-1*H*-benzo[*d*][1.2.3]triazol-1'-yl)propanoate (103)

To a solution of methyl (2*S*)-2-[(benzyloxycarbonyl)amino]-3-[(5'-bromo-2'-nitrophenyl)amino]propanoate (**105**) (9.00 g, 19.9 mmol) in methanol (100 mL) was added tin(II) dichloride dihydrate (22.0 g, 99.5 mmol). The reaction mixture was stirred under reflux for 20 h. After cooling the reaction to ambient temperature, the solvent was removed *in vacuo*. The resulting residue was dissolved in ethyl acetate (50 mL) and mixed with a saturated solution of aqueous sodium hydrogen carbonate (30 mL). The biphasic mixture was filtered through Celite® and the organic layer separated. The aqueous layer was extracted with ethyl acetate (2 × 50 mL) and the combined organic layers were washed with brine (50 mL), dried (MgSO$_4$), filtered and concentrated *in vacuo*. Purification by flash column chromatography, eluting with 10% ethyl acetate in dichloromethane gave methyl (2*S*)-2-[(benzyloxycarbonyl)amino]-3-[(5'-bromo-2'-aminophenyl)amino]propanoate (**106**) as a brown oil (6.42 g, 76%). This material was then used immediately in the following step. To a solution of methyl (2*S*)-2-[(benzyloxycarbonyl)amino]-3-[(5'-bromo-2'-aminophenyl)amino]propanoate (**106**) (6.30 g, 14.9 mmol) in acetonitrile

(200 mL) at −10 °C was added *p*-toluenesulfonic acid (8.50 g, 44.7 mmol) and polymer-supported nitrite (12.8 g, containing 44.7 mmol of NO_2^-). The reaction mixture was stirred at this temperature for 3 h. The reaction mixture was filtered, and the resin washed with dichloromethane (50 mL). The reaction mixture was concentrated *in vacuo* and dissolved in ethyl acetate (100 mL). The organic layer was then washed with a saturated solution of aqueous sodium hydrogen carbonate (50 mL) and brine (50 mL), dried (MgSO₄), filtered and concentrated *in vacuo*. Purification by flash column chromatography, eluting with 10% ethyl acetate in dichloromethane gave methyl (2*S*)-2-[(benzyloxycarbonyl)amino]-3-(5'-bromo-1*H*-benzo[*d*][1.2.3]triazol-1'-yl)propanoate (**103**) as a white solid (4.25 g, 66%). Mp 110–114 °C; ν_{max}/cm⁻¹ (neat) 3321 (NH), 2954 (CH), 1717 (C=O), 1512, 1211, 1057, 752; $[\alpha]_D^{22}$ −22.2 (*c* 1.0, CHCl₃); δ_H (500 MHz, CDCl₃) 3.77 (3H, s, OCH₃), 4.84 (1H, dt, *J* 6.6, 4.5 Hz, 2-H), 5.00–5.20 (4H, m, 3-H₂ and OC*H₂*Ph), 5.69 (1H, d, *J* 6.6 Hz, NH), 7.22–7.47 (7H, m, 6'-H, 7'-H and Ph), 8.15 (1H, d, *J* 1.0 Hz, 4'-H); δ_C (126 MHz, CDCl₃) 48.6 (CH₂), 53.3 (CH₃), 54.2 (CH), 67.3 (CH₂), 110.4 (CH), 117.4 (C), 122.6 (CH), 128.3 (2 × CH), 128.4 (CH), 128.6 (2 × CH), 131.2 (CH), 132.8 (C), 135.8 (C), 146.7 (C), 155.6 (C), 169.1 (C); *m/z* (ESI) 455.0325 (MNa⁺. $C_{18}H_{17}^{79}BrN_4NaO_4$ requires 455.0325).

Methyl (2*S*)-2-[(benzyloxycarbonyl)amino]-3-[(2'-nitro-4'-iodophenyl)amino]propanoate (110)

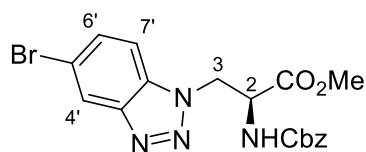Methyl (2*S*)-2-[(benzyloxycarbonyl)amino]-3-[(2'-nitro-4'-iodophenyl)amino]propanoate (**110**) was synthesised as described for methyl (2*S*)-2-[(benzyloxycarbonyl)amino]-3-[(4'-bromo-2'-nitrophenyl)amino]propanoate (**105**) using methyl (2*S*)-3-amino-2-[(benzyloxycarbonyl)amino]propanoate hydrochloride (**102**) (2.21 g, 7.70 mmol), 5-iodo-2-fluoro-1-nitrobenzene (6.16 g, 23.1 mmol) and triethylamine (3.20 mL, 23.1 mmol) in acetonitrile (50 mL). Purification by flash column chromatography, eluting with 0–20% ethyl acetate in dichloromethane gave methyl (2*S*)-2-[(benzyloxycarbonyl)amino]-3-[(2'-nitro-4'-

iodophenyl)amino]propanoate (**110**) as an orange solid (3.40 g, 89%). Mp 103–107 °C; v_{max}/cm^{-1} (neat) 3356 (NH), 2953 (CH), 1719 (C=O), 1611 (C=O), 1503, 1230, 1060; $[α]_D^{21}$ +46.5 (*c* 1.0, CHCl₃); $δ_H$ (500 MHz, CDCl₃) 3.73–3.80 (5H, m, 3-H₂ and OCH₃), 4.58–4.65 (1H, m, 2-H), 5.10 (1H, d, *J* 12.1 Hz, OC*H*HPh), 5.15 (1H, d, *J* 12.1 Hz, OCH*H*Ph), 5.60 (1H, d, *J* 6.0 Hz, NH), 6.78 (1H, d, *J* 8.8 Hz, 6'-H), 7.30–7.41 (5H, m, Ph), 7.57 (1H, br d, *J* 8.8 Hz, 5'-H), 8.21 (1H, t, *J* 5.5 Hz, NH), 8.46 (1H, d, *J* 1.1 Hz, 3'-H); $δ_C$ (126 MHz, CDCl₃) 44.5 (CH₂), 53.1 (CH₃), 53.4 (CH), 67.4 (CH₂), 75.4 (C), 115.8 (CH), 128.3 (2 × CH), 128.4 (CH), 128.6 (2 × CH), 133.5 (C), 135.0 (CH), 135.8 (C), 144.3 (CH), 144.3 (C), 155.8 (C), 170.4 (C); *m/z* (ESI) 522.0143 (MNa⁺. C₁₈H₁₈IN₃NaO₆ requires 522.0132).

Methyl (2*S*)-2-[(benzyloxycarbonyl)amino]-3-[(4'-iodo-2'-aminophenyl)amino]propanoate (111)
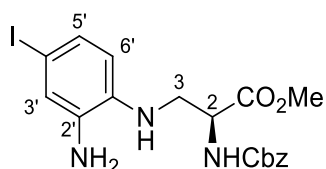
To a solution of methyl (2*S*)-2-[(benzyloxycarbonyl)amino]-3-[(2'-nitro-4'-iodophenyl)amino]propanoate (**110**) (3.30 g, 6.60 mmol) in methanol (100 mL) was added zinc (2.16 g, 33.0 mmol) and acetic acid (1.90 mL, 33.0 mmol) under argon. The reaction mixture was stirred for 0.5 h at room temperature and then filtered through Celite®. The mixture was concentrated *in vacuo*, and the resulting residue was dissolved in ethyl acetate (50 mL). The organic layer was washed with water (3 × 50 mL), brine (50 mL), dried (MgSO₄), filtered and concentrated *in vacuo*. Purification by flash column chromatography eluting with 10% ethyl acetate in dichloromethane gave methyl (2*S*)-2-[(benzyloxycarbonyl)amino]-3-[(4'-iodo-2'-aminophenyl)amino]propanoate (**111**) as a brown solid (2.65 g, 85%). Mp 117–119 °C; v_{max}/cm^{-1} (neat) 3337 (NH), 2951 (CH), 1709 (C=O), 1500, 1217, 1059; $[α]_D^{22}$ +4.2 (*c* 0.3, CHCl₃); $δ_H$ (500 MHz, CDCl₃) 3.37 (2H, br s, NH₂), 3.42 (1H, dd, *J* 12.4, 5.6 Hz, 3-*H*H), 3.54 (1H, dd, *J* 12.4, 3.5 Hz, 3-H*H*), 3.75 (3H, s, OCH₃), 4.59–4.66 (1H, m, 2-H), 5.09 (1H, d, *J* 12.3 Hz, OC*H*HPh), 5.12 (1H, d, *J* 12.3 Hz, OCH*H*Ph), 5.69 (1H, d, *J* 6.2 Hz, NH), 6.39 (1H, d, *J* 8.1 Hz, 6'-H), 6.97 (1H, d, *J* 1.9 Hz, 3'-H), 7.04 (1H, br d, *J* 8.1 Hz, 5'-H), 7.31–7.37 (5H, m, Ph); $δ_C$ (126 MHz,

CDCl$_3$) 46.2 (CH$_2$), 52.9 (CH$_3$), 53.9 (CH), 67.3 (CH$_2$), 81.1 (C), 114.2 (CH), 124.8 (CH), 128.2 (2 × CH), 128.3 (CH), 128.6 (2 × CH), 129.1 (CH), 136.0 (C), 136.3 (C), 136.6 (C), 156.1 (C), 171.3 (C); *m/z* (ESI) 492.0409 (MNa$^+$. C$_{18}$H$_{20}$IN$_3$NaO$_4$ requires 492.0391).
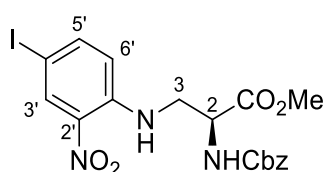
Methyl (2*S*)-2-[(benzyloxycarbonyl)amino]-3-(5'-iodo-1*H*-benzo[*d*][1.2.3]triazol-1'-yl)propanoate (113)
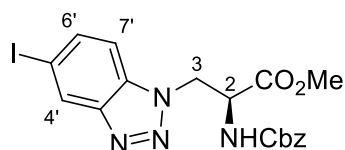
To a solution of methyl (2*S*)-2-[(benzyloxycarbonyl)amino]-3-[(5'-iodo-2'-aminophenyl)amino]propanoate (**111**) (2.50 g, 5.32 mmol) in acetonitrile (140 mL) at −10 °C was added *p*-toluenesulfonic acid (3.00 g, 16.0 mmol) and polymer-supported nitrite (4.60 g, containing 16.0 mmol of NO$_2^-$). The reaction mixture was stirred for 3 h, filtered and the resin washed with dichloromethane (50 mL). The solution was concentrated *in vacuo* and dissolved in ethyl acetate (100 mL). The organic layer was washed with a saturated solution of aqueous sodium hydrogen carbonate (50 mL), brine (50 mL), dried (MgSO$_4$), filtered and concentrated *in vacuo*. Purification by flash column chromatography, eluting with 10% ethyl acetate in dichloromethane gave methyl (2*S*)-2-[(benzyloxycarbonyl)amino]-3-(5'-iodo-1*H*-benzo[*d*][1.2.3]triazol-1'-yl)propanoate (**113**) as a pale orange solid (1.66 g, 65%). Mp 152–156 °C; ν_{max}/cm^{-1} (neat) 3329 (NH), 2953 (CH), 1717 (C=O), 1533, 1213, 1058, 754; [α]$_D^{22}$ +27.5 (*c* 0.3, CHCl$_3$); δ$_H$ (500 MHz, CDCl$_3$) 3.78 (3H, s, OCH$_3$), 4.84 (1H, dt, *J* 6.5, 4.3 Hz, 2-H), 4.95–5.24 (4H, m, 3-H$_2$ and OC*H$_2$*Ph), 5.56 (1H, d, *J* 6.5 Hz, NH), 7.17 (1H, d, *J* 8.7 Hz, 7'-H), 7.29–7.42 (5H, m, Ph), 7.57 (1H, br d, *J* 8.7 Hz, 6'-H), 8.40 (1H, br s, 4'-H); δ$_C$ (126 MHz, CDCl$_3$) 48.5 (CH$_2$), 53.3 (CH$_3$), 54.2 (CH), 67.3 (CH$_2$), 87.6 (C), 110.7 (CH), 128.3 (2 × CH), 128.5 (CH), 128.6 (2 × CH), 129.1 (CH), 133.2 (C), 135.8 (C), 136.4 (CH), 147.4 (C), 155.6 (C), 169.1 (C); *m/z* (ESI) 503.0201 (MNa$^+$. C$_{18}$H$_{17}$IN$_4$NaO$_4$ requires 503.0187).

Methyl (2*S*)-2-[(benzyloxycarbonyl)amino]-3-[5'-(phenylethynyl)-1*H*-benzo[*d*][1.2.3]triazol-1'-yl]propanoate (114a)
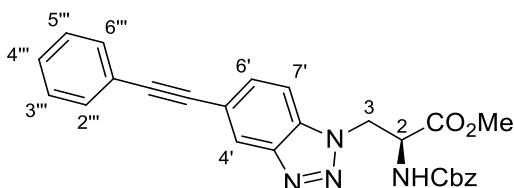
To a solution of methyl (2*S*)-2-[(benzyloxycarbonyl)amino]-3-(5'-iodo-1*H*-benzo[*d*][1.2.3]triazol-1'-yl)propanoate (**113**) (0.300 g, 0.260 mmol) in *N,N'*-dimethylformamide was added copper iodide (0.0228 g, 0.120 mmol) and bis(triphenylphosphine)palladium(II) dichloride (0.0420 g, 0.0600 mmol). Phenylacetylene (0.0880 mL, 0.800 mmol) was dissolved in degassed triethylamine (40 mL) and added to the reaction mixture. The solution was heated to 100 °C for 0.1 h and then left to stir at room temperature for 2 h. The solution was concentrated *in vacuo*, dissolved in ethyl acetate (20mL), washed with water (5 × 10 mL) and brine (2 × 10 mL), dried (MgSO$_4$) and concentrated *in vacuo*. Purification by flash column chromatography, eluting with 0−10% ethyl acetate in dichloromethane gave methyl (2*S*)-2-[(benzyloxycarbonyl)amino]-3-[5'-(phenylethynyl)-1*H*-benzo[*d*][1.2.3]triazol-1'-yl]propanoate (**114a**) as a yellow solid (0.265 g, 94%). Mp 128–132 °C; v_{max}/cm^{-1} (neat) 3331 (NH), 2951 (CH), 2365 (C≡C), 1716 (C=O), 1512, 1213, 1060, 742; $[\alpha]_D^{17}$ +9.1 (*c* 0.1, CHCl$_3$); δ_H (500 MHz, CDCl$_3$) 3.76 (3H, s, OCH$_3$), 4.87 (1H, dt, *J* 7.0, 4.3 Hz, 2-H), 5.01–5.19 (4H, m, 3-H$_2$ and OC*H*$_2$Ph), 5.66 (1H, d, *J* 7.0 Hz, NH), 7.29–7.41 (9H, m, 7'-H and 8 × ArH), 7.51 (1H, dd, *J* 8.6, 1.1 Hz, 6'-H), 7.55–7.59 (2H, m, 2 × ArH), 8.21 (1H, br s, 4'-H); δ_C (126 MHz, CDCl$_3$) 48.6 (CH$_2$), 53.3 (CH$_3$), 54.2 (CH), 67.3 (CH$_2$), 88.6 (C), 89.6 (C), 109.2 (CH), 119.5 (C), 122.9 (C), 123.3 (CH), 128.2 (2 × CH), 128.4 (CH), 128.4 (2 × CH), 128.5 (CH), 128.6 (2 × CH), 131.4 (CH), 131.7 (2 × CH), 133.4 (C), 135.8 (C), 145.6 (C), 155.6 (C), 169.2 (C); *m/z* (ESI) 477.1533 (MNa$^+$. C$_{26}$H$_{22}$N$_4$NaO$_4$ requires 477.1527).

Methyl (2*S*)-2-[(benzyloxycarbonyl)amino]-3-{5'-[(4'''-fluorophenyl)ethynyl]-1*H*-benzo[*d*][1.2.3]triazol-1'-yl}propanoate (114b)
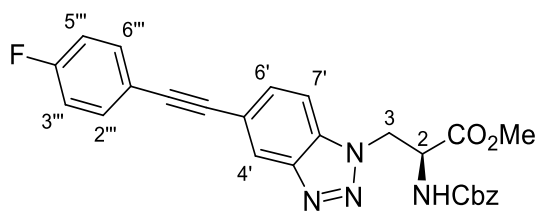
Methyl (2*S*)-2-[(benzyloxycarbonyl)amino]-3-{5'-[(4'''-fluorophenyl)ethynyl]-1*H*-benzo[*d*][1.2.3]triazol-1'-yl}propanoate (**114b**) was synthesised as described for methyl (2*S*)-2-[(benzyloxycarbonyl)amino]-3-[5'-(phenylethynyl)-1*H*-benzo[*d*][1.2.3]triazol-1'-yl]propanoate (**114a**) using methyl (2*S*)-2-[(benzyloxycarbonyl)amino]-3-(5'-iodo-1*H*-benzo[*d*][1.2.3]triazol-1'-yl)propanoate (**113**) (0.0500 g, 0.100 mmol) in *N,N'*-dimethylformamide (3 mL), copper iodide (0.00380 g, 0.0200 mmol), bis(triphenylphosphine)palladium(II) dichloride (0.00700 g, 0.0100 mmol), 4-fluorophenylacetylene (0.0150 mL, 0.130 mmol) and degassed triethylamine (7 mL). Purification by flash column chromatography, eluting with 0−10% ethyl acetate in dichloromethane gave methyl (2*S*)-2-[(benzyloxycarbonyl)amino]-3-{5'-[(4'''-fluorophenyl)ethynyl]-1*H*-benzo[*d*][1.2.3]triazol-1'-yl}propanoate (**114b**) as a yellow solid (0.0370 g, 79%). Mp 115–118 °C; ν_{max}/cm^{-1} (neat) 3313 (NH), 2954 (CH), 2366 (C≡C), 1720 (C=O), 1508, 1219, 835; $[\alpha]_D^{14}$ +7.1 (*c* 0.5, CHCl$_3$); δ_H (500 MHz, CDCl$_3$) 3.77 (3H, s, OCH$_3$), 4.87 (1H, dt, *J* 6.7, 4.4 Hz, 2-H), 5.06–5.17 (4H, m, 3-H$_2$ and OC*H*$_2$Ph), 5.65 (1H, d, *J* 6.7 Hz, NH), 7.04–7.10 (2H, m, 3'''-H and 5'''-H), 7.29–7.42 (6H, m, 7'-H and Ph), 7.50 (1H, dd, *J* 8.6, 1.2 Hz, 6'-H), 7.53–7.57 (2H, m, 2'''-H and 6'''-H), 8.18 (1H, br s, 4'-H); δ_C (126 MHz, CDCl$_3$) 48.6 (CH$_2$), 53.3 (CH$_3$), 54.2 (CH), 67.3 (CH$_2$), 88.3 (C), 88.5 (C), 109.3 (CH), 115.8 (d, $^2J_{C-F}$ 22.1 Hz, 2 × CH), 119.0 (d, $^4J_{C-F}$ 3.5 Hz, C), 119.3 (C), 123.3 (CH), 128.2 (2 × CH), 128.4 (2 × CH), 128.6 (CH), 131.3 (CH), 133.4 (C), 133.6 (d, $^3J_{C-F}$ 8.4 Hz, 2 × CH), 135.8 (C), 145.6 (C), 155.6 (C), 162.7 (d, $^1J_{C-F}$ 250.0 Hz, C), 169.2 (C); *m/z* (ESI) 495.1443 (MNa$^+$. C$_{26}$H$_{21}$FN$_4$NaO$_4$ requires 495.1439).

(2*S*)-2-[(*tert*-Butoxycarbonyl)amino]-3-aminopropanoic acid (118)[115]
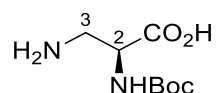
A suspension of N_α-[(*tert*-butoxycarbonyl)amino-L-asparagine (10.0 g, 43.0 mmol and (diacetoxyiodo)benzene (16.6 g, 51.7 mmol) in acetonitrile (50 mL), ethyl acetate (50 mL) and water (25 mL) was stirred at 10 °C, then allowed to warm to room temperature with stirring for 18 h. The reaction mixture was filtered and the filtrate was washed with cold ethyl acetate (50 mL) and diethyl ether (50 mL) which gave (2*S*)-2-[(*tert*-butoxycarbonyl)amino]-3-aminopropionic acid (**118**) (7.40 g, 84%) as a white solid. Mp 202–204 °C (lit.[115] 206 °C); $[\alpha]_D^{20}$ +21.3 (*c* 1.0, MeOH); δ_H (400 MHz, DMSO-*d6*) 1.39 (9H, s, 3 × CH₃), 2.75 (1H, dd, *J* 11.8, 9.1 Hz, 3-*H*H), 3.02 (1H, dd, *J* 11.8, 4.7 Hz, 3-H*H*), 3.60–3.69 (1H, m, 2-H), 6.20 (1H, d, *J* 5.0 Hz, NH); δ_C (101 MHz, DMSO-*d6*) 28.2 (3 × CH₃), 40.7 (CH₂), 51.4 (CH), 78.1 (C), 155.1 (C), 171.5 (C); *m/z* (ESI) 277 (MNa⁺. 100%).

(2*S*)-2-[(*tert*-Butoxycarbonyl)amino]-3-(benzyloxycarbonyl)aminopropanoic acid (119)[115]
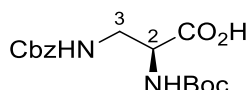
To (2*S*)-2-[(*tert*-butoxycarbonyl)amino]-3-aminopropionic acid (**118**) (7.00 g, 34.2 mmol) in water (80 mL) was added sodium hydrogen carbonate (7.20 g, 85.7 mmol). A solution of benzyl chloroformate (5.80 mL, 41.1 mmol) in toluene (16 mL) was added and the mixture was stirred at room temperature for 18 h. The reaction mixture was concentrated *in vacuo* and the solid residue was filtered and washed with diethyl ether (100 mL). The resulting solid was dissolved in water (200 mL), and a concentrated citric acid solution was added until the solution reached pH 2. The aqueous layer was then extracted with ethyl acetate (2 × 200 mL). The combined organic layers were washed with water (200 mL) and brine (150 mL), dried (MgSO₄), filtered and concentrated *in vacuo* to give (2*S*)-2-[(*tert*-butoxycarbonyl)amino]-3-(benzyloxycarbonyl)aminopropanoic acid (**119**) as a white solid (8.70 g, 75%).

Spectroscopic data were consistent with the literature.[115] Mp 45–47 °C; $[\alpha]_D^{19}$ −4.6 (c 0.1, MeOH); δ_H (400 MHz, DMSO-d_6) 1.38 (9H, s, 3 × CH$_3$), 3.25–3.32 (2H, m, 3-H$_2$), 4.04 (1H, dt, J 8.0, 5.4 Hz, 2-H), 5.02 (2H, s, OCH$_2$Ph), 6.95 (1H, d, J 8.0 Hz, NH), 7.26–7.39 (5H, m, Ph), 12.63 (1H, br s, CO$_2$H); δ_C (101 MHz, DMSO-d_6) 28.6 (3 × CH$_3$), 42.1 (CH$_2$), 54.1 (CH), 65.8 (CH$_2$), 78.7 (C), 128.1 (2 × CH), 128.2 (CH), 128.8 (2 × CH), 137.5 (C), 155.8 (C), 156.7 (C), 172.7 (C); m/z (ESI) 361 (MNa$^+$. 100%).

Methyl (2S)-2-[(tert-butoxycarbonyl)amino]-3-(benzyloxycarbonyl)aminopropanoate (120)[191]
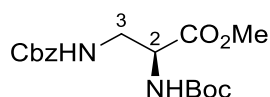
To a solution of (2S)-2-[(tert-butoxycarbonyl)amino]-3-(benzyloxycarbonyl)aminopropanoic acid (119) (6.50 g, 8.80 mmol) and potassium carbonate (5.30 g, 38.4 mmol) in N,N'-dimethylformamide (50 mL) at 10 °C was added methyl iodide (5.97 mL, 96.1 mmol) dropwise. The reaction mixture was stirred at room temperature for 18 h and then concentrated in vacuo. The residue was dissolved in water (200 mL), extracted with ethyl acetate (3 × 200 mL), dried (MgSO$_4$), filtered and concentrated in vacuo. Purification by column chromatography, eluting with 40% ethyl acetate in hexane gave methyl (2S)-2-[(tert-butoxycarbonyl)amino]-3-(benzyloxycarbonyl)aminopropanoate (120) as a colourless oil (5.07 g, 83%). Spectroscopic data were consistent with the literature.[192] $[\alpha]_D^{19}$ −5.7 (c 0.1, MeOH); δ_H (400 MHz, CDCl$_3$) 1.43 (9H, s, 3 × CH$_3$), 3.56−3.59 (2H, m, 3-H$_2$), 3.72 (3H, s, OCH$_3$), 4.32–4.41 (1H, m, 2-H), 5.08 (2H, s, OCH$_2$Ph), 5.28 (1H, br s, NH), 5.51 (1H, d, J 7.4 Hz, NH), 6.95 (1H, d, J 8.0 Hz, NH), 7.28–7.38 (5H, m, Ph); δ_C (101 MHz, CDCl$_3$) 28.3 (3 × CH$_3$), 42.9 (CH$_2$), 52.7 (CH$_3$), 54.0 (CH), 67.0 (CH$_2$), 80.3 (C), 128.1 (2 × CH), 128.2 (CH), 128.5 (2 × CH), 136.3 (C), 155.5 (C), 156.7 (C), 171.2 (C); m/z (ESI) 375 (MNa$^+$. 100%).

Methyl (2*S*)-2-[(*tert*-butoxycarbonyl)amino]-3-aminopropanoate (121)[115]
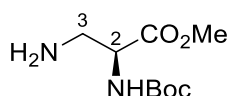
To a solution of methyl (2*S*)-2-[(*tert*-butoxycarbonyl)amino]-3-(benzyloxycarbonyl)aminopropanoate (**120**) (5.00 g, 14.2 mmol) in methanol (75 mL) under argon was added palladium on activated charcoal (10% palladium basis, 0.151 g, 1.42 mmol). The reaction mixture was then was stirred under a hydrogen atmosphere at room temperature for 5 h. The solution was filtered through Celite®, washed with methanol (300 mL) and concentrated *in vacuo* to give methyl (2*S*)-2-[(*tert*-butoxycarbonyl)amino]-3-aminopropanoate (**121**) as a colourless oil (3.09 g, 100%). Spectroscopic data were consistent with the literature.[115] $[\alpha]_D^{20}$ −16.4 (*c* 1.0, MeOH); δ_H (400 MHz, DMSO-*d₆*) 1.40 (9H, s, 3 × CH_3), 2.99 (1H, dd, *J* 13.0, 8.6 Hz, 3-*H*H), 3.13 (1H, dd, *J* 13.0, 4.8 Hz, 3-H*H*), 3.67 (3H, s, OCH_3), 4.31 (1H, td, *J* 8.6, 4.8 Hz, 2-H), 7.40 (1H, d, *J* 8.6 Hz, NH), 7.81 (2H, br s, NH_2); δ_C (101 MHz, DMSO-*d₆*) 28.6 (3 × CH_3), 39.9 (CH_2), 52.5 (CH_3), 52.8 (CH), 79.4 (C), 155.9 (C), 170.8 (C); *m/z* (ESI) 219 (MNa⁺. 100%).

Methyl (2*S*)-2-[(*tert*-butoxycarbonyl)amino]-3-[(2'-nitro-4'-iodophenyl)amino]propanoate (122)
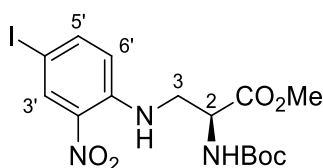
To a solution of methyl (2*S*)-2-[(*tert*-butoxycarbonyl)amino]-3-aminopropanoate (**121**) (1.50 g, 6.99 mmol) in acetonitrile (50 mL) under argon was added 5-iodo-2-fluoronitrobenzene (5.60 g, 21.0 mmol) and triethylamine (2.92 mL, 21.0 mmol). The reaction mixture stirred under reflux for 18 h. After cooling the reaction to ambient temperature, the solvent was removed *in vacuo*. The resulting residue was dissolved in ethyl acetate (50 mL), washed with water (3 × 50 mL) and brine (50 mL). The organic layer was dried (MgSO₄), filtered and concentrated *in vacuo*. Purification by flash column chromatography, eluting with 0–10% ethyl acetate in

dichloromethane gave methyl (2*S*)-2-[(*tert*-butoxycarbonyl)amino]-3-[(2'-nitro-4'-iodophenyl)amino]propanoate (**122**) as a yellow solid (2.54 g, 78%). Mp 103–105 °C; ν_{max}/cm^{-1} (neat) 3363 (NH), 2978 (CH), 1744 (C=O), 1709 (C=O), 1611, 1500, 1159 cm^{-1}; [α]$_D^{21}$ +51.5 (*c* 1.0, CHCl$_3$); δ$_H$ (400 MHz, CDCl$_3$) 1.45 (9H, s, 3 × CH$_3$), 3.68 (1H, dt, *J* 13.2, 5.6 Hz, 3-*H*H), 3.72–3.79 (1H, m, 3-H*H*), 3.80 (3H, s, OCH$_3$), 4.54–4.62 (1H, m, 2-H), 5.37 (1H, d, *J* 6.3 Hz, NH), 6.80 (1H, d, *J* 9.0 Hz, 6'-H), 7.66 (1H, dd, *J* 9.0, 2.1 Hz, 5'-H), 8.22 (1H, t, *J* 5.6 Hz, NH), 8.46 (1H, d, *J* 2.1 Hz, 3'-H); δ$_C$ (101 MHz, CDCl$_3$) 28.3 (3 × CH$_3$), 44.8 (CH$_2$), 53.0 (CH$_3$), 53.0 (CH), 75.3 (C), 80.7 (C), 115.9 (CH), 133.5 (C), 134.9 (CH), 144.3 (CH), 144.4 (C), 155.2 (C), 170.7 (C); *m/z* (ESI) 488.0290 (MNa$^+$. C$_{15}$H$_{20}$IN$_3$NaO$_6$ requires 488.0289).

Methyl (2*S*)-2-[(*tert*-butoxycarbonyl)amino]-3-[(4'-iodo-2'-aminophenyl)amino]propanoate (123)
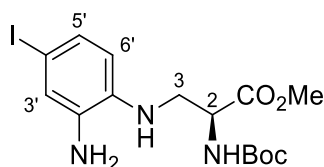
To a solution of methyl (2*S*)-2-[(*tert*-butoxycarbonyl)amino]-3-[(2'-nitro-4'-iodophenyl)amino]propanoate (**122**) (1.80 g, 3.87 mmol) in methanol (40 mL) was added zinc (1.26 g, 19.3 mmol) and acetic acid (1.20 mL, 19.3 mmol). The reaction mixture was stirred for 0.75 h at room temperature, then filtered through Celite® and concentrated *in vacuo*. Purification by flash column chromatography, eluting with 10% ethyl acetate in dichloromethane gave methyl (2*S*)-2-[(*tert*-butoxycarbonyl)amino]-3-[(4'-iodo-2'-aminophenyl)amino]propanoate (**123**) as a brown solid (1.53 g, 91%). Mp 176–180 °C; ν_{max}/cm^{-1} (neat) 3396 (NH), 2987 (CH), 2901, 1795 (C=O), 1697 (C=O), 1503, 1250, 1066; [α]$_D^{18}$ +24.7 (*c* 0.1, CHCl$_3$); δ$_H$ (400 MHz, CDCl$_3$) 1.44 (9H, s, 3 × CH$_3$), 3.31–3.44 (3H, m, 3-*H*H and NH$_2$), 3.52 (1H, dd, *J* 12.5, 4.4 Hz, 3-H*H*), 3.76 (3H, s, OCH$_3$), 4.53–4.62 (1H, m, 2-H), 5.41 (1H, d, *J* 6.7 Hz, NH), 6.40 (1H, d, *J* 8.3 Hz, 6'-H), 6.99 (1H, d, *J* 2.0 Hz, 3'-H), 7.06 (1H, dd, *J* 8.3, 2.0 Hz, 5'-H); δ$_C$ (101 MHz, CDCl$_3$) 28.3 (3 × CH$_3$), 46.5 (CH$_2$), 52.7 (CH$_3$), 53.6 (CH), 80.5 (C), 80.9 (C), 114.1 (CH), 124.7 (CH), 129.1 (CH), 136.5 (C), 136.6 (C), 155.6 (C), 171.6 (C); *m/z* (ESI) 458.0545 (MNa$^+$. C$_{15}$H$_{22}$IN$_3$NaO$_4$ requires 458.0547).

Methyl (2*S*)-2-[(*tert*-butoxycarbonyl)amino]-3-(5'-iodo-1*H*-benzo[*d*][1.2.3]triazol-1'-yl)propanoate (125)

To a solution of methyl (2*S*)-2-[(*tert*-butoxycarbonyl)amino]-3-[(4'-iodo-2'-aminophenyl)amino]propanoate (**123**) (0.700 g, 1.61 mmol) in ethyl acetate (35 mL) at −10 °C was added *p*-toluenesulfonic acid (0.917 g, 4.82 mmol) and polymer-supported nitrite (1.37 g, containing 4.82 mmol of NO_2^-). The reaction mixture was stirred for 1 h, filtered and the resin washed with ethyl acetate (50 mL). The organic layer was washed with a saturated solution of aqueous sodium hydrogen carbonate (50 mL) and brine (50 mL), dried (MgSO$_4$), filtered and concentrated *in vacuo*. Purification by flash column chromatography eluting with 0−5% ethyl acetate in dichloromethane gave methyl (2*S*)-2-[(*tert*-butoxycarbonyl)amino]-3-(5'-iodo-1*H*-benzo[*d*][1.2.3]triazol-1'-yl)propanoate (**125**) as a grey solid (0.505 g, 70%). Mp 113–116 °C; ν_{max}/cm^{-1} (neat) 3676 (NH), 2972 (CH), 2901, 1701 (C=O), 1406, 1250, 1066; $[\alpha]_D^{19}$ +21.9 (*c* 0.1, CHCl$_3$); δ_H (400 MHz, CDCl$_3$) 1.42 (9H, s, 3 × CH$_3$), 3.78 (3H, s, OCH$_3$), 4.77 (1H, dt, *J* 6.0, 4.4 Hz, 2-H), 5.09 (2H, d, *J* 4.4 Hz, 3-H$_2$), 5.31 (1H, d, *J* 6.0 Hz, NH), 7.32 (1H, br d, *J* 8.7 Hz, 7'-H), 7.73 (1H, dd, *J* 8.7, 1.3 Hz, 6'-H), 8.43 (1H, dd, *J* 1.3, 0.6 Hz, 4'-H); δ_C (101 MHz, CDCl$_3$) 28.2 (3 × CH$_3$), 48.8 (CH$_2$), 53.2 (CH$_3$), 53.9 (CH), 80.8 (C), 87.6 (C), 111.0 (CH), 129.1 (CH), 133.3 (C), 136.2 (CH), 147.5 (C), 155.0 (C), 169.5 (C); *m/z* (ESI) 469.0359 (MNa$^+$. C$_{15}$H$_{19}$IN$_4$NaO$_4$ requires 469.0343).

Methyl (2*S*)-2-[(*tert*-butoxycarbonyl)amino]-3-[5'-(phenylethynyl)-1*H*-benzo[*d*][1.2.3]triazol-1'-yl]propanoate (126a)
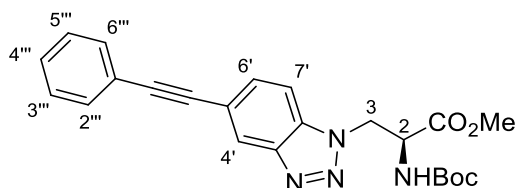
To a solution of methyl (2*S*)-2-[(*tert*-butoxycarbonyl)amino]-3-(5'-iodo-1*H*-benzo[*d*][1.2.3]triazol-1'-yl)propanoate (**125**) (0.050 g, 0.11 mmol) in *N,N'*-dimethylformamide (3 mL) was added copper iodide (0.0042 g, 0.022 mmol) and bis(triphenylphosphine)palladium(II) dichloride (0.0077 g, 0.011 mmol). Phenylacetylene (0.015 mL, 0.14 mmol) was dissolved in degassed triethylamine (7 mL) and added to the reaction mixture. The solution was heated to 100 °C for 0.1 h and stirred at room temperature for 2 h. The solution was concentrated *in vacuo*, dissolved in ethyl acetate (20 mL), washed with water (5 × 10 mL) and brine (2 × 10 mL), dried (MgSO₄) and concentrated *in vacuo*. Purification by flash column chromatography eluting with 0−5% ethyl acetate in dichloromethane gave met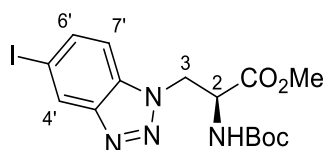hyl (2*S*)-2-[(*tert*-butoxycarbonyl)amino]-3-[5'-(phenylethynyl)-1*H*-benzo[*d*][1.2.3]triazol-1'-yl]propanoate (**126a**) as a yellow oil (0.039 g, 85%). v_{max}/cm⁻¹ (neat) 3357 (NH), 2978 (CH), 2360 (C≡C), 1745 (C=O), 1708 (C=O), 1498, 1162, 755; $[\alpha]_D^{19}$ +21.1 (*c* 0.1, CHCl₃); δ_H (400 MHz, CDCl₃) 1.43 (9H, s, 3 × CH₃), 3.78 (3H, s, OCH₃), 4.79 (1H, dt, *J* 6.6, 4.5 Hz, 2-H), 5.12 (2H, d, *J* 4.5 Hz, 3-H₂), 5.39 (1H, d, *J* 6.6 Hz, NH), 7.34–7.39 (3H, m, 3'''-H, 4'''-H and 5'''-H), 7.50 (1H, d, *J* 8.6 Hz, 7'-H), 7.57 (2H, dd, *J* 6.5, 3.2 Hz, 6'''-H and 2'''-H), 7.63 (1H, dd, *J* 8.6, 0.6 Hz, 6'-H), 8.43 (1H, br s, 4'-H); δ_C (101 MHz, CDCl₃) 28.2 (3 × CH₃), 48.7 (CH₂), 53.2 (CH₃), 53.9 (CH), 80.7 (C), 88.7 (C), 89.5 (C), 109.5 (CH), 119.4 (C), 122.9 (C), 123.3 (CH), 128.4 (2 × CH), 128.5 (CH), 131.2 (CH), 131.7 (2 × CH), 133.5 (C), 145.6 (C), 155.0 (C), 169.5 (C); *m/z* (ESI) 443.1687 (MNa⁺. C₂₃H₂₄N₄NaO₄ requires 443.1690).

Methyl (2S)-2-[(*tert*-butoxycarbonyl)amino]-3-{5'-[(4'''-methoxyphenyl)ethynyl]-1*H*-benzo[*d*][1.2.3]triazol-1'-yl}propanoate (126b)
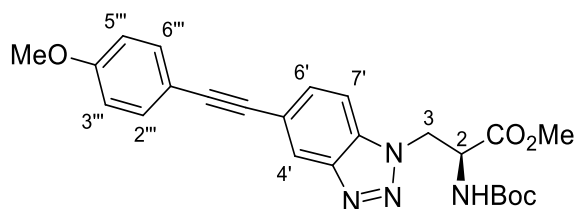
Methyl (2S)-2-[(*tert*-butoxycarbonyl)amino]-3-{5'-[(4'''-methoxyphenyl)ethynyl]-1*H*-benzo[*d*][1.2.3]triazol-1'-yl}propanoate (**126b**) was synthesised as described for methyl (2S)-2-[(*tert*-butoxycarbonyl)amino]-3-[5'-(phenylethynyl)-1*H*-benzo[*d*][1.2.3]triazol-1'-yl]propanoate (**126a**) using methyl (2S)-2-[(*tert*-butoxycarbonyl)amino]-3-(5'-iodo-1*H*-benzo[*d*][1.2.3]triazol-1'-yl)propanoate (**125**) (0.100 g, 0.220 mmol), *N,N'*-dimethylformamide (7 mL), copper iodide (0.00840 g, 0.0440 mmol), bis(triphenylphosphine)palladium(II) dichloride (0.0154 g, 0.0220 mmol), 4-methoxyphenylacetylene (0.0400 g, 0.280 mmol) and triethylamine (14 mL). Purification by flash column chromatography eluting with 5% ethyl acetate in dichloromethane gave methyl (2S)-2-[(*tert*-butoxycarbonyl)amino]-3-{5'-[(4'''-methoxyphenyl)ethynyl]-1*H*-benzo[*d*][1.2.3]triazol-1'-yl}propanoate (**126b**) as a yellow solid (0.0970 g, 97%). Mp 155–158 °C; ν_{max}/cm^{-1} (neat) 3369 (NH), 2976 (CH), 2357 (C≡C), 1748 (C=O), 1714 (C=O), 1514, 1250, 1170, 833; $[\alpha]_D^{18}$ +17.3 (*c* 0.1, CHCl$_3$); δ_H (400 MHz, CDCl$_3$) 1.43 (9H, s, 3 × CH$_3$), 3.78 (3H, s, OCH$_3$), 3.84 (3H, s, OCH$_3$), 4.79 (1H, dt, *J* 6.5, 4.3 Hz, 2-H), 5.11 (2H, d, *J* 4.3 Hz, 3-H$_2$), 5.32 (1H, d, *J* 6.5 Hz, NH), 6.90 (2H, d, *J* 8.8 Hz, 3'''-H and 5'''-H), 7.47–7.53 (2H, m, 7'-H, 2'''-H and 6'''-H), 7.61 (1H, dd, *J* 8.6, 0.8 Hz, 6'-H), 8.19 (1H, br s, 4'-H); δ_C (101 MHz, CDCl$_3$) 28.3 (3 × CH$_3$), 48.7 (CH$_2$), 53.2 (CH$_3$), 53.9 (CH), 55.3 (CH$_3$), 80.7 (C), 87.4 (C), 89.6 (C), 109.4 (CH), 114.1 (2 × CH), 115.0 (C), 119.8 (C), 123.0 (CH), 131.2 (CH), 133.1 (2 × CH), 133.4 (C), 145.7 (C), 155.0 (C), 159.8 (C), 169.6 (C); *m/z* (ESI) 473.1792 (MNa$^+$. C$_{24}$H$_{26}$N$_4$NaO$_5$ requires 473.1795).

Methyl (2S)-2-[(*tert*-butoxycarbonyl)amino]-3-{5'-[(4'''-dimethylaminophenyl)ethynyl]-1*H*-benzo[*d*][1.2.3]triazol-1'-yl}propanoate (126c)

Methyl (2S)-2-[(*tert*-butoxycarbonyl)amino]-3-{5'-[(4'''-dimethylaminophenyl)ethynyl]-1*H*-benzo[*d*][1.2.3]triazol-1'-yl}propanoate (**126c**) was synthesised as described for methyl (2S)-2-[(*tert*-butoxycarbonyl)amino]-3-[5'-(p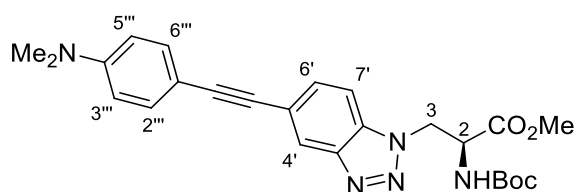henylethynyl)-1*H*-benzo[*d*][1.2.3]triazol-1'-yl]propanoate (**126a**) using methyl (2S)-2-[(*tert*-butoxycarbonyl)amino]-3-(5'-iodo-1*H*-benzo[*d*][1.2.3]triazol-1'-yl)propanoate (**125**) (0.400 g, 0.900 mmol), *N,N'*-dimethylformamide (18 mL), copper iodide (0.0340 g, 0.180 mmol), bis(triphenylphosphine)palladium(II) dichloride (0.0630 g, 0.0900 mmol), 4-dimethylaminophenylacetylene (0.170 g, 1.17 mmol) and triethylamine (42 mL). Purification by flash column chromatography, eluting with 80% diethyl ether in hexane gave methyl (2S)-2-[(*tert*-butoxycarbonyl)amino]-3-{5'-[(4'''-dimethylaminophenyl)ethynyl]-1*H*-benzo[*d*][1.2.3]triazol-1'-yl}propanoate (**126c**) as a yellow oil (0.346 g, 83%). ν_{max}/cm^{-1} (neat) 3318 (NH), 2926 (CH), 2359 (C≡C), 1746 (C=O), 1708 (C=O), 1605, 1510, 1364, 835, 1164, 757; $[\alpha]_D^{17}$ +12.9 (*c* 0.2, CHCl$_3$); δ_H (400 MHz, CDCl$_3$) 1.43 (9H, s, 3 × CH$_3$), 3.00 (6H, s, N(CH$_3$)$_2$), 3.77 (3H, s, OCH$_3$), 4.79 (1H, dt, *J* 6.8, 4.3 Hz, 2-H), 5.10 (2H, d, *J* 4.3 Hz, 3-H$_2$), 5.33 (1H, d, *J* 6.8 Hz, NH), 6.90 (2H, d, *J* 8.8 Hz, 3'''-H and 5'''-H), 7.47–7.53 (3H, m, 7'-H, 2'''-H and 6'''-H), 7.60 (1H, dd, *J* 8.6, 1.1 Hz, 6'-H), 8.17 (1H, br s, 4'-H); δ_C (101 MHz, CDCl$_3$) 28.3 (3 × CH$_3$), 40.2 (2 × CH$_3$), 48.7 (CH$_2$), 53.1 (CH$_3$), 53.9 (CH), 80.7 (C), 86.7 (C), 90.9 (C), 109.3 (CH), 109.6 (C), 111.9 (2 × CH), 120.4 (C), 122.5 (CH), 131.3 (CH), 132.8 (2 × CH), 133.1 (C), 145.8 (C), 150.3 (C), 155.0 (C), 169.6 (C); *m/z* (ESI) 486.2114 (MNa$^+$. C$_{25}$H$_{29}$N$_5$NaO$_4$ requires 486.2112).

Methyl (2*S*)-2-[(*tert*-butoxycarbonyl)amino]-3-{5'-[(4'''-fluorophenyl)ethynyl]-1*H*-benzo[*d*][1.2.3]triazol-1'-yl}propanoate (126d)

Methyl (2*S*)-2-[(*tert*-butoxycarbonyl)amino]-3-{5'-[(4'''-fluorophenyl)ethynyl]-1*H*-benzo[*d*][1.2.3]triazol-1'-yl}propanoate (**126d**) was synthesised as described for methyl (2*S*)-2-[(*tert*-butoxycarbonyl)amino]-3-[5'-(phenylethynyl)-1*H*-benzo[*d*][1.2.3]triazol-1'-yl]propanoate (**126a**) using methyl (2*S*)-2-[(*tert*-butoxycarbonyl)amino]-3-(5'-iodo-1*H*-benzo[*d*][1.2.3]triazol-1'-yl)propanoate (**125**) (0.100 g, 0.220 mmol), *N,N'*-dimethylformamide (6 mL), copper iodide (0.00840 g, 0.0440 mmol), bis(triphenylphosphine)palladium(II) dichloride (0.0154 g, 0.0220 mmol), 4-fluorophenylacetylene (0.0336 g, 0.280 mmol) and triethylamine (14 mL). Purification by flash column chromat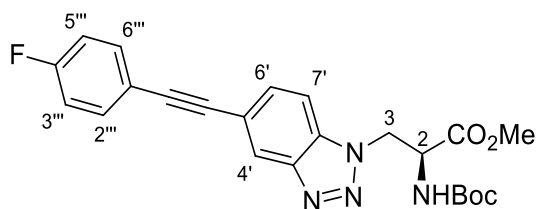ography, eluting with 0−5% ethyl acetate in dichloromethane gave methyl (2*S*)-2-[(*tert*-butoxycarbonyl)amino]-3-{5'-[(4'''-fluorophenyl)ethynyl]-1*H*-benzo[*d*][1.2.3]triazol-1'-yl}propanoate (**126d**) as an off-white solid (0.0770 g, 80%). Mp 145–147 °C; ν_{max}/cm^{-1} (neat) 3358 (NH), 2976 (CH), 2359 (C≡C), 1748 (C=O), 1708 (C=O), 1510, 1220, 1157, 835; $[\alpha]_D^{18}$ +21.4 (*c* 0.1, CHCl$_3$); δ_H (400 MHz, CDCl$_3$) 1.43 (9H, s, 3 × CH$_3$), 3.78 (3H, s, OCH$_3$), 4.79 (1H, dt, *J* 6.6, 4.4 Hz, 2-H), 5.12 (2H, d, *J* 4.4 Hz, 3-H$_2$), 5.33 (1H, d, *J* 6.6 Hz, NH), 7.07 (2H, t, *J* 8.7 Hz, 3'''-H and 5'''-H), 7.38–7.51 (3H, m, 7'-H, 2'''-H and 6'''-H), 7.61 (1H, dd, *J* 8.6, 1.1 Hz, 6'-H), 8.21 (1H, br s, 4'-H); δ_C (101 MHz, CDCl$_3$) 28.2 (3 × CH$_3$), 48.7 (CH$_2$), 53.2 (CH$_3$), 53.9 (CH), 80.8 (C), 88.4 (d, $^5J_{C-F}$ 1.2 Hz, C), 88.5 (C), 89.6 (C), 109.6 (CH), 115.8 (d, $^2J_{C-F}$ 22.1 Hz, 2 × CH), 119.1 (d, $^4J_{C-F}$ 3.6 Hz, C), 119.2 (C), 123.3 (CH), 131.1 (CH), 133.6 (d, $^3J_{C-F}$ 8.4 Hz, 2 × CH), 145.6 (C), 155.0 (C), 162.7 (d, $^1J_{C-F}$ 250.0 Hz, C), 169.5 (C); *m/z* (ESI) 461.1592 (MNa$^+$. C$_{23}$H$_{23}$FN$_4$NaO$_4$ requires 461.1596).

Methyl (2*S*)-2-[(*tert*-butoxycarbonyl)amino]-3-{5'-[(4'''-nitrophenyl)ethynyl]-1*H*-benzo[*d*][1.2.3]triazol-1'-yl}propanoate (126e)

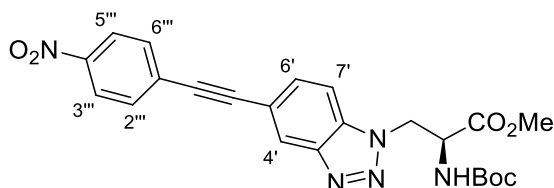
Methyl (2*S*)-2-[(*tert*-butoxycarbonyl)amino]-3-{5'-[(4'''-nitrophenyl)ethynyl]-1*H*-benzo[*d*][1.2.3]triazol-1'-yl}propanoate (**126e**) was synthesised as described for methyl (2*S*)-2-[(*tert*-butoxycarbonyl)amino]-3-[5'-(phenylethynyl)-1*H*-benzo[*d*][1.2.3]triazol-1'-yl]propanoate (**126a**) using methyl (2*S*)-2-[(*tert*-butoxycarbonyl)amino]-3-(5'-iodo-1*H*-benzo[*d*][1.2.3]triazol-1'-yl)propanoate (**125**) (0.200 g, 0.450 mmol), *N,N'*-dimethylformamide (9 mL), copper iodide (0.0171 g, 0.0900 mmol), bis(triphenylphosphine)palladium(II) dichloride (0.0314 g, 0.0448 mmol), 4-nitrophenylacetylene (0.0850 g, 0.580 mmol) and triethylamine (21 mL). Purification by flash column chromatography, eluting with 60% diethyl ether in hexane gave methyl (2*S*)-2-[(*tert*-butoxycarbonyl)amino]-3-{5'-[(4'''-nitrophenyl)ethynyl]-1*H*-benzo[*d*][1.2.3]triazol-1'-yl}propanoate (**126e**) as an orange solid (0.163 g, 78%). Mp 75–78 °C; v_{max}/cm^{-1} (neat) 3368 (NH), 2927 (CH), 2360 (C≡C), 1745 (C=O), 1709 (C=O), 1517, 1367, 1162, 784; $[\alpha]_D^{17}$ +3.8 (*c* 0.2, CHCl$_3$); δ_H (500 MHz, CDCl$_3$) 1.43 (9H, s, 3 × CH$_3$), 3.80 (3H, s, OCH$_3$), 4.80 (1H, dt, *J* 6.3, 4.4 Hz, 2-H), 5.14 (2H, d, *J* 4.4 Hz, 3-H$_2$), 5.34 (1H, d, *J* 6.3 Hz, NH), 7.56 (1H, d, *J* 8.6 Hz, 7'-H), 7.65 (1H, dd, *J* 8.6, 0.6 Hz, 6'-H), 7.71 (2H, d, *J* 8.8 Hz, 2'''-H and 6'''-H), 8.25 (1H, d, *J* 8.8 Hz, 3'''-H and 5'''-H), 8.27 (1H, br s, 4'-H); δ_C (101 MHz, CDCl$_3$) 28.2 (3 × CH$_3$), 48.8 (CH$_2$), 53.2 (CH$_3$), 53.9 (CH), 80.8 (C), 87.7 (C), 93.9 (C), 109.9 (CH), 118.2 (C), 123.7 (2 × CH), 124.0 (CH), 129.9 (C), 131.0 (CH), 132.3 (2 × CH), 134.0 (C), 145.5 (C), 147.2 (C), 155.0 (C), 169.5 (C); *m/z* (ESI) 488.1540 (MNa$^+$. C$_{23}$H$_{23}$N$_5$NaO$_6$ requires 488.1541).

Methyl (2*S*)-2-[(*tert*-butoxycarbonyl)amino]-3-{5'-[(4'''-cyanophenyl)ethynyl]-1*H*-benzo[*d*][1.2.3]triazol-1'-yl}propanoate (126g)
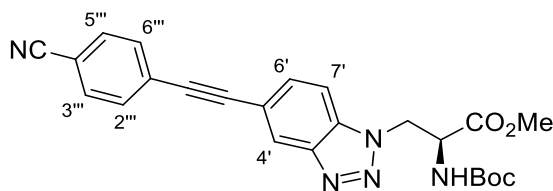

Methyl (2*S*)-2-[(*tert*-butoxycarbonyl)amino]-3-{5'-[(4'''-cyanophenyl)ethynyl]-1*H*-benzo[*d*][1.2.3]triazol-1'-yl}propanoate (**126g**) was synthesised as described for methyl (2*S*)-2-[(*tert*-butoxycarbonyl)amino]-3-[5'-(phenylethynyl)-1*H*-benzo[*d*][1.2.3]triazol-1'-yl]propanoate (**126a**) using methyl (2*S*)-2-[(*tert*-butoxycarbonyl)amino]-3-(5'-iodo-1*H*-benzo[*d*][1.2.3]triazol-1'-yl)propanoate (**125**) (0.150 g, 0.340 mmol), *N,N'*-dimethylformamide (9 mL), copper iodide (0.0130 g, 0.0680 mmol), bis(triphenylphosphine)palladium(II) dichloride (0.0239 g, 0.0340 mmol), 4-cyanophenylacetylene (0.0520 mL, 0.442 mmol) and triethylamine (21 mL). Purification by flash column chromatography, eluting with 5% ethyl acetate in dichloromethane gave methyl (2*S*)-2-[(*tert*-butoxycarbonyl)amino]-3-{5'-[(4'''-cyanophenyl)ethynyl]-1*H*-benzo[*d*][1.2.3]triazol-1'-yl}propanoate (**126g**) as a yellow solid (0.125 g, 83%). Mp 110–115 °C; ν_{max}/cm^{-1} (neat) 3361 (NH), 2983 (CH), 2230 (C≡C), 1747 (C=O), 1690 (C=O), 1519, 1252, 1108, 837; $[\alpha]_D^{22}$ +6.1 (*c* 0.1, CHCl$_3$); δ_H (500 MHz, CDCl$_3$) 1.43 (9H, s, 3 × CH$_3$), 3.79 (3H, s, OCH$_3$), 4.79 (1H, dt, *J* 6.4, 4.5 Hz, 2-H), 5.13 (2H, d, *J* 4.5 Hz, 3-H$_2$), 5.33 (1H, d, *J* 6.4 Hz, NH), 7.54 (1H, d, *J* 8.6 Hz, 7'-H), 7.65 (5H, m, 6'-H, 2'''-H, 3'''-H, 5'''-H and 6'''-H), 8.25 (1H, s, 4'-H); δ_C (126 MHz, CDCl$_3$) 28.4 (3 × CH$_3$), 48.9 (CH$_2$), 53.4 (CH$_3$), 54.0 (CH), 80.9 (C), 88.0 (C), 93.2 (C), 109.9 (CH), 111.9 (C), 118.4 (C), 118.6 (C), 124.1 (CH), 128.0 (C), 131.2 (CH), 132.3 (4 × CH), 134.1 (C), 145.6 (C), 155.1 (C), 169.6 (C); *m/z* (ESI) 446.1832 (MH$^+$. C$_{24}$H$_{24}$N$_5$O$_4$ requires 446.1823).

Methyl (2*S*)-2-[(*tert*-butoxycarbonyl)amino]-3-{5'-[(napthalen-2'''-yl)ethynyl]-1*H*-benzo[*d*][1.2.3]triazol-1'-yl}propanoate (126i)

Methyl (2*S*)-2-[(*tert*-butoxycarbonyl)amino]-3-{5'-[(napthalen-2'''-yl)ethynyl]-1*H*-benzo[*d*][1.2.3]triazol-1'-yl}propanoate (**126i**) was synthesised as described for methyl (2*S*)-2-[(*tert*-butoxycarbonyl)amino]-3-[5'-(phenylethynyl)-1*H*-benzo[*d*][1.2.3]triazol-1'-yl]propanoate (**126a**) using methyl (2*S*)-2-[(*tert*-butoxycarbonyl)amino]-3-(5'-iodo-1*H*-benzo[*d*][1.2.3]triazol-1'-yl)propanoate (**125**) (0.150 g, 0.340 mmol), *N,N'*-dimethylformamide (9 mL), copper iodide (0.0128 g, 0.0670 mmol), bis(triphenylphosphine)palladium(II) dichloride (0.0239 g, 0.0340 mmol), 2-ethynylnapthalene (0.0670 g, 0.440 mmol) and triethylamine (21 mL). The reaction mixture was stirred at room temperature for 4 h. Purification by flash column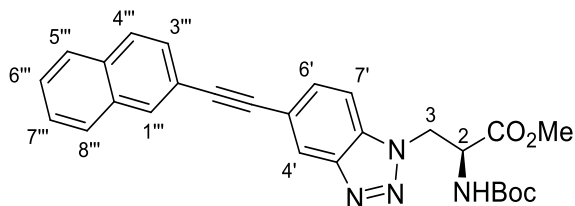 chromatography, eluting with 40% ethyl acetate in hexane gave methyl (2*S*)-2-[(*tert*-butoxycarbonyl)amino]-3-{5'-[(napthalen-2'''-yl)ethynyl]-1*H*-benzo[*d*][1.2.3]triazol-1'-yl}propanoate (**126i**) as a yellow solid (0.112 g, 70%). Mp 180–182 °C; ν_{max}/cm^{-1} (neat) 2979 (NH), 2360 (C≡C), 1746 (C=O), 1708 (C=O), 1502, 1163, 752; $[\alpha]_D^{21}$ +5.5 (*c* 0.2, CHCl₃); δ_H (500 MHz, CDCl₃) 1.44 (9H, s, 3 × CH₃), 3.78 (3H, s, OCH₃), 4.79 (1H, dt, *J* 6.5, 4.5 Hz, 2-H), 5.11 (2H, d, *J* 4.5 Hz, 3-H₂), 5.45 (1H, d, *J* 6.5 Hz, NH), 7.47–7.53 (3H, m, 6'-H, 6'''-H and 7'''-H), 7.60 (1H, dd, *J* 8.5, 1.5 Hz, 3'''-H), 7.67 (1H, dd, *J* 8.5, 0.8 Hz, 7'-H), 7.79–7.84 (3H, m, 4'''-H, 5'''-H and 8'''-H), 8.08 (1H, br s, 1'''-H), 8.24 (1H, br s, 4'-H); δ_C (126 MHz, CDCl₃) 28.4 (3 × CH₃), 48.7 (CH₂), 53.3 (CH₃), 54.0 (CH), 80.8 (C), 89.1 (C), 90.1 (C), 109.6 (CH), 119.5 (C), 120.3 (C), 123.4 (CH), 126.7 (CH), 126.9 (CH), 127.9 (3 × CH), 128.2 (CH), 128.4 (CH), 131.7 (CH), 133.0 (C), 133.1 (C), 133.6 (C), 145.7 (C), 155.1 (C), 169.7 (C); *m/z* (ESI) 493.1844 (MNa⁺. C₂₇H₂₆N₄NaO₄ requires 483.1846).

1-(3',4'-Methylenedioxyphenyl)-2-trimethylsilylacetylene (129)[193]
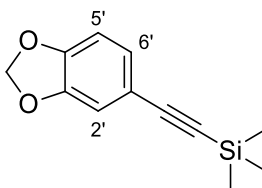
To bis(triphenylphosphine)palladium(II) dichloride (0.102 g, 0.145 mmol) and copper iodide (0.0550 g, 0.29 mmol) in *N,N'*-dimethylformamide (0.6 mL) was added 4-bromo-1,2-(methylenedioxy)benzene (0.350 mL, 2.90 mmol) and triethylamine (17 mL). The solution was degassed and trimethylsilylacetylene (0.600 mL, 4.35 mmol) was added. The reaction mixture was stirred at 90 °C and after 6 h, further bis(triphenylphosphine)palladium(II) dichloride (0.102 g, 0.145 mmol) and copper iodide (0.0550 g, 0.29 mmol) were added. The reaction mixture was stirred at 90 °C for a further 18 h. Upon cooling, the reaction mixture was concentrated *in vacuo*. Purification by flash column chromatography, eluting with 0–2% ethyl acetate in hexane gave 1-(3',4'-methylenedioxyphenyl)-2-trimethylsilylacetylene (**129**) (0.569 g, 90%) as a yellow oil. Spectroscopic data were consistent with the literature.[193] δ_H (500 MHz, CDCl$_3$) 0.23 (9H, s, 3 × CH$_3$), 5.96 (2H, s, OCH$_2$O), 6.73 (1H, d, *J* 8.0 Hz, 5'-H), 6.91 (1H, d, *J* 1.5 Hz, 2'-H), 7.00 (1H, dd, *J* 8.0, 1.5 Hz, 6'-H); δ_C (126 MHz, CDCl$_3$) 0.2 (3 × CH$_3$), 92.4 (C), 101.4 (CH$_2$), 105.1 (C), 108.5 (CH), 112.0 (CH), 116.5 (C), 126.9 (CH), 147.4 (C), 148.2 (C); *m/z* (EI) 218 (M$^+$. 80%), 203 (100).

3,4-Methylenedioxyphenylethyne (130)[194]
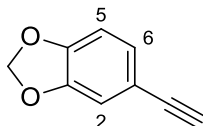
To 1-(3',4'-methylenedioxyphenyl)-2-trimethylsilylacetylene (**129**) (0.695 g, 3.18 mmol) in methanol (20 mL) was added potassium carbonate (1.30 g, 9.55 mmol). The reaction was stirred at room temperature for 1 h, and then concentrated *in vacuo*. The resulting residue was diluted with ethyl acetate (40 mL), washed with water (3 × 30 mL) and brine (30 mL), dried (MgSO$_4$), filtered, and concentrated *in vacuo*. Purification by column chromatography, eluting with 2% ethyl acetate in

hexane gave 3,4-methylenedioxyphenylethyne (**130**) as a yellow oil (0.320 g, 69%). Spectroscopic data were consistent with the literature.[194] δ_H (500 MHz, CDCl$_3$) 2.98 (1H, s, C≡CH), 5.97 (2H, s, OCH$_2$O), 6.75 (1H, d, *J* 8.0 Hz, 5-H), 6.93 (1H, d, *J* 1.5 Hz, 2-H), 7.02 (1H, dd, *J* 8.0, 1.5 Hz, 6-H); δ_C (126 MHz, CDCl$_3$) 75.6 (CH), 83.7 (C), 101.4 (CH$_2$), 108.4 (CH), 112.0 (CH), 115.3 (C), 126.9 (CH), 147.4 (C), 148.3 (C); *m/z* (EI) 146 (M$^+$. 100%).

Methyl (2*S*)-2-[(*tert*-butoxycarbonyl)amino]-3-{5'-[(3''',4'''-methylenedioxyphenyl)ethynyl]-1*H*-benzo[*d*][1.2.3]triazol-1'-yl}propanoate (126h)
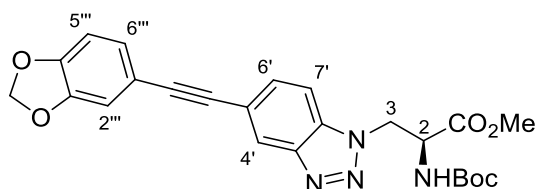
Methyl (2*S*)-2-[(*tert*-butoxycarbonyl)amino]-3-{5'-[(3''',4'''-methylenedioxyphenyl)ethynyl]-1*H*-benzo[*d*][1.2.3]triazol-1'-yl}propanoate (**126h**) was synthesised as described for methyl (2*S*)-2-[(*tert*-butoxycarbonyl)amino]-3-[5'-(phenylethynyl)-1*H*-benzo[*d*][1.2.3]triazol-1'-yl]propanoate (**126a**) using methyl (2*S*)-2-[(*tert*-butoxycarbonyl)amino]-3-(5'-iodo-1*H*-benzo[*d*][1.2.3]triazol-1'-yl)propanoate (**125**) (0.150 g, 0.340 mmol), *N,N'*-dimethylformamide (9 mL), copper iodide (0.0128 g, 0.0670 mmol), bis(triphenylphosphine)palladium(II) dichloride (0.0239 g, 0.0340 mmol), 3,4-methylenedioxyphenylethyne (**130**) (0.0640 g, 0.440 mmol) and triethylamine (21 mL). Purification by flash column chromatography, eluting with 80% diethyl ether in hexane gave methyl (2*S*)-2-[(*tert*-butoxycarbonyl)amino]-3-{5'-[(3,4-methylenedioxyphenyl)ethynyl]-1*H*-benzo[*d*][1.2.3]triazol-1'-yl}propanoate (**126h**) as a yellow solid (0.146 g, 92%). Mp 77–80 °C; ν_{max}/cm^{-1} (neat) 3383 (NH), 2977 (CH), 2360 (C≡C), 1746 (C=O), 1706 (C=O), 1502, 1227, 1036, 733; $[\alpha]_D^{21}$ +10.2 (*c* 0.2, CHCl$_3$); δ_H (500 MHz, CDCl$_3$) 1.43 (9H, s, 3 × CH$_3$), 3.78 (3H, s, OCH$_3$), 4.79 (1H, dt, *J* 6.6, 4.4 Hz, 2-H), 5.11 (2H, d, *J* 4.4 Hz, 3-H$_2$), 5.33 (1H, d, *J* 6.6 Hz, NH), 6.00 (2H, s, OCH$_2$O), 6.81 (1H, d, *J* 8.0 Hz, 5'''-H), 7.01 (1H, d, *J* 1.5 Hz, 2'''-H), 7.10 (1H, dd, *J* 8.0, 1.5 Hz, 6'''-H), 7.49 (1H, d, *J* 8.6 Hz, 7'-H), 7.60 (1H, dd, *J* 8.6, 0.7 Hz, 6'-H), 8.18 (1H, br s, 4'-H); δ_C (126 MHz, CDCl$_3$) 28.2 (3 × CH$_3$), 48.7 (CH$_2$), 53.2 (CH$_3$), 53.9 (CH), 80.7 (C), 87.1

(C), 89.5 (C), 101.4 (CH_2), 108.6 (CH), 109.5 (CH), 111.6 (CH), 116.1 (C), 119.6 (C), 123.1 (CH), 126.4 (CH), 131.2 (CH), 133.4 (C), 145.6 (C), 147.5 (C), 148.1 (C), 155.0 (C), 169.5 (C); *m/z* (ESI) 487.1592 (MNa^+. $C_{24}H_{24}N_4NaO_6$ requires 487.1588).

1-(4-Bromophenyl)azetidine (131)
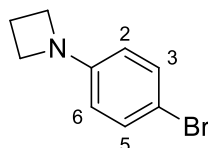
To tris(dibenzylideneacetone)dipalladium(0) (0.0160 g, 0.0175 mmol), (±)-2,2′-bis(diphenylphosphino)-1,1′-binaphthalene (0.0310 g, 0.050 mmol) and sodium *tert*-butoxide (0.200 g, 2.10 mmol) in tetrahydrofuran (12.5 mL) was added 1-bromo-4-iodobenzene (0.500 g, 1.75 mmol) and 1,4,7,10,13,16-hexaoxacyclooctadecane (0.610 g, 2.30 mmol). The solution was degassed and azetidine (0.150 mL, 2.10 mmol) was added. The reaction mixture was stirred at room temperature for 20 h, filtered through Celite® and concentrated *in vacuo*. The reaction mixture was diluted with water (50 mL), extracted with ethyl acetate (3 × 30 mL), dried ($MgSO_4$) and concentrated *in vacuo*. Purification by flash column chromatography, eluting with 0–5% ethyl acetate in hexane gave 1-(4-bromophenyl)azetidine (**131**) as a white solid (0.322 g, 87%). Mp 57–50 °C; ν_{max}/cm^{-1} (neat) 2848 (CH), 1589, 1346, 1122, 806; δ_H (500 MHz, $CDCl_3$) 2.36 (2H, pent, *J* 7.3 Hz, CH_2), 3.84 (4H, t, *J* 7.3 Hz, $N(CH_2)_2$), 6.31 (2H, d, *J* 8.7 Hz, 2-H and 6-H), 7.28 (2H, d, *J* 8.7 Hz, 3-H and 5-H); δ_C (126 MHz, $CDCl_3$) 16.9 (CH_2), 52.5 (2 × CH_2), 109.2 (C), 113.0 (2 × CH), 131.6 (2 × CH), 151.1 (C); *m/z* (ESI) 212.0068 (MH^+. $C_9H_{11}{}^{79}BrN$ requires 212.0069).

1-(4-Bromophenyl)-2-(trimethylsilyl)acetylene (133)[195]
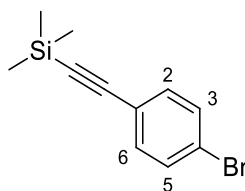
To a solution of 1-bromo-4-iodobenzene (0.500 g, 1.77 mmol) in *N,N'*-dimethylformamide (1 mL) was added copper iodide (0.0700 g, 0.350 mmol) and bis(triphenylphosphine)palladium(II) dichloride (0.120 g, 0.175 mmol). Trimethylsilylacetylene (0.350 mL, 2.63 mmol) was dissolved in degassed triethylamine (12.5 mL) and added to the reaction mixture. The solution was stirred at room temperature for 0.5 h, concentrated *in vacuo* and dissolved in ethyl acetate (40 mL). The organic layer was washed with water (5 × 20 mL) and brine (20 mL), dried (MgSO$_4$) and concentrated *in vacuo*. Purification by flash column chromatography, eluting with hexane gave 1-(4-bromophenyl)-2-(trimethylsilyl)acetylene (**133**) as a white solid (0.418 g, 95%). Mp 58–60 °C (lit.[195] 56–59 °C); δ$_H$ (500 MHz, CDCl$_3$) 0.25 (9H, s, 3 × CH$_3$), 7.32 (2H, d, *J* 8.3 Hz, 2-H and 6-H), 7.43 (2H, d, *J* 8.3 Hz, 3-H and 5-H); δ$_C$ (126 MHz, CDCl$_3$) 0.0 (3 × CH$_3$), 95.7 (C), 104.0 (C), 122.2 (C), 122.9 (C), 131.6 (2 × CH), 133.5 (2 × CH); *m/z* (EI) 254 (M$^+$. 60%), 252 (60), 237 (100).

1-(4-Azetidinephenyl)-2-(trimethylsilyl)acetylene (132)
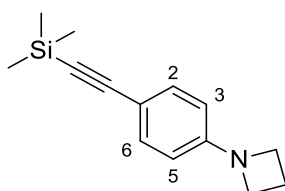
To bis(dibenzylideneacetone)palladium(0) (0.0730 g, 0.0800 mmol), (±)-2,2′-bis(diphenylphosphino)-1,1′-binaphthalene (0.100 g, 0.160 mmol) and sodium *tert*-butoxide (0.183 g, 1.90 mmol) was added 1-(4-bromophenyl)-2-(trimethylsilyl)acetylene (**133**) (0.400 g, 1.58 mmol) in toluene (8 mL). The solution was degassed, and azetidine (0.130 mL, 1.90 mmol) was added. The reaction mixture was stirred at 80 °C for 2 h, filtered through Celite® and concentrated *in*

vacuo. The resulting residue was dissolved in ethyl acetate (50 mL), washed with water (3 × 25 mL), dried (MgSO$_4$) and concentrated *in vacuo*. Purification by flash column chromatography, eluting with 5% ethyl acetate in hexane gave 1-(4-azetidinephenyl)-2-(trimethylsilyl)acetylene (**132**) (0.300 g, 83%) as a yellow solid. Mp 81–84 °C; ν_{max}/cm^{-1} (neat) 2955 (CH), 2855, 2140 (C≡C), 1607, 1515, 1246, 815; δ_H (400 MHz, CDCl$_3$) 0.23 (9H, s, 3 × CH$_3$), 2.37 (2H, pent, *J* 7.3 Hz, CH$_2$), 3.89 (4H, t, *J* 7.3 Hz, N(CH$_2$)$_2$), 6.31 (2H, d, *J* 8.7 Hz, 3-H and 5-H), 7.31 (2H, d, *J* 8.7 Hz, 2-H and 6-H); δ_C (126 MHz, CDCl$_3$) 0.0 (3 × CH$_3$), 16.8 (CH$_2$), 52.1 (2 × CH$_2$), 91.3 (C), 106.7 (C), 110.7 (2 × CH), 110.9 (C), 133.1 (2 × CH), 151.8 (C); *m/z* (ESI) 230.1366 (MH$^+$. C$_{13}$H$_{20}$NSi requires 230.1360).

4-Azetidine-phenylacetylene (134)[196]
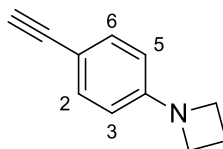
To 1-(4-azetidinephenyl)-2-(trimethylsilyl)acetylene (**132**) (0.300 g, 0.650 mmol) in methanol (6 mL) was added potassium carbonate (0.540 g, 1.96 mmol), and the reaction mixture stirred at room temperature for 1 h. Upon completion, the reaction mixture was concentrated *in vacuo*, dissolved in ethyl acetate (50 mL), washed with water (2 × 25 mL) and brine (25 mL), then dried (MgSO$_4$) and concentrated *in vacuo* to give 4-azetidine-phenylacetylene (**134**) (0.196 g, 98%) as a yellow solid. Spectroscopic data were consistent with the literature.[196] Mp 64–66 °C; δ_H (500 MHz, CDCl$_3$) 2.37 (2H, pent, *J* 7.3 Hz, CH$_2$), 2.96 (1H, s, C≡CH), 3.89 (4H, t, *J* 7.3 Hz, N(CH$_2$)$_2$), 6.33 (2H, d, *J* 8.7 Hz, 3-H and 5-H), 7.33 (2H, d, *J* 8.7 Hz, 2-H and 6-H); δ_C (126 MHz, CDCl$_3$) 16.7 (CH$_2$), 52.0 (2 × CH$_2$), 74.8 (C), 84.9 (CH), 109.6 (C), 110.7 (2 × CH), 133.1 (2 × CH), 151.9 (C); *m/z* (ESI) 158 (MH$^+$. 100%).

Methyl (2*S*)-2-[(*tert*-butoxycarbonyl)amino]-3-{5'-[(4'''-azetidine)ethynyl]-1*H*-benzo[*d*][1.2.3]triazol-1'-yl}propanoate (126f)
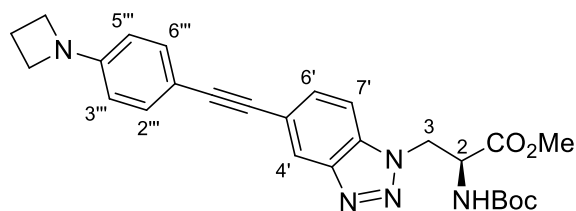
Methyl (2*S*)-2-[(*tert*-butoxycarbonyl)amino]-3-{5'-[(4'''-azetidine)ethynyl]-1*H*-benzo[*d*][1.2.3]triazol-1'-yl}propanoate (**126f**) was synthesised as described for methyl (2*S*)-2-[(*tert*-butoxycarbonyl)amino]-3-[5'-(phenylethynyl)-1*H*-benzo[*d*][1.2.3]triazol-1'-yl]propanoate (**126a**) using methyl (2*S*)-2-[(*tert*-butoxycarbonyl)amino]-3-(5'-iodo-1*H*-benzo[*d*][1.2.3]triazol-1'-yl)propanoate (**125**) (0.200 g, 0.450 mmol), *N,N'*-dimethylformamide (10 mL), copper iodide (0.0171 g, 0.0900 mmol), bis(triphenylphosphine)palladium(II) dichloride (0.0315 g, 0.0450 mmol), 4-azetidine-phenylacetylene (**134**) (0.102 g, 0.580 mmol) and degassed triethylamine (28 mL). Purification by flash column chromatography, eluting with 80% diethyl ether in hexane gave methyl (2*S*)-2-[(*tert*-butoxycarbonyl)amino]-3-{5'-[(4'''-azetidine)ethynyl]-1*H*-benzo[*d*][1.2.3]triazol-1'-yl}propanoate (**126f**) as a yellow solid (0.190 g, 89%). Mp 154–158 °C; v_{max}/cm^{-1} (neat) 3369 (NH), 2970 (CH), 2207 (C≡C), 1762 (C=O), 1687, 1521, 1347, 866; [α]$_D^{20}$ +12.5 (*c* 0.5, CHCl$_3$); δ$_H$ (400 MHz, CDCl$_3$) 1.42 (9H, s, 3 × CH$_3$), 2.37 (2H, pent, *J* 7.2 Hz, CH$_2$), 3.76 (3H, s, OCH$_3$), 3.91 (4H, t, *J* 7.2 Hz, N(CH$_2$)$_2$), 4.78 (1H, dt, *J* 6.6, 4.3 Hz, 2-H), 5.09 (2H, d, *J* 4.3 Hz, 3-H$_2$), 5.40 (1H, d, *J* 6.6 Hz, NH), 6.37 (2H, d, *J* 8.6 Hz, 3'''-H and 5'''-H), 7.40 (2H, d, *J* 8.6 Hz, 2'''-H and 6'''-H), 7.45 (1H, d, *J* 8.6 Hz, 7'-H), 7.58 (1H, d, *J* 8.6 Hz, 6'-H), 8.14 (1H, s, 4'-H); δ$_C$ (101 MHz, CDCl$_3$) 16.7 (CH$_2$), 28.2 (3 × CH$_3$), 48.6 (CH$_2$), 52.0 (2 × CH$_2$), 53.1 (CH$_3$), 53.9 (CH), 80.7 (C), 86.7 (C), 90.9 (C), 109.3 (CH), 110.4 (C), 110.8 (2 × CH), 120.3 (C), 122.5 (CH), 131.2 (CH), 132.6 (2 × CH), 133.1 (C), 145.7 (C), 151.7 (C), 155.0 (C), 169.6 (C); *m/z* (ESI) 476.2301 (MH$^+$. C$_{26}$H$_{30}$N$_5$O$_4$ requires 476.2292).

1-Iodo-4-methoxynapthalene (136)[197]
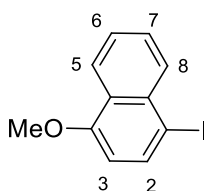
Iron(III) chloride (0.0050 g, 0.032 mmol) was dissolved in 1-butyl-3-methylimidazolium bis(trifluoromethanesulfonyl)imide (0.028 mL, 0.095 mmol), stirred for 0.5 h at room temperature and then added to a solution of *N*-iodosuccinimide (0.34 g, 1.5 mmol) in dichloromethane (2.0 mL). 1-methoxylnapthalene (0.20 g, 1.3 mmol) was then added, and the mixture was stirred at 40 °C for 3 h. Additional *N*-iodosuccinimide was added (0.085 g, 0.38 mmol) and the reaction mixture stirred for a further 1 h at 40 °C. Upon completion, the reaction mixture was diluted with dichloromethane (20 mL) and washed with 0.5 M sodium thiosulfate solution (3 × 10 mL), dried (MgSO$_4$) and concentrated *in vacuo*. Purification by flash column chromatography, eluting with 2% ethyl acetate in hexane gave 1-iodo-4-methoxynapthalene (**136**) (0.347, 97%) as a white solid. Mp 51–53 °C (lit.[197] 52–54 °C); δ$_H$ (400 MHz, CDCl$_3$) 3.99 (3H, s, OCH$_3$), 6.60 (1H, d, *J* 8.2 Hz, 3-H), 7.51 (1H, ddd, *J* 8.3, 6.9, 1.1 Hz, 7-H), 7.59 (1H, ddd, *J* 8.5, 6.9, 1.3 Hz, 6-H), 7.95 (1H, d, *J* 8.2, 2-H), 8.03 (1H, ddd, *J* 8.5, 1.1, 0.5 Hz, 5-H), 8.24 (1H, ddd, *J* 8.3, 1.3, 0.5 Hz, 8-H); δ$_C$ (101 MHz, CDCl$_3$) 55.7 (CH$_3$), 88.1 (C), 105.6 (CH), 122.5 (CH), 126.0 (CH), 126.6 (C), 128.1 (CH), 131.7 (CH), 134.7 (C), 136.9 (CH), 156.3 (C); *m/z* (EI) 284 (M$^+$, 100%), 269 (35), 241 (31), 114 (30).

1-(Trimethylsilylethynyl)-4-methoxynaphthalene (137)[198]
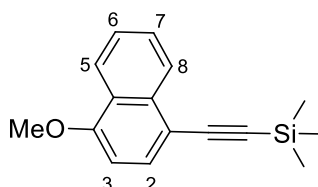
To 1-iodo-4-methoxynapthalene (**136**) (0.300 g, 1.06 mmol), in *N,N'*-dimethylformamide (0.4 mL) and triethylamine (10 mL) was added copper iodide (0.0400 g, 0.212 mmol), and bis(triphenylphosphine)palladium(II) dichloride (0.0740

g, 0.106 mmol). The reaction was degassed and trimethylsilylacetylene (0.220 mL, 1.60 mmol) was added. The reaction mixture was stirred at 25 °C for 4 h. Upon completion, the reaction mixture was diluted with ethyl acetate (50 mL), washed with water (4 × 25 mL), dried (MgSO$_4$) and concentrated *in vacuo* to give 1-methoxy-4-(trimethylsilylethynyl)napthalene (**137**) (0.215 g, 80%) as a yellow solid. Mp 64–68 °C (lit.[198] 68–71 °C); δ_H (500 MHz, CDCl$_3$) 0.35 (9H, s, 3 × CH$_3$), 4.00 (3H, s, OCH$_3$), 6.75 (1H, d, *J* 8.0 Hz, 3-H), 7.52 (1H, ddd, *J* 8.0, 6.7, 0.8 Hz, 6-H), 7.61 (1H, ddd, *J* 8.0, 6.7, 1.0 Hz, 7-H), 7.66 (1H, d, *J* 8.0, 2-H), 8.25–8.32 (2H, m, 5'-H and 8'-H); δ_C (126 MHz, CDCl$_3$) 0.4 (3 × CH$_3$), 55.7 (CH$_3$), 97.5 (C), 103.5 (CH), 103.7 (C), 113.1 (C), 122.4 (CH), 125.4 (C), 125.8 (CH), 126.1 (CH), 127.4 (CH), 131.7 (CH), 134.5 (C), 156.3 (C); *m/z* (ESI) 255 (MH$^+$. 100%).

1-Ethynyl-4-methoxynapthalene (138)[199]
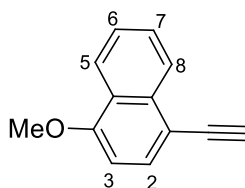
To 1-methoxy-4-(trimethylsilylethynyl)napthalene (**137**) (0.150 g, 0.590 mmol) in methanol (2.5 mL) was added potassium carbonate (0.245 g, 1.77 mmol), and the reaction mixture was stirred at room temperature for 1 h. Upon completion, the reaction mixture was concentrated *in vacuo*, dissolved in ethyl acetate (30 mL), washed with water (2 × 20 mL) and brine (20 mL), then dried (MgSO$_4$) and concentrated *in vacuo* to give 1-ethynyl-4-methoxynapthalene (**138**) (0.103 g, 90%) as a yellow oil. Spectroscopic data were consistent with the literature.[199] δ_H (400 MHz, CDCl$_3$) 3.38 (1H, s, C≡CH), 4.00 (3H, s, OCH$_3$), 6.76 (1H, d, *J* 8.0 Hz, 3-H), 7.51 (1H, ddd, *J* 8.3, 6.9, 1.3 Hz, 6-H), 7.59 (1H, ddd, *J* 8.3, 6.9, 1.4 Hz, 7-H), 7.67 (1H, d, *J* 8.0 Hz, 2-H), 8.29 (2H, m, 5-H and 8-H); δ_C (101 MHz, CDCl$_3$) 55.7 (CH$_3$), 80.3 (CH), 82.1 (C), 103.4 (CH), 111.8 (C), 122.3 (CH), 125.3 (C), 125.8 (CH), 125.9 (CH), 127.3 (CH), 131.9 (CH), 134.4 (C), 156.3 (C); *m/z* (ESI) 183.08 (MH$^+$. 100%).

Methyl (2*S*)-2-[(*tert*-butoxycarbonyl)amino]-3-{5'-[(4'''-methoxynapthyl)ethynyl]-1*H*-benzo[*d*][1.2.3]triazol-1'-yl}propanoate (126j)
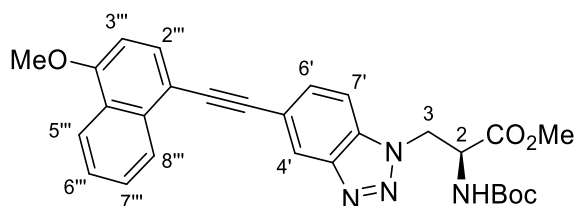

Methyl (2*S*)-2-[(*tert*-butoxycarbonyl)amino]-3-{5'-[(4'''-methoxynapthyl)ethynyl]-1*H*-benzo[*d*][1.2.3]triazol-1'-yl}propanoate (**126j**) was synthesised as described for methyl (2*S*)-2-[(*tert*-butoxycarbonyl)amino]-3-[5'-(phenylethynyl)-1*H*-benzo[*d*][1.2.3]triazol-1'-yl]propanoate (**126a**) using methyl (2*S*)-2-[(*tert*-butoxycarbonyl)amino]-3-(5'-iodo-1*H*-benzo[*d*][1.2.3]triazol-1'-yl)propanoate (**125**) (0.150 g, 0.336 mmol) in *N,N*'-dimethylformamide (6 mL), copper iodide (0.0128 g, 0.0672 mmol), bis(triphenylphosphine)palladium(II) dichloride (0.0236 g, 0.0336 mmol), 1-ethynyl-4-methoxynapthalene (**138**) (0.0800 g, 0.440 mmol) and degassed triethylamine (14 mL). Purification by flash column chromatography, eluting with 70% diethyl ether in hexane gave methyl (2*S*)-2-[(*tert*-butoxycarbonyl)amino]-3-{5'-[(4'''-methoxynapthyl)ethynyl]-1*H*-benzo[*d*][1.2.3]triazol-1'-yl}propanoate (**126j**) as a yellow solid (0.140 g, 83%). Mp 99–101 °C; ν_{max}/cm^{-1} (neat) 3350 (NH), 2974 (CH), 2160 (C≡C), 1743 (C=O), 1701 (C=O), 1581, 1238, 1088, 763; $[\alpha]_D^{19}$ +9.8 (*c* 0.1, CHCl$_3$); δ_H (400 MHz, CDCl$_3$) 1.44 (9H, s, 3 × CH$_3$), 3.79 (3H, s, OCH$_3$), 4.05 (3H, s, OCH$_3$), 4.81 (1H, dt, *J* 6.7, 4.2 Hz, 2-H), 5.13 (2H, d, *J* 4.2 Hz, 3-H$_2$), 5.36 (1H, d, *J* 6.7 Hz, NH), 6.83 (1H, d, *J* 8.1 Hz, 3'''-H), 7.49–7.58 (2H, m, 7'-H and 7'''-H), 7.64 (1H, ddd, *J* 8.3, 6.8, 1.3 Hz, 6'''-H), 7.69–7.76 (2H, m, 6'-H and 2'''-H), 8.26–8.34 (2H, m, 4'-H and 5'''-H), 8.40 (1H, d, *J* 8.1 Hz, 8'''-H); δ_C (101 MHz, CDCl$_3$) 28.3 (3 × CH$_3$), 48.7 (CH$_2$), 53.2 (CH$_3$), 53.9 (CH), 55.7 (CH$_3$), 80.8 (C), 88.1 (C), 92.0 (C), 103.7 (CH), 109.5 (CH), 112.6 (C), 120.0 (C), 122.4 (CH), 123.0 (CH), 125.4 (C), 125.8 (CH), 125.9 (CH), 127.4 (CH), 131.3 (2 × CH), 133.4 (C), 134.2 (C), 145.7 (C), 155.1 (C), 156.3 (C), 169.6 (C); *m/z* (ESI) 501.2138 (MH$^+$. C$_{28}$H$_{28}$N$_4$O$_5$ requires 501.2132).

(2S)-2-Amino-3-[5'-(phenylethynyl)-1H-benzo[d][1.2.3]triazol-1'-yl]propanoic acid hydrochloride (128a)
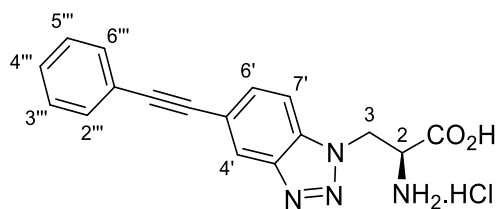
To a solution of methyl (2S)-2-[(*tert*-butoxycarbonyl)amino]-3-[5'-(phenylethynyl)-1H-benzo[d][1.2.3]triazol-1'-yl]propanoate (**126a**) (0.100 g, 0.240 mmol) in a mixture of methanol (6 mL) and 1,4-dioxane (6 mL) was added a solution of caesium carbonate (0.101 g, 0.310 mmol) in water (3 mL). The reaction mixture was stirred at room temperature for 20 h and then concentrated *in vacuo.* The resulting residue was dissolved in water (50 mL) and acidified to pH 1 with 2 M aqueous hydrochloric acid. The aqueous layer was extracted with dichloromethane (3 × 30 mL) and the combined organic layers were washed with water (30 mL), dried (MgSO₄) and concentrated *in vacuo* to give (2S)-2-[(*tert*-butoxycarbonyl)amino]-3-[5'-(phenylethynyl)-1H-benzo[d][1.2.3]triazol-1'-yl]propanoic acid (**127a**) as a yellow solid (0.0630 g, 65%). This was used for the next reaction without any further purification. To a solution of (2S)-2-[(*tert*-butoxycarbonyl)amino]-3-[5'-(phenylethynyl)-1H-benzo[d][1.2.3]triazol-1'-yl]propanoic acid (**127a**) (0.0500 g, 0.120 mmol) in acetonitrile (0.1 mL) was added 2 M aqueous hydrochloric acid (3 mL). The reaction mixture was stirred at room temperature for 6 h and then concentrated *in vacuo*. Trituration with chloroform gave (2S)-2-amino-3-[5'-(phenylethynyl)-1H-benzo[d][1.2.3]triazol-1'-yl]propanoic acid hydrochloride (**128a**) as an off-white solid (0.0340 g, 83%). Mp 245–247 °C (decomposition); ν_{max}/cm⁻¹ (neat) 2920 (OH), 2359 (C≡C), 1732 (C=O), 1472, 1338, 686; $[\alpha]_D^{18}$ +4.9 (*c* 0.1, MeOH); δ_H (400 MHz, CD₃OD) 4.77 (1H, dd, *J* 4.1, 5.8 Hz, 2-H), 5.27 (1H, dd, *J* 15.5, 4.1 Hz, 3-*H*H), 5.37 (1H, dd, *J* 15.5, 5.8 Hz, 3-H*H*), 7.35–7.45 (3H, m, 3'''-H, 4'''-H and 5'''-H), 7.51–7.61 (2H, m, 2'''-H and 6'''-H), 7.75 (1H, dd, *J* 8.7, 1.3 Hz, 6'-H), 7.85 (1H, dd, *J* 8.7, 0.6 Hz, 7'-H), 8.22 (1H, br s, 4'-H); δ_C (101 MHz, CD₃OD) 46.8 (CH₂), 52.2 (CH), 87.8 (C), 89.3 (C), 110.3 (CH), 120.0 (C), 122.0 (CH), 122.7 (C), 128.3 (2 × CH), 128.4 (CH), 131.2 (2 × CH), 131.3 (CH), 133.2 (C), 145.4 (C), 167.6 (C); *m/z* (ESI) 307.1191 (MH⁺. C₁₇H₁₅N₄O₂ requires 307.1190).

(2*S*)-2-Amino-3-{5'-[(4'''-methoxyphenyl)ethynyl]-1*H*-benzo[*d*][1.2.3]triazol-1'-yl}propanoic acid hydrochloride (128b)
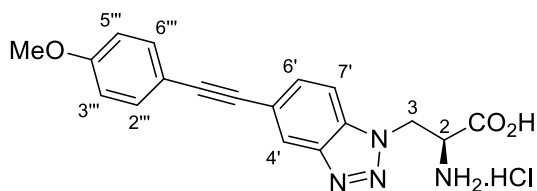

(2*S*)-2-[(*tert*-Butoxycarbonyl)amino]-3-{5'-[(4'''-methoxyphenyl)ethynyl]-1*H*-benzo[*d*][1.2.3]triazol-1'-yl}propanoic acid (**127b**) was prepared as described for (2*S*)-2-[(*tert*-butoxycarbonyl)amino]-3-[5'-(phenylethynyl)-1*H*-benzo[*d*][1.2.3]triazol-1'-yl]propanoic acid (**127a**) using methyl (2*S*)-2-[(*tert*-butoxycarbonyl)amino]-3-{5'-[(4'''-methoxyphenyl)ethynyl]-1*H*-benzo[*d*][1.2.3]triazol-1'-yl}propanoate (**126b**) (0.0800 g, 0.180 mmol) and caesium carbonate (0.0750 g, 0.230 mmol) to give (2*S*)-2-[(*tert*-butoxycarbonyl)amino]-3-{5'-[(4'''-methoxyphenyl)ethynyl]-1*H*-benzo[*d*][1.2.3]triazol-1'-yl}propanoic acid (**127b**) (0.0710 g, 91%) as a yellow solid. This was used for the next reaction without any further purification. To a solution of (2*S*)-2-[(*tert*-butoxycarbonyl)amino]-3-{5'-[(4'''-methoxyphenyl)ethynyl]-1*H*-benzo[*d*][1.2.3]triazol-1'-yl}propanoic acid (**127b**) (0.0500 g, 0.110 mmol) in dioxane (2 mL) was added 2 M aqueous hydrochloric acid (0.8 mL). The reaction mixture was stirred at room temperature for 24 h and concentrated *in vacuo*. Purification by recrystallisation from methanol and chloroform gave (2*S*)-2-amino-3-{5'-[(4'''-methoxyphenyl)ethynyl]-1*H*-benzo[*d*][1.2.3]triazol-1'-yl}propanoic acid hydrochloride (**128b**) as an off-white solid (0.0340 g, 83%). Mp 274–276 °C (decomposition); ν_{max}/cm^{-1} (neat) 3394 (OH), 2931 (CH), 2214 (C≡C), 1728 (C=O), 1604, 1512, 1107, 826; $[\alpha]_D^{17}$ +5.7 (*c* 0.1, MeOH); δ_H (400 MHz, DMSO-*d6*) 3.81 (3H, s, OCH$_3$), 4.58 (1H, t, *J* 5.0 Hz, 2-H), 5.17 (1H, dd, *J* 15.0, 5.0 Hz, 3-*H*H), 5.22 (1H, dd, *J* 15.0, 5.0 Hz, 3-H*H*), 7.01 (2H, d, *J* 8.9 Hz, 3'''-H and 5'''-H), 7.54 (2H, d, *J* 8.9 Hz, 2'''-H and 6'''-H), 7.72 (1H, dd, *J* 8.6, 1.2 Hz, 6'-H), 7.96 (1H, dd, *J* 8.6, 0.7 Hz, 7'-H), 8.13 (1H, dd, *J* 1.2, 0.7 Hz, 4'-H); δ_C (126 MHz, DMSO-*d6*) 47.2 (CH$_2$), 52.0 (CH), 55.3 (CH$_3$), 87.8 (C), 89.4 (C), 110.5 (CH), 114.0 (2 × CH), 114.5 (C), 118.7 (C), 121.9 (CH), 130.7 (CH), 133.1 (2 × CH), 133.3 (C), 145.2 (C), 159.7 (C), 168.3 (C); *m/z* (ESI) 359.1105 (MNa$^+$. C$_{18}$H$_{16}$N$_4$NaO$_3$ requires 359.1115).

(2*S*)-2-Amino-3-{5'-[(4'''-dimethylaminophenyl)ethynyl]-1*H*-benzo[*d*][1.2.3]triazol-1'-yl}propanoic acid hydrochloride (128c)
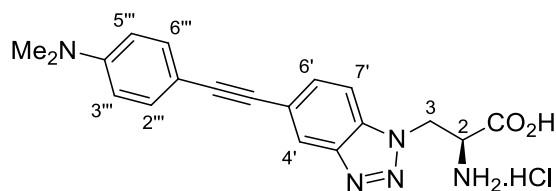
(2*S*)-2-[(*tert*-Butoxycarbonyl)amino]-3-{5'-[(4'''-dimethylaminophenyl)ethynyl]-1*H*-benzo[*d*][1.2.3]triazol-1'-yl}propanoic acid (**127c**) was prepared as for (2*S*)-2-[(*tert*-butoxycarbonyl)amino]-3-[5'-(phenylethynyl)-1*H*-benzo[*d*][1.2.3]triazol-1'-yl]propanoic acid (**127a**) using methyl (2*S*)-2-[(*tert*-butoxycarbonyl)amino]-3-{5'-[(4'''-dimethylaminophenyl)ethynyl]-1*H*-benzo[*d*][1.2.3]triazol-1'-yl}propanoate (**126c**) (0.100 g, 0.220 mmol) and caesium carbonate (0.0910 g, 0.280 mmol). Purification by recrystallisation from methanol gave (2*S*)-2-[(*tert*-butoxycarbonyl)amino]-3-{5'-[(4'''-dimethylaminophenyl)ethynyl]-1*H*-benzo[*d*][1.2.3]triazol-1'-yl}propanoic acid (**127c**) (0.0450 g, 66%) as an off-white solid. This was used for the next step without further purification. To a solution of (2*S*)-2-[(*tert*-butoxycarbonyl)amino]-3-{5'-[(4'''-dimethlaminophenyl)ethynyl]-1*H*-benzo[*d*][1.2.3]triazol-1'-yl}propanoic acid (**127c**) (0.0400 g, 0.0890 mmol) in acetonitrile (0.05 mL) was added 1 M aqueous hydrochloric acid (1 mL). The reaction mixture was stirred at room temperature for 0.5 h and concentrated *in vacuo*. Purification by trituration with chloroform gave (2*S*)-2-amino-3-{5'-[(4'''-dimethylaminophenyl)ethynyl]-1*H*-benzo[*d*][1.2.3]triazol-1'-yl}propanoic acid hydrochloride (**128c**) as a yellow oil (0.0300 g, 88%); v_{max}/cm^{-1} (neat) 3406 (OH), 2920 (CH), 2360 (C≡C), 1740 (C=O), 1508, 1211, 1130, 841; $[\alpha]_D^{19}$ −4.5 (*c* 0.1, MeOH); δ_H (400 MHz, CD$_3$OD) 3.27 (6H, s, N(CH$_3$)$_2$), 4.78 (1H, dd, *J* 5.4, 4.4 Hz, 2-H), 5.29 (1H, dd, *J* 15.5, 4.4 Hz, 3-*H*H), 5.40 (1H, dd, *J* 15.5, 5.4 Hz, 3-H*H*), 7.59 (2H, d, *J* 8.9 Hz, 3'''-H and 5'''-H), 7.74 (2H, d, *J* 8.9 Hz, 2'''-H and 6'''-H), 7.77 (1H, dd, *J* 8.7, 1.3 Hz, 6'-H), 7.89 (1H, dd, *J* 8.7, 0.7 Hz, 7'-H), 8.23–8.25 (1H, m, 4'-H); δ_C (101 MHz, CD$_3$OD) 44.9 (2 × CH$_3$), 46.8 (CH$_2$), 52.2 (CH), 87.8 (C), 89.5 (C), 109.7 (C), 110.6 (CH), 111.5 (C), 119.6 (2 × CH), 122.3 (CH), 130.9 (C), 131.4 (CH), 133.2 (2 × CH), 143.6 (C), 145.2 (C), 167.8 (C); *m/z* (ESI) 350.1616 (MH$^+$. C$_{19}$H$_{20}$N$_5$O$_2$ requires 350.1612).

(2*S*)-2-Amino-3-{5'-[(4'''-fluorophenyl)ethynyl]-1*H*-benzo[*d*][1.2.3]triazol-1'-yl}propanoic acid hydrochloride (128d)
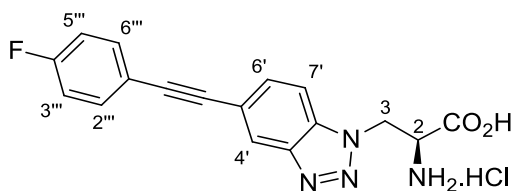

(2*S*)-2-[(*tert*-Butoxycarbonyl)amino]-3-{5'-[(4'''-fluorophenyl)ethynyl]-1*H*-benzo[*d*][1.2.3]triazol-1'-yl}propanoic acid (**127d**) was prepared as described for (2*S*)-2-[(*tert*-butoxycarbonyl)amino]-3-[5'-(phenylethynyl)-1*H*-benzo[*d*][1.2.3]triazol-1'-yl]propanoic acid (**127a**) using methyl (2*S*)-2-[(*tert*-butoxycarbonyl)amino]-3-{5'-[(4'''-fluorophenyl)ethynyl]-1*H*-benzo[*d*][1.2.3]triazol-1'-yl}propanoate (**126d**) (0.0800 g, 0.180 mmol) and caesium carbonate (0.0750 g, 0.230 mmol). This gave (2*S*)-2-[(*tert*-butoxycarbonyl)amino]-3-{5'-[(4'''-fluorophenyl)ethynyl]-1*H*-benzo[*d*][1.2.3]triazol-1'-yl}propanoic acid (**127d**) (0.0610 g, 79%) as an off-white solid. This was used for the next step without further purification. To a solution of (2*S*)-2-[(*tert*-butoxycarbonyl)amino]-3-{5'-[(4'''-fluorophenyl)ethynyl]-1*H*-benzo[*d*][1.2.3]triazol-1'-yl}propanoic acid (**127d**) (0.0500 g, 0.120 mmol) in acetonitrile (3 mL) was added 6 M aqueous hydrochloric acid (2 mL). The reaction mixture was stirred at room temperature for 3 h and concentrated *in vacuo*. Purification by trituration with chloroform gave (2*S*)-2-amino-3-{5'-[(4'''-fluorophenyl)ethynyl]-1*H*-benzo[*d*][1.2.3]triazol-1'-yl}propanoic acid hydrochloride (**128d**) as a white solid (0.0270 g, 64%). Mp 280–285 °C (decomposition); v_{max}/cm^{-1} (neat) 2921 (OH), 2851 (CH), 2359 (C≡C), 1742 (C=O), 1508, 1219, 833; $[\alpha]_D^{17}$ +12.9 (*c* 0.1, MeOH); δ_H (400 MHz, CD$_3$OD) 4.72–4.79 (1H, m, 2-H), 5.27 (1H, dd, *J* 15.4, 3.8 Hz, 3-*H*H), 5.36 (1H, dd, *J* 15.4, 5.5 Hz, 3-H*H*), 7.14 (2H, t, *J* 8.5 Hz, 3'''-H and 5'''-H), 7.59 (2H, dd, *J* 8.5, 5.5 Hz, 2'''-H and 6'''-H), 7.73 (1H, d, *J* 8.6 Hz, 6'-H), 7.85 (1H, d, *J* 8.6 Hz, 7'-H), 8.19 (1H, s, 4'-H); δ_C (101 MHz, CD$_3$OD) 46.8 (CH$_2$), 52.2 (CH), 87.5 (C), 88.2 (C), 110.3 (CH), 115.4 (d, $^2J_{C-F}$ 22.5 Hz, 2 × CH), 119.0 (d, $^4J_{C-F}$ 3.5 Hz, C), 119.9 (C), 122.0 (CH), 131.2 (CH), 133.2 (C), 133.4 (d, $^3J_{C-F}$ 8.5 Hz, 2 × CH), 145.4 (C), 162.8 (d, $^1J_{C-F}$ 247.8 Hz, C), 167.5 (C); *m/z* (ESI) 347.0913 (MNa$^+$. C$_{17}$H$_{13}$FN$_4$NaO$_2$ requires 347.0915).

(2*S*)-2-Amino-3-{5'-[(4'''-nitrophenyl)ethynyl]-1*H*-benzo[*d*][1.2.3]triazol-1'-yl}propanoic acid hydrochloride (128e)
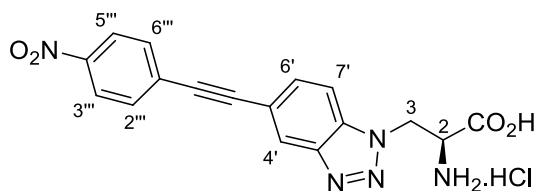

(2*S*)-2-[(*tert*-Butoxycarbonyl)amino]-3-{5'-[(4'''-nitrophenyl)ethynyl]-1*H*-benzo[*d*][1.2.3]triazol-1'-yl}propanoic acid (**127e**) was prepared as described for (2*S*)-2-[(*tert*-butoxycarbonyl)amino]-3-[5'-(phenylethynyl)-1*H*-benzo[*d*][1.2.3]triazol-1'-yl]propanoic acid (**127a**) using methyl (2*S*)-2-[(*tert*-butoxycarbonyl)amino]-3-{5'-[(4'''-nitrophenyl)ethynyl]-1*H*-benzo[*d*][1.2.3]triazol-1'-yl}propanoate (**126e**) (0.0410 g, 0.107 mmol) and caesium carbonate (0.0456 g, 0.140 mmol). This gave (2*S*)-2-[(*tert*-butoxycarbonyl)amino]-3-{5'-[(4'''-nitrophenyl)ethynyl]-1*H*-benzo[*d*][1.2.3]triazol-1'-yl}propanoic acid (**127e**) (0.0360 g, 90%) as an orange solid. This was used for the next reaction without any further purification. To a solution of (2*S*)-2-[(*tert*-butoxycarbonyl)amino]-3-{5'-[(4'''-nitrophenyl)ethynyl]-1*H*-benzo[*d*][1.2.3]triazol-1'-yl}propanoic acid (**127e**) (0.0500 g, 0.110 mmol) in acetonitrile (1 mL) and 1,4-dioxane (1 mL) was added 6 M aqueous hydrochloric acid (1 mL). The reaction mixture was stirred at room temperature for 3 h and concentrated *in vacuo*. Purification by recrystallisation from methanol followed by trituration with chloroform gave (2*S*)-2-amino-3-{5'-[(4'''-nitrophenyl)ethynyl]-1*H*-benzo[*d*][1.2.3]triazol-1'-yl}propanoic acid hydrochloride (**128e**) as an orange solid (0.0260 g, 60%). Mp 188–191 °C (decomposition); v_{max}/cm^{-1} (neat) 3410 (OH), 2962 (CH), 2214 (C≡C), 1593, 1512, 1307, 1103, 852; $[\alpha]_D^{18}$ +5.8 (*c* 0.1, MeOH); δ_H (400 MHz, CD$_3$OD) 4.76 (1H, dd, *J* 5.5, 4.2 Hz, 2-H), 5.30 (1H, dd, *J* 15.5, 4.2 Hz, 3-*H*H), 5.40 (1H, dd, *J* 15.5, 5.5 Hz, 3-H*H*), 7.81–7.85 (3H, m, 6'-H, 2'''-H and 6'''-H), 7.92 (1H, dd, *J* 8.7, 0.4 Hz, 7'-H), 8.29–8.34 (3H, m, 4'-H, 3'''-H and 5'''-H); δ_C (101 MHz, CD$_3$OD) 46.9 (CH$_2$), 52.3 (CH), 87.5 (C), 92.7 (C), 110.7 (CH), 118.9 (C), 122.8 (CH), 123.5 (2 × CH), 129.5 (C), 131.4 (CH), 132.3 (2 × CH), 133.6 (C), 145.2 (C), 147.3 (C), 167.9 (C); *m/z* (ESI) 352.1041 (MH$^+$. C$_{17}$H$_{13}$N$_5$O$_4$ requires 352.1040).

(2*S*)-2-Amino-3-{5'-[(4'''-cyanophenyl)ethynyl]-1*H*-benzo[*d*][1.2.3]triazol-1'-yl}propanoic acid hydrochloride (128g)
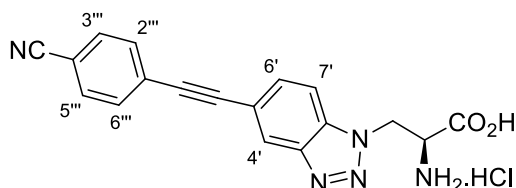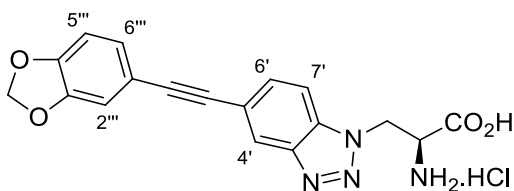

(2*S*)-2-[(*tert*-Butoxycarbonyl)amino]-3-{5'-[(4'''-cyanophenyl)ethynyl]-1*H*-benzo[*d*][1.2.3]triazol-1'-yl}propanoic acid (**127g**) was prepared as described for (2*S*)-2-[(*tert*-butoxycarbonyl)amino]-3-[5'-(phenylethynyl)-1*H*-benzo[*d*][1.2.3]triazol-1'-yl]propanoic acid (**127a**) using methyl (2*S*)-2-[(*tert*-butoxycarbonyl)amino]-3-{5'-[(4'''-cyanophenyl)ethynyl]-1*H*-benzo[*d*][1.2.3]triazol-1'-yl}propanoate (**126g**) (0.100 g, 0.220 mmol) and caesium carbonate (0.0950 g, 0.290 mmol). This gave (2*S*)-2-[(*tert*-butoxycarbonyl)amino]-3-{5'-[(4'''-cyanophenyl)ethynyl]-1*H*-benzo[*d*][1.2.3]triazol-1'-yl}propanoic acid (**127g**) (0.0895 g, 94%) as a yellow solid. This was used for the next reaction without any further purification. To a solution of (2*S*)-2-[(*tert*-butoxycarbonyl)amino]-3-{5'-[(4'''-cyanophenyl)ethynyl]-1*H*-benzo[*d*][1.2.3]triazol-1'-yl}propanoic acid (**127g**) (0.0500 g, 0.0890 mmol) in acetonitrile (0.1 mL) was added 2 M aqueous hydrochloric acid (1 mL). The reaction mixture was stirred at room temperature for 3 h and concentrated *in vacuo*. Purification by recrystallisation from methanol and diethyl ether gave (2*S*)-2-amino-3-{5'-[(4'''-cyanophenyl)ethynyl]-1*H*-benzo[*d*][1.2.3]triazol-1'-yl}propanoic acid hydrochloride (**128g**) as a yellow solid (0.0300 g, 88%). Mp 215–218 °C; v_{max}/cm^{-1} (neat) 2862 (CH), 2360 (C≡N), 2229 (C≡C), 1747 (C=O), 1600 (C=C), 1497, 814; $[\alpha]_D^{20}$ +12.4 (*c* 0.2, MeOH); δ_H (500 MHz, DMSO-d_6) 4.65 (1H, t, *J* 5.0 Hz, 2-H), 5.21–5.24 (2H, m, 3-H$_2$), 7.76–7.81 (3H, m, 6'-H, 2'''-H and 6'''-H), 7.93 (2H, d, *J* 8.5 Hz, 3'''-H and 5'''-H), 8.09 (1H, d, *J* 8.5 Hz, 7'-H), 8.39 (1H, s, 4'-H); δ_C (126 MHz, DMSO-d_6) 47.4 (CH$_2$), 52.2 (CH), 88.2 (C), 93.5 (C), 111.5 (C), 112.3 (CH), 117.8 (C), 118.9 (C), 123.4 (CH), 127.5 (C), 131.2 (CH), 132.7 (2 × CH), 133.2 (2 × CH), 134.3 (C), 145.4 (C), 168.9 (C); *m/z* (ESI) 332.1140 (MH$^+$. C$_{18}$H$_{14}$N$_5$O$_2$ requires 332.1142).

(2S)-2-Amino-3-{5'-[(3''',4'''-methylenedioxyphenyl)ethynyl]-1H-benzo[d][1.2.3]triazol-1'-yl}propanoic acid hydrochloride (128h)

(2S)-2-[(*tert*-Butoxycarbonyl)amino]-3-{5'-[(3''',4'''-methylenedioxyphenyl)ethynyl]-1H-benzo[d][1.2.3]triazol-1'-yl}propanoic acid (**127h**) was prepared as described for (2S)-2-[(*tert*-butoxycarbonyl)amino]-3-[5'-(phenylethynyl)-1H-benzo[d][1.2.3]triazol-1'-yl]propanoic acid (**127a**) using methyl (2S)-2-[(*tert*-butoxycarbonyl)amino]-3-{5'-[(methylenedioxyphenyl)ethynyl]-1H-benzo[d][1.2.3]triazol-1'-yl}propanoate (**126h**) (0.100 g, 0.220 mmol) and caesium carbonate (0.0890 g, 0.280 mmol). This gave (2S)-2-[(*tert*-butoxycarbonyl)amino]-3-{5'-[(methylenedioxyphenyl)ethynyl]-1H-benzo[d][1.2.3]triazol-1'-yl}propanoic acid (**127h**) (0.0850 g, 93%) as an orange solid. This was used for the next reaction without any further purification. To a solution of (2S)-2-[(*tert*-butoxycarbonyl)amino]-3-{5'-[(methylenedioxyphenyl)ethynyl]-1H-benzo[d][1.2.3]triazol-1'-yl}propanoic acid (**127h**) (0.0500 g, 0.110 mmol) in 1,4-dioxane (1mL) was added 4 M aqueous hydrochloric acid (1 mL). The reaction mixture was stirred at room temperature for 3 h and concentrated *in vacuo*. Purification by trituration with chloroform gave (2S)-2-amino-3-{5'-[(3''',4'''-methylenedioxyphenyl)ethynyl]-1H-benzo[d][1.2.3]triazol-1'-yl}propanoic acid hydrochloride (**128h**) as an orange solid (0.0300 g, 70%). Mp 190–192 °C (decomposition); v_{max}/cm^{-1} (neat) 3408 (OH), 2898 (CH), 2208 (C≡C), 1739 (C=O), 1500, 1225, 1036, 811; $[\alpha]_D^{20}$ +8.2 (*c* 0.2, MeOH); δ_H (500 MHz, CD$_3$OD) 4.79–4.84 (1H, m, 2-H), 5.29 (1H, dd, *J* 15.4, 3.9 Hz, 3-*H*H), 5.38 (1H, dd, *J* 15.4, 5.4 Hz, 3-H*H*), 6.00 (2H, s, OCH$_2$O), 6.85 (1H, d, *J* 8.0 Hz, 5'''-H), 7.00 (1H, d, *J* 1.4 Hz, 2'''-H), 7.09 (1H, dd, *J* 8.0, 1.4 Hz, 6'''-H), 7.71 (d, *J* 8.6 Hz, 1H, 6'-H), 7.86 (1H, d, *J* 8.6 Hz, 7'-H), 8.14 (1H, s, 4'-H); δ_C (126 MHz, CD$_3$OD) 46.8 (CH$_2$), 52.1 (CH), 86.2 (C), 89.4 (C), 101.6 (CH$_2$), 108.2 (CH), 110.3 (CH), 110.9 (CH), 120.2 (C), 121.6 (CH), 126.1 (CH), 131.3 (CH), 133.1 (C), 145.5 (C), 147.7 (C), 147.7 (C), 148.4 (C), 167.5 (C); *m/z* (ESI) 373.0905 (MNa$^+$. C$_{18}$H$_{14}$N$_4$NaO$_4$ requires 373.0907).

(2*S*)-2-Amino-3-{5'-[(napthalen-2''-yl)ethynyl]-1*H*-benzo[*d*][1.2.3]triazol-1'-yl}propanoic acid hydrochloride (128i)
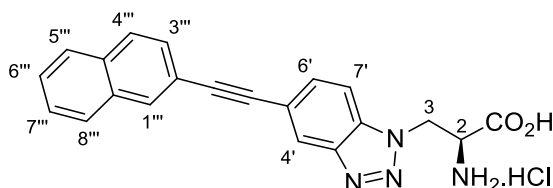

(2*S*)-2-[(*tert*-Butoxycarbonyl)amino]-3-{5'-[(napthalen-2''-yl)ethynyl]-1*H*-benzo[*d*][1.2.3]triazol-1'-yl}propanoic acid (**127i**) was prepared as described for (2*S*)-2-[(*tert*-butoxycarbonyl)amino]-3-[5'-(phenylethynyl)-1*H*-benzo[*d*][1.2.3]triazol-1'-yl]propanoic acid (**127a**) using methyl (2*S*)-2-[(*tert*-butoxycarbonyl)amino]-3-{5'-[(napthalen-2''-yl)ethynyl]-1*H*-benzo[*d*][1.2.3]triazol-1'-yl}propanoate (**126i**) (0.100 g, 0.210 mmol) and caesium carbonate (0.0890 g, 0.270 mmol). This gave (2*S*)-2-[(*tert*-butoxycarbonyl)amino]-3-{5'-[(napthalen-2''-yl)ethynyl]-1*H*-benzo[*d*][1.2.3]triazol-1'-yl}propanoic acid (**127i**) (0.0850 g, 91%) as a yellow solid. This was used for the next reaction without any further purification. To a solution of (2*S*)-2-[(*tert*-butoxycarbonyl)amino]-3-{5'-[(napthalen-2''-yl)ethynyl]-1*H*-benzo[*d*][1.2.3]triazol-1'-yl}propanoic acid (**127i**) (0.0500 g, 0.109 mmol) in 1,4-dioxane (0.1 mL) was added 2 M aqueous hydrochloric acid (1 mL). The reaction mixture was stirred at room temperature for 3 h and concentrated *in vacuo*. Purification by recrystallisation from methanol and diethyl ether gave (2*S*)-2-amino-3-{5'-[(napthalen-2''-yl)ethynyl]-1*H*-benzo[*d*][1.2.3]triazol-1'-yl}propanoic acid hydrochloride (**128i**) as a yellow solid (0.0200 g, 80%). Mp 195–198 °C; ν_{max}/cm^{-1} (neat) 3320 (OH), 2849 (CH), 2352 (C≡C), 1742 (C=O), 1487, 1234, 1057, 810; $[\alpha]_D^{23}$ +14.7 (*c* 0.1, MeOH); δ_H (400 MHz, CD$_3$OD) 4.81 (1H, br s, 2-H), 5.28 (1H, dd, *J* 15.3, 3.0 Hz, 3-*H*H), 5.38 (1H, dd, *J* 15.3, 4.9 Hz, 3-H*H*), 7.50–7.56 (2H, m, 5'''-H and 8'''-H), 7.60 (1H, dd, *J* 8.5, 1.4 Hz, 6'-H), 7.79 (1H, d, *J* 8.4 Hz, 3'''-H), 7.84–7.92 (4H, m, 7'-H, 4'''-H, 6'''-H and 7'''-H), 8.10 (1H, br s, 4'-H), 8.25 (1H, s, 1'''-H); δ_C (101 MHz, CD$_3$OD) 46.8 (CH$_2$), 52.2 (CH), 88.1 (C), 89.7 (C), 110.4 (CH), 120.0 (C), 120.0 (C), 122.1 (CH), 126.5 (CH), 126.7 (CH), 127.4 (CH), 127.5 (CH), 127.8 (CH), 127.9 (CH), 131.2 (CH), 131.3 (CH), 133.1 (C), 133.1 (C), 133.2 (C), 145.5 (C), 167.6 (C); *m/z* (ESI) 357.1350 (MNa$^+$. C$_{21}$H$_{17}$N$_4$O$_2$ requires 357.1346).

(2S)-2-Amino-3-{5'-[(4'''-methoxynapthalene)- 2''-chloroethenyl]-1H-benzo[d][1.2.3]triazol-1'-yl}propanoic acid hydrochloride (139)
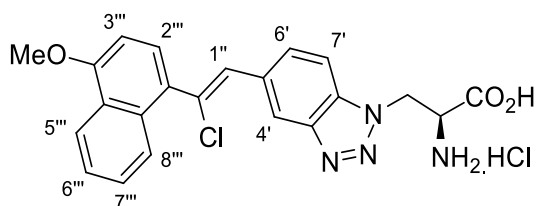

(2S)-2-[(*tert*-Butoxycarbonyl)amino]-3-{5'-[(4'''-methoxynapthyl)ethynyl]-1H-benzo[d][1.2.3]triazol-1'-yl}propanoic acid (**127j**) was prepared as for (2S)-2-[(*tert*-butoxycarbonyl)amino]-3-[5'-(phenylethynyl)-1H-benzo[d][1.2.3]triazol-1'-yl]propanoic acid (**127a**) using methyl (2S)-2-[(*tert*-butoxycarbonyl)amino]-3-{5'-[(4'''-methoxynapthyl)ethynyl]-1H-benzo[d][1.2.3]triazol-1'-yl}propanoate (**126j**) (0.100 g, 0.200 mmol) and caesium carbonate (0.0850 g, 0.260 mmol). Purification by trituration with chloroform gave gave (2S)-2-[(*tert*-butoxycarbonyl)amino]-3-{5'-[(4'''-methoxynapthyl)ethynyl]-1H-benzo[d][1.2.3]triazol-1'-yl}propanoic acid (**127j**) as a yellow solid (0.0820 g, 85%). To a solution of (2S)-2-[(*tert*-butoxycarbonyl)amino]-3-{5'-[(4'''-methoxynapthyl)ethynyl]-1H-benzo[d][1.2.3]triazol-1'-yl}propanoic acid (**127j**) (0.0500 g, 0.110 mmol) in 1,4-dioxane (0.1 mL) was added 2 M aqueous hydrochloric acid (2 mL). The reaction mixture was stirred at room temperature for 24 h and concentrated *in vacuo*. Purification by trituration with chloroform gave (2S)-2-Amino-3-{5'-[(4'''-methoxynapthalene)- 2''-chloroethenyl]-1H-benzo[d][1.2.3]triazol-1'-yl}propanoic acid hydrochloride (**139**) as a grey solid (0.0350 g, 78%). Mp 150–153 °C (decomposition); v_{max}/cm^{-1} (neat) 3333 (OH), 2932 (CH), 1743 (C=O), 1636 (C=C), 1582, 1508, 1242, 1087, 768; $[\alpha]_D^{20}$ −10.8 (*c* 0.2, MeOH); δ_H (400 MHz, CD$_3$OD) 4.04 (1H, s, OCH$_3$), 4.54 (1H, br s, 2-H), 5.09 (1H, dd, *J* 15.6, 3.1 Hz, 3-*H*H), 5.16 (1H, dd, *J* 15.6, 6.0 Hz, 3-H*H*), 6.93 (1H, d, *J* 8.1 Hz, 3'''-H), 7.17 (1H, d, *J* 8.8 Hz, 7'-H), 7.38–7.45 (2H, m, 1''-H and 2'''-H), 7.45–7.54 (4H, m, 4'-H, 6'-H, 6'''-H and 7'''-H), 7.94–8.00 (1H, m, 5'''-H), 8.26–8.33 (1H, m, 8'''-H); δ_C (101 MHz, CD$_3$OD) 46.9 (CH$_2$), 52.2 (CH), 55.1 (CH$_3$), 103.6 (CH), 109.6 (CH), 118.1 (CH), 122.3 (CH), 124.3 (CH), 125.5 (CH), 125.9 (C), 127.2 (CH), 127.3 (C), 127.9 (CH), 128.8 (CH), 130.3 (CH), 131.0 (C), 131.0 (C), 132.4 (C), 132.9 (C), 132.9 (C), 156.6 (C), 167.3 (C); *m/z* (ESI) 423.1220 (MH$^+$. C$_{22}$H$_{20}$^{35}ClN$_4$O$_3$ requires 423.1218).

(2*S*)-2-[(9*H*-Fluoren-9-ylmethoxycarbony)amino]-3-{5'-[(4'''-methoxyphenyl)ethynyl]-1*H*-benzo[*d*][1.2.3]triazol-1'-yl}propanoic acid (147)
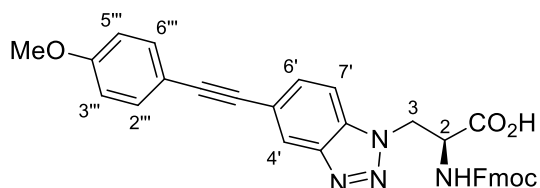
To a solution of (2*S*)-2-amino-3-{5'-[(4'''-methoxyphenyl)ethynyl]-1*H*-benzo[*d*][1.2.3]triazol-1'-yl}propanoic acid hydrochloride (**128b**) (0.140 g, 0.376 mmol) in 1,4-dioxane (1.5 mL) and water (1.5 mL) was added sodium hydrogen carbonate (0.126 g, 1.50 mmol) followed by *N*-(9-fluorenylmethoxycarbonyloxy)succinimide (0.124 g, 0.368 mmol). The reaction mixture was stirred at room temperature for 24 h and concentrated *in vacuo*. The resulting residue was dissolved in water, acidified to pH 2 with 1 M aqueous hydrochloric acid and the aqueous layer extracted with ethyl acetate (3 × 20 mL). The organic layers were dried (MgSO₄), filtered and concentrated *in vacuo*. Purification by flash column chromatography eluting with 0–10% methanol in acetone gave (2*S*)-2-[(9*H*-fluoren-9-ylmethoxycarbony)amino]-3-{5'-[(4'''-methoxyphenyl)ethynyl]-1H-benzo[d][1.2.3]triazol-1'-yl}propanoic acid (**147**) (0.133 g, 63%) as a white solid. Mp 213–214 °C (decomposition); v_{max}/cm⁻¹ (neat) 3390 (OH), 2955 (CH), 1701 (C=O), 1600 (C=C), 1512, 1411, 1246, 1030, 829; $[\alpha]_D^{22}$ +4.3 (*c* 0.1, DMSO); δ_H (400 MHz, DMSO-*d₆*) 3.80 (3H, s, OCH₃), 3.92–4.10 (3H, m, OC*H₂*CH and OCH₂C*H*), 4.21 (1H, td, *J* 7.5, 4.0 Hz, 2-H), 4.89 (1H, dd, *J* 14.0, 7.5 Hz, 3-*H*H), 5.21 (1H, dd, *J* 14.0, 4.0 Hz, 3-H*H*), 6.90 (1H, d, *J* 7.5 Hz, NH), 7.00 (2H, d, *J* 8.8 Hz, 3'''-H and 5'''-H), 7.24–7.32 (2H, m, 2 × ArH), 7.38 (2H, t, *J* 7.4 Hz, 2 × ArH), 7.45 (1H, d, *J* 8.7 Hz, 6'-H), 7.50 (2H, d, *J* 8.8 Hz, 2'''-H and 6'''-H), 7.56 (2H, d, *J* 7.4 Hz, 2 × ArH), 7.84 (2H, dd, *J* 7.4, 3.7 Hz, 2 × ArH), 7.93 (1H, d, *J* 8.7 Hz, 7'-H), 8.12 (1H, s, 4'-H); ¹³C data unavailable due to compound decomposition in DMSO;[200] *m/z* (ESI) 559.1977 (MNa⁺. C₃₃H₂₇N₄O₅ requires 559.1976).

Preparation of Zinc Iodide (1 M in tetrahydrofuran)

To zinc (0.200 g, 3.06 mmol) in anhydrous tetrahydrofuran (1 mL) under argon at 0 °C, was added a solution of iodine (0.500 g, 1.97 mmol) in anhydrous tetrahydrofuran (1 mL) in five portions. Between additions, the solution was warmed

to room temperature until the solution became colourless, and then cooled to 0 °C for the next addition.

Methyl 2-[(benzyloxycarbonyl)amino]acrylate (141)[190]
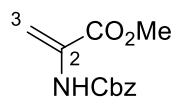
To a solution of methyl (2*S*)-2-[(benzyloxycarbonyl)amino]-3-(5'-bromo-1*H*-benzo[*d*][1.2.3]triazol-1'-yl)propanoate (**103**) (0.0500 g, 0.115 mmol) in *N,N'*-dimethylformamide (1.5 mL) under argon was added styrene (0.0330 mL, 0.289 mmol) and *N,N'*-diisopropylethylamine (0.100 mL, 0.575 mmol), followed by bis(triphenylphosphine)palladium(II) dichloride (0.00400 g, 0.00580 mmol). The reaction mixture was heated to 100 °C for 18 h, allowed to cool to room temperature and filtered through Celite®. The solution was diluted with ethyl acetate (20 mL), washed with water (5 × 10 mL) and brine (2 × 10 mL), dried (MgSO$_4$) and concentrated *in vacuo*. Purification by flash column chromatography, eluting with dichloromethane gave methyl 2-[(benzyloxycarbonyl)amino]acrylate (**141**) as a colourless oil (0.00800 g, 30%). Spectroscopic data were consistent with the literature.[190] δ$_H$ (400 MHz, CDCl$_3$) 3.83 (3H, s, OCH$_3$), 5.17 (2H, s, OC*H*$_2$Ph), 5.79 (1H, d, *J* 1.2 Hz, 3-*H*H), 6.25 (1H, br s, *3*-H*H*), 7.24 (1H, br s, NH), 7.29–7.42 (5H, m, Ph); δ$_C$ (101 MHz, CDCl$_3$) 52.9 (CH$_3$), 67.1 (CH$_2$), 106.1 (CH$_2$), 128.3 (2 × CH), 128.4 (CH), 128.6 (2 × CH), 131.0 (C), 135.9 (C), 153.1 (C), 164.2 (C); *m/z* (ESI) 258 (MNa$^+$. 100%).

Methyl (2*S*)-2-[(Benzyloxycarbonyl)amino]-3-(1*H*-benzo[*d*][1.2.3]triazol-1′-yl)propanoate (144)[81]
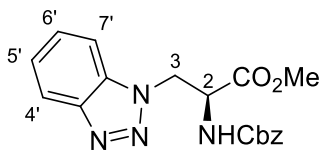
To a solution of methyl (2*S*)-2-[(benzyloxycarbonyl)amino]-3-(5′-iodo-1*H*-benzo[*d*][1.2.3]triazol-1′-yl)propanoate (**113**) (0.050 g, 0.10 mmol) in *N,N′*-dimethylformamide (1 mL) under argon was added styrene (0.034 mL, 0.30 mmol) and *N,N′*-diisopropylethylamine (0.052 mL, 0.30 mmol), followed by palladium(II) acetate (0.0022 g, 0.0010 mmol) and triphenylphosphine (0.0053 g, 0.020 mmol). The reaction mixture was heated to 75 °C for 2 h, then allowed to cool to room temperature and filtered through Celite®. The solution was diluted with ethyl acetate (20 mL), washed with water (5 × 10 mL) and brine (2 × 10 mL), dried (MgSO$_4$) and concentrated *in vacuo*. Purification by flash column chromatography, eluting with dichloromethane gave methyl (2*S*)-2-[(benzyloxycarbonyl)amino]-3-(1*H*-benzo[*d*][1.2.3]triazol-1′-yl)propanoate (**144**) as a white solid (0.010 g, 31%). Mp 82–85 °C; [α]$_D^{25}$ +37.0 (*c* 0.4, CHCl$_3$); δ$_H$ (400 MHz, CDCl$_3$) 3.75 (3H, s, OCH$_3$), 4.88 (1H, dt, *J* 7.0, 4.4 Hz, 2-H), 5.05–5.18 (4H, m, 3-H$_2$ and OC*H*$_2$Ph), 5.66 (1H, d, *J* 7.0 Hz, NH), 7.29–7.45 (8H, m, Ph, 5′-H, 6′-H and 7′-H), 8.03 (1H, br d, *J* 8.0 Hz, 4′-H); δ$_C$ (101 MHz, CDCl$_3$) 48.7 (CH$_2$), 53.3 (CH$_3$), 54.4 (CH), 67.4 (CH$_2$), 109.2 (CH), 120.2 (CH), 124.2 (CH), 127.9 (CH), 128.3 (2 × CH), 128.5 (CH), 128.7 (2 × CH), 133.9 (C), 136.0 (C), 145.8 (C), 155.8 (C), 169.5 (C); *m/z* (ESI) 377 (MNa$^+$. 100%).

Methyl (2*S*,1''*E*)-2-[(benzyloxycarbonyl)amino]-3-(5'-styryl-1*H*-benzo[*d*][1,2,3]triazol-1'-yl)propanoate (140a)
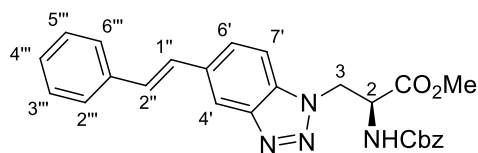

To a solution of methyl (2*S*)-2-[(benzyloxycarbonyl)amino]-3-(5'-bromo-1*H*-benzo[*d*][1.2.3]triazol-1'-yl)propanoate (**103**) (0.200 g, 0.460 mmol) in *N,N'*-dimethylformamide (6 mL) under argon was added styrene (0.132 mL, 1.14 mmol) and *N,N'*-diisopropylethylamine (0.260 mL, 1.38 mmol), followed by bis(triphenylphosphine)palladium(II) dichloride (0.0168 g, 0.0240 mmol). The reaction mixture was heated to 100 °C for 18 h, then allowed to cool to room temperature and filtered through Celite®. The solution was diluted with ethyl acetate (20 mL), washed with water (5 × 10 mL) and brine (2 × 10 mL), dried (MgSO$_4$) and concentrated *in vacuo*. Purification by flash column chromatography, eluting with 0−5% acetonitrile in dichloromethane gave methyl (2*S*,1''*E*)-2-[(benzyloxycarbonyl)amino]-3-(5'-styryl-1*H*-benzo[*d*][1,2,3]triazol-1'-yl)propanoate (**140a**) as a white solid (0.0488 g, 23%). Mp 140–144 °C; ν_{max}/cm^{-1} (neat) 3327 (NH), 1730 (C=O), 1680 (C=C), 1529, 1267, 698; [α]$_D^{24}$ +3.7 (*c* 0.1, CHCl$_3$); δ$_H$ (400 MHz, CDCl$_3$) 3.77 (3H, s, OCH$_3$), 4.88 (1H, dt, *J* 7.0, 4.2 Hz, 2-H), 5.03–5.22 (4H, m, 3-H$_2$ and OC*H*$_2$Ph), 5.63 (1H, d, *J* 7.0 Hz, NH), 7.14 (1H, d, *J* 16.3 Hz, 2''-H), 7.23 (1H, d, *J* 16.3 Hz, 1''-H), 7.28–7.43 (9H, m, 7'-H and 8 × ArH), 7.55 (2H, d, *J* 7.3 Hz, 2 × ArH), 7.60 (1H, dd, *J* 8.7, 0.8 Hz, 6'-H), 8.21 (1H, br s, 4'-H); δ$_C$ (101 MHz, CDCl$_3$) 48.6 (CH$_2$), 53.3 (CH$_3$), 54.3 (CH), 67.3 (CH$_2$), 109.3 (CH), 117.7 (CH), 126.5 (CH), 126.6 (2 × CH), 127.9 (CH), 127.9 (CH), 128.3 (2 × CH), 128.4 (CH), 128.6 (2 × CH), 128.8 (2 × CH), 129.6 (CH), 133.5 (C), 134.1 (C), 135.9 (C), 137.0 (C), 146.4 (C), 155.7 (C), 169.3 (C); *m/z* (ESI) 479.1696 (MNa$^+$. C$_{26}$H$_{24}$N$_4$NaO$_4$ requires 479.1690).

Methyl (2*S*,1''*E*)-2-[(benzyloxycarbonyl)amino]-3-(5'-[(4'''-methoxyphenyl)ethenyl]-1*H*-benzo[*d*][1,2,3]triazol-1'-yl)propanoate (140b)
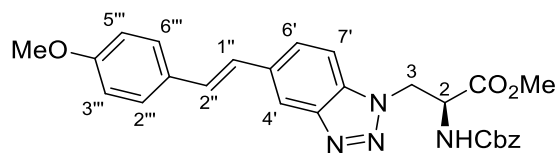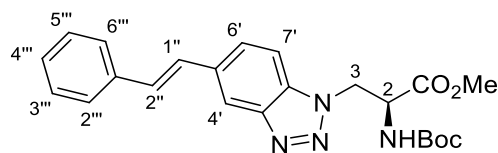

To a solution of methyl (2*S*)-2-[(benzyloxycarbonyl)amino]-3-(5'-bromo-1*H*-benzo[*d*][1.2.3]triazol-1'-yl)propanoate (**103**) (0.250 g, 0.577 mmol) in 1,4-dioxane (3.0 mL) and water (0.30 mL) was added *trans*-2-(4-methoxyphenyl)vinylboronic acid (0.171 g, 1.15 mmol), potassium fluoride (0.100 g, 1.73 mmol) and [1,1'-bis(diphenylphosphino)ferrocene]dichloropalladium(II) (0.0706 g, 0.0870 mmol). The mixture was degassed under argon for 0.25 h before heating to 80 °C for 60 h. The reaction mixture was then cooled to ambient temperature and filtered through a pad of Celite®. The filtrate was diluted with ethyl acetate (20 mL) and washed with water (3 × 20 mL) and brine (20 mL). The organic layer was dried (MgSO$_4$), filtered and concentrated *in vacuo*. Purification by flash column chromatography, eluting with dichloromethane gave methyl (2*S*,1''*E*)-2-[(benzyloxycarbonyl)amino]-3-(5'-[(4'''-methoxyphenyl)ethenyl]-1*H*-benzo[*d*][1,2,3]triazol-1'-yl)propanoate (**140b**) as a yellow solid (0.0780 g, 25%). Mp 168–171 °C; v_{max}/cm^{-1} (neat) 3342 (NH), 2954 (CH), 1719 (C=O), 1605 (C=C), 1512, 1251, 1174; [α]$_D^{21}$ +10.6 (*c* 1.0, CHCl$_3$); δ$_H$ (400 MHz, CDCl$_3$) 3.76 (3H, s, OCH$_3$), 3.84 (3H, s, OCH$_3$), 4.87 (1H, dt, *J* 7.2, 4.2 Hz, 2-H), 5.00–5.22 (4H, m, 3-H$_2$ and OC*H*$_2$Ph), 5.66 (1H, d, *J* 7.2 Hz, NH), 6.93 (2H, d, *J* 8.8 Hz, 3'''-H and 5'''-H), 7.09 (2H, br s, 1''-H and 2''-H), 7.29–7.40 (6H, m, 7'-H and Ph), 7.48 (2H, d, *J* 8.8 Hz, 2'''-H and 6'''-H), 7.57 (1H, dd, *J* 8.7, 1.0 Hz, 6'-H), 8.01 (1H, br s, 4'-H); δ$_C$ (101 MHz, CDCl$_3$) 48.6 (CH$_2$), 53.2 (CH$_3$), 54.3 (CH), 55.4 (CH$_3$), 67.3 (CH$_2$), 109.2 (CH), 114.2 (2 × CH), 117.2 (CH), 125.8 (CH), 126.4 (CH), 127.8 (2 × CH), 128.2 (2 × CH), 128.3 (CH), 128.6 (2 × CH), 129.1 (CH), 129.8 (C), 133.3 (C), 134.5 (C), 135.9 (C), 146.5 (C), 155.7 (C), 159.6 (C), 169.3 (C); *m/z* (ESI) 509.1794 (MNa$^+$. C$_{27}$H$_{26}$N$_4$NaO$_5$ requires 509.1795).

Methyl (2*S*,1''*E*)-2-[(*tert*-butyloxycarbonyl)amino]-3-(5'-styryl-1*H*-benzo[*d*][1,2,3]triazol-1'-yl)propanoate (145a)

To a dry microwave vial containing zinc (0.0470 g, 0.720 mmol) and bis(triphenylphosphine)palladium(II) dichloride (0.0337 g, 0.0480 mmol), under argon, was added a solution of methyl (2*S*)-2-[(*tert*-butoxycarbonyl)amino]-3-[5'-(phenylethynyl)-1*H*-benzo[*d*][1.2.3]triazol-1'-yl]propanoate (**126a**) (0.100 g, 0.240 mmol) in tetrahydrofuran (1.2 mL). A 1 M solution of zinc iodide (0.240 mL, 0.240 mmol) in tetrahydrofuran was added and then the reaction mixture was degassed, purged with hydrogen and stirred at 40 °C for 20 h. The reaction mixture was allowed to cool to room temperature and diluted with ethyl acetate (40 mL), washed with water (3 × 20 mL), dried (MgSO$_4$) and concentrated *in vacuo*. Purification by flash column chromatography, eluting with 70% diethyl ether in hexane gave methyl (2*S*,1''*E*)-2-[(*tert*-butyloxycarbonyl)amino]-3-(5'-styryl-1*H*-benzo[*d*][1,2,3]triazol-1'-yl)propanoate (**145a**) as an off-white solid (0.0660 g, 65%). Mp 170–172 °C; ν_{max}/cm^{-1} (neat) 3367 (NH), 2978 (CH), 1755 (C=O), 1690 (C=O), 1589, 1267, 698; $[\alpha]_D^{22}$ +7.0 (*c* 0.5, CHCl$_3$); δ_H (400 MHz, CDCl$_3$) 1.42 (9H, s, 3 × CH$_3$), 3.77 (3H, s, OCH$_3$), 4.81 (1H, dt, *J* 6.8, 4.4 Hz, 2-H), 5.04–5.15 (2H, m, 3-H$_2$), 5.39 (1H, d, *J* 6.8 Hz, NH), 7.16 (1H, d, *J* 16.3 Hz, 2''-H), 7.22–7.31 (3H, m, 1''-H and 4'''-H), 7.34–7.44 (2H, m, 3'''-H and 5'''-H), 7.50 (1H, d, *J* 8.7 Hz, 7'-H), 7.53–7.57 (2H, m, 2'''-H and 6'''-H), 7.73 (1H, dd, *J* 8.7, 0.9 Hz, 6'-H), 8.08 (1H, br s, 4'-H); δ_C (101 MHz, CDCl$_3$) 28.3 (3 × CH$_3$), 48.7 (CH$_2$), 53.1 (CH$_3$), 53.9 (CH), 80.7 (C), 109.5 (CH), 117.7 (CH), 126.4 (CH), 126.6 (2 × CH), 127.9 (CH), 127.9 (CH), 128.8 (2 × CH), 129.5 (CH), 133.6 (C), 134.1 (C), 137.0 (C), 146.4 (C), 155.1 (C), 169.6 (C); *m/z* (ESI) 423.2035 (MH$^+$. C$_{23}$H$_{27}$N$_4$O$_4$ requires 423.2027).

Methyl (2S,1''E)-2-[(tert-butyloxycarbonyl)amino]-3-(5'-{[(4'''-methoxyphenyl)ethenyl]-1H-benzo[d][1,2,3]triazol-1'-yl)propanoate (145b)
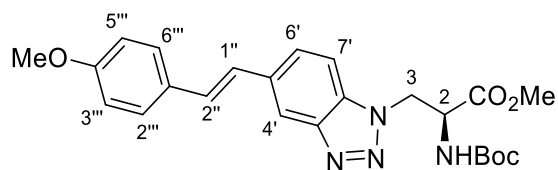

Methyl (2S,1''E)-2-[(tert-butyloxycarbonyl)amino]-3-(5'-[(4'''-methoxyphenyl)ethenyl]-1H-benzo[d][1,2,3]triazol-1'-yl)propanoate (**145b**) was synthesised as described for methyl (2S,1''E)-2-[(tert-butyloxycarbonyl)amino]-3-(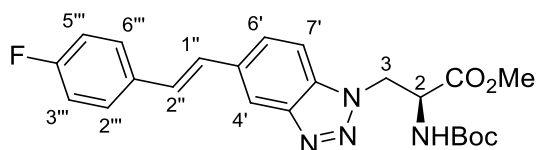5'-styryl-1H-benzo[d][1,2,3]triazol-1'-yl)propanoate (**145a**) using zinc (0.0610 g, 0.930 mmol), bis(triphenylphosphine)palladium(II) dichloride (0.0436 g, 0.0620 mmol), methyl (2S)-2-[(tert-butoxycarbonyl)amino]-3-{5'-[(4'''-methoxyphenyl)ethynyl]-1H-benzo[d][1.2.3]triazol-1'-yl}propanoate (**126b**) (0.140 g, 0.310 mmol), tetrahydrofuran (1.7 mL) and a 1 M solution of zinc iodide (0.310 mL, 0.310 mmol) in tetrahydrofuran. Purification by flash column chromatography, eluting with 75% diethyl ether in hexane gave methyl (2S,1''E)-2-[(tert-butyloxycarbonyl)amino]-3-(5'-[(4'''-methoxyphenyl)ethenyl]-1H-benzo[d][1,2,3]triazol-1'-yl)propanoate (**145b**) as a yellow solid (0.0895 g, 64%). Mp 164–168 °C; v_{max}/cm^{-1} (neat) 3306 (NH), 2966 (CH), 1739 (C=O), 1701 (C=O), 1604, 1512, 1300, 821; $[\alpha]_D^{21}$ +15.0 (c 0.2, CHCl$_3$); δ_H (500 MHz, CDCl$_3$) 1.44 (9H, s, 3 × CH$_3$), 3.77 (3H, s, OCH$_3$), 3.85 (3H, s, OCH$_3$), 4.81 (1H, dt, J 6.7, 4.2 Hz, 2-H), 5.04–5.16 (2H, m, 3-H$_2$), 5.37 (1H, d, J 6.7 Hz, NH), 6.92 (2H, d, J 8.4 Hz, 3'''-H and 5'''-H), 7.12 (2H, s, 1''-H and 2''-H), 7.46–7.53 (3H, m, 7'-H, 2'''-H and 6'''-H), 7.71 (1H, d, J 8.7 Hz, 6'-H), 8.05 (1H, s, 4'-H); δ_C (126 MHz, CDCl$_3$) 28.3 (3 × CH$_3$), 48.7 (CH$_2$), 53.1 (CH$_3$), 53.9 (CH), 55.4 (CH$_3$), 80.6 (C), 109.5 (CH), 114.2 (2 × CH), 117.1 (CH), 125.8 (CH), 126.3 (CH), 127.8 (2 × CH), 129.0 (CH), 129.8 (C), 133.3 (C), 134.5 (C), 146.4 (C), 155.1 (C), 159.5 (C), 169.7 (C); m/z (ESI) 475.1954 (MNa$^+$. C$_{24}$H$_{28}$N$_4$NaO$_5$ requires 475.1952).

Methyl (2*S*,1''*E*)-2-[(*tert*-butyloxycarbonyl)amino]-3-(5'-[(4'''-fluorophenyl)ethenyl]-1*H*-benzo[*d*][1,2,3]triazol-1'-yl)propanoate (145d)

Methyl (2*S*,1''*E*)-2-[(tert-butyloxycarbonyl)amino]-3-(5'-[(4'''-fluorophenyl)ethenyl]-1*H*-benzo[*d*][1,2,3]triazol-1'-yl)propanoate (**145d**) was synthesised as described for methyl (2*S*,1''*E*)-2-[(*tert*-butyloxycarbonyl)amino]-3-(5'-styryl-1*H*-benzo[*d*][1,2,3]triazol-1'-yl)propanoate (**145a**) using zinc (0.0445 g, 0.680 mmol), bis(triphenylphosphine)palladium(II) dichloride (0.0323 g, 0.0460 mmol), methyl (2*S*)-2-[(*tert*-butyloxycarbonyl)amino]-3-(5'-[(4'''-fluorophenyl)ethynyl]-1*H*-benzo[*d*][1.2.3]triazol-1'-yl)propanoate (**126d**) (0.100 g, 0.230 mmol), tetrahydrofuran (1.4 mL) and a 1 M solution of zinc iodide (0.230 mL, 0.230 mmol) in tetrahydrofuran. The reaction mixture was stirred at 40 °C for 24 h. Purification by flash column 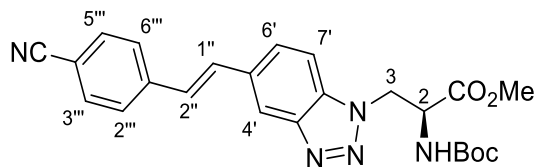chromatography, eluting with 70% diethyl ether in hexane gave methyl (2*S*,1''*E*)-2-[(*tert*-butyloxycarbonyl)amino]-3-(5'-[(4'''-fluorophenyl)ethenyl]-1*H*-benzo[*d*][1,2,3]triazol-1'-yl)propanoate (**145d**) as a yellow solid (0.0580 g, 57%). Mp 162–165 °C; v_{max}/cm^{-1} (neat) 3383 (NH), 2982 (CH), 1759 (C=O), 1700 (C=O), 1508, 1157, 829; $[\alpha]_D^{24}$ +6.2 (*c* 0.2, CHCl$_3$); δ_H (400 MHz, DMSO-*d$_6$*) 1.22 (9H, s, 3 × CH$_3$), 3.67 (3H, s, OCH$_3$), 4.81 (1H, td, *J* 9.0, 4.5 Hz, 2-H), 4.95 (1H, dd, *J* 14.4, 9.0 Hz, 3-*H*H), 5.08 (1H, dd, *J* 14.4, 4.5 Hz, 3-H*H*), 7.24 (2H, t, *J* 8.9 Hz, 3'''-H and 5'''-H), 7.40 (2H, s, 1''-H and 2''-H), 7.43 (1H, d, *J* 9.0 Hz, NH), 7.68 (2H, dd, *J* 8.9, 5.6 Hz, 2'''-H and 6'''-H), 7.85 (1H, d, *J* 8.8 Hz, 7'-H), 7.90 (1H, dd, *J* 8.8, 0.9 Hz, 6'-H), 8.16 (1H, br s, 4'-H); δ_C (101 MHz, DMSO-*d$_6$*) 28.4 (3 × CH$_3$), 48.3 (CH$_2$), 52.8 (CH$_3$), 53.9 (CH), 79.1 (C), 111.4 (CH), 116.1 (d, $^2J_{C-F}$ 21.6 Hz, 2 × CH), 117.2 (CH), 126.3 (CH), 128.0 (CH), 128.4 (CH), 128.8 (d, $^3J_{C-F}$ 8.0 Hz, 2 × CH), 133.6 (C), 133.9 (C), 134.1 (d, $^4J_{C-F}$ 3.2 Hz, C), 146.3 (C), 155.4 (C), 162.2 (d, $^1J_{C-F}$ 244.9 Hz, C), 170.5 (C); *m/z* (ESI) 463.1752 (MNa$^+$. C$_{23}$H$_{25}$FN$_4$NaO$_4$ requires 463.1752).

Methyl (2*S*,1''*E*)-2-[(*tert*-butyloxycarbonyl)amino]-3-(5'-[(4'''-cyanophenyl)ethenyl]-1*H*-benzo[*d*][1,2,3]triazol-1'-yl)propanoate (145g)

Methyl (2*S*,1''*E*)-2-[(*tert*-butyloxycarbonyl)amino]-3-(5'-[(4'''-cyanophenyl)ethenyl]-1*H*-benzo[*d*][1,2,3]triazol-1'-yl)propanoate (**145g**) was synthesised as described for methyl (2*S*,1''*E*)-2-[(*tert*-butyloxycarbonyl)amino]-3-(5'-styryl-1*H*-benzo[*d*][1,2,3]triazol-1'-yl)propanoate (**145a**) using zinc (0.0440 g, 0.670 mmol), bis(triphenylphosphine)palladium(II) dichloride (0.0310 g, 0.0440 mmol), methyl (2*S*)-2-[(*tert*-butyloxycarbonyl)amino]-3-{5'-[(4'''-cyanophenyl)ethynyl]-1*H*-benzo[*d*][1.2.3]triazol-1'-yl}propanoate (**126g**) (0.100 g, 0.220 mmol), tetrahydrofuran (1.4 mL) and a 1 M solution of zinc iodide (0.220 mL, 0.220 mmol) in tetrahydrofuran. Purification by flash column chromatography, eluting with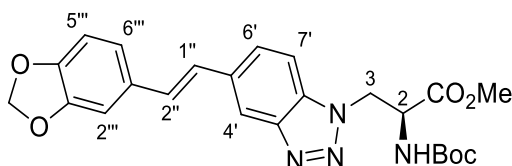 70% diethyl ether in hexane gave methyl (2*S*,1''*E*)-2-[(*tert*-butyloxycarbonyl)amino]-3-(5'-[(4'''-cyanophenyl)ethenyl]-1*H*-benzo[*d*][1,2,3]triazol-1'-yl)propanoate (**145g**) as a yellow solid (0.0200 g, 20%). Mp 142–144 °C; v_{max}/cm^{-1} (neat) 3364 (NH), 2978 (CH), 2222 (C≡N), 1748 (C=O), 1690 (C=O), 1600 (C=C), 1504, 1250, 826; $[\alpha]_D^{19}$ +4.4 (*c* 0.1, CHCl$_3$); δ_H (400 MHz, CDCl$_3$) 1.42 (9H, s, 3 × CH$_3$), 3.78 (3H, s, OCH$_3$), 4.80 (1H, dt, *J* 6.6, 4.4 Hz, 2-H), 5.11 (2H, d, *J* 4.4 Hz, 3-H$_2$), 5.36 (1H, d, *J* 6.6 Hz, NH), 7.15 (1H, d, *J* 16.3 Hz, 2''-H), 7.35 (1H, d, *J* 16.3 Hz, 1''-H), 7.54 (1H, d, *J* 8.7 Hz, 7'-H), 7.59–7.68 (4H, m, 2'''-H, 3'''-H, 5'''-H and 6'''-H), 7.73 (1H, dd, *J* 8.7, 0.7 Hz, 6'-H), 8.12 (1H, br s, 4'-H); δ_C (101 MHz, CDCl$_3$) 28.3 (3 × CH$_3$), 48.8 (CH$_2$), 53.2 (CH$_3$), 53.9 (CH), 80.7 (C), 109.9 (CH), 110.9 (C), 118.6 (CH), 119.0 (C), 126.4 (CH), 126.9 (2 × CH), 127.4 (CH), 131.7 (CH), 132.6 (2 × CH), 133.0 (C), 134.0 (C), 141.5 (C), 146.3 (C), 155.0 (C), 169.6 (C); *m/z* (ESI) 448.1981 (MH$^+$. C$_{24}$H$_{28}$N$_5$O$_4$ requires 448.1979).

Methyl (2*S*,1''*E*)-2-[(*tert*-butyloxycarbonyl)amino]-3-(5'-[(3''',4'''-methylenedioxyphenyl)ethenyl]-1*H*-benzo[*d*][1,2,3]triazol-1'-yl)propanoate (145h)

Methyl (2*S*,1''*E*)-2-[(*tert*-butyloxycarbonyl)amino]-3-(5'-[(3''',4'''-methylenedioxyphenyl)ethenyl]-1*H*-benzo[*d*][1,2,3]triazol-1'-yl)propanoate (**145h**) was synthesised as described for methyl (2*S*,1''*E*)-2-[(*tert*-butyloxycarbonyl)amino]-3-(5'-styryl-1*H*-benzo[*d*][1,2,3]triazol-1'-yl)propanoate (**145a**) using zinc (0.0420 g, 0.640 mmol), bis(triphenylphosphine)palladium(II) dichloride (0.0290 g, 0.0420 mmol), methyl (2*S*)-2-[(*tert*-butyloxycarbonyl)amino]-3-{5'-[(4'''-methylenedioxyphenyl)ethynyl]-1*H*-benzo[*d*][1.2.3]triazol-1'-yl}propanoate (**126h**) (0.100 g, 0.210 mmol), tetrahydrofuran (1.4 mL) and a 1 M solution of zinc iodide (0.210 mL, 0.210 mmol) in tetrahydrofuran. The reaction mixture was stirred at 40 °C for 24 h. Purification by flash column chromatography, eluting with 80% diethyl ether in hexane gave methyl (2*S*,1''*E*)-2-[(*tert*-butyloxycarbonyl)amino]-3-(5'-[(3''',4'''- methylenedioxyphenyl)ethenyl]-1*H*-benzo[*d*][1,2,3]triazol-1'-yl)propanoate (**145h**) as a yellow solid (0.0230 g, 23%). Mp 195–198 °C; ν_{max}/cm^{-1} (neat) 3368 (NH), 2974 (CH), 1740 (C=O), 1701 (C=O), 1500, 1443, 1250, 752; $[\alpha]_D^{19}$ +7.0 (*c* 0.1, CHCl₃); δ_H (500 MHz, CDCl₃) 1.43 (9H, s, 3 × CH₃), 3.77 (3H, s, OCH₃), 4.80 (1H, dt, *J* 6.7, 4.4 Hz, 2-H), 5.04–5.15 (2H, m, 3-H₂), 5.37 (1H, d, *J* 6.7 Hz, NH), 6.82 (1H, d, *J* 8.0 Hz, 5'''-H), 6.97 (1H, dd, *J* 8.0, 1.7 Hz, 6'''-H), 7.07 (2H, s, 1''-H and 2''-H), 7.10 (1H, d, *J* 1.7 Hz, 2'''-H), 7.49 (1H, d, *J* 8.5 Hz, 7'-H), 7.69 (1H, d, *J* 8.5 Hz, 6'-H), 8.05 (1H, s, 4'-H); δ_C (126 MHz, CDCl₃) 28.3 (3 × CH₃), 48.7 (CH₂), 53.2 (CH), 53.9 (CH₃), 80.7 (C), 101.2 (CH₂), 105.5 (CH), 108.5 (CH), 109.5 (CH), 117.3 (CH), 121.7 (CH), 126.2 (CH), 126.4 (CH), 129.2 (CH), 131.5 (C), 133.4 (C), 133.5 (C), 147.6 (C), 147.6 (C), 148.2 (C), 155.0 (C), 169.6 (C); *m/z* (ESI) 467.1933 (MH⁺. C₂₄H₂₇N₄O₆ requires 467.1925).

(2*S*,1''*E*)-2-amino-3-(5'-styryl-1*H*-benzo[*d*][1,2,3]triazol-1'-yl)propanoic acid hydrochloride (142a)
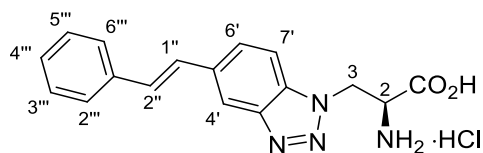
To a solution of methyl (2*S*,1''*E*)-2-[(*tert*-butyloxycarbonyl)amino]-3-(5'-styryl-1*H*-benzo[*d*][1,2,3]triazol-1'-yl)propanoate (**145a**) (0.0500 g, 0.120 mmol) in a mixture of methanol (1.5 mL) and 1,4-dioxane (1.5 mL) was added a solution of caesium carbonate (0.0500 g, 0.150 mmol) in water (0.75 mL). The reaction mixture was stirred at room temperature for 20 h and then concentrated *in vacuo.* The resulting residue was dissolved in water (50 mL) and acidified to pH 1 with 1 M aqueous hydrochloric acid. The aqueous layer was extracted with dichloromethane (3 × 30 mL), dried (MgSO$_4$) and concentrated *in vacuo* to give (2*S*,1''*E*)-2-[(*tert*-butyloxycarbonyl)amino]-3-(5'-styryl-1*H*-benzo[*d*][1,2,3]triazol-1'-yl)propanoic acid (**146a**) as a yellow solid (0.0430 g, 88%). This was used for the next reaction without further purification. To a solution of (2*S*,1''*E*)-2-[(*tert*-butyloxycarbonyl)amino]-3-(5'-styryl-1*H*-benzo[*d*][1,2,3]triazol-1'-yl)propanoic acid (**146a**) (0.0300 g, 0.0700 mmol) in 1,4-dioxane (0.1 mL) was added 2 M aqueous hydrochloric acid (2.5 mL). The reaction mixture was stirred at room temperature for 3 h and then concentrated *in vacuo.* This gave (2*S*,1''*E*)-2-amino-3-(5'-styryl-1*H*-benzo[*d*][1,2,3]triazol-1'-yl)propanoic acid hydrochloride (**142a**) as an off-white solid (0.0230 g, 92%). Mp 215–219 °C; v_{max}/cm^{-1} (neat) 3368 (NH$_2$), 2955 (CH), 1748 (C=O), 1689, 1500, 1204, 1161, 691; $[\alpha]_D^{22}$ +5.6 (*c* 0.1, MeOH); δ_H (500 MHz, CD$_3$OD) 4.74 (1H, br s, 2-H), 5.25 (1H, dd, *J* 14.9, 2.3 Hz, 3-*H*H), 5.34 (1H, dd, *J* 14.9, 4.9 Hz, 3-H*H*), 7.23–7.43 (5H, m, 1''-H, 2''-H, 3'''-H, 4'''-H and 5'''-H), 7.59 (2H, br d, *J* 7.5 Hz, 2'''-H and 6'''-H), 7.82 (1H, d, *J* 8.5 Hz, 7'-H), 7.93 (1H, d, *J* 8.5 Hz, 6'-H), 8.09 (1H, s, 4'-H); δ_C (126 MHz, CD$_3$OD) 46.7 (CH$_2$), 52.1 (CH), 110.0 (CH), 116.4 (CH), 126.3 (2 × CH), 126.7 (CH), 127.2 (CH), 127.6 (CH), 128.4 (2 × CH), 129.7 (CH), 133.1 (C), 135.1 (C), 137.1 (C), 146.2 (C), 167.6 (C); *m/z* (ESI) 309.1344 (MH$^+$. C$_{17}$H$_{17}$N$_4$O$_2$ requires 309.1346).

(2S,1''E)-2-Amino-3-(5'-[(4'''-methoxyphenyl)ethenyl]-1H-benzo[d][1,2,3]triazol-1'-yl)propanoic acid hydrochloride (142b)
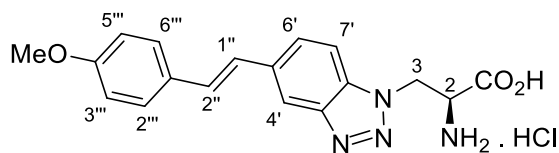
(2S,1''E)-2-Amino-3-(5'-[(4'''-methoxyphenyl)ethenyl]-1H-benzo[d][1,2,3]triazol-1'-yl)propanoic acid hydrochloride (**142b**) was synthesised as described for (2S,1''E)-2-amino-3-(5'-styryl-1H-benzo[d][1,2,3]triazol-1'-yl)propanoic acid hydrochloride (**142a**) using methyl (2S,1''E)-2-[(tert-butyloxycarbonyl)amino]-3-(5'-[(4'''-methoxyphenyl)ethenyl]-1H-benzo[d][1,2,3]triazol-1'-yl)propanoate (**145b**) (0.0300 g, 0.0660 mmol) and caesium carbonate (0.0280 g, 0.0860 mmol). This gave (2S,1''E)-2-amino-3-(5'-[(4'''-methoxyphenyl)ethenyl]-1H-benzo[d][1,2,3]triazol-1'-yl)propanoic acid (**146b**) as an off-white solid (0.0250 g, 87%). This was used for the next reaction without further purification using (2S,1''E)-2-amino-3-(5'-[(4'''-methoxyphenyl)ethenyl]-1H-benzo[d][1,2,3]triazol-1'-yl)propanoic acid (**146b**) (0.0250 g, 0.0570 mmol), 1,4-dioxane (2 mL) and 6 M aqueous hydrochloric acid (1 mL). This gave (2S,1''E)-2-amino-3-(5'-[(4'''-methoxyphenyl)ethenyl]-1H-benzo[d][1,2,3]triazol-1'-yl)propanoic acid hydrochloride (**142b**) as a yellow solid (0.0220 g, 88%). Mp 210–213 °C; ν_{max}/cm^{-1} 3430 (OH), 2932 (CH), 1728 (C=O), 1601 (C=C), 1501, 1443, 1242; $[\alpha]_D^{21}$ +10.1 (c 0.1, MeOH); δ_H (400 MHz, DMSO-d_6) 3.79 (3H, s, OCH$_3$), 4.63–4.69 (1H, m, 2-H), 5.17 (1H, dd, J 15.2, 4.9 Hz, 3-HH), 5.24 (1H, dd, J 15.2, 5.5 Hz, 3-HH), 6.98 (2H, d, J 8.8 Hz, 3'''-H and 5'''-H), 7.29 (1H, d, J 16.5 Hz, 1''-H), 7.36 (1H, d, J 16.5 Hz, 2''-H), 7.58 (2H, d, J 8.8 Hz, 2'''-H and 6'''-H), 7.89–7.93 (2H, m, 6'-H and 7'-H), 8.16 (1H, s, 4'-H), 8.71 (1H, br s, OH); δ_C (101 MHz, DMSO-d_6) 47.3 (CH$_2$), 52.2 (CH), 55.7 (CH$_3$), 111.4 (CH), 114.7 (2 × CH), 116.7 (CH), 126.1 (CH), 126.5 (CH), 128.3 (2 × CH), 129.1 (CH), 130.1 (C), 133.5 (C), 134.7 (C), 146.4 (C), 159.5 (C), 168.9 (C); m/z (ESI) 361.1270 (MNa$^+$. C$_{18}$H$_{18}$N$_4$NaO$_3$ requires 361.1271).

(2S,1''E)-2-Amino-3-(5'-[(4'''-fluorophenyl)ethenyl]-1H-benzo[d][1,2,3]triazol-1'-yl)propanoic acid hydrochloride (142d)
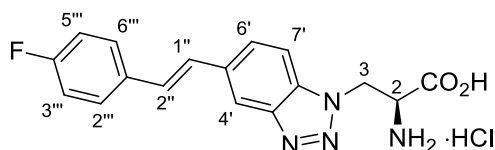
(2S,1''E)-2-Amino-3-(5'-[(4'''-fluorophenyl)ethenyl]-1H-benzo[d][1,2,3]triazol-1'-yl)propanoic acid hydrochloride (**142d**) was synthesised as described for (2S,1''E)-2-amino-3-(5'-styryl-1H-benzo[d][1,2,3]triazol-1'-yl)propanoic acid hydrochloride (**142a**) using methyl (2S,1''E)-2-[(tert-butyloxycarbonyl)amino]-3-(5'-[(4'''-fluorophenyl)ethenyl]-1H-benzo[d][1,2,3]triazol-1'-yl)propanoate (**145d**) (0.0800 g, 0.180 mmol) and caesium carbonate (0.0770 g, 0.240 mmol). This gave (2S,1''E)-2-[(tert-butyloxycarbonyl)amino]-3-(5'-[(4'''-fluorophenyl)ethenyl]-1H-benzo[d][1,2,3]triazol-1'-yl)propanoic acid (**146d**) as an off-white solid (0.0690 g, 90%). This was used for the next reaction without further purification using (2S,1''E)-2-[(tert-butyloxycarbonyl)amino]-3-(5'-[(4'''-fluorostyryl)ethenyl]-1H-benzo[d][1,2,3]triazol-1'-yl)propanoic acid (**146d**) (0.0500 g, 0.117 mmol), 1,4-dioxane (0.2 mL), and 2 M aqueous hydrochloric acid (2.5 mL). This gave (2S,1''E)-2-amino-3-(5'-[(4'''-fluorophenyl)ethenyl]-1H-benzo[d][1,2,3]triazol-1'-yl)propanoic acid hydrochloride (**142d**) as an off-white solid (0.0344 g, 81%). Mp 195–199 °C; ν_{max}/cm^{-1} 3371 (OH), 2951 (CH), 1728 (C=O), 1597 (C=C), 1497, 1200; $[\alpha]_D^{23}$ +7.3 (c 0.1, MeOH); δ_H (500 MHz, DMSO-d_6) 4.61–4.69 (1H, m, 2-H), 5.21 (1H, dd, J 15.2, 4.8 Hz, 3-HH), 5.27 (1H, dd, J 15.2, 5.2 Hz, 3-HH), 7.25 (2H, t, J 8.3 Hz, 3'''-H and 5'''-H), 7.42 (2H, s, 1''-H and 2''-H), 7.69 (2H, dd, J 8.3, 5.8 Hz, 2'''-H and 6'''-H), 7.92–7.99 (2H, m, 6'-H and 7'-H), 8.21 (1H, br s, 4'-H); δ_C (126 MHz, CDCl$_3$) 47.3 (CH$_2$), 52.2 (CH), 111.5 (CH), 116.1 (d, $^2J_{C\text{-}F}$ 21.5 Hz, 2 × CH), 117.2 (CH), 126.6 (CH), 128.3 (CH), 128.4 (CH), 128.9 (d, $^3J_{C\text{-}F}$ 8.0 Hz, 2 × CH), 133.7 (C), 134.1 (d, $^4J_{C\text{-}F}$ 2.7 Hz, C), 134.2 (C), 146.3 (C), 162.2 (d, $^1J_{C\text{-}F}$ 245.1 Hz, C), 168.9 (C); m/z (ESI) 327.1260 (MH$^+$. C$_{17}$H$_{16}$FN$_4$O$_2$ requires 327.1252).

5.4 Fluoroprolines Experimental

Di-*tert*-butyl (2*S*,4*R*)-4-hydroxypyrrolidine-1,2-dicarboxylate (168)[172]
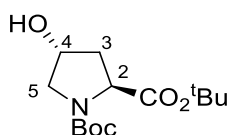
To a solution of *N*-(*tert*-butoxycarbonyl)-(2*S*,4*R*)-4-hydroxypyrrolidine-2-carboxylic acid (0.500 g, 2.16 mmol) in dry tetrahydrofuran (2.5 mL), under argon at 0 °C was added *tert*-butyl *N,N'*-diisopropylcarbamimidate (0.500 mL, 2.16 mmol). The reaction mixture was heated to 70 °C for 3 h, followed by further addition of *tert*-butyl *N,N'*-diisopropylcarbamimidate (0.500 mL, 2.16 mmol). The reaction mixture was heated for a further 18 h. The reaction mixture was filtered through Celite® and then concentrated *in vacuo*. Purification by flash column chromatography eluting with 50% ethyl acetate in hexane gave di-*tert*-butyl (2*S*,4*R*)-4-hydroxypyrrolidine-1,2-dicarboxylate (168) as a white solid (0.420 g, 68%). Mp 65–67 °C; $[\alpha]_D^{14}$ –55.3 (*c* 0.2, CHCl$_3$) (lit.[172] $[\alpha]_D^{25}$ –51.3 (*c* 1.3, CHCl$_3$)); NMR spectra showed a 2:1 mixture of rotamers. Only data for the major rotamer were recorded: δ_H (500 MHz, CDCl$_3$) 1.44 (9H, s, 3 × CH$_3$), 1.46 (9H, s, 3 × CH$_3$), 2.03 (1H, ddd, *J* 12.3, 8.0, 4.4 Hz, 3-*H*H), 2.29 (1H, ddd, *J* 12.3, 8.0, 4.6 Hz, 3-H*H*), 2.88 (1H, d, *J* 3.6 Hz, OH), 3.53 (1H, br d, *J* 11.6 Hz, 5-*H*H), 3.59 (1H, dd, *J* 11.6, 4.3 Hz, 5-H*H*), 4.27 (1H, t, *J* 8.0 Hz, 2-H), 4.41–4.49 (1H, m, 4-H); δ_C (126 MHz, CDCl$_3$) 28.0 (3 × CH$_3$), 28.3 (3 × CH$_3$), 39.2 (CH$_2$), 54.6 (CH$_2$), 58.5 (CH), 69.3 (CH), 80.2 (C), 81.1 (C), 154.2 (C), 172.1 (C); *m/z* (ESI) 310 (MNa$^+$. 100%).

Di-*tert*-butyl (2*S*,4*R*)-4-(tosyloxy)pyrrolidine-1,2-dicarboxylate (169)[201]
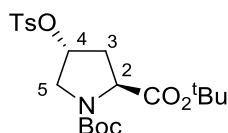
To a solution of di-*tert*-butyl (2*S*,4*R*)-4-hydroxypyrrolidine-1,2-dicarboxylate (168) (1.50 g, 5.22 mmol) in dichloromethane (30 mL) at 0 °C was added pyridine (0.840 mL, 10.4 mmol), 4-dimethylaminopyridine (0.0640 g, 0.520 mmol) and *p*-toluenesulfonyl chloride (1.99 g, 10.4 mmol). The reaction mixture was heated to 40 °C for 96 h and then concentrated *in vacuo*. Purification by flash column

chromatography eluting with 20% ethyl acetate in hexane gave di-*tert*-butyl (2*S*,4*R*)-4-(tosyloxy)pyrrolidine-1,2-dicarboxylate (**169**) as a white solid (1.90 g, 81%). Mp 74–76 °C; $[\alpha]_D^{17}$ −27.0 (*c* 0.1, CHCl$_3$); Spectroscopic data were consistent with the literature.[201] NMR spectra showed a 2:1 mixture of rotamers. Only data for the major rotamer were recorded: δ_H (500 MHz, CDCl$_3$) 1.42 (9H, s, 3 × CH$_3$), 1.44 (9H, s, 3 × CH$_3$), 2.12 (1H, ddd, *J* 12.6, 7.4, 5.5 Hz, 3-*H*H), 2.45 (3H, s, ArCH$_3$), 2.51–2.58 (1H, m, 3-H*H*), 3.53 (1H, dd, *J* 12.5, 5.0 Hz, 5-*H*H), 3.57–3.63 (1H, m, 5-H*H*), 4.24 (1H, t, *J* 7.4 Hz, 2-H), 4.97–5.02 (1H, m, 4-H), 7.36 (2H, d, *J* 8.1 Hz, 2 × ArH), 7.78 (2H, d, *J* 8.1 Hz, 2 × ArH); δ_C (126 MHz, CDCl$_3$) 21.7 (CH$_3$), 28.0 (3 × CH$_3$), 28.3 (3 × CH$_3$), 37.3 (CH$_2$), 51.7 (CH$_2$), 58.0 (CH), 78.3 (CH), 80.5 (C), 81.6 (C), 127.8 (2 × CH), 130.0 (2 × CH), 133.4, (C), 145.2 (C), 153.4, (C), 171.3 (C); *m/z* (ESI) 464 (MNa$^+$. 100%).

Di-*tert*-butyl (2*S*)-3,4-dehydroprolinate (173)[174]

To a solution of di-*tert*-butyl (2*S*,4*R*)-4-(tosyloxy)pyrrolidine-1,2-dicarboxylate (**169**) (0.100 g, 0.230 mmol) in dry tetrahydrofuran (2 mL) at 0 °C was added tetrabutylammonium fluoride (1 M solution in tetrahydrofuran) (5.80 mL, 0.580 mmol). The reaction mixture was stirred at room temperature for 24 h and subsequently concentrated *in vacuo*. Purification by flash column chromatography, eluting with 20% ethyl acetate in hexane gave di-*tert*-butyl (2*S*)-3,4-dehydroprolinate (**173**) as a colourless oil (0.0250 g, 40%). $[\alpha]_D^{20}$ −65.2 (*c* 0.5, CHCl$_3$); Spectroscopic data were consistent with the literature.[174] NMR spectra showed a 2:1 mixture of rotamers. Only data for the major rotamer were recorded: δ_H (500 MHz, CDCl$_3$) 1.45 (9H, s, 3 × CH$_3$), 1.45 (9H, s, 3 × CH$_3$), 4.20–4.24 (2H, m, 5-H$_2$), 4.81 (1H, td, *J* 5.2, 2.1 Hz, 2-H), 5.69 (1H, dq, *J* 6.3, 2.1 Hz, 3-H), 5.95 (1H, dq, *J* 6.3, 2.1 Hz, 4-H); δ_C (126 MHz, CDCl$_3$) 28.0 (3 × CH$_3$), 28.4 (3 × CH$_3$), 53.3 (CH$_2$), 67.2 (CH), 80.0 (C), 81.4 (C), 125.2 (CH), 129.0 (CH) 153.6 (C), 169.6 (C); *m/z* (ESI) 292 (MNa$^+$. 100%).

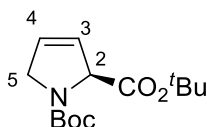## Di-*tert*-butyl (2S,4S)-4-fluoropyrrolidine-1,2-dicarboxylate (166)

To a solution of di-*tert*-butyl (2S,4R)-4-hydroxypyrrolidine-1,2-dicarboxylate (**168**) (0.150 g, 0.522 mmol) in dry dichloromethane (3 mL), under argon, was added dropwise morpholinosulfur trifluoride (0.330 mL, 2.61 mmol). The reaction mixture was stirred at room temperature for 48 h, concentrated *in vacuo* and water (20 mL) was added to the resulting residue. The aqueous layer was extracted with ethyl acetate (3 × 10 mL) and the combined extracts then washed with water (3 × 10 mL) and sodium bicarbonate (3 × 10 mL), dried over MgSO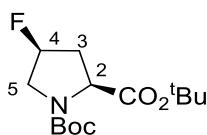₄, filtered and concentrated *in vacuo*. Purification by flash column chromatography, eluting with 30% ethyl acetate in hexane gave di-*tert*-butyl (2S,4S)-4-fluoropyrrolidine-1,2-dicarboxylate (**166**) as a colourless oil (0.092 g, 63%). v_{max}/cm⁻¹ (neat) 2976 (CH), 1736 (C=O), 1701 (C=O), 1395, 1366, 1151, 1117, 1070, 769; $[\alpha]_D^{15}$ −33.3 (*c* 0.2, CHCl₃); NMR spectra showed a 2:1 mixture of rotamers. Only data for the major rotamer were recorded: δ_H (500 MHz, CDCl₃) 1.45 (9H, s, 3 × CH₃), 1.48 (9H, s, 3 × CH₃), 2.20–2.51 (2H, m, 3-H₂), 3.57–3.73 (1H, m, 5-*H*H), 3.79 (1H, dt, *J* 27.0, 13.0 Hz, 5-H*H*), 4.29 (1H, d, *J* 9.3 Hz, 2-H), 5.18 (1H, dt, *J* 53.0, 4.2 Hz, 4-H); δ_C (126 MHz, CDCl₃) 27.9 (3 × CH₃), 28.3 (3 × CH₃), 37.7 (d, $^2J_{C-F}$ 22.0 Hz, CH₂), 53.0 (d, $^2J_{C-F}$ 24.6 Hz, CH₂), 58.4 (CH), 80.1 (C), 81.4 (C), 91.2 (d, $^1J_{C-F}$ 177.3 Hz, CH), 153.8 (C), 170.8 (C); *m/z* (ESI) 312.1579 (MNa⁺. C₁₄H₂₄FNNaO₄ requires 312.1582).

(2S,4S)-4-Fluoropyrrolidine-2-carboxylic acid hydrochloride (150)
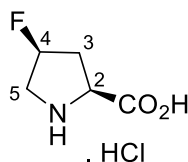
To a solution of di-*tert*-butyl (2S,4S)-4-fluoropyrrolidine-1,2-dicarboxylate (**166**) (0.0500 g, 0.170 mmol) in acetonitrile (0.2 mL) was added 2 M aqueous hydrochloric acid (2 mL). The reaction mixture was stirred at room temperature for 5 h and then concentrated *in vacuo*. Purification by trituration with chloroform yielded (2S,4S)-4-fluoropyrrolidine-2-carboxylic acid (**150**) as a white solid (0.0180 g, 64%). Mp 130–136 °C (decomposition); v_{max}/cm⁻¹ (neat) 3358 (NH), 2947 (CH), 1742 (C=O), 1717

(C=O), 1603, 1499, 1263, 1246, 1179, 1026; $[\alpha]_D^{15}$ −13.9 (*c* 0.1, MeOH); δ_H (500 MHz, CD$_3$OD) 2.58–2.78 (2H, m, 3-H$_2$), 3.56 (1H, ddd, *J* 35.7, 13.5, 3.6 Hz, 5-*H*H), 3.74 (1H, ddd, *J* 20.0, 13.5, 1.5 Hz, 5-H*H*), 4.59–4.65 (1H, m, 2-H), 5.44 (1H, dt, *J* 52.1, 3.6 Hz, 4-H); δ_C (126 MHz, CD$_3$OD) 35.4 (d, $^2J_{C\text{-}F}$ 22.0 Hz, CH$_2$), 52.0 (d, $^2J_{C\text{-}F}$ 24.0 Hz, CH$_2$), 58.2 (CH), 91.5 (d, $^1J_{C\text{-}F}$ 177.2 Hz, CH), 169.5 (C); *m/z* (ESI) 134.0611 (MH$^+$. C$_5$H$_9$FNO$_2$ requires 134.0612).

tert-Butyl (1*S*,4*S*)-2-oxa-3-oxo-5-azabicyclo[2.2.1]heptane-5-carboxylate (158)[202]
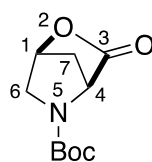
To a solution of *N*-(*tert*-butoxycarbonyl)-(2*S*,4*R*)-4-hydroxypyrrolidine-2-carboxylic acid (6.00 g, 26.0 mmol) in dry tetrahydrofuran (200 mL), under argon at 0 °C was added triphenylphosphine (8.17 g, 31.1 mmol), followed by dropwise addition of diisopropyl azodicarboxylate (6.13 mL, 31.1 mmol). The reaction mixture was stirred at room temperature for 18 h and concentrated *in vacuo*. Purification by column chromatography, eluting with 80% diethyl ether in hexane gave *tert*-butyl (1*S*,4*S*)-2-oxa-3-oxo-5-azabicyclo[2.2.1]heptane-5-carboxylate (**158**) as a white solid (4.30 g, 77%). Mp 90–93 °C; $[\alpha]_D^{19}$ +43.8 (*c* 1.0, CHCl$_3$) (lit.[202] $[\alpha]_D^{20}$ +46.3 (*c* 1.0, CHCl$_3$)); δ_H (400 MHz, CDCl$_3$) 1.48 (9H, s, 3 × CH$_3$), 2.01 (1H, br d, *J* 10.7 Hz, 7-*H*H), 2.21 (1H, ddt, *J* 10.7, 2.5, 1.3 Hz, 7-H*H*), 3.46 (1H, br d, *J* 11.0 Hz, 6-*H*H), 3.53 (1H, dd, *J* 11.0, 1.1 Hz, 6-H*H*), 4.42–4.65 (1H, m, 4-H), 5.07–5.09 (1H, m, 1-H); δ_C (101 MHz, CDCl$_3$) 28.3 (3 × CH$_3$), 39.1 (CH$_2$), 49.8 (CH$_2$), 57.7 (CH), 78.3 (CH), 81.4 (C), 153.9 (C), 170.9 (C); *m/z* (ESI) 236 (MNa$^+$. 100%).

N-(*tert*-Butoxycarbonyl)-(2S,4S)-4-hydroxypyrrolidine-2-carboxylic acid (159)[203]
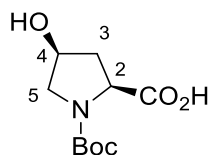
To a solution of *tert*-butyl (1*S*,4*S*)-2-oxa-3-oxo-5-azabicyclo[2.2.1]heptane-5-carboxylate (**158**) (4.00 g, 18.8 mmol) in a mixture of water (60 mL), tetrahydrofuran (40 mL) and methanol (40 mL) was added lithium hydroxide monohydrate (2.36 g, 56.3 mmol). The reaction mixture was stirred at room temperature for 18 h, concentrated *in vacuo* and ethyl acetate (100 mL) was added to the oily residue. The solution was acidified using a saturated aqueous solution of potassium hydrogen sulfate and the aqueous layer extracted with ethyl acetate (3 × 150 mL). The combined extracts were dried over $MgSO_4$ and concentrated *in vacuo* to give *N*-(*tert*-butoxycarbonyl)-(2*S*,4*S*)-4-hydroxypyrrolidine-2-carboxylic acid (**159**) as a white solid (4.00 g, 92%). Mp 132–135 °C; $[\alpha]_D^{21}$ –38.5 (*c* 0.3, MeOH) (lit.[203] $[\alpha]_D$ –39.0 (*c* 0.7, MeOH)); NMR spectra showed a 2:1 mixture of rotamers. Only data for the major rotamer were recorded: δ_H (400 MHz, DMSO-d_6) 1.34 (9H, s, 3 × CH₃), 1.81 (1H, ddd, *J* 11.1, 6.2, 2.2 Hz, 3-*H*H), 2.24–2.38 (1H, m, 3-H*H*), 3.06–3.14 (1H, m, 5-*H*H), 3.48 (1H, dt, *J* 10.9, 6.4 Hz, 5-H*H*), 4.08 (1H, dd, *J* 9.0, 6.2 Hz, 2-H), 4.15–4.23 (1H, m, 4-H), 5.01 (1H, br s, OH), 12.25 (1H, br s, CO_2H); δ_C (101 MHz, DMSO-d_6) 28.4 (3 × CH₃), 38.8 (CH_2), 54.0 (CH_2), 57.9 (CH), 68.1 (CH), 79.1 (C), 153.6 (C), 174.2 (C); *m/z* (ESI) 254 (MNa⁺. 100%).

Di-*tert*-butyl (2S,4S)-4-hydroxypyrrolidine-1,2-dicarboxylate (170)[204]

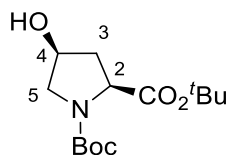Di-*tert*-butyl (2*S*,4*S*)-4-hydroxypyrrolidine-1,2-dicarboxylate (**170**) was prepared as for di-*tert*-butyl (2*S*,4*R*)-4-hydroxypyrrolidine-1,2-dicarboxylate (**168**) using *N*-(*tert*-butoxycarbonyl)-(2*S*,4*S*)-4-hydroxypyrrolidine-2-carboxylic acid (**159**) (1.00 g, 4.32 mmol), dry tetrahydrofuran (5.0 mL), and *tert*-butyl *N,N*-diisopropylcarbamimidate

(0.965 mL, 4.33 mmol). A second portion of *tert*-butyl *N,N'*-diisopropylcarbamimidate (0.965 mL, 4.33 mmol) was added after 3 h. Purification by column chromatography, eluting with 40% ethyl acetate in hexane gave di-*tert*-butyl (2*S*,4*S*)-4-hydroxypyrrolidine-1,2-dicarboxylate (**170**) as a white solid (0.650 g, 87%). Mp 58–60 °C (lit.[204] 53–55 °C); $[\alpha]_D^{20}$ −7.0 (*c* 0.1, CHCl₃); NMR spectra showed a 2:1 mixture of rotamers. Only data for the major rotamer were recorded: δ_H (400 MHz, CDCl₃) 1.44 (9H, s, 3 × CH₃), 1.48 (9H, s, 3 × CH₃), 1.96–2.07 (1H, m, 3-*H*H), 2.22–2.37 (1H, m, 3-H*H*), 3.47 (1H, d, *J* 10.4 Hz, OH), 3.54 (1H, dd, *J* 11.6, 4.4 Hz, 5-*H*H), 3.67 (1H, d, *J* 11.6 Hz, 5-H*H*), 4.16 (1H, dd, *J* 9.9, 1.2 Hz, 2-H), 4.26–4.34 (1H, m, 4-H); δ_C (101 MHz, CDCl₃) 27.9 (3 × CH₃), 28.4 (3 × CH₃), 38.7 (CH₂), 55.8 (CH₂), 58.8 (CH), 70.4 (CH), 80.3 (C), 82.4 (C), 153.9 (C), 174.4 (C); *m/z* (ESI) 310 (MNa⁺. 100%).

Di-*tert*-butyl (2*S*,4*S*)-4-(tosyloxy)pyrrolidine-1,2-dicarboxylate (171)[204]

Di-*tert*-butyl (2*S*,4*S*)-4-(tosyloxy)pyrrolidine-1,2-dicarboxylate (**171**) was prepared as described for di-*tert*-butyl (2*S*,4*R*)-4-(tosyloxy)pyrrolidine-1,2-dicarboxylate (**169**) using di-*tert*-butyl (2*S*,4*S*)-4-hydroxypyrrolidine-1,2-dicarboxylate (**170**) (0.500 g, 1.74 mmol), dry dichloromethane (10 mL), pyridine (0.280 mL, 3.48 mmol), 4-dimethylaminopyridine (0.0210 g, 0.174 mmol) and *p*-toluenesulfonyl chloride (0.663 g, 3.48 mmol). The reaction was heated for 48 h. Purification by column chromatography, eluting with 20% ethyl acetate in hexane gave di-*tert*-butyl (2*S*,4*S*)-4-(tosyloxy)pyrrolidine-1,2-dicarboxylate (**171**) as a white solid (0.500 g, 66%). Mp 69–71 °C; $[\alpha]_D^{20}$ −25.4 (*c* 0.5, CHCl₃) (lit.[204] $[\alpha]_D^{34}$ −28.3 (*c* 0.5, CHCl₃); NMR spectra showed a 2:1 mixture of rotamers. Only data for the major rotamer were recorded: δ_H (400 MHz, CDCl₃) 1.42 (9H, s, 3 × CH₃), 1.46 (9H, s, 3 × CH₃), 2.21–2.39 (1H, m, 3-*H*H), 2.40–2.51 (4H, m, 3-H*H* and ArCH₃), 3.55 (1H, dd, *J* 13.4, 1.6 Hz, 5-*H*H), 3.64 (1H, dd, *J* 13.4, 5.5 Hz, 5-H*H*), 4.21 (1H, dd, *J* 9.2, 2.8 Hz, 2-H), 4.97–5.05 (1H, m, 4-H), 7.34 (2H, d, *J* 8.2 Hz, 2 × ArH), 7.76 (2H, d, *J* 8.2 Hz, 2 × ArH); δ_C (101 MHz, CDCl₃) 21.7 (CH₃), 27.8 (3 × CH₃), 28.3 (3 × CH₃), 37.2 (CH₂),

51.8 (CH$_2$), 58.2 (CH), 78.0 (CH), 80.3 (C), 81.8 (C), 127.8 (2 × CH), 130.0 (2 × CH), 133.6 (C), 145.1 (C), 153.4 (C), 170.4 (C); *m/z* (ESI) 464 (MNa$^+$. 100%).
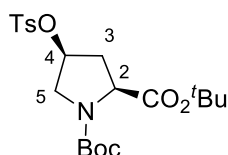
Di-*tert*-butyl (2*S*,4*R*)-4-fluoropyrrolidine-1,2-dicarboxylate (172)

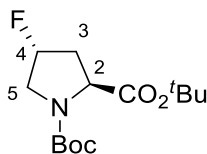Di-*tert*-butyl (2*S*,4*R*)-4-fluoropyrrolidine-1,2-dicarboxylate (**172**) was prepared as described for di-*tert*-butyl (2*S*,4*S*)-4-fluoropyrrolidine-1,2-dicarboxylate (**168**) using di-*tert*-butyl (2*S*,4*S*)-4-hydroxypyrrolidine-1,2-dicarboxylate (**170**) (0.150 g, 0.522 mmol), dry dichloromethane (3 mL), and morpholinosulfur trifluoride (0.330 mL, 2.61 mmol). Purification by column chromatography, eluting with 20% ethyl acetate in hexane gave di-*tert*-butyl (2*S*,4*R*)-4-fluoropyrrolidine-1,2-dicarboxylate (**172**) as a colourless oil (0.084 g, 57%). v_{max}/cm^{-1} (neat) 2978 (CH), 1744 (C=O), 1703 (C=O), 1398, 1368, 1152; [α]$_D^{20}$ −8.8 (*c* 0.2, CHCl$_3$); NMR spectra showed a 2:1 mixture of rotamers. Only data for the major rotamer were recorded: δ$_H$ (400 MHz, CDCl$_3$) 1.42 (9H, s, 3 × CH$_3$), 1.44 (9H, s, 3 × CH$_3$), 1.92–2.14 (1H, m, 3-*H*H), 2.44–2.64 (1H, m, 3-H*H*), 3.55 (1H, ddd, *J* 36.1, 13.0, 3.0 Hz, 5-*H*H), 3.89 (1H, ddd, *J* 21.8, 13.0, 3.0 Hz, 5-H*H*), 4.26 (1H, t, *J* 8.3 Hz, 2-H), 5.16 (1H, dt, *J* 52.6, 3.0 Hz, 4-H); δ$_C$ (101 MHz, CDCl$_3$) 28.0 (3 × CH$_3$), 28.3 (3 × CH$_3$), 37.6 (d, $^2J_{C-F}$ 22.8 Hz, CH$_2$), 53.0 (d, $^2J_{C-F}$ 22.8 Hz, CH$_2$), 58.2 (CH), 80.4 (C), 81.4 (C), 91.0 (d, $^1J_{C-F}$ 178.7 Hz, CH), 153.8 (C), 171.7 (C); *m/z* (ESI) 312.1580 (MNa$^+$. C$_{14}$H$_{24}$FNNaO$_4$ requires 312.1582).

(2*S*,4*R*)-4-Fluoropyrrolidine-2-carboxylic acid hydrochloride (149)
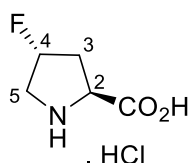
(2*S*,4*R*)-4-Fluoropyrrolidine-2-carboxylic acid hydrochloride (**149**) was prepared as described for (2*S*,4*S*)-4-fluoropyrrolidine-2-carboxylic acid hydrochloride (**150**) using di-*tert*-butyl (2*S*,4*R*)-4-fluoropyrrolidine-1,2-dicarboxylate (**172**) (0.0800 g, 0.280 mmol), acetonitrile (0.25 mL) and 2 M aqueous hydrochloric acid (2.5 mL).

This gave (2*S*,4*S*)-4-fluoropyrrolidine-2-carboxylic acid (**149**) as an off-white solid (0.0331 g, 70%). Mp 148–152 °C (decomposition); ν_{max}/cm^{-1} (neat) 3672 (NH), 2987 (CH), 1738 (C=O), 1682, 1406, 1242, 1220, 1067, 1051; $[\alpha]_D^{17}$ –6.5 (*c* 0.1, MeOH); δ_H (400 MHz, CD$_3$OD) 2.39 (1H, dddd, *J* 38.5, 14.8, 10.5, 3.6 Hz, 3-*H*H), 2.70–2.84 (1H, m, 3-H*H*), 3.52–3.73 (2H, m, 5-H$_2$), 4.61 (1H, dd, *J* 10.5, 7.9 Hz, 2-H), 5.47 (1H, dt, *J* 51.8, 3.6 Hz, 4-H); δ_C (101 MHz, CD$_3$OD) 35.4 (d, $^2J_{C\text{-}F}$ 22.1 Hz, CH$_2$), 51.7 (d, $^2J_{C\text{-}F}$ 24.0 Hz, CH$_2$), 58.0 (CH), 92.0 (d, $^1J_{C\text{-}F}$ 177.0 Hz, CH), 169.3 (C); *m/z* (ESI) 134.0613 (MH$^+$. C$_5$H$_9$FNO$_2$ requires 134.0612).

6.0 References

1   J. V. Jun, D. M. Chenoweth and E. J. Petersson, *Org. Biomol. Chem.*, 2020, **18**, 5747–5763.

2   Y. Fu and N. S. Finney, *RSC Adv.*, 2018, **8**, 29051–29061.

3   B. Valeur and M. N. Berberan-Santos, *J. Chem. Educ.*, 2011, **88**, 731–738.

4   Z. Cheng, E. Kuru, A. Sachdeva and M. Vendrell, *Nat. Rev. Chem.*, 2020, **4**, 275–290.

5   A. H. Harkiss and A. Sutherland, *Org. Biomol. Chem.*, 2016, **14**, 8911–8921.

6   J. Lotze, U. Reinhardt, O. Seitz and A. G. Beck-Sickinger, *Mol. Biosyst.*, 2016, **12**, 1731–1745.

7   Y. Zhang, K. Y. Park, K. F. Suazo and M. D. Distefano, *Chem. Soc. Rev.*, 2018, **47**, 9106–9136.

8   Y. L. Pak, K. M. K. Swamy and J. Yoon, *Sensors,* 2015, **15**, 24374–24396.

9   A. T. Krueger and B. Imperiali, *ChemBioChem*, 2013, **14**, 788–799.

10   J. R. Lakowicz, *Principles of Fluorescence Spectroscopy*, Springer, New York, 2006.

11   *Molecular Probes Handbook*, Thermo Fisher Scientific, 2010.

12   J. C. Del Valle and J. Catalán, *Phys. Chem. Chem. Phys.*, 2019, **21**, 10061–10069.

13   M. Y. Berezin and S. Achilefu, *Chemical Reviews*, 2010, **110**, 2641–2684.

14   S. L. Zheng, N. Lin, S. Reid and B. Wang, *Tetrahedron*, 2007, **63**, 5427–5436.

15   M. Nepraš, N. Almonasy, F. Bureš, J. Kulhánek, M. Dvořák and M. Michl, *Dyes Pigm.*, 2011, **91**, 466–473.

16   Y. Koide, Y. Urano, K. Hanaoka, T. Terai and T. Nagano, *ACS Chem. Biol.*, 2011, **6**, 600–608.

17   S. Benson, A. Fernandez, N. D. Barth, F. de Moliner, M. H. Horrocks, C. S. Herrington, J. L. Abad, A. Delgado, L. Kelly, Z. Chang, Y. Feng, M. Nishiura, Y. Hori, K. Kikuchi and M. Vendrell, *Angew. Chemie Int. Ed.*, 2019, **58**, 6911–6915.

18   J. B. Grimm, B. P. English, H. Choi, A. K. Muthusamy, B. P. Mehl, P. Dong, T. A. Brown, J. Lippincott-Schwartz, Z. Liu, T. Lionnet and L. D. Lavis, *Nat. Methods*, 2016, **13**, 985–988.

19   J. B. Grimm, A. K. Muthusamy, Y. Liang, T. A. Brown, W. C. Lemon, R. Patel, R. Lu, J. J. Macklin, P. J. Keller, N. Ji and L. D. Lavis, *Nat. Methods*, 2017, **14**, 987–994.

20   J. D. Bell, A. H. Harkiss, D. Nobis, E. Malcolm, A. Knuhtsen, C. R. Wellaway, A. G. Jamieson, S. W. Magennis and A. Sutherland, *Chem. Commun.*, 2020, **56**, 1887–1890.

21   M. S. Michie, R. Götz, C. Franke, M. Bowler, N. Kumari, V. Magidson, M. Levitus, J. Loncarek, M. Sauer and M. J. Schnermann, *J. Am. Chem. Soc.*, 2017, **139**, 12406–12409.

22   J. B. Grimm, A. N. Tkachuk, H. Choi, B. Mohar, N. Falco, R. Patel, J. Lippincott-Schwartz, T. A. Brown and L. D. Lavis, *Nat. Methods*, 2019, **17**, 815–821.

23   C. Reichardt, *Chemical Reviews*, 1994, **94**, 2319–2358.

24   M. A. Haidekker and E. A. Theodorakis, *J. Biol. Eng.*, 2010, **4**, 1–14.

25   B. Sk, P. K. Thakre, R. S. Tomar and A. Patra, *Chem. - Asian J.*, 2017, **12**, 2501–2509.

26   X. Zhou, K. J. Belavek and E. W. Miller, *Biochemistry*, 2021, **60**, 3547–3554.

27   N. Mataga, Y. Kaifu and M. Koizumi, *Bull. Chem. Soc. Jpn.*, 1956, **29**, 465–470.

28   S. Kumari, J. Sindhu and J. M. Khurana, *Synth. Commun.*, 2015, **45**, 1101–1113.

29   M. Nagy, B. Fiser, M. Szőri, L. Vanyorek and B. Viskolcz, *Int. J. Mol. Sci.*, 2022, **23**, 1315.

30   F. Le Guern, V. Mussard, A. Gaucher, M. Rottman and D. Prim, *Int. J. Mol. Sci.*, 2020, **21**, 23.

31   L. Ma, Q. Ouyang, G. C. Werthmann, H. M. Thompson and E. M. Morrow, *Frontiers in Cell and Developmental Biology*, 2017, **5**, 71.

32   H. Ihmels, A. Meiswinkel, C. J. Mohrschladt, D. Otto, M. Waidelich, M. Towler, R. White, M. Albrecht and A. Schnurpfeil, *J. Org. Chem.*, 2005, **70**, 3929–3938.

33   M. A. Haidekker and E. A. Theodorakis, *Org. Biomol. Chem.*, 2007, **5**, 1669–1678.

34   C. Wang, W. Chi, Q. Qiao, D. Tan, Z. Xu and X. Liu, *Chem. Soc. Rev.*, 2021, **50**, 12656–12678.

35   A. R. Katritzky and T. Narindoshvili, *Org. Biomol. Chem.*, 2009, **7**, 627–634.

36   A. H. Harkiss, J. D. Bell, A. Knuhtsen, A. G. Jamieson and A. Sutherland, *J. Org. Chem.*, 2019, **84**, 2879–2890.

37   Y. Xiong, C. Shi, L. Li, Y. Tang, X. Zhang, S. Liao, B. Zhang, C. Sun and C. Ren, *New J. Chem.*, 2021, **45**, 15180–15194.

38   M. R. Hilaire, I. A. Ahmed, C. W. Lin, H. Jo, W. F. DeGrado and F. Gai, *Proc.*

Natl. Acad. Sci. U. S. A., 2017, **114**, 6005–6009.

39   L. J. G. W. Van Wilderen, H. Brunst, H. Gustmann, J. Wachtveitl, J. Broos and J. Bredenbeck, *Phys. Chem. Chem. Phys.*, 2018, **20**, 19906–19915.

40   F. Bartoccini, S. Bartolucci, M. Mari and G. Piersanti, *Org. Biomol. Chem.*, 2016, **14**, 10095–10100.

41   C. E. Boville, D. K. Romney, P. J. Almhjell, M. Sieben and F. H. Arnold, *J. Org. Chem.*, 2018, **83**, 7447–7452.

42   K. Zhang, I. A. Ahmed, H. T. Kratochvil, W. F. Degrado, F. Gai and H. Jo, *Chem. Commun.*, 2019, **55**, 5095–5098.

43   R. O. Duthaler, *Tetrahedron*, 1994, **50**, 1539–1650.

44   H. K. Chenaull, J. Dahmer and G. M. Whitesides, *J. Am. Chem. Soc.*, 1989, **111**, 6354–6364.

45   R. Micikas, A. Acharyya, F. Gai and A. B. Smith, *Org. Lett.*, 2021, **23**, 1247–1250.

46   J. Ku, B. Jeong, S. Jew and H. Park, *J. Org. Chem.*, 2007, **72**, 8115–8118.

47   G. Loidl, H. J. Musiol, N. Budisa, R. Huber, S. Poirot, D. Fourmy and L. Moroder, *J. Pept. Sci.*, 2000, **6**, 139–144.

48   Y. S. Moroz, W. Binder, P. Nygren, G. A. Caputo and I. V. Korendovych, *Chem. Commun.*, 2013, **49**, 490–492.

49   E. Stempel, R. F. X. Kaml, N. Budisa and M. Kalesse, *Bioorganic Med. Chem.*, 2018, **26**, 5259–5269.

50   E. J. Watkins, P. J. Almhjell and F. H. Arnold, *ChemBioChem*, 2020, **21**, 80–83.

51   H. Gruß, C. Belu, L. M. Bernhard, A. Merschel and N. Sewald, *Chem. - A Eur. J.*, 2019, **25**, 5880–5883.

52   M. Frese and N. Sewald, *Angew. Chemie - Int. Ed.*, 2015, **54**, 298–301.

53   M. Frese, C. Schnepel, H. Minges, H. Voß, R. Feiner and N. Sewald, *ChemCatChem*, 2016, **8**, 1799–1803.

54   P. Cheruku, J. H. Huang, H. J. Yen, R. S. Iyer, K. D. Rector, J. S. Martinez and H. L. Wang, *Chem. Sci.*, 2015, **6**, 1150–1158.

55   D. Summerer, S. Chen, N. Wu, A. Deiters, J. W. Chin and P. G. Schultz, *Proc. Natl. Acad. Sci. U. S. A.,* 2006, **103**, 9785–9789.

56   M. Noden and S. D. Taylor, *J. Org. Chem.*, 2021, **86**, 11407–11418.

57   M. Sholokh, O. M. Zamotaiev, R. Das, V. Y. Postupalenko, L. Richert, D. Dujardin, O. A. Zaporozhets, V. G. Pivovarenko, A. S. Klymchenko and Y. Mély, *J. Phys. Chem. B*, 2015, **119**, 2585–2595.

58 L. Mendive-Tapia, R. Subiros-Funosas, C. Zhao, F. Albericio, N. D. Read, R. Lavilla and M. Vendrell, *Nat. Protoc.*, 2017, **12**, 1588.

59 R. Subiros-Funosas, V. C. L. Ho, N. D. Barth, L. Mendive-Tapia, M. Pappalardo, X. Barril, R. Ma, C. Bin Zhang, B. Z. Qian, M. Sintes, O. Ghashghaei, R. Lavilla and M. Vendrell, *Chem. Sci.*, 2020, **11**, 1368–1374.

60 A. Chakrabarti, *Biochem. Biophys. Res. Commun.*,1996, **497**, 495–497.

61 K. Tainaka, K. Tanaka, S. Ikeda, K. I. Nishiza, T. Unzai, Y. Fujiwara, I. Saito and A. Okamoto, *J. Am. Chem. Soc.*, 2007, **129**, 4776–4784.

62 G. Weber and F. J. Farris, *Biochemistry*, 1979, **18**, 3075–3078.

63 M. Nitz, A. R. Mezo, M. H. Ali and B. Imperiali, *Chem. Commun.*, 2002, **17**, 1912–1913.

64 S. L. Hyun, J. Guo, E. A. Lemke, R. D. Dimla and P. G. Schultz, *J. Am. Chem. Soc.*, 2009, **131**, 12921–12923.

65 Z. Diwu, C. Beachdel and D. H. Klaubert, *Tetrahedron Lett.*, 1998, **39**, 4987–4990.

66 A. Chatterjee, J. Guo, H. S. Lee and P. G. Schultz, *J. Am. Chem. Soc.*, 2013, **135**, 12540–12543.

67 B. Imperiali and M. Sainlos, *Nat. Protoc.*, 2007, **2**, 3201–3209.

68 M. E. Vázquez, D. M. Rothman and B. Imperiali, *Org. Biomol. Chem.*, 2004, **2**, 1965–1966.

69 M. E. Vázquez, J. B. Blanco and B. Imperiali, *J. Am. Chem. Soc.*, 2005, **127**, 1300–1306.

70 B. Imperiali and M. Sainlos, *Nat. Protoc.*, 2007, **2**, 3210–3218.

71 S. Wörner, F. Rönicke, A. S. Ulrich and H. A. Wagenknecht, *ChemBioChem*, **21**, 2019, 618–622.

72 T. Soujanya, R. W. Fessenden and A. Samanta, *J. Phys. Chem.*, 1996, **100**, 3507–3512.

73 Y. Zhao, M. C. Pirrung and J. Liao, *Mol. Biosyst.*, 2012, **8**, 879–887.

74 P. Talukder, S. Chen, P. M. Arce and S. M. Hecht, *Org. Lett.*, 2014, **16**, 556–559.

75 Int. Pat., WO2011079804A1, 2011.

76 X. G. Liang, J. Cheng, S. Qin, L. X. Shao, M. Z. Huang, G. Wang, Y. Han, F. Han and X. Li, *Chem. Commun.*, 2018, **54**, 12010–12013.

77 L. S. Fowler, D. Ellis and A. Sutherland, *Org. Biomol. Chem.*, 2009, **7**, 4309–4316.

78   A. H. Harkiss and A. Sutherland, *Org. Biomol. Chem.*, 2016, **14**, 8911–8921.

79   L. Gilfillan, R. Artschwager, A. H. Harkiss, R. M. J. Liskamp and A. Sutherland, *Org. Biomol. Chem.*, 2015, **13**, 4514–4523.

80   S. Danishefsky and M. Bednarski, *Tetrahedron Lett.*, 1984, **25**, 721–724.

81   J. D. Bell, T. E. F. Morgan, N. Buijs, A. H. Harkiss, C. R. Wellaway and A. Sutherland, *J. Org. Chem.*, 2019, **84**, 10436–10448.

82   H. Hori, Y. Nishida, H. Ohrui and H. Meguro, *J. Org. Chem.*, 1989, **54**, 1346–1353.

83   M. A. B. Mostafa, E. D. D. Calder, D. T. Racys and A. Sutherland, *Chem. - A Eur. J.*, 2017, **23**, 1044–1047.

84   H. Gruß, C. Belu, L. M. Bernhard, A. Merschel and N. Sewald, *Chem. - A Eur. J.*, 2019, **25**, 5880–5883.

85   U. Salzner and A. Aydin, *J. Chem. Theory Comput.*, 2011, **7**, 2568–2583.

86   F. Weigend and R. Ahlrichs, *Phys. Chem. Chem. Phys.*, 2005, **7**, 3297–3305.

87   S. Umar, A. K. Jha and A. Goel, *Asian J. Org. Chem.*, 2016, **5**, 187–191.

88   L. Espinar-Barranco, M. Meazza, A. Linares-Perez, R. Rios, J. M. Paredes and L. Crovetto, *Sensors*, 2019, **19**, 4932.

89   T. Rudrappa, *Int. J. Sci. Technol. Res.*, 2014, **3**, 107.

90   A. Filarowski, M. Kluba, K. Cieślik-Boczula, A. Koll, A. Kochel, L. Pandey, W. M. De Borggraeve, M. Van Der Auweraer, J. Catalán and N. Boens, *Photochem. Photobiol. Sci.*, 2010, **9**, 996–1008.

91   N. Dash, F. A. S. Chipem, R. Swaminathan and G. Krishnamoorthy, *Chem. Phys. Lett.*, 2008, **460**, 119–124.

92   K. Melánová, D. Cvejn, F. Bureš, V. Zima, J. Svoboda, L. Beneš, T. Mikysek, O. Pytela and P. Knotek, *Dalt. Trans.*, 2014, **43**, 10462–10470.

93   R. Hu, E. Lager, A. Aguilar-Aguilar, J. Liu, J. W. Y. Lam, H. H. Y. Sung, I. D. Williams, Y. Zhong, K. S. Wong, E. Peña-Cabrera and B. Z. Tang, *J. Phys. Chem. C*, 2009, **113**, 15845–15853.

94   C. Weber, M. Sipos, A. Paczal, B. Balint, V. Kun, N. Foloppe, P. Dokurno, A. J. Massey, D. L. Walmsley, R. E. Hubbard, J. Murray, K. Benwell, T. Edmonds, D. Demarles, A. Bruno, M. Burbridge, F. Cruzalegui and A. Kotschy, *J. Med. Chem.*, 2021, **64**, 6745–6764.

95   Z. Li, Y. Wang, C. Fu, X. Wang, J. J. Wang, Y. Zhang, D. Zhou, Y. Zhao, L. Luo, H. Ma, W. Lu, J. Zheng and X. Zhang, *Eur. J. Med. Chem.*, 2018, **149**, 30–44.

96   B. Lygo and P. G. Wainwright, *Tetrahedron Lett.*, 1997, **38**, 8595–8598.

97   E. J. Corey, F. Xu and M. C. Noe, *J. Am. Chem. Soc.*, 1997, **119**, 12414–12415.

98   L. H. Zhang, G. S. Kauffman, J. A. Pesti and J. Yin, *J. Org. Chem.*, 1997, **62**, 6918–6920.

99   V. D. Filimonov, M. Trusova, P. Postnikov, E. A. Krasnokutskaya, Y. M. Lee, H. Y. Hwang, H. Kim and K. W. Chi, *Org. Lett.*, 2008, **10**, 3961–3964.

100   R. J. Faggyas, N. L. Sloan, N. Buijs and A. Sutherland, *European J. Org. Chem.*, 2019, 5344–5353.

101   P. Cheruku, J. Huang, H. Yen, R. S. Iyer, K. D. Rector, J. S. Martinez and H. Wang, *Chem. Sci.*, 2015, **6**, 1150–1158.

102   L. H. Zhang, G. S. Kauffman, J. A. Pesti and J. Yin, *J. Org. Chem.*, 1997, **62**, 6918–6920.

103   M. A. B. Mostafa, A. E. McMillan and A. Sutherland, *Org. Biomol. Chem.*, 2017, **15**, 3035–3045.

104   M. Rubin, A. Trofimov and V. Gevorgyan, *J. Am. Chem. Soc.*, 2005, **127**, 10243–10249.

105   R. Chinchilla and C. Nájera, *Chem. Soc. Rev.*, 2011, **40**, 5084–5121.

106   R. Chinchilla and C. Nájera, *Chem. Rev.*, 2007, **107**, 874–922.

107   B. Li, J. Zhang, Y. Xu, X. Yang and L. Li, *Tetrahedron Lett.*, 2017, **58**, 2374–2377.

108   R. M. Williams, D. J. Aldous and S. C. Aldous, *J. Org. Chem.*, 1990, **55**, 4657–4663.

109   Y. Kiso, K. Ukawa and T. Akita, *J. Chem. Soc. Chem. Commun.*, 1980, 101–102.

110   R. B. Silverman and M. W. Holladay, *J. Am. Chem. Soc.*, 1981, **103**, 7357–7358.

111   T. R. Bailey, R. S. Garigipati, J. A. Morton and S. M. Weinreb, *J. Am. Chem. Soc.*, 1984, **106**, 3240–3245.

112   R. Y. Y. Ko, J. C. K. Chu and P. Chiu, *Tetrahedron*, 2011, **67**, 2542–2547.

113   S. I. Kozhushkov, K. Wagner-Gillen, A. F. Khlebnikov and A. de Meijere, *Synthesis*, 2010, 23, 3967–3973.

114   J. M. Beierle, W. S. Horne, J. H. Van Maarseveen, B. Waser, J. C. Reubi and M. R. Ghadiri, *Angew. Chemie - Int. Ed.*, 2009, **48**, 4725–4729.

115   M. Radić Stojković, P. Piotrowski, C. Schmuck and I. Piantanida, *Org. Biomol. Chem.*, 2015, **13**, 1629–1633.

116   V. Murugesan, R. De Bettignies, R. Mercier, S. Guillerez and L. Perrin, *Synth.*

Met., 2012, **162**, 1037–1045.

117 S. Ling, M. Polymenidou, D. W. Cleveland, A. Revyakin, R. Patel, J. J. Macklin, D. Normanno and H. Robert, *Nat. Methods*, 2015, **79**, 244–250.

118 J. N. Abrams, Q. Zhao, I. Ghiviriga and Minaruzzaman, *Tetrahedron*, 2012, **68**, 423–428.

119 S. M. Crawford, C. A. Wheaton, V. Mishra and M. Stradiotto, *Can. J. Chem.*, 2018, **96**, 578–586.

120 S. Mikami, S. Nakamura, T. Ashizawa, I. Nomura, M. Kawasaki, S. Sasaki, H. Oki, H. Kokubo, I. D. Hoffman, H. Zou, N. Uchiyama, K. Nakashima, N. Kamiguchi, H. Imada, N. Suzuki, H. Iwashita and T. Taniguchi, *J. Med. Chem.*, 2017, **60**, 7677–7702.

121 D. T. Racys, C. E. Warrilow, S. L. Pimlott and A. Sutherland, *Org. Lett.*, 2015, **17**, 4782–4785.

122 D. G. Patel, F. Feng, Y. Y. Ohnishi, K. A. Abboud, S. Hirata, K. S. Schanze and J. R. Reynolds, *J. Am. Chem. Soc.*, 2012, **134**, 2599–2612.

123 A. Khalaf, D. Grée, H. Abdallah, N. Jaber, A. Hachem and R. Grée, *Tetrahedron*, 2011, **67**, 3881–3886.

124 J. Sherwood, J. H. Clark, I. J. S. Fairlamb and J. M. Slattery, *Green Chem.*, 2019, **21**, 2164–2213.

125 D. M. Knapp, E. P. Gillis and M. D. Burke, *J. Am. Chem. Soc.*, 2009, **131**, 6961–6963.

126 S. Jagtap, *Catalysts*, 2017, **7**, 267.

127 T. Jeffery, *Experientia*, 1996, **52**, 25–30.

128 M. Suhartono, M. Weidlich, T. Stein, M. Karas, G. Dürner and M. W. Göbel, *European J. Org. Chem.*, 2008, 1608–1614.

129 M. Safir Filho, S. Fiorucci, A. R. Martin and R. Benhida, *New J. Chem.*, 2017, **41**, 13760–13772.

130 H. Lindlar, *Helv. Chim. Acta.*, 1952, **35**, 446–450.

131 B. M. Trost, Z. T. Ball and T. Jöge, *J. Am. Chem. Soc.*, 2002, **124**, 7922–7923.

132 D. Srimani, Y. Diskin-Posner, Y. Ben-David and D. Milstein, *Angew. Chemie - Int. Ed.*, 2013, **52**, 14131–14134.

133 K. Higashida and K. Mashima, *Chem. Lett.*, 2016, **45**, 866–868.

134 R. Maazaoui, R. Abderrahim, F. Chemla, F. Ferreira, A. Perez-Luna and O. Jackowski, *Org. Lett.*, 2018, **20**, 7544–7549.

135 I. Torres-Moya, C. Benitez-Martin, B. Donoso, C. Tardío, R. Martín, J. R. Carrillo, Á. Díaz-Ortiz, F. Najera, P. Prieto and E. Perez-Inestrosa, *Chem. - A*

Eur. J., 2019, **25**, 15572–15579.

136 R. K. P. Benninger and D. W. Piston, *Curr. Protoc. Cell Biol.*, 2013, **4**, 1–24.

137 A. Diaspro, G. Chirico and M. Collini, *Q. Rev. Biophys.*, 2005, **38**, 97–166.

138 L. Mendive-Tapia, C. Zhao, A. R. Akram, S. Preciado, F. Albericio, M. Lee, A. Serrels, N. Kielland, N. D. Read, R. Lavilla and M. Vendrell, *Nat. Commun.*, 2016, **7**, 1–9.

139 J. Yao and L. V. Wang, *Laser Photonics Rev.*, 2013, **7**, 758–778.

140 D. B. Nowak, A. J. Lawrence and E. J. Sánchez, *Appl. Opt.*, 2010, **49**, 6766.

141 J. A. Gomez, V. Gama, T. Yoshida, W. Sun, P. Hayes, K. Leskov, D. Boothman and S. Matsuyama, *Biochem. Soc. Trans.*, 2007, **35**, 797–801.

142 P. K. Mykhailiuk, *J. Org. Chem.*, 2022, **87**, 6961–7005.

143 A. M. P. Koskinen, J. Helaja, E. T. T. Kumpulainen, J. Koivisto, H. Mansikkamäki and K. Rissanen, *J. Org. Chem.*, 2005, **70**, 6447–6453.

144 M. D. Shoulders, F. W. Kotch, A. Choudhary, I. A. Guzei and R. T. Raines, *J. Am. Chem. Soc.*, 2010, **132**, 10857–10865.

145 J. A. Hodgest and R. T. Raines, *J. Am. Chem. Soc.*, 2003, **125**, 9262–9263.

146 S. P. Nadarajan, K. Deepankumar, J.-H. Seo and H. Yun, *Biotechnol. Bioprocess Eng.*, 2017, **22**, 504–511.

147 A. A. Gottlieb, Y. Fujita, S. Udenfriend and B. Witkop, *Biochemistry*, 1965, **4**, 2507–2513.

148 R. T. Raines, S. Moghe, N. Bhoite, M. V. Mandlecha and M. S. Chorghade, *J. Fluor. Chem.*, 2008, **129**, 781–784.

149 E. M. Smith, G. F. Swiss, B. R. Neustadt, E. H. Gold, J. A. Sommer, A. D. Brown, P. J. S. Chiu, R. Moran, E. J. Sybertz and T. Baum, *J. Med. Chem.*, 1988, **31**, 875–885.

150 T. Komai, S. Higashida, M. Sakurai, T. Nitta, A. Kasuya, S. Miyamaoto, R. Yagi, Y. Ozawa, H. Handa, H. Mohri, A. Yasuoka, S. Oka, T. Nishigaki, S. Kimura, K. Shimada and Y. Yabe, *Bioorg. Med. Chem.*, 1996, **4**, 1365–1377.

151 M. Hudlický, *J. Fluor. Chem.*, 1993, **60**, 193–210.

152 T. T. Tran, N. Patino, R. Condom, T. Frogier and R. Guedj, *J. Fluor. Chem.*, 1997, **82**, 125–130.

153 L. Demange, A. Ménez and C. Dugave, *Tetrahedron Lett.*, 1998, **39**, 1169–1172.

154 M. Doi, Y. Nishi, N. Kiritoshi, T. Iwata, M. Nago, H. Nakano, S. Uchiyama, T. Nakazawa, T. Wakamiya and Y. Kobayashi, *Tetrahedron*, 2002, **58**, 8453–8459.

155 R. P. Singh and T. Umemoto, *J. Org. Chem.*, 2011, **76**, 3113–3121.

156 M. K. Nielsen, C. R. Ugaz, W. Li and A. G. Doyle, *J. Am. Chem. Soc.*, 2015, **137**, 9571–9574.

157 J. Guo, C. Kuang, J. Rong, L. Li, C. Ni and J. Hu, *Chem. – A Eur. J.*, 2019, **25**, 7259–7264.

158 P. W. Miller, N. J. Long, R. Vilar and A. D. Gee, *Angew. Chemie Int. Ed.*, 2008, **47**, 8998–9033.

159 S. L. Pimlott and A. Sutherland, *Chem. Soc. Rev.*, 2011, **40**, 149–162.

160 J. Ermert and H. H. Coenen, *J. Label. Compd. Radiopharm.*, 2013, **56**, 225–236.

161 P. L. Jager, W. Vaalburg, J. Pruim, E. G. E. De Vries, K. Langen and D. A. Piers, *J. Nucl. Med.*, 2001, **42**, 432–445.

162 S. Geisler, J. Ermert, G. Stoffels, A. Willuweit, N. Galldiks, C. Filss, N. Shah, H. Coenen and K.-J. Langen, *Curr. Radiopharm.*, 2015, **7**, 123–132.

163 O. Couturier, A. Luxen, J. F. Chatal, J. P. Vuillez, P. Rigo and R. Hustinx, *Eur. J. Nucl. Med. Mol. Imaging*, 2004, **31**, 1182–1206.

164 J. McConathy and M. M. Goodman, *Cancer Metastasis Rev.*, 2008, **27**, 555–573.

165 E. Nurmi, H. M. Ruottinen, J. Bergman, M. Haaparanta, O. Solin, P. Sonninen and J. O. Rinne, *Mov. Disord.*, 2001, **16**, 608–615.

166 W. E. Wallace, N. C. Gupta, A. F. Hubbs, S. M. Mazza, H. A. Bishop, M. J. Keane, L. A. Battelli, J. Ma and P. Schleiff, *J. Nucl. Med.*, 2002, **43**, 413–420.

167 K.-J. Langen, H. Mühlensiepen, S. Schmieder, K. Hamacher, S. Bröer, A. R. Börner, F. H. . Schneeweiss and H. H. Coenen, *Nucl. Med. Biol.*, 2002, **29**, 685–692.

168 J. Lavalaye, J. C. Grutters, E. M. W. van de Garde, M. M. C. van Buul, J. M. M. van den Bosch, A. D. Windhorst and F. J. Verzijlbergen, *Mol. Imaging Biol.*, 2009, **11**, 123–127.

169 K. Hamacher, *J. Label. Compd. Radiopharm.*, 1999, **42**, 1135–1144.

170 H. H. Coenen, A. D. Gee, M. Adam, G. Antoni, C. S. Cutler, Y. Fujibayashi, J. M. Jeong, R. H. Mach, T. L. Mindt, V. W. Pike and A. D. Windhorst, *Nucl. Med. Biol.*, 2017, **55**, v–xi.

171 B. B. Azad, R. Ashique, N. R. Labiris and R. Chirakal, *J. Label. Compd. Radiopharm.*, 2012, **55**, 23–28.

172 P. Chabaud, G. Pèpe, J. Courcambeck and M. Camplo, *Tetrahedron*, 2005, **61**, 3725–3731.

173 C. Donthulachitti, S. R. Kothakapu, R. K. Shekunti and C. K. Neella,

ChemistrySelect, 2017, **2**, 5321–5328.

174 F. Brackmann, H. Schill and A. De Meijere, *Chem. - A Eur. J.*, 2005, **11**, 6593–6600.

175 P. A. Messina, K. C. Mange and W. J. Middleton, *J. Fluor. Chem.*, 1989, **42**, 137–143.

176 S. J. M. Verhoork, P. M. Killoran and C. R. Coxon, *Biochemistry*, 2018, **57**, 6132–6143.

177 C. Siebler, B. Maryasin, M. Kuemin, R. S. Erdmann, C. Rigling, C. Grünenfelder, C. Ochsenfeld and H. Wennemers, *Chem. Sci.*, 2015, **6**, 6725–6730.

178 G. J. Hofman, E. Ottoy, M. E. Light, B. Kieffer, I. Kuprov, J. C. Martins, D. Sinnaeve and B. Linclau, *Chem. Commun.*, 2018, **54**, 5118–5121.

179 J. Seo, P. Martásek, L. J. Roman and R. B. Silverman, *Bioorganic Med. Chem.*, 2007, **15**, 1928–1938.

180 R. W. Newberry and R. T. Raines, *Top. Heterocycle. Chem.*, 2017, **48**, 1–25.

181 K. Langen, K. Hamacher, D. Bauer, S. Bröer, D. Pauleit, H. Herzog, F. Floeth, K. Zilles and H. H. Coenen, *J. Cereb. Blood Flow Metab.*, 2005, **25**, 607–616.

182 K. Langen, D. Salber, K. Hamacher, G. Stoffels, G. Reifenberger, D. Pauleit, H. H. Coenen and K. Zilles, *J. Nucl. Med.*, 2007, **48**, 1482–1491.

183 P. Gmeiner, P. L. Feldman, M. Y. Chu-Moyer and H. Rapoport, *J. Org. Chem.*, 1990, **55**, 3068–3074.

184 I. Abrunhosa-Thomas, A. Plas, N. Kandepedu, P. Chalard and Y. Troin, *Beilstein J. Org. Chem.*, 2013, **9**, 486–495.

185 D. E. Rudisill and J. P. Whitten, *Synthesis*, 1994, **8**, 851–854.

186 W. Kurosawa, T. Kan and T. Fukuyama, *J. Am. Chem. Soc.*, 2003, **125**, 8112–8113.

187 W. Delong, W. Lanying, W. Yongling, S. Shuang, F. Juntao and Z. Xing, *Eur. J. Med. Chem.*, 2017, **130**, 286–307.

188 P. de Macédo, C. Marrano and J. W. Keillor, *Bioorg. Med. Chem.*, 2002, **10**, 355–360.

189 M. S. Egbertson, J. J. Cook, B. Bednar, J. D. Prugh, R. A. Bednar, S. L. Gaul, R. J. Gould, G. D. Hartman, C. F. Homnick, M. A. Holahan, L. A. Libby, J. J. Lynch, R. J. Lynch, G. R. Sitko, M. T. Stranieri and L. M. Vassallo, *J. Med. Chem.*, 1999, **42**, 2409–2421.

190 Y. Yang, M. Ji, Z. Lu, M. Jiang, W. Huang and X. He, *Synth. Commun.*, 2016, **46**, 977–982.

191 H. Teng, Z. Jiang, L. Wu, J. Su, X. Feng, G. Qiu, S. Liang and X. Hu, *Synth.*

Commun., 2006, **36**, 3803–3807.

192 A. Isidro-Llobet, K. Hadje Georgiou, W. R. J. D. Galloway, E. Giacomini, M. R. Hansen, G. Méndez-Abt, Y. S. Tan, L. Carro, H. F. Sore and D. R. Spring, *Org. Biomol. Chem.*, 2015, **13**, 4570–4580.

193 Y. Jeong, J. Lee and J. Ryu, *Bioorg. Med. Chem.*, 2016, **24**, 2114–2124.

194 X. Jiang, Z. Zeng, D. Shi, C. Liu and Y. Zhang, *Tetrahedron Lett.*, 2021, **66**, 152839.

195 M. Shigeta, J. Watanabe and G. Konishi, *Tetrahedron Lett.*, 2013, **54**, 1761–1764.

196 GB. Pat., WO2021009506, 2021.

197 A. Bose and P. Mal, *Tetrahedron Lett.*, 2014, **55**, 2154–2156.

198 M. Yamaji, H. Maeda, K. Minamida, T. Maeda, K. Asai, G. Konishi and K. Mizuno, *Res. Chem. Intermed.*, 2013, **39**, 321–345.

199 C. D. Wight, Q. Xiao, H. R. Wagner, E. A. Hernandez, V. M. Lynch and B. L. Iverson, *J. Am. Chem. Soc.*, 2020, **142**, 17630–17643.

200 S. Höck, R. Marti, R. Riedl and M. Simeunovic, *Chimia.*, 2010, **64**, 200.

201 A. del Prado, M. Pintado-Sierra, M. Juan-y-Seva, R. Navarro, H. Reinecke, J. Rodríguez-Hernández, C. Elvira, A. Fernández-Mayoralas and A. Gallardo, *J. Polym. Sci. Part A Polym. Chem.*, 2017, **55**, 1228–1236.

202 J. Y. Lu, M. Riedrich, K. P. Wojtas and H. D. Arndt, *Synth.*, 2013, **45**, 1300–1311.

203 D. Torino, A. Mollica, F. Pinnen, F. Feliciani, S. Spisani and G. Lucente, *Bioorganic Med. Chem.*, 2009, **17**, 251–259.

204 P. Barraclough, P. Dieterich, C. A. Spray and D. W. Young, *Org. Biomol. Chem.*, 2006, **4**, 1483–1491.

Appendix A - HPLC Traces of [18F]-Fluoroproline Precursors

## Di-*tert*-butyl (2S,4R)-4-(tosyloxy)pyrrolidine-1,2-dicarboxylate (169)

<Chromatogram>

mV
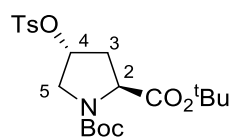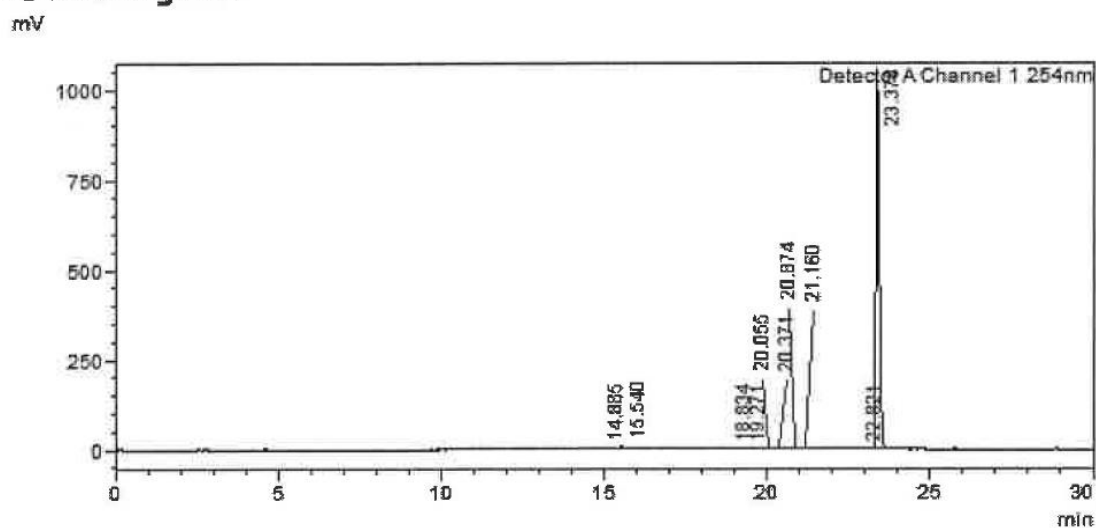
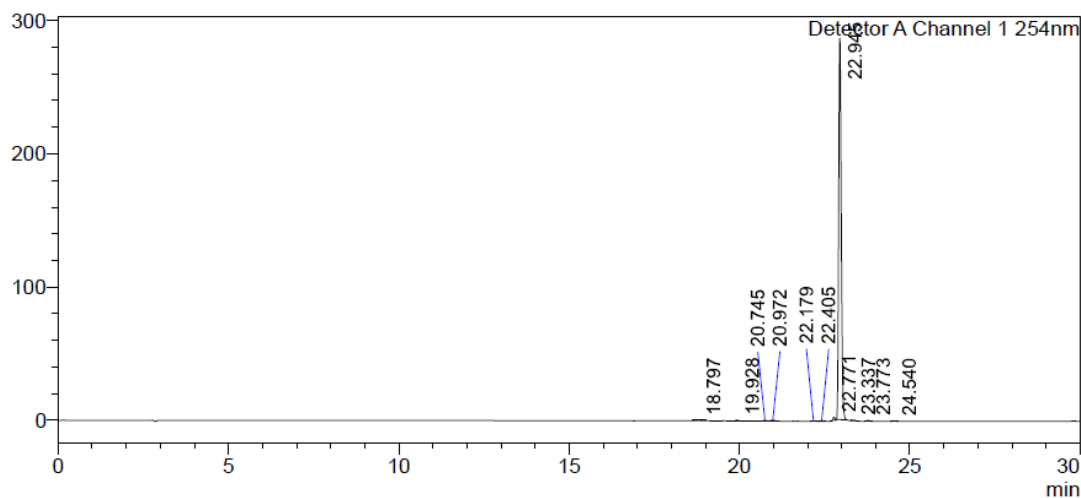| Peak#	Ret. Time	Area	Height	Conc.	Unit	Mark	Name
1	14.885	6759	786	0.090		M	
2	15.540	46928	5660	0.622		M	
3	18.834	2058	421	0.027		M	
4	19.271	5567	761	0.074		M	
5	20.055	1630	403	0.022		M	
6	20.371	469	103	0.006		M	
7	20.874	37316	6946	0.495		M	
8	21.160	12629	994	0.168		M	
9	22.821	9833	1536	0.130		M	
10	23.378	7415946	1012037	98.366		M	
Total		7539135	1029649				

Peak #10 corresponds to compound **169**, with an overall purity of 98%.

Di-*tert*-butyl (2*S*,4*S*)-4-(tosyloxy)pyrrolidine-1,2-dicarboxylate (171)

<Chromatogram>
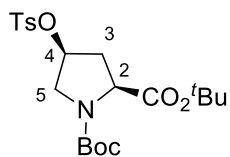
Peak#	Ret. Time	Area	Height	Conc.	Unit	Mark	Name
1	18.797	2148	242	0.139		M	
2	19.928	3745	758	0.243		M	
3	20.745	2032	429	0.132		M	
4	20.972	3490	655	0.227		M	
5	22.179	1179	202	0.077		M	
6	22.405	392	84	0.025		M	
7	22.771	9121	2239	0.592		M	
8	22.945	1510801	286148	98.084		M	
9	23.337	3049	636	0.198		M	
10	23.773	3004	626	0.195		M	
11	24.540	1358	276	0.088		M	
Total		1540319	292294				

Peak #8 corresponds to compound **171**, with an overall purity of 98%.